

DISSERTATION

ELECTRON PARAMAGNETIC RESONANCE DOSIMETRY AND THE USE OF
JAPANESE WILD BOAR TOOTH ENAMEL AS A DOSIMETER FOR RECONSTRUCTION
OF LIFETIME EXTERNAL ABSORBED DOSES FROM THE FUKUSHIMA EXCLUSION
ZONE

Submitted by

Amber Harshman

Department of Environmental and Radiological Health Sciences

In partial fulfillment of the requirements

For the Degree of Doctor of Philosophy

Colorado State University

Fort Collins, Colorado

Fall 2018

Doctoral Committee:

Advisor: Thomas E. Johnson

Alexander Brandl

Ralf Sudowe

Gwen Fisher

Copyright by Amber Melissa Harshman 2018

All Rights Reserved

ABSTRACT

ELECTRON PARAMAGNETIC RESONANCE DOSIMETRY AND THE USE OF JAPANESE WILD BOAR TOOTH ENAMEL AS A DOSIMETER FOR RECONSTRUCTION OF LIFETIME EXTERNAL ABSORBED DOSES FROM THE FUKUSHIMA EXCLUSION ZONE¹

The goal of this study was to establish characteristics of Japanese wild boar tooth enamel in the region of 0.25 – 12.0 Gy and to reconstruct external doses to wild boar native to the Fukushima Exclusion Zone using Electron Paramagnetic Resonance Dosimetry. The significance of Japanese wild boar in their ecosystem and their position within the trophic hierarchy make the wild boar a species of particular importance and therefore the focus of this study. Dose response, linearity, and variability of enamel originating from various wild boar were investigated. Radiation dose response of Japanese wild boar tooth enamel in the range of 0.25 – 12.0 Gy was found to be linear, and the average variation in dose response between teeth originating from the same boar specimen was 30%. Analysis of dose response of permanent and deciduous tooth enamel revealed a statistically significant difference in both the degree of dose response and also variation. No statistically significant difference in dose response was found in permanent molar teeth of boar of differing ages or in boar of different sex. Doses were successfully reconstructed with large associated uncertainties. The critical level dose value for the calibration curve was 1.0 Gy, and the detection limit dose was 1.8 Gy, suggesting that this method would be more

¹ Based on: Harshman A, Johnson T. 2018. Dose Reconstruction Using Tooth Enamel from Wild Boar Living in the Fukushima Exclusion Zone with Electron Paramagnetic Resonance Dosimetry. Health Physics Journal. Submitted.

beneficial for boar with lifetime doses over 1 Gy. The method of reconstructing external doses using EPR dosimetry with tooth enamel from Japanese wild boar as dosimeters has proven to be a viable method which can be used to reconstruct doses to wildlife in accident-stricken areas in the absence of alternative dosimetry.

ACKNOWLEDGEMENTS

The author was supported in part by the U.S. Nuclear Regulatory Commission under Grant Award Number, NRC-HQ-84-14-G-0034, Modification M0003 (Program B). The contents herein, however, are solely the responsibility of the author and do not represent the official views of the U.S. Nuclear Regulatory Commission.

I would like to thank my advisor, Dr. Thomas Johnson, whose guidance and mentorship were a great encouragement to me during the completion of this research project and also my time at Colorado State University. I am immensely grateful to Dr. Shin Toyoda, whose expertise and advice were invaluable to this project. Many thanks go to Josh Hayes, Sami Pederson, and Maggie Li Puma for collecting the boar specimens used in this research endeavor. I would like to acknowledge Ashley Sorcic of Colorado State University and Mika Murahashi of the Okayama University of Science for their assistance with the various analysis techniques used in this research. I would like to share my sincere appreciation to Dr. Alexander Romanyukha of the US Naval Dosimetry Center, Dr. Albrecht Wieser of Helmholtz Zentrum München-German Research Center for Environmental Health, and Dr. Gareth Eaton and Dr. Sandra Eaton from the University of Denver for their various areas of expertise and contributions to this project. Much gratitude goes to all of the individuals at the Institute of Environmental Radioactivity at Fukushima University in Fukushima, Japan, for their support throughout the summer I spent there. I would also like to thank my committee members for their support during the course of this project.

I would like to thank Brian Perri, a dear friend whose life ended too soon. His friendship meant more to me than he could have known. I would also like to thank Jaimie Daum, Lucas

Boron-Brenner, and Scott Braley for making life in Fort Collins fun. Finally, I would like to thank my husband, Frank Harshman Jr., for his support and encouragement even at my most difficult times.

TABLE OF CONTENTS

ABSTRACT.....	ii
ACKNOWLEDGEMENTS.....	iv
EXECUTIVE SUMMARY	1
Chapter 1.....	4
SCOPE AND PURPOSE OF THE PROJECT	4
1.1 Background	4
1.2 Motivation.....	5
1.3 Project Goals	7
1.3.1 Research Objectives	7
1.3.2 Supporting Objectives	8
1.4 Significance of the Study	9
Chapter 2.....	10
HISTORY AND BACKGROUND OF ELECTRON PARAMAGNETIC RESONANCE DOSIMETRY	10
2.1 Electron Paramagnetic Resonance Dosimetry	10
2.1.1 Theory.....	10
2.1.2 EPR Measurements.....	11
2.1.3 Measurement Parameters.....	12
2.1.3.1 Microwave Parameters	12
2.1.3.2 Magnetic Field Parameters	14
2.1.3.3 Signal Channel Parameters.....	14
2.1.4 EPR Spectra.....	15
2.1.5 Methods Used for Dose Reconstruction.....	16
2.1.6 EPR Spectrometers	17
2.2. The Origins and Uses of EPR	19
2.3 Teeth as Radiation Dosimeters.....	21
2.4 Tooth Characteristics & EPR	22
2.5 Summary of Studies	23
2.5.1 Canines	23

2.5.2 Bovines	24
2.5.3 Goats	25
2.5.4 Mice	26
2.5.5 Pacific Walrus.....	27
2.5.6 Pigs	28
2.5.7 Rats	29
2.5.8 Reindeer.....	29
2.5.9 Rhesus Monkey Studied by In Vivo EPR Dosimetry.....	31
2.6 Synthesis of Results, Their Meaning and Future Needs	32
2.7 Conclusion.....	32
Chapter 3.....	35
SAMPLE PROCEDURES.....	35
3.1 Sample Collection	35
3.2 Tooth Extraction.....	37
Chapter 4.....	38
SUITABILITY DETERMINATION PART I: DOSE RESPONSE EVALUATION (1.2 – 12 GY)	38
4.1 Introduction.....	38
4.2 Materials & Methods.....	39
4.2.1 Sample Selection	39
4.2.2 Sample Preparation.....	39
4.2.3 Sample Irradiation	41
4.3 EPR Measurement.....	42
4.4 Processing of the Spectra and Statistical Analysis.....	43
4.5 Results	46
4.5.1 Variation in Dose Response	46
4.5.2 Possible Causes of Dose Response Variation.....	46
4.6 Discussion and Synthesis of Results	48
4.7 Conclusion.....	49
Chapter 5.....	50

SUITABILITY DETERMINATION PART II: DOSE RESPONSE EVALUATION (0.25- 2.0 GY)	50
5.1 Introduction.....	50
5.2 Materials and Methods	50
5.2.1 Sample Selection	50
5.2.2 Sample Preparation.....	52
5.2.3 Sample Irradiation	52
5.3 EPR Measurement.....	53
5.4 Spectral Processing and Statistical Analysis.....	55
5.5 Results	56
5.5.1 Variation in Dose Response	56
5.6 Discussion and Synthesis of Results	57
5.7 Conclusion.....	58
Chapter 6.....	59
CONSTRUCTION OF CALIBRATION CURVES.....	59
6.1 Introduction	59
6.2 Materials & Methods.....	59
6.2.1 Sample Selection	59
6.2.2 Sample Preparation.....	60
6.2.3 Sample Irradiation	60
6.3 EPR Sample Measurement.....	60
6.4 Spectral Processing and Statistical Analysis.....	61
6.5 Results	62
6.6 Discussion and Synthesis of Results	62
6.7 Conclusion.....	63
Chapter 7.....	65
EPR DOSE RECONSTRUCTION.....	65
7.1 Introduction	65
7.2 Materials & Methods.....	65
7.2.1 Sample Selection	65
7.2.2 Sample Preparation.....	65

7.3 EPR Sample Measurement.....	66
7.4 Spectral Processing	66
7.5 Results	66
7.5.1 Determination of Retrospective Doses	66
7.5.2 Measurement Uncertainty.....	67
7.6 Discussion and Synthesis of Results	68
7.7 Conclusion.....	69
Chapter 8.....	70
CESIUM-137 ANALYSIS	70
8.1 Introduction	70
8.2 Materials & Methods.....	70
8.2.1 Tooth Selection.....	70
8.2.2 Detector System and Software	71
8.3 Sample Measurement	71
8.4 Results	71
8.5 Discussion	73
Chapter 9.....	74
STRONTIUM-90 ANALYSIS	74
9.1 Introduction	74
9.2 Materials & Methods.....	74
9.2.1 Tooth Selection.....	74
9.2.2 The Autoradiography Method	75
9.3 Sample Measurement	75
9.4 Results	76
9.5 Discussion	77
9.6 Conclusion.....	77
Chapter 10.....	78
IMPROVEMENT OF METHODS.....	78
10.1 Introduction	78
10.2 Improvement of Methods	78
10.2.1 Samples.....	78

10.2.2 Experimental Design	79
10.2.3 Least Squares Regression Analysis	80
10.2.4. Dose Reconstruction Method Used	80
10.3 Conclusion.....	81
Chapter 11	82
SUMMARY AND CONCLUSIONS	82
11.1 Introduction	82
11.2 Characteristics of Wild Boar Tooth Enamel	82
11.3 Dose Reconstruction of Lifetime Doses to Wild Boar using EPR Dosimetry	83
11.4 Future Work	83
References.....	85
Appendix A.....	90
IACUC Exemption.....	90
Appendix B	91
Wild Boar Tooth Extraction Procedure	91
Appendix C	95
Sample Weights	95
Appendix D.....	96
EPR Signal Intensities (1.2 – 12.0 Gy).....	96
Appendix E	98
Critical Level Dose (D_{CL}) and Decision Level Dose (D_{DL}) Equations and Values.....	98
Appendix F.....	104
Deciduous versus Permanent Tooth Slope Comparison.....	104
Appendix G.....	105
Tooth Sample Preparation Procedure	105
Appendix H.....	111
Individual RIS values and Irradiation Doses: 0.25 Gy – 2.0 Gy Range	111
Appendix I	113
R Code for Tooth Slope Comparison.....	113
Appendix J	116
Results for the Linear Regression and Correlation Analysis: Chapters 4 – 6.....	116

Appendix K.....	168
EPR Spectra of samples: Chapters 4 – 6.....	168
Appendix L.....	176
Signal Intensity Versus Irradiation Dose with Linear Regression Analysis.....	176
Appendix M.....	180
Excel LINEST Results: Uncertainty in Retrospective Dose Calculations.....	180
Appendix N.....	182
Dose Reconstruction Measurement Results.....	182
Appendix O.....	183
Reconstructed Dose Confidence Interval Calculations.....	183
Appendix P.....	185
Calculation of Effective Half-Life of Air Dose Rates and Estimated Lifetime Doses.....	185
Appendix Q.....	187
¹³⁷ Cs Measurements for Combined Tooth Enamel Samples and Background Measurements...	187
Appendix R.....	212
USDA Permit for Shipment of Tooth Samples.....	212
Appendix S.....	216
⁹⁰ Sr Analysis Results.....	216

EXECUTIVE SUMMARY²

The accident that occurred at the Fukushima Daiichi Nuclear Power Plant on March 11, 2011 resulted in widespread environmental contamination and exposed numerous animal species to radioactive materials (Koarai et al., 2016). Wildlife inhabiting the Fukushima Exclusion zone are being exposed to chronic low levels of radiation as a result of the radioactive contamination which remains in the area. This event presented another unfortunate situation in which EPR dosimetry could prove useful in determining external radiation doses to exposed wildlife. Because of the significance of the Japanese wild boar within this ecosystem, continuous low dose exposures to the boar and their associated biological effects are of particular interest.

Quantification of radiation doses to wildlife is a challenge faced in radioecology studies when dosimeters are not present in a location where an unplanned exposure has occurred. In order to reconstruct absorbed radiation doses received by wildlife when dosimetry is not available, other techniques must be utilized. Electron Paramagnetic Resonance (EPR) tooth enamel dosimetry has proven to be a reliable method for performing dose reconstructions in humans, as well as in a small number of animal species. The EPR dosimetry technique has been employed using permanent teeth in adults for a number of individuals involved in radiological accidents such as the atomic bomb survivors (Ikeya, et al., 1984), individuals affected by the Chernobyl accident (Bugai et al., 1996), as well as others.

Animal teeth have not been studied as comprehensively as human teeth, however several studies have shown their effectiveness as dosimeters in retrospective dose reconstruction (Khan et al., 2003; Serezhenkov et al., 1996). In order to establish suitability of tooth enamel from

² Based on: Harshman A, Johnson T. 2018. Dose Reconstruction Using Tooth Enamel from Wild Boar Living in the Fukushima Exclusion Zone with Electron Paramagnetic Resonance Dosimetry. Health Physics Journal. Submitted.

different species for use as a dosimeter with EPR dosimetry, further studies are necessary. The goal of the present study was to establish reliability of Japanese wild boar (*Sus scrofa leucomystax*) tooth enamel for use in performing retrospective dose reconstructions with EPR dosimetry, and to ultimately reconstruct absorbed doses to wild boar inhabiting the Fukushima Exclusion Zone.

A review of prior research that has been done which investigated a variety of different animal teeth for use as EPR dosimeters is provided in Chapter 2 along with their findings and conclusions. The information contained in Chapter 2 provides a foundation for the research carried out in the present study. Chapter 3 gives specific information on samples which were obtained for this project. Samples used in this study were collected from boar living in various areas of Fukushima Prefecture, in Fukushima, Japan. Details such as estimated age of the boar, GPS coordinates and dose rates for sample collection sites, as well as sex are provided.

Chapters 4 and 5 outline the investigation of the suitability of wild boar tooth enamel as an EPR dosimeter in the range of 0.25 – 12.0 Gy. Characteristics of wild boar tooth enamel are determined including linearity and variability in dose response. Additionally, radiation sensitivity is compared between permanent and deciduous teeth, molar teeth of different ages, teeth from boar of different sex, as well as teeth from the same boar. Possible causes for differences in radiation sensitivity between different types of tooth enamel are presented.

Chapters 6 and 7 detail the steps taken to perform dose reconstructions using EPR dosimetry for wild boar inhabiting the Fukushima Exclusion Zone, which were introduced in Chapter 3. Chapter 6 gives information on the construction of the calibration curve used to reconstruct lifetime doses that are presented in Chapter 7. Lifetime dose estimates using decay

corrected air dose rates are compared with EPR reconstructed doses, and possible explanations for their differences are provided. Tooth enamel used for dose reconstructions were analyzed for the presence of radionuclides, specifically ^{137}Cs and ^{90}Sr . Different methods are used to identify the existence of these radionuclides within the samples, and results of testing are provided in Chapters 8 and 9.

A number of different techniques were used throughout this research to obtain necessary data and to meet research goals. An analysis of the methods used throughout this project and ways in which they can be improved is given in Chapter 10. Implementation of different approaches or experimental designs are expected to produce improved results in future work. Finally, Chapter 11 provides a summary of conclusions drawn during the course of this research and outlines findings that were presented in each of the previous chapters. Additional data including: tables, graphs, and figures are provided in the appendices at the end of this document. In total, the chapters in this dissertation provide the full picture of the research carried out investigating tooth enamel of Japanese wild boar for use as an EPR dosimeter.

Chapter 1

SCOPE AND PURPOSE OF THE PROJECT

1.1 Background

On March 11, 2011, a series of catastrophic events occurred, beginning with a 9.0 earthquake in the Pacific Ocean, with an epi-center located nearly 163 km from the Fukushima Daiichi Nuclear Power Plant (FDNPP) (Thielen, 2012). A resulting tsunami engulfed areas of the coast, including the site of the Fukushima Daiichi Nuclear Power Plant. Tsunami barriers at the FDNPP were overcome by waves, causing flooding of vital plant equipment, loss of heat removal systems, and loss of on-site power for an extended period of time. As a result of the prolonged loss of cooling capabilities, breaches occurred in the reactor pressure vessels as well as in primary containment vessels of Units 1-3, ultimately resulting in the release of radioactive materials into the environment (IAEA, 2015). In total, nearly 520 PBq of radioactive materials were released (Steinhauser et al., 2014), including 12 PBq of ^{137}Cs (Chino et al., 2011) and 0.02 PBq of ^{90}Sr (Steinhauser et al., 2014). Large areas of land were contaminated, the most highly contaminated of which was a 60 km area of land stretching northwest of the FDNPP (Hirose, 2012). The release of radionuclides resulted in the evacuation of tens of thousands of residents (Hasegawa et al., 2016) in the most severely impacted areas. Over time, residents were able to return to less affected areas, however some areas still remain uninhabitable, and they make up what is known as the Fukushima Exclusion Zone.

^{137}Cs and ^{90}Sr are of particular concern in the Fukushima Exclusion Zone due to their long half-lives, 30.17 years and 28.79 years respectively, and their effect on living organisms and the environment. Although the concentrations of ^{137}Cs and ^{90}Sr in the contaminated areas of

Fukushima Prefecture have decreased, these nuclides are still present today, resulting in low levels of ionizing radiation exposure to biota. Affected biota in this area which are of special interest include wild boar (*Sus scrofa leucomystax*) due to their significance in the ecosystem.



Figure 1.1 Japanese wild boar (*Sus scrofa leucomystax*). Photo courtesy of Donovan Anderson.

1.2 Motivation

It is currently recognized that there is a need to understand and determine the interrelation between exposure to animals, the resulting dose, and ultimately the effects and risks associated with the doses received when animals are exposed to radiation in the environment.

Understanding this interrelation will assist in the effort to preserve and protect species, and to ensure sufficient biological diversity within ecosystems (ICRP, 2007), as well as providing more confidence when using animals as surrogates to better understand radiation effects on humans. It is therefore necessary to have a sufficient amount of information which can be used to give

sound advice and determine appropriate actions when protection of animals and the environment is the goal.

One of the most significant issues for radioecology studies is the ability to quantify radiation dose to wildlife, and to have accurate data on which to base predictions of radiation effects (ICRP, 2008; UNSCEAR, 1996). There is a large body of scientific data documenting the deleterious effects of acute high doses in humans (Grant et al., 2017) as well as plants and animals (UNSCEAR, 1996), however much less is known regarding the effects of chronic low doses to wildlife (Moller and Mousseau 2006). Current results for in-vivo animal models have concluded that the deleterious effects of radiation are suppressed as the dose rate is decreased (Olipitz et al., 2012). Although the radiation risks are expected to be lower for lower dose rates, more extensive data are crucial for determining true risk factors and dose-effect relationships for low dose exposures (Brenner et al., 2003). Developing a method for more rigorously assessing radiation dose will serve to reduce the uncertainties that currently exist in the establishment of risk factors as well as in determining the lowest dose for which biological effects can be seen (Brenner et al., 2003).

Research has shown that after an event, dose rates and contamination levels are not sufficient to determine the amount of absorbed radiation dose that has been received in exposed populations (IAEA, 2002). If the goal of preserving and protecting animal species is to be met, it is necessary that a process be established in which the dose to an animal can ultimately be linked to corresponding risks and effects of the radiation dose. It is especially important to determine an accurate lifetime dose when investigating radiation effects in animals so that when detectable effects manifest, they can be correlated to a particular radiation dose.

The ability to perform retrospective dose reconstruction after a nuclear accident, or an incident involving the release of radioactive materials, is dependent upon having a suitable dosimeter present at the time of the exposure. Electron Paramagnetic Resonance (EPR) dosimetry (also known as Electron Spin Resonance or ESR) is one method which can be used to quantify absorbed doses.

Electron Spin Resonance (ESR) dosimetry, utilizing teeth as dosimeters, has been shown to be an effective method for determining absorbed dose in humans, using primarily adult permanent teeth, for a number of historical radiological accidents, as summarized by IAEA (2002) and Fattibene and Callens (2010). The potential for use of animal teeth as dosimeters using ESR has also been investigated in studies such as those by Khan et al. (2003), Serezhnikov et al. (1996), Klevezal et al. (1999), and Toyoda et al. (2003). More research is needed to confirm the appropriateness of teeth from different animal species and their ability to provide reliable measurements of absorbed doses in wildlife. (Harshman et al., 2018)

1.3 Project Goals

1.3.1 Research Objectives

The first goal of this project was to determine the suitability of teeth of Japanese wild boar for use as a dosimeter in performing retrospective dose reconstructions with EPR dosimetry. The suitability of a tooth for EPR dosimetry can be determined in part through investigation of the response of tooth enamel to gamma radiation. The following characteristics of wild boar tooth enamel were evaluated:

- the degree of linearity in dose response of teeth irradiated to different known doses ranging between 0.25 Gy – 12.0 Gy,

- the extent of variability in dose response between deciduous and permanent teeth, teeth taken from opposite sides of the mouth of the same boar, as well as molar teeth extracted from wild boar of different ages and of different sex, and
- the characteristic g-values of the radiation induced signal and native signal

Through investigation of these aspects, suitability of tooth enamel of Japanese wild boar for use in measuring radiation dose using EPR was determined.

Ultimately, the goal of this research was to use EPR dosimetry to determine the cumulative lifetime doses received by Japanese wild boar residing in the area of interest. Results from the investigation of the suitability of wild boar tooth enamel for use as an EPR dosimeter helped to determine the most suitable dose reconstruction method. Finally, characteristic information about the boar tooth enamel was used to establish uncertainty values for reconstructed dose estimates.

1.3.2 Supporting Objectives

1. A minimally destructive technique for extracting teeth from Japanese wild boar with the assistance of a veterinary dentist was devised.
2. A preparation procedure for animal tooth samples based on guidance from the IAEA, review of previous studies conducted using EPR dosimetry and animal teeth, as well as through collaboration with EPR experts was developed.
3. A procedure for analysis of the EPR spectrum using ESR Dosimetry software to reconstruct doses received by boar was created.

Methods developed and utilized for sample collection, preparation, and EPR analysis of teeth from Japanese wild boar inhabiting the contaminated areas of the Fukushima Exclusion Zone assisted in achieving the desired goals. Procedures were developed for future use and will

allow for more reliable and reproducible results. This research will serve to increase the knowledge that currently exists with respect to low level chronic exposures to wild boar.

1.4 Significance of the Study

Currently, there are limited data from a small number of studies that have been performed regarding the dose response of teeth of different animal species for retrospective dose reconstruction. This study will increase knowledge in regard to what is currently known about the suitability of animal teeth for use as a dosimeter. Moreover, the methods developed in the course of this research project for preparation and analysis of boar tooth enamel could potentially be used to estimate the cumulative dose to biota (Khan et al., 2003) living in the Fukushima Exclusion Zone and elsewhere. A tested and validated method to establish lifetime doses in Japanese wild boar can be used to provide additional knowledge with respect to low level chronic exposures to wildlife and their associated biological effects. As a result, more reliable and accurate extrapolations regarding dose-effect relationships can be made.

The International Commission on Radiological Protection (ICRP) has developed a model using the concept of Reference Animals, which represents typical organisms in a given environment along with associated data. The ICRP model was developed with the goal of creating a structure and framework for gaining a deeper insight into how exposure, and ultimately the risks and consequences of the exposure are related (ICRP, 2008). The methods and techniques developed during the course of this research can assist in collecting the necessary data needed to add to this relevant data set. A tested and validated technique used to determine doses received by wildlife using EPR dosimetry could help to reduce uncertainty and fill current knowledge gaps and to strengthen and bolster current models utilizing reference animals.

Chapter 2

HISTORY AND BACKGROUND OF ELECTRON PARAMAGNETIC RESONANCE DOSIMETRY³

2.1 Electron Paramagnetic Resonance Dosimetry

2.1.1 Theory

Electron Paramagnetic Resonance tooth enamel dosimetry is based on quantifying the relative abundance of radiation-induced radicals trapped in hydroxyapatite crystals ($\text{Ca}_{10}(\text{PO}_4)_6(\text{OH})_2$) within calcium components of teeth. Hydroxyapatite crystals in tooth enamel contain carbonate impurities, which are transformed into trapped stable CO_2^- radicals as a result of radiation exposure (IAEA, 2002). The CO_2^- radicals in enamel increase as a function of the absorbed dose (Dansoreanu and Fildan 2009). The CO_2^- radicals can be reliably detected, quantified, and related to an absorbed dose using the EPR dosimetry technique. Ideal materials for use in EPR dosimetry are materials that are highly mineralized with a significant calcium content (IAEA, 2002).

In EPR spectroscopy, a varying magnetic field is applied to a tooth sample with a fixed frequency. This is different from traditional spectroscopy where the frequency used varies. An unpaired electron only has two possible energy states, $+\frac{1}{2}$ or $-\frac{1}{2}$, and when applied, the energy states are proportionally split in the magnetic field (Fattibene and Callens 2010). The spins are either parallel or anti-parallel with the direction of the magnetic field, with the lower energy state being parallel to the direction of the magnetic field, and the higher energy state being anti-

³This chapter is based on a non-final version of an article published in final form: Harshman Amber, Johnson, Thomas. A Brief Review- EPR Dosimetry and the Use of Animal Teeth as Dosimeters. *Health Physics Journal* 115(5): 600-607; 2018. <https://journals.lww.com/health-physics/pages/default.aspx>

parallel (Eaton et al., 2010). The EPR spectrum is created when resonance absorption occurs, which is at the point when the applied microwave energy equals the energy difference between the two electron energy states.

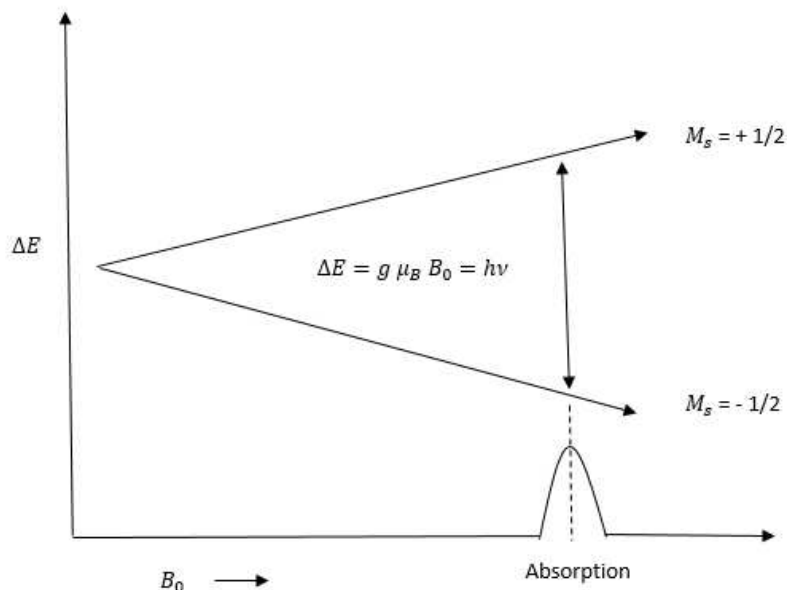


Fig. 2.1 The divergence of the energy levels for the spin $-1/2$ and spin $+1/2$ states for an unpaired electron and its dependence on magnetic field strength.

The energy difference between the $+\frac{1}{2}$ and $-\frac{1}{2}$ spin states, ΔE , is determined by the g -value, g , the Bohr magneton, μ_B , and the applied magnetic field, B_0 . As shown in equation 2.1 describing the condition for resonance, there is a linear relationship between the resonance frequency, ν , and the applied magnetic field, B_0 (Eaton et al., 2010).

$$h\nu = g\mu_B B_0 = \Delta E \quad (2.1)$$

2.1.2 EPR Measurements

There are several steps that must be taken in order to turn a whole tooth into a pure powder enamel sample suitable for EPR analysis, and those steps are discussed in detail in Chapters 4 and 5. Once the powder sample has been prepared, it is put into an EPR tube and

placed into the EPR spectrometer resonant cavity. The appropriate parameters for the sample being measured are selected, measurements are performed, and a spectrum is obtained.

Measurements are typically repeated 3-5 times and averaged, and the sample is removed and either shaken or rotated between measurements (IAEA, 2002).

2.1.3 Measurement Parameters

Based on current research, the parameters used to perform EPR analysis on animal teeth vary somewhat from study to study. Furthermore, some of the parameters necessary for analysis are spectrometer specific while others are sample specific. Spectrometer dependent parameters include: microwave frequency, microwave power, and modulation frequency. Table 2.1 provides a summary of studies conducted utilizing animal teeth and parameters used.

The parameters that need to be selected in order to produce the desired EPR spectrum include: microwave, magnetic field, and signal channel parameters. Parameters should be optimized to get the most precise results (IAEA, 2002). Other factors which influence results and thus need to be considered are: sweep width, modulation amplitude, time constant, and number of scans.

2.1.3.1 Microwave Parameters

The frequency of the resonant cavity in an EPR spectrometer is termed the microwave frequency, and the characteristics of the cavity will determine this parameter. The most common microwave frequency used in EPR analysis of teeth is X band (~9.8 GHz). All of the studies included in this chapter were performed using X-band EPR dosimetry.

Microwave Power is an important parameter in that the selected value will impact the dosimetric signal to native signal ratio, as well as the ratio of dosimetric signal to noise (IAEA, 2002). This is because the dosimetric signal as well as the native signal increase with increasing

Table 2.1. Summary of parameters used in EPR Dosimetry studies using animal teeth. *Data not available. ^a (IAEA, 2002), ^b (Zdravkova et al., 2005), ^c (Brik et al., 2000), ^d (Khan et al., 2003), ^e (Toyoda et al., 2003), ^f (Hassan et al., 2010), ^g (Toyoda et al., 2006), ^h (Toyoda et al., 2007), ⁱ (Jiao et al., 2014), ^j (Hayes et al., 1998), ^k (Khan et al., 2005), ^l (Dansoreanu and Fildan 2009), ^m (Junwang et al., 2014)

Animal Studied	Magnetic Field Parameters		Microwave Parameters		Signal Channel Parameters			
	Sweep Width	Time of Sweep	Microwave Frequency	Power	Modulation Frequency	Modulation Amplitude	Time Constant	Number of Scans
Humans ^a	5 or 10 mT	20-80 s	9.8 GHz (X-band)	1-25 mW	50 or 100 kHz	0.1-0.4 mT	40 -700 ms	10-160
Rat ^b	5 mT	*	9.7 GHz (X-band)	5 mW	100 kHz	0.34 mT	10.24 ms	20
Rat ^c	*	*	X-band	80 mW	100 kHz	0.1 mT	*	*
Mouse ^d	5 mT	30s	9.4 GHz (X-band)	18 mW	100 kHz	0.5 mT	30 ms	40
Cow/Mouse ^e	10 mT	60 s	*	5 mW	100 kHz	0.2 mT	*	30
Cow ^f	10 mT	82s	9.7 GHz (X-band)	25 mW	100 kHz	0.4 mT	20 ms	10
Cow ^g	*	60 s	*	5 mW	100 kHz	0.3 mT	30 ms	40
Cow ^h	10 mT	60 s	*	10 mW	100 kHz	0.2 mT	30 ms	40
Cow/Goat ⁱ	10 mT	166.9 s	X-band	2 mW	100 kHz	0.3 mT	163 ms	10
Pacific Walrus ^j	10 mT	*	*	25 mW	100 kHz	0.5 mT	41 ms	60
Canine ^k	5 mT	*	9.4 GHz (X-band)	18 mW	100 kHz	0.5 mT	30 ms	40
Pig ^l	130 mT	*	9.1 GHz (X-band)	8.5 mW	100 kHz	0.3 mT	100 ms	30
Rhesus Monkey ^m	10 mT	20-300 s	9.5 GHz (X-band)	20 mW	*	0.2 mT	30-100 ms	*

microwave power, however the native signal will reach its saturation point first (Fattibene and Callens 2010). Additionally, the signals which are considered noise also increase as the microwave power is increased, thus interfering with the spectrum of the dosimetric signal (Fattibene and Callens 2010). This parameter is dependent on the resonant cavity and not on the sample being analyzed.

2.1.3.2 Magnetic Field Parameters

The choice of magnetic field sweep width will depend on the procedure used for spectrum manipulation (IAEA, 2002). Values of 5 mT or 10 mT are commonly used. Magnetic field sweep time is determined by the spectrum resolution, or the total channels used to obtain the spectrum, and the channel conversion time (IAEA, 2002). It is also dependent on the sample being analyzed (Eaton et al., 2010).

2.1.3.3 Signal Channel Parameters

In order to attain the optimal signal-to-noise ratio, the magnetic field modulation frequency should be set to the upper limit (IAEA, 2002). In general, modulation frequencies of 50 kHz or 100 kHz are used in commercial EPR spectrometers (IAEA, 2002). As seen in Table 2.1, a modulation frequency of 100 kHz was used in all animal studies listed.

Modulation Amplitude is selected such that the signal resolution is optimized and broadening or distortion of the dosimetric signal is minimized. If a modulation amplitude is selected that is too high, it will result in signal distortion and loss of resolution, and if the value is too low, it will result in a decline in detection limits (Fattibene and Callens 2010; IAEA 2002). Values in the range of 0.1-0.4 mT are recommended. (IAEA, 2002)

The number of scans selected is important in that it will impact the signal-to-noise ratio. If a number of scans n is selected, it will produce an improvement of the signal-to-noise ratio of

\sqrt{n} (Eaton et al., 2010). The number of scans used in EPR animal studies listed in Table 2.1 range from 10-60.

2.1.4 EPR Spectra

In EPR spectroscopy, unlike most other types of spectroscopy, due to the nature of the system used, the first derivative of the absorption curve (dy/dB) is what is actually detected and not the actual absorption curve itself (Fattibene and Callens 2010). The first derivative of the absorption curve is what makes up the EPR signal or spectrum.

There are several useful and important characteristics of the EPR spectrum, which include peak-to-peak amplitude and g-value, amongst others (IAEA, 2002). In EPR dosimetry, radiation sensitivity is related to the peak-to-peak amplitude of the radiation induced signal, which is proportional to the number of radicals trapped in pure enamel, per unit mass and dose (Khan et al., 2005). Both the number of radicals created in human tooth enamel and the intensity of the EPR spectrum increase with absorbed dose (IAEA, 2002). The relation between peak-to-peak signal amplitude and concentration of spins is the basis of EPR dosimetry. The g-value is characteristic for the material, and for electrons having spin $\frac{1}{2}$, the value is approximately equal to 2 (IAEA, 2002). The characteristic parameters will be determined by the type of free radicals being measured (IAEA, 2002).

The main components of the EPR signal are the native signal (NS) and the radiation induced signal (RIS). The native signal conceals the RIS somewhat due to the similarities in their intensities as well as their g-values, making it more difficult to measure the peak-to-peak signal amplitude of the RIS (Fattibene and Callens 2010). The native signal, sometimes called the “radiation-insensitive component,” is believed to be a consequence of radicals stemming from

organic material, such as dentin that remains in the tooth, although its origin hasn't been fully determined (Fattibene and Callens 2010).

Several different types of radicals contribute to the dosimetric signal, which are mostly carbonate radicals, however stable CO_2^- radicals are the main contributor (IAEA, 2002). The contribution to the dosimetric signal from ionizing radiation can be either from external sources or internal sources such as radionuclides embedded in the teeth, gums, or mandible of the animal. The EPR signal from exposure to different types of radiation is virtually indistinguishable such as gamma-rays, beta particles, as well as alpha particles (IAEA, 2002). Fig. 2.2a shows a basic EPR signal. Fig. 2.2b shows an idealized spectrum including a radiation induced signal (RIS).

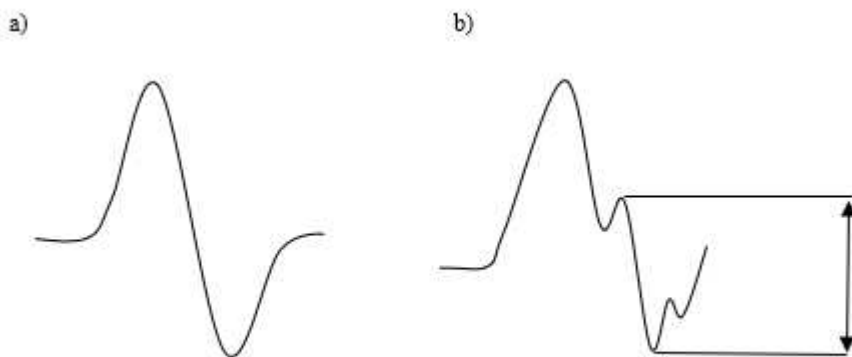


Fig. 2.2. a) EPR spectra are displayed as the first derivative of the resonant absorption curve. b) Idealized EPR spectrum showing a radiation induced signal (RIS). The peak-to-peak amplitude of the RIS is used to perform EPR dose reconstructions.

2.1.5 Methods Used for Dose Reconstruction

Two primary methods used in reconstructing doses with EPR dosimetry after the EPR spectrum is obtained are the calibration curve method and the additive dose method. Both require a least-square fitting linear regression analysis, and both methods rely on a linear dose

response of the tooth enamel sample (IAEA, 2002). With the calibration curve method, powder enamel samples consisting of a mixture from a minimum of 5 different molars are used and irradiated to a series of four or more additional known doses (IAEA, 2002). A plot of signal intensity and irradiation dose is created and a least-square fitting linear regression is performed to determine the calibration curve parameters. The dose axis intercept corresponding with the RIS intensity of the sample is the intrinsic reconstructed dose once the background dose has been subtracted (IAEA, 2002). The calibration curve method is often used for samples with a small to moderate variation in dose response.

The additive dose method, or individual sample calibration, is often used for samples that have a significant variation in dose response. With the additive dose method, a sample from a specific tooth is measured and then irradiated incrementally to typically at least 14 different additional doses (IAEA, 2002). Linear regression analysis is performed using the plot of signal intensity versus irradiation dose. The dose is reconstructed using the linear regression line and its negative intercept with the dose axis (IAEA, 2002). Definitive evidence supporting the use of one method over another has not been found (Fattibene and Callens 2010). Studies have shown, however, the importance of the acquisition and spectrum processing methods on both the reproducibility and accuracy of results (Fattibene and Callens 2010).

2.1.6 EPR Spectrometers

Two different EPR spectrometers were used to perform measurements for this research. The first was a JEOL JES-PX2300 ESR Spectrometer, located in Okayama, Japan, at the Okayama University of Science as shown in Fig. 2.3. The second spectrometer used to perform measurements in this study was a Bruker ELEXSYS II E 500 ESR Spectrometer, located at Colorado State University, shown in Fig. 2.4.



Fig. 2.3. JEOL JES-PX2300 ESR Spectrometer.

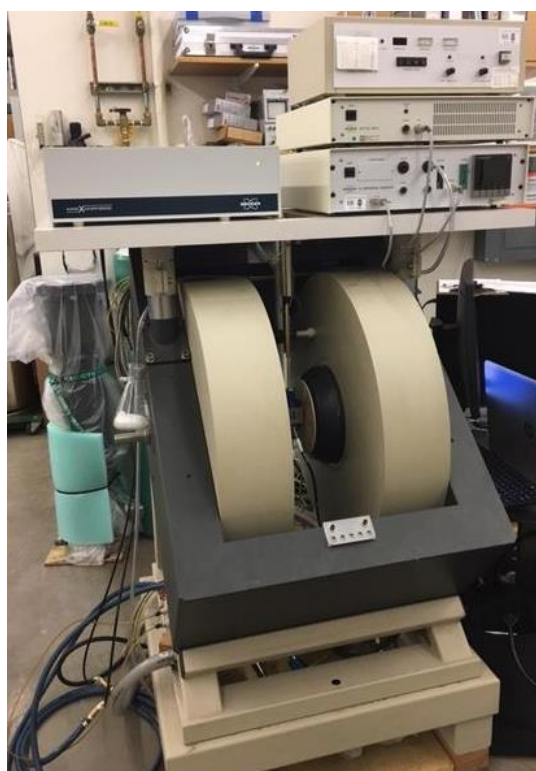


Fig. 2.4. Bruker ELEXSYS II E 500 ESR Spectrometer.

Although there may be small differences between EPR spectrometers used, each is made up of similar components necessary to obtain an EPR spectrum. An EPR spectrometer consists of the following main components: an electromagnet, a microwave generator, a resonant cavity, detectors, and the signal channel. A basic diagram of the system is shown below in Fig. 2.5.

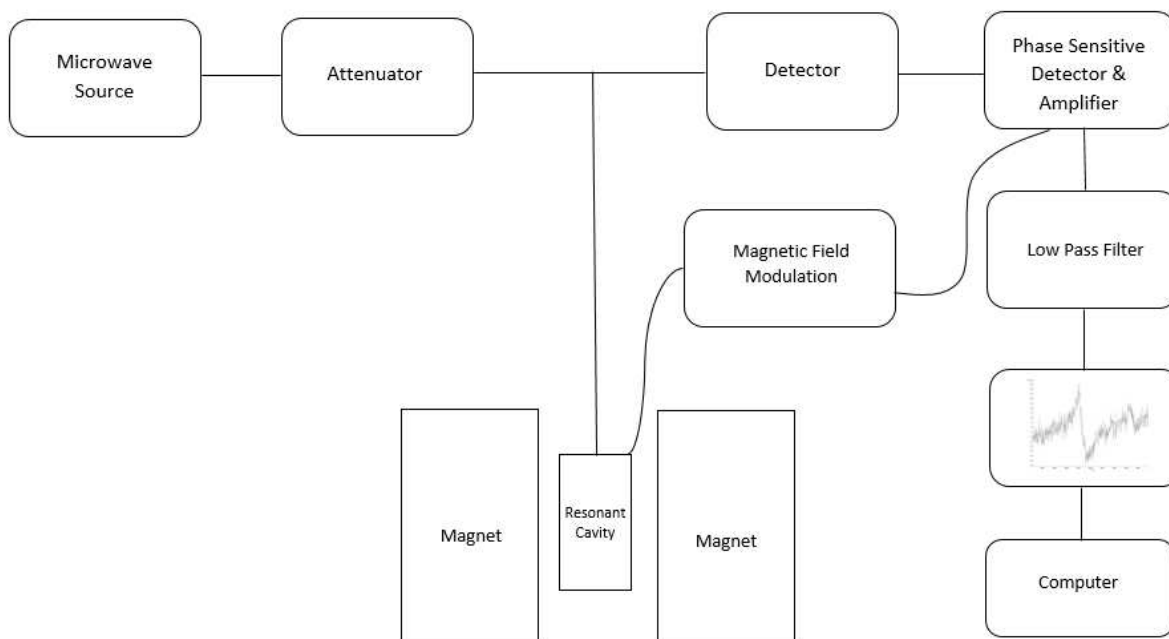


Fig. 2.5. Typical EPR spectrometer setup.

Further information on the function and purpose of each component of an EPR spectrometer can be found in Eaton et al. (2010).

2.2. The Origins and Uses of EPR

EPR dosimetry using human teeth was first developed nearly five decades ago (Brady et al., 1968). In addition to EPR studies using tooth enamel, EPR has been investigated as a dosimetric technique using a wide range of materials including: human blood (Swartz et al., 1965), bone (Swartz, 1965; Ikeya et al., 1996), antlers of deer (Huang et al., 1985), shell buttons (Ikeya et al., 1984), and egg shells (Kai et al., 1988). Materials such as fingernails, toenails (Gordy et al., 1955; Symons et al., 1995), as well as hair (Gordy et al., 1955) have also been

studied. Biological materials originating from animals which have been investigated include: incisors and tissues of rats (Brady et al., 1968), fish scales, feathers, and hides of cattle (Gordy et al., 1955), canine heart, lung, and liver (Swartz and Molenda 1965), and femurs of rats (Swartz, 1965).

EPR dosimetry is the preferred method for retrospective human dose reconstruction (Wieser et al., 2000), and the technique has been used in a variety of scenarios, accident situations, and for dosimetry in research experiments for doses administered in laboratory settings. Dose reconstructions utilizing EPR spectroscopy have been performed for groups such as: the atomic bomb survivors of Hiroshima and Nagasaki (Ikeya et al., 1984), residents of the affected areas of Chernobyl (Bugai et al., 1996), survivors of accidents that occurred in the Southern Ural region of the Soviet Union (Wieser et al., 1996), and also for radiation workers (Romanyukha et al., 1994). Although human teeth have been the focus of a significant proportion of studies conducted using EPR dosimetry, research has also been devoted to understanding the characteristics of the teeth of wildlife and their suitability as a dosimeter or to reconstruct doses in accident situations, such as in the case of Chernobyl (Bugai et al., 1996).

There are important advantages to using EPR dosimetry which make it the preferred technique in retrospective dose reconstructions. First, materials in the vicinity of an event can be analyzed for potential use as a dosimeter. Furthermore, specimens such as teeth can be used to provide an individual dose to an exposed person (Toyoda et al., 2003; Khan et al., 2003). Because of the stability of the EPR signal in enamel, dose reconstructions can be performed long after the exposure occurs (IAEA, 2002).

There are also conditions which must be met in order to establish the validity of EPR dosimetry. Although there are many different types of materials that can be used to perform

retrospective dose reconstructions, the dose response of each of these materials must be known in order to estimate an absorbed dose. Additionally, the exposure timeline for the material must also be known in order to accurately assess the dose. Additional uncertainties in the final EPR results can occur as a result of processing techniques used to prepare samples for analysis. Small absorbed doses are difficult to measure with EPR, and the type and energy of radiation add additional uncertainty to the results using EPR dosimetry (IAEA, 2002).

2.3 Teeth as Radiation Dosimeters

As previously discussed, enamel and its large proportion of inorganic material is the preferred substance on which to perform EPR spectroscopy. Molars and premolars are the most useful for EPR dosimetry due to their mineralization and the limited UV radiation impact from sunlight exposure due to their position (IAEA, 2002). Only healthy teeth are used in EPR dosimetry since studies have shown that cavities, fillings, and chemical treatments can affect the results (IAEA, 2002).

There are advantages to using teeth as dosimeters compared to other materials that have been studied. First, teeth have been found to have a dose response that is linear for exposures that range up to 300 Gy. Secondly, there is little fading of the radiation induced signals, and the radicals are estimated to be stable in humans up to 10^7 years (IAEA, 2002). A considerable number of studies have been performed on EPR dosimetry and human teeth, although a much smaller number of studies have focused on animal teeth and their use as dosimeters for the purpose of retrospective dose reconstruction.

2.4 Tooth Characteristics & EPR

Teeth are made up of four major constituents: enamel, dentin, cementum, and pulp. For the purposes of EPR dosimetry, the enamel and dentin, and their relative fractions, are the two most important components. A diagram of the human tooth can be seen in Fig. 2.6 below.

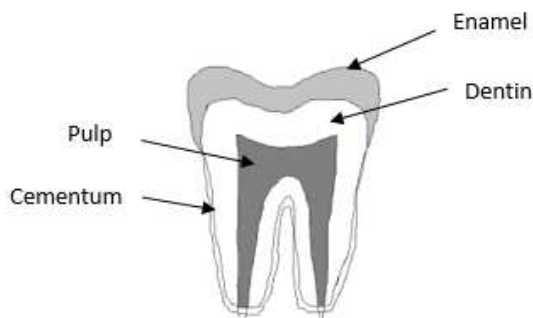


Fig. 2.6. Constituents that make up the anatomy of the tooth.

There are two different types of teeth in mammals, brachydont and hypsodont. Human teeth, as well as the teeth of many animals that are carnivores and omnivores, such as Japanese wild boar, are classified as brachydont. Hypsodont teeth are found primarily in herbivores, and unlike brachydont teeth, these teeth are constantly growing and regenerating during the lifetime of the animal due to the composition of the tooth and the constant wear on it (Fattibene and Callens 2010). For this reason, brachydont teeth are more suitable for EPR dosimetry. The amount of enamel and dentin in a tooth varies from species to species and differs from what is contained in a human tooth. Although it is possible to gather information regarding dose using the dentin in the tooth, the enamel is more desirable for a few reasons. First, enamel is the tissue with the largest amount of mineralization, consisting of almost entirely inorganic material, in this case hydroxyapatite crystals (IAEA, 2002).

Tooth enamel is very stable in humans, although it can vary in animal teeth. In human teeth, once the tooth is formed, the amount of enamel does not change, and as a result, the number of radicals that have formed is retained. (IAEA, 2002). As described above, this is not

always the case in animals, and the structure of the teeth of some animals is constantly changing throughout their lifespan (Khan et al., 2003). An understanding of how the tooth of the particular animal that is being studied is formed throughout its life and the time period when the radiation interaction occurs is useful in determining an accurate dose.

2.5 Summary of Studies

The following section provides a summary of the studies which have investigated animal teeth for use as dosimeters with EPR dosimetry and their findings.

2.5.1 Canines

Canines (dogs) are popular domestic pets in many parts of the world. Further, canines inhabit many of the same areas as humans, and in the event of a radiation accident, would be exposed to many of the same hazards. The motivation for wanting to formulate an EPR procedure for analyzing the teeth of canines and to understand their radiation sensitivity compared to human teeth is to have the ability to use them for the purposes of retrospective dose reconstruction (Khan et al., 2005). Furthermore, reconstructed doses could give an indication of the dose to the environment in addition to the accidental dose to the canine (Khan et al., 2005). A procedure was developed by Khan et al for canine tooth analysis which included: methods for chemical processing, evaluation of the dosimetric signal, and EPR dose reconstruction techniques. Additionally, signal intensity variability versus age of the tooth specimen was explored.

Canine teeth were found to have an average radiation sensitivity of 1399 ± 93 (Gy-100 mg)⁻¹ which is similar to the average value of 1664.42 ± 49.30 (Gy-100 mg)⁻¹ for human teeth. Additionally, comparisons of the g-value and EPR spectrum from canine and human teeth showed that the radicals trapped in canine teeth after irradiation are the same as those trapped in

human teeth. It was noted that a 10-25% deviation was seen from the average value of the dosimetric signal in the canine specimens (Khan et al., 2005). A linear dose response in canine tooth enamel is present from 200 mGy up to 50 Gy. The study also concluded that canine tooth enamel was sufficiently similar to that of humans for use in retrospective dose reconstructions using EPR dosimetry. (Khan et al., 2005)

2.5.2 Bovines

Cattle are the most widely studied mammalian species with regard to EPR dosimetry. Much of the research performed using bovine teeth was done in order to determine the dose response and native enamel signal relative to that of human teeth. Cattle are of particular interest because they live in close proximity to humans and are therefore likely to receive similar doses (Hassan et al., 2010; Toyoda et al., 2003; Toyoda et al., 2007). Additionally, the anatomy and chemical structure of bovine teeth are similar to that of humans (Toyoda et al., 2006). A primary goal for establishing radiation sensitivity of bovine teeth relative to human teeth is to use them as an alternative measure of radiation exposure when human teeth are not available or cannot be easily obtained.

Some disparities were found during investigation of bovine teeth that make comparison to human teeth more challenging. Samples taken from cows exposed to ^{90}Sr in the South Ural region of Russia had a variation greater than a factor of 10 in radiation sensitivity and dosimetric signal (Toyoda et al., 2007). This variation is not seen in human teeth, nor was it seen in the control teeth analyzed from cows inhabiting Japan. There is currently no explanation for this anomaly, but it has been suggested that the nature of the hydroxyapatite crystals and their organic components could be the source of the discrepancy (Toyoda et al., 2007). Furthermore, the native signal in bovine tooth samples was found to be lower than that of human tooth

samples. This is believed to be due to the differences in organic material and thus the organic radical content in the bovine tooth samples (Toyoda et al., 2006), and could also be due to the choice of chemical or mechanical methods used when preparing the tooth sample for analysis (Jiao et al., 2014).

Numerous studies demonstrate that bovine teeth are a suitable alternative to human teeth when used for EPR dose reconstruction based on radiation sensitivity and dose response, with bovine teeth being 10% more sensitive than human teeth (Hassan et al., 2010; Jiao et al., 2014; Toyoda et al., 2003). Additionally, cow teeth were estimated to have a signal stability of approximately 7×10^6 years, comparable to that of human teeth, at nearly 1.1×10^7 years (Hassan et al., 2010). The dose response of bovine tooth enamel was found to be linear at doses from 0.2 to 2 Gy (Hassan et al., 2010; Toyoda et al., 2003). Reconstructed doses as low as 29 mGy were achieved with human teeth, and due to their similarities, it is believed that a similar threshold would apply to bovine teeth as well (Toyoda et al., 2003).

2.5.3 Goats

Only one study has been performed which analyzed teeth taken from goats, and the goal of the study was to compare the dose response and native signal of goat and cattle teeth with that of humans (Jiao et al., 2014). Goats typically live in close proximity to humans, and much like cows, they are seen as a reasonable alternative to human teeth when dose reconstruction using EPR dosimetry is necessary. The native signal in the samples taken from goat teeth was lower than that of human teeth (Jiao et al., 2014). Additionally, the radiation sensitivity of goat teeth was found to be much the same as in human teeth. These findings led the study to conclude that goat teeth could be used as a surrogate for human teeth to determine exposures using EPR analysis, although more research is needed to confirm their results (Jiao et al., 2014).

2.5.4 Mice

There are several reasons why studying mice for the purpose of reconstructing doses using EPR dosimetry is of particular interest. Rats, dogs, cows, and mice live in close proximity to humans and are typically present in areas where there have been radiation events or accidental exposures (Khan et al., 2003). There are also situations in which there are no human victims, but doses to the environment are needed (Khan et al., 2003; Toyoda et al., 2003). The objectives of the studies that were undertaken using mice were to: determine the appropriate EPR techniques utilizing the tooth enamel of mice, to compare the radiation sensitivity of mouse teeth to that of humans with the goal of determining if they are a suitable substitute for the purpose of retrospective dose reconstruction in an accident situation, to have the ability to determine a dose to animals used in radiobiology studies, as well as to determine doses to the environment (Khan et al., 2003; Toyoda et al., 2003).

Mouse teeth present a different set of issues related to EPR dosimetry. A sufficient amount of tooth enamel is required in order to perform EPR analysis (20-100 mg), and a single mouse tooth does not provide the necessary sample mass. It is therefore necessary to use multiple molar teeth from several mice in a single aliquot (Toyoda et al., 2003). When multiple specimens are combined, EPR analysis will produce a dose that is representative of the mean dose to the teeth used to make up the sample. Furthermore, mice, as well as other rodents, have a short lifespan, which limits the available time in which a specimen must be collected and analyzed (Khan et al., 2003). Additional time constraints on the usefulness of mouse teeth may exist when the turnover time of the tooth is considered (Khan et al., 2003). All of these factors could restrict their use.

Mouse tooth specimens responded linearly to doses ranging from 0.8 to 5.5 Gy, and the EPR analysis revealed doses that matched closely with administered doses (Khan et al., 2003). In one study, a slight variation in the reconstructed dose versus the administered dose was seen. This was possibly due to the time that lapsed between irradiation and EPR analysis of the sample, which was 2.5 weeks, or the chemical treatments used (Toyoda et al., 2003). Furthermore, the EPR dose response characteristics of mouse tooth samples were similar to that of humans, although it was lower by approximately 25-50% (Khan et al., 2003). Possible origins for the discrepancy include the age or sex of the specimen (Toyoda et al., 2003). The similarity in dose response implies the ability to use data determined using mouse tooth specimens for estimating dose to humans found in the same area (Khan et al., 2003).

2.5.5 Pacific Walrus

The study which investigated walrus teeth was performed as a result of the discovery that radioactive waste had been dumped into the Arctic Ocean by the former Soviet Union. The goal of the study was to determine the feasibility of using walrus teeth as an EPR dosimeter to assess the extent of unintentional exposures to marine wildlife and the ecosystem inhabiting the Arctic Ocean, as well as to humans (Hayes et al., 1998). Due to the morphological features of the walrus tooth, such as the ability to determine its age due to growth rings consisting of cementum, as well as the ability to separate those layers and measure them individually, their use was considered advantageous for this purpose (Hayes et al., 1998).

Numerous properties of the EPR response of walrus teeth were investigated for the purpose of dose reconstruction. The EPR dose response of the tooth samples was found to be linear up to $6.6 \text{ kGy} \pm 0.6 \text{ kGy}$. The response for microwave power saturation using the walrus tooth specimens was found to be the same as that in the human specimens. Additionally, the g-

value of the native signal for the walrus cementum sample was found to be the same as that of dentin and enamel of human teeth (Hayes et al., 1998). The native signal was successfully removed using a Soxhlet extraction technique; however, this method resulted in a factor of 10 reduction in the dosimetric signal. The lowest dose measurement achievable was concluded to be 350 mGy, and that was on the condition that the native signal of the sample and the LET of the incident radiation was known prior to analysis. Based on the findings of this investigation, it was concluded that dose reconstructions using EPR dosimetry for low level exposures utilizing the teeth from walrus was not achievable at that time (Hayes et al., 1998).

2.5.6 Pigs

An EPR technique related to measuring radiation doses utilizing porcine molars was investigated by a dentistry radiology group. The aim of the study was to develop a methodology for performing dose evaluations and profiling the X-ray radiation dose to teeth during experimental diagnostic or therapeutic procedures. Because humans cannot be used in these situations, porcine teeth were selected due to the similarities in physiology between pigs and humans in development of the jaw and face region as well as in the occurrence of injury and disease (Dansoreanu and Fildan 2009). The radiation dose absorbed by the lingual enamel was found to be only 45% of the dose to the vestibular or buccal side of the tooth from dental x-rays (Dansoreanu and Fildan 2009), and relative doses based on the position of the X-ray beam in relation to the tooth were able to be determined (Dansoreanu and Fildan 2009). It was concluded that due to the similarities in both anatomy as well as native and dosimetric signal characteristics between humans and pigs, this methodology was sufficient to perform reconstructions of radiation doses resulting from diagnostic X-rays in humans.

2.5.7 Rats

One of the earliest studies to have been performed using the teeth of animals investigated rat incisors and their characteristics related to EPR dosimetry (Brady et al., 1968). This study showed that rat incisors have a linear dose response in the range of 9 – 270 Gy, and doses as low as 1 Gy could reliably be measured (Brady et al., 1968). It was concluded that rat incisors could be used to perform dose reconstructions in situations involving accidental exposures.

Several subsequent studies have been performed utilizing the teeth of rats, each with goals rather different from the studies already discussed. One study investigated the consequences of tooth disease and metabolic processes on EPR dosimetry and the ability to accurately reconstruct dose (Brik et al., 2000). It was shown that CO_2^- radicals and the number of CO_2^- molecules in enamel is significantly impacted by metabolic processes (Brik et al., 2000). Additionally, teeth affected by caries will experience a greater rate of change in the quality of the tooth enamel (Brik et al., 2000). This study concluded that as a result of metabolic processes, when the same radiation doses are delivered, a different number of CO_2^- radicals are created depending on whether the animal is alive or dead when exposed (Brik et al., 2000).

A subsequent study was conducted in 2005 by Zdravkova et.al, which attempted to verify the results of Brik et al., which was able to confirm that teeth which were removed and irradiated had a greater signal intensity than teeth analyzed from live irradiated rats, although there were large standard deviations noted for much of the data collected (Zdravkova et al., 2005).

2.5.8 Reindeer

Although the origin of the doses reconstructed using EPR dosimetry are chiefly external gamma radiation, internal alpha and beta emitting radionuclides integrated into bone tissue or fixed in the enamel of the teeth can also contribute to the dose accumulated (Klevezal et al.,

1999). Depending on the phase of tooth formation and the quantities ingested, a significant radionuclide content in the enamel of the tooth can result (Klevezal et al., 1999). Klevezal et al. attempted to determine to what extent the radionuclides present in teeth and bone contributed to the overall dose established using EPR dosimetry. Analysis was performed using enamel taken from the molars of 77 reindeer of differing ages, living in areas with varying levels of contamination, specifically Novaya Zemlya, Taimyr and Wrangel Island. The specific activities were estimated for both alpha and beta emitters present. Mandibles from a subset of reindeer were also analyzed to determine their radionuclide content.

It was determined through the course of the research that as the age of the animal from which the enamel was taken increased, the beta-emitting radionuclide content in enamel also increased, however no increase in the levels of alpha-emitting radionuclides was found (Klevezal et al., 1999). Beta-emitting radionuclide content for the tooth enamel samples and the mandibles were found to be equal in nearly half of the samples. In 16 of the samples, the enamel had a concentration of beta-emitters 1.5 times higher than the mandible, and only two samples showed a lower value for the tooth enamel. It was concluded that radionuclides present in the enamel of the teeth do not contribute in a significant way to the EPR reconstructed dose (Klevezal et al., 1999). There is, however, a considerable contribution to the accumulated tooth enamel dose from the radionuclides present in the adjacent bone tissue (Klevezal et al., 1999).

A second study, similar to that of Klevezal, et al. (1999), was conducted which examined reindeer teeth from the same three areas (Klevezal et al., 2001). The analysis included measurements of the specific activity of certain radionuclides in the tooth enamel as well as in the mandible of the specimens, and also the accumulated dose the specimens received. The study did not produce unique information about the characteristics of the reindeer teeth related to EPR

dosimetry, but instead confirmed environmental levels of contamination in the areas that were being investigated and also considered the effect of radiation on several biological parameters.

2.5.9 Rhesus Monkey Studied by In Vivo EPR Dosimetry

Having the ability to determine a potential victim's dose in situ after a nuclear or radiological accident is critical to emergency response efforts (Junwang et al., 2014). Until recently, the capability to perform in vivo EPR analysis of tooth samples was not a viable option (Junwang et al., 2014), and typical EPR analysis was performed on powder enamel samples. A cylindrical TM010 X-band EPR spectrometer cavity was developed and tested, which is to be used to perform in vivo analysis on intact teeth (Junwang et al., 2014). The novel cavity was tested using various samples including the irradiated teeth from a Rhesus Monkey. Although no specific information was gathered regarding the characteristics of the rhesus monkey tooth specimens themselves, a spectrum was obtained that showed a dosimetric signal with a high intensity, which demonstrated the potential practicality of this instrument. (Junwang et al., 2014).

2.5.10 Other Mammals

Serezhenkov et al examined the teeth from several species including: European bison, polar fox, moose, polar bear, as well as from humans. The goal of this study was to gather further information on the use of animal teeth for EPR dosimetry. Several properties of the EPR signals were compared among the different types of animal teeth used, as well as with the human specimens including: the effect of microwave power on the intensity of the EPR signal, techniques to isolate the dosimetric signal from the total EPR signal, dose response of the enamel from the different types of wildlife as well as humans, and EPR signal relaxation parameters (Serezhenkov et al., 1996).

The characteristics of EPR signals of analyzed enamel originating from different animal species, as well as humans, were found to have many similarities (Serezhnikov et al., 1996). Furthermore, no substantial differences in the radiosensitivity were found amongst the samples analyzed based on a comparison of regression coefficients (Serezhnikov et al., 1996).

2.6 Synthesis of Results, Their Meaning and Future Needs

The study of tooth enamel from various species of animals has resulted in much new information about their attributes and use with EPR dosimetry. A summary of some specific characteristics can be seen in Table 2.2. One important conclusion is that the teeth of many animals have been found to be suitable alternatives to human teeth for use in retrospective dose reconstructions. Furthermore, it was shown that the radiation induced radicals trapped in many different types of animal teeth are the same type, i.e., CO_2^- , that are trapped in the teeth of humans. Additionally, the dose response of tooth enamel from several species was found to vary significantly.

Although much has been learned regarding EPR dosimetry and animal teeth, there are still important unanswered questions. In addition, specific characteristics of tooth enamel from a greater number of animals must be established to allow for more rapid and reliable reconstructed doses in humans, wildlife, and the environment. The technique of EPR Dosimetry using animal teeth as dosimeters would greatly benefit from continued studies and by use of a wider array of species.

2.7 Conclusion

EPR Dosimetry with teeth as dosimeters is a technique that has proven useful for several decades. Although a variety of materials have been studied to gauge their usefulness for a multitude of scenarios, tooth enamel has been found to be particularly advantageous due to a

Table 2.2. Summary of X-Band EPR animal studies written and pertinent findings. * Data not available.

Animal Studied	Study Referenced	Lowest Measured Dose	g-value (Native Signal)	g-value (Radiation Induced Signal)		Dose Response compared to humans	Linearity Range
				g _i	g _±		
Canine	Khan et al. (2005)	0.44 Gy	2.0045	1.9973	2.0018	~1	0.44-4.42 Gy
	Hassan et al. (2010)	200 mGy	*	1.9976	2.0019	1.1 Higher	0.2-2 Gy
Cow	Toyoda et al. (2006)	5 Gy	*	*	*	*	*
	Toyoda et al. (2007)	4.9 Gy	*	*	*	*	*
	Jiao et al. (2014)	2 Gy	2.0046	1.9975	2.0018	~1	*
	Toyoda et al. (2003)	*	2.0046	1.9972	2.0031	~1	0-18 Gy
European Bison	Serezhenkov et al. (1996)	0.48 Gy	*	*	*	~1	0.48-10.08 Gy
Goat	Jiao et al. (2014)	2 Gy	2.0046	1.9975	2.0015	~1	*
Moose	Serezhenkov et al. (1996)	0.48 Gy	*	*	*	~1	0.48-10.08 Gy
Mouse	Toyoda et al. (2003)	2.8 Gy	2.0046	1.9972	2.0031	25-30% lower	0-18 Gy
	Khan et al. (2003)	1.4 ± 0.2 Gy	2.0045	*	*	50% lower	0.8-5.5 Gy
Pacific Walrus	Hayes et al. (1998)	790 mGy	2.005	*	2.0018	*	up to 6 kGy
Pig	Dansoreanu et al. (2009)	0.05 Gy	2.0044	1.9971	2.0032	*	*
Polar Bear	Serezhenkov et al. (1996)	0.48 Gy	*	*	*	~1	0.48-10.08 Gy
Polar Fox	Serezhenkov et al. (1996)	0.48 Gy	*	*	*	~1	0.48-10.08 Gy
Rat	Brady et al. (1968)	0.8 Gy	*	*	2.0	*	9 - 270 Gy
	Zdravkova et al. (2004)	*	*	*	*	*	*
	Brik et al. (2000)	*	*	*	*	*	*
Reindeer	Klevezal et al. (1999)	0.03 Gy	*	*	*	*	*
	Serezhenkov et al. (1996)	0.48 Gy	*	*	*	~1	0.48-10.08 Gy
	Klevezal et al. (2001)	*	*	*	*	*	*
Rhesus Monkey	Junwang et al. (2014)	2 Gy	*	*	*	*	*

number of inherent characteristics. EPR tooth dosimetry has been widely used in situations involving unintended exposures when no other suitable alternatives were available and has enabled the reconstruction of retrospective doses to affected humans and a select number of wildlife. The need exists for more materials to be studied to determine their suitability as dosimeters for future situations where their use may be necessary.

Chapter 3

SAMPLE PROCEDURES⁴

3.1 Sample Collection

This study was reviewed by the Colorado State University Institutional Animal Care and Use Committee and was deemed to be exempt from oversight (Appendix A).

Boar were collected for use in this research project during a period of approximately two-months in June and July, 2017. Mandibles were procured from Japanese wild boar living in various areas within the Fukushima Exclusion Zone. Wild boar in the Exclusion Zone are being culled by hunters at the behest of the Japanese Government to prevent destruction and invasion by the creatures. A field team, which included a veterinarian, accompanied hunters to boar trap locations to collect specimens. Mandibles were collected and taken to the laboratory at the Institute of Environmental Radioactivity, at Fukushima University, for processing. Pertinent data were recorded for each boar from which mandibles and tooth samples were extracted including: collection location, approximate age and sex of the boar from which the sample was taken, date of collection, and unique sample identification number. Figure 3.1 shows a map of the boar collection site locations (red stars) in relation to the FDNPP (black x). Boar trap locations were selected due to their location within the Fukushima Exclusion Zone. Additionally, two boar specimens, designated as control boar, were collected outside the Fukushima Exclusion Zone due to lower levels of background radiation. Table 3.1 lists specific data for boar collected for use in this investigation.

⁴ This chapter is based on: Harshman A, Toyoda, S, Johnson T. Suitability of Japanese Wild Boar Tooth Enamel for Use as an Electron Spin Resonance Dosimeter. *Radiation Measurements* 116(2018) 46-50; 2018.

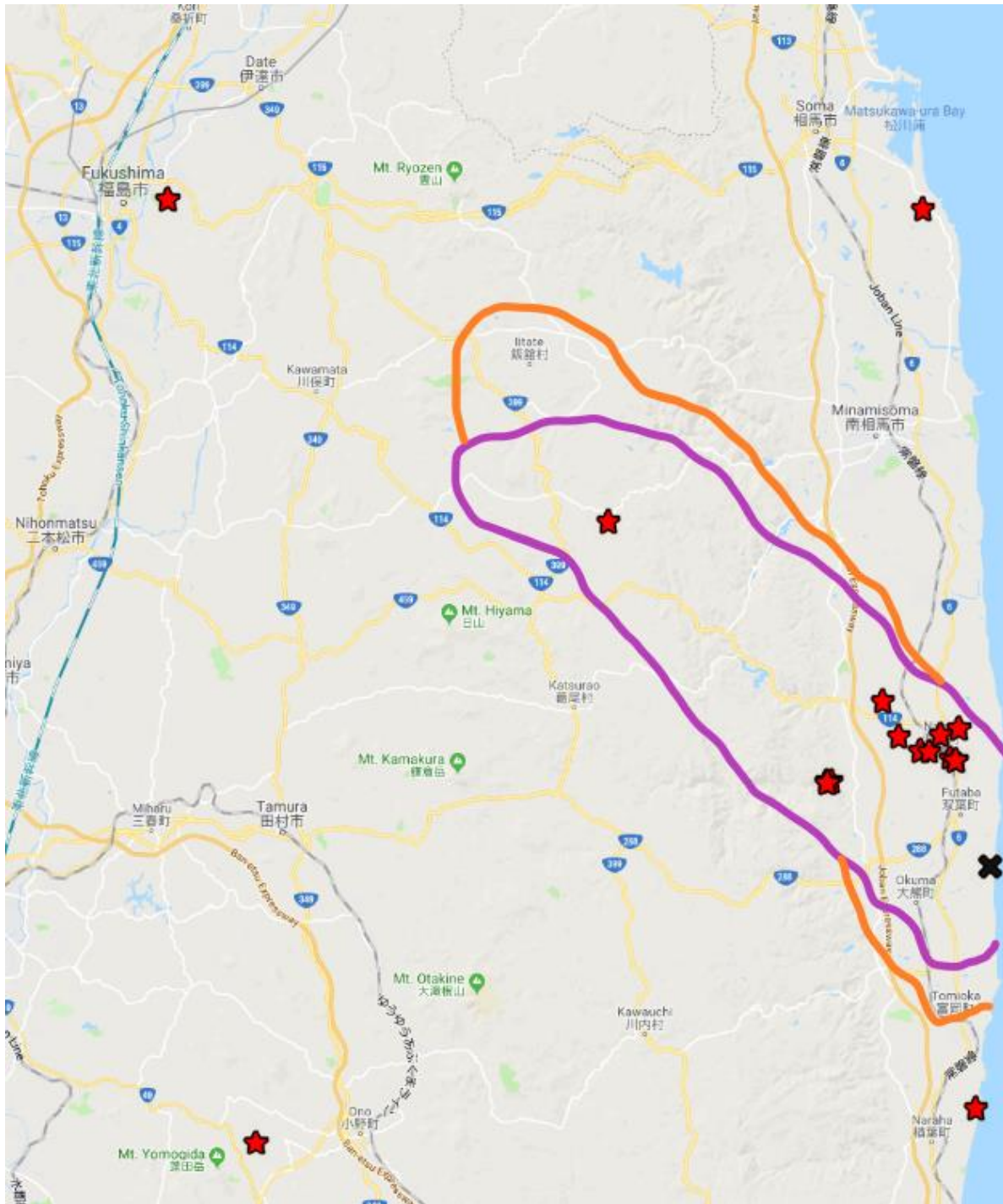


Figure 3.1. Map showing the locations of the boar collection sites indicated by red stars. The Fukushima Daiichi Nuclear Power Plant is indicated with a black x. The areas outlined in magenta and orange show the approximate areas of the Fukushima Exclusion Zone (HamsterMap.com, 2018)

Table 3.1 Summary of data for boar collected.

^a Estimated ages, ^b Control boar ^c Measurements taken at boar capture site using a Hitachi TCS-172 NaI Scintillation Survey meter, ^d Estimated using collection site dose rate and estimated age of boar, neglecting possible contribution from internally deposited radionuclides. *Data not available.

Sample Number	Estimated Age ^a	Sex	Collection Site	GPS Coordinates	Dose Rate (μGy/hr) ^c	Estimated Lifetime dose (Gy) ^d
170609 B-1	*	*	*	*	*	*
Ba20170605	26 weeks	Male	Namie	N37.48048, E140.98898	3.05	0.014
Ba20170608	30 weeks	Female	Namie	N37.48922, E140.99678	0.34	0.002
Ba20170609	4 years	Female	Namie	N37.46531, E 140.92621	8.1	0.492
Bb20170609	47-52 weeks	Male	Namie	N37.47610, E 141.00615	0.68	0.006
Ba20170615 ^b	>220 weeks	Female	Fukushima	N37.76129, E140.49994	0.46	0.031
Ba20170616	47-52 weeks	Male	Namie	N37.47610, E141.00615	0.68	0.006
Bb20170616	62 weeks	Male	Namie	N37.49222, E141.00841	0.14	0.002
Ba20170617 ^b	26 weeks	Male	Soma	N37.75646, E 140.98490	0.09	0.0004
Ba20170620	62 weeks	Female	Namie	N37.46532, E140.92326	10.1	0.123
Ba20170623	127 weeks	Female	Namie	*	0.98	0.029
Bb20170623	88-106 weeks	Male	Namie	N37.59710, E140.78300	2.98	0.062
Ba20170627	62 weeks	Male	Namie	N37.46444, E140.92354	10.5	0.128
Ba20170704	56-62 weeks	Male	Namie	N37.28049, E140.55695	10.5	0.121
Ba20170717	57-61 weeks	Female	Namie	N37.50570, E140.95948	1.7	0.020
Bb20170717	127 weeks	Male	Namie	N37.48788, E140.96959	0.75	0.022
Bc20170717	127 weeks	Male	Namie	N37.47685, E141.00258	0.35	0.010
Ba20170720	*	*	Namie	N37.29833 E141.01931	0.12	*
Ba20170724	*	Female	Namie	N37.48092 E140.98351	2.8	*

3.2 Tooth Extraction

Mandibles were stored in a freezer under environmentally stable conditions until the start of the sample processing procedure. Frozen mandibles were thawed overnight prior to processing. Steps listed in the “Wild Boar Tooth Extraction Procedure” (Appendix B) were used to remove all tooth samples. A low-speed water-cooled 10.16 cm (4-inch) saw (Ameritool, Inc., Redding, CA) with a diamond blade was used to carry out the crown amputation of molars and pre-molars. After tooth specimens were harvested, they were submerged in a 1-5% Sodium Hypochlorite solution for 24 hours for the purpose of sterilization. Specimens not being immediately processed were then shipped back to Colorado State University (Appendix R).

Chapter 4

SUITABILITY DETERMINATION PART I: DOSE RESPONSE EVALUATION (1.2 – 12 GY)⁵

4.1 Introduction

When determining suitability of wild boar tooth enamel for use as an EPR dosimeter, linearity of dose response must be established as well as the degree to which the dose response varies from sample to sample. Dose response variation can be ascertained for distinct tooth samples taken from the same boar and also those originating from different boar specimens. Confirmation of these characteristics is necessary because the methods used in EPR dose reconstruction rely on a linear dose response (IAEA, 2002). Furthermore, the appropriate dose reconstruction method will be determined by the extent of variation in dose response. The calibration curve method is more appropriate for samples with a less substantial variation, where the additive dose method, or individual calibration method, would be more applicable to samples with a significant diversity in dose response (IAEA, 2002).

Human teeth, as well as all animal teeth that have been studied thus far, have exhibited a dose response which is linear. Differences have been seen, however, in the variation in dose response or radiation sensitivity between species, as discussed in Chapter 2. Therefore, the characteristic variation in radiation sensitivity must be established in order to select the technique best suited for EPR analysis and dose reconstruction using tooth enamel of wild boar. The characteristics of wild boar tooth enamel in the range of 1.2 – 12.0 Gy are outlined below.

⁵ This chapter is based on: Harshman A, Toyoda, S, Johnson T. Suitability of Japanese Wild Boar Tooth Enamel for Use as an Electron Spin Resonance Dosimeter. Radiation Measurements 116(2018) 46-50; 2018.

4.2 Materials & Methods

4.2.1 Sample Selection

A subset of eight tooth samples was selected to determine linearity and variation in EPR dose response. Samples were selected from boar of different ages and from different positions within the mouth. Table 4.1 shows the sample number, tooth position, as well as the age of the boar for each of the samples selected. Fig. 4.1 shows molar teeth from boar Ba20170609. Boar ages were estimated by an experienced wildlife biologist using eruption and wear patterns in the teeth. An estimate of accumulated lifetime dose based on the boar's age and the dose rate at the collection site at the time of collection is also included. Although attempts were made to properly classify tooth specimens used, uncertainty in the age of the boar and tooth developmental stages created the potential for misclassification of tooth position. This does not impact the validity of the results shown, as both molars and pre-molars have been found to be useful with EPR dosimetry (IAEA, 2002).

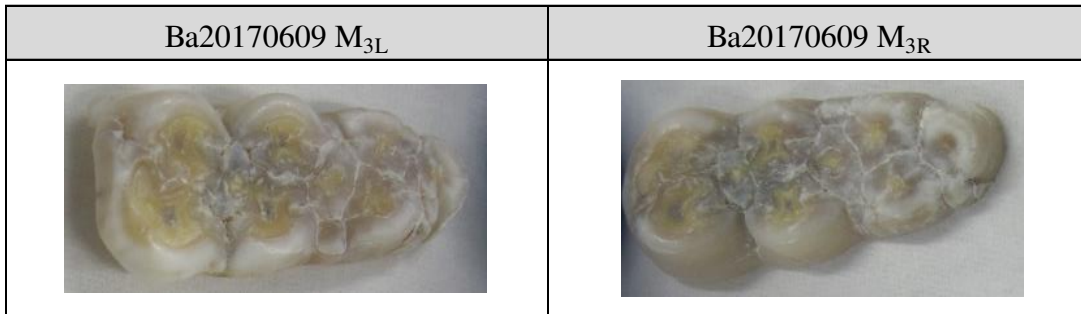


Fig. 4.1 Molar teeth used to determine linearity and variability in the 1.2 – 12.0 Gy range.

4.2.2 Sample Preparation

The selected tooth samples were rinsed in acetone and placed in deionized water for a period of 24 hours. Once the samples were removed from the deionized water, they were cut into smaller pieces using the water-cooled saw to aid in removal of dentin from the tooth enamel.

Table 4.1 Summary of tooth samples selected for irradiation. Linear regression data including R², R, and dose response (slope) values from irradiated tooth sample measurements and differences in slope values for the right versus left tooth from the same boar are listed. Retrospective (intercept) doses for samples in this study with their associated uncertainty are also shown. Critical level doses (D_{CL}) and detection limit doses (D_{DL}) for each sample were calculated using methodology in Fattibene et. al. (2011).

^a Control boar tooth sample, ^b Based on measurements made using a Hitachi TCS-172 NaI Scintillation Survey meter at the site of capture, ^c Average spectral data values for Ba20170608 P_{3L}, Sample 6 were calculated using Microsoft Excel. ^d Based on dose rate and age of boar, assuming negligible contribution from internally deposited nuclides.

*Projected doses approach zero

Sample #	Est. Age in Weeks	Collection Site	GPS Coord	Site Dose Rate (μGy/hr) ^b	Tooth Used	Linear Eqn of Trendline	Slope ± σ	% Variation relative to the average	Average Slope by boar ± σ	R ² Value	R Value	Est. Lifetime Dose (Gy) ^d	Retrospective Dose ± uncertainty (Gy)	D _{CL} (Gy)	D _{DL} (Gy)
Ba20170608	30	Namie	N37.4 8922, E140. 99678	0.34	P _{3R}	y = 138.27x - 31.43	138.27 ± 4.12	11.48	130.76 ± 5.34	0.99	0.99	0.0017	*	0.9	1.6
					P _{3L}	y = 123.25 x - 52.04 ^c	123.25 ± 6.33						0.98 ^c	0.99	*
Ba20170609	> 220	Namie	N37.4 6531, E140. 92621	8.1	M _{3R}	y = 110.41x + 84.26	110.41 ± 3.15	27.14	97.22 ± 3.43	0.99	0.99	0.2994	0.8 ± 0.2	0.8	1.5
					M _{3L}	y = 84.02x + 116.15	84.02 ± 3.69						0.99	0.99	1.4 ± 0.3
Ba20170615 ^a	> 220	Fukushima	N37.7 6129, E140. 49994	0.46	M _{2R}	y = 36.74x + 18.26	36.74 ± 1.52	79.98	61.23 ± 3.11	0.99	0.99	0.017	0.5 ± 0.3	1.2	2.2
					M _{2L}	y = 85.72x + 14.81	85.72 ± 4.13						0.99	0.99	0.2 ± 0.3
Ba20170617 ^a	26	Soma	N37.7 5646, E140. 98490	0.09	P _{3R}	y = 130.99x - 29.603	130.99 ± 5.23	3.44	133.29 ± 3.83	0.99	0.99	0.0004	*	1.2	2.1
					P _{3L}	y = 135.58x + 12.99	135.58 ± 1.40						0.99	0.99	*

Dentin removal was performed using a combination of chemical and mechanical separation. First, a dental drill with water-cooling was used to remove as much visible dentin as possible from each tooth segment. Tooth segments were then placed in beakers containing a solution of 20% Potassium Hydroxide (KOH) for 24 hours. Tooth specimens were removed from the solution and rinsed with deionized water. A water-cooled dental drill was again used to remove visible dentin. This process was repeated twice. Remaining enamel was rinsed in a solution of 70% Ethanol and dried at 40°C in an oven for a period of 4 hours.

An agate mortar and pestle were used to grind the dried enamel segments into a powder. Because the ideal grain size for EPR analysis is between 0.10-1.00 mm (IAEA, 2002), a system of calibrated sieves was used, which consisted of a 1.00 mm sieve, a 0.50 mm sieve, and a 0.177 mm sieve. The powder enamel was poured through the series of sieves, and the material remaining between the sieves measured between 0.177 -1.00 mm. Enamel larger than 1.00 mm was further crushed until the desired particle size was achieved. Powder enamel samples were then placed into plastic vials and stored at room temperature awaiting further processing. This step additionally served the purpose of allowing time for spurious signals, which may have been created as a result of sample processing, to fade (IAEA, 2002). Samples were dried again at 40°C in an oven overnight just prior to EPR analysis to remove residual moisture.

4.2.3 Sample Irradiation

Processed powder enamel from each tooth was separated into six individual aliquots, with Ba20170617 P_{3L} having only 5 aliquots. A total of forty-seven 90-mg aliquots were used and verified to be uniform in weight to within 0.1 mg. Data regarding individual sample measurements are listed in Appendix C. Aliquots were separated into batches based on irradiation dose. One aliquot from each tooth was segregated and left unirradiated. The

remaining aliquots were then placed into containers made of acrylic plates whose dimensions were 40 x 70 x 10 mm with a top and bottom thickness of 4 mm. The samples were sent to Takasaki Advanced Radiation Research facility in Japan for irradiation. A Co-60 source was used, and aliquot batches were irradiated using a dose rate of 0.13 C/kg-h to the following doses: 1.2 Gy, 2.2 Gy, 4.4 Gy, 7.6 Gy, and 12.0 Gy. Table 4.2 shows exposure rate, irradiation time, and actual absorbed doses for each sample. Irradiated samples were then sent to Okayama University of Science for analysis.

Table 4.2. Sample irradiation information.

Aliquot #	Rate (C/kg-h)	Time (h)	Exposure (C/kg)	Absorbed Dose (Gy)
1	0.1295	0.25	0.0324	1.2
2	0.1295	0.50	0.0648	2.2
3	0.1295	1.00	0.1295	4.4
4	0.1295	1.75	0.2266	7.6
5	0.1295	2.75	0.3561	12.0
6	0	0	0	0

4.3 EPR Measurement

Irradiated powder tooth enamel samples were analyzed at Okayama University of Science using a JEOL JES-PX2300 ESR Spectrometer. Individual aliquots were repeatedly measured 3-5 times in the ESR spectrometer depending on irradiation dose. Samples were analyzed at room temperature. The following analysis parameters were used: sweep width: 10 mT, microwave frequency: 9.42 GHz, microwave power: 2 mW, modulation frequency: 100 kHz, modulation amplitude: 0.2 mT, time constant: 0.03 s, and number of scans: 40, scan time 30 s.

Spectra obtained from the set of aliquots from Ba20170608 P_{3L} and Ba20170609 M_{3R} are displayed in Fig. 4.2. Spectra from all 4 boar are shown in Appendix K. The radiation induced

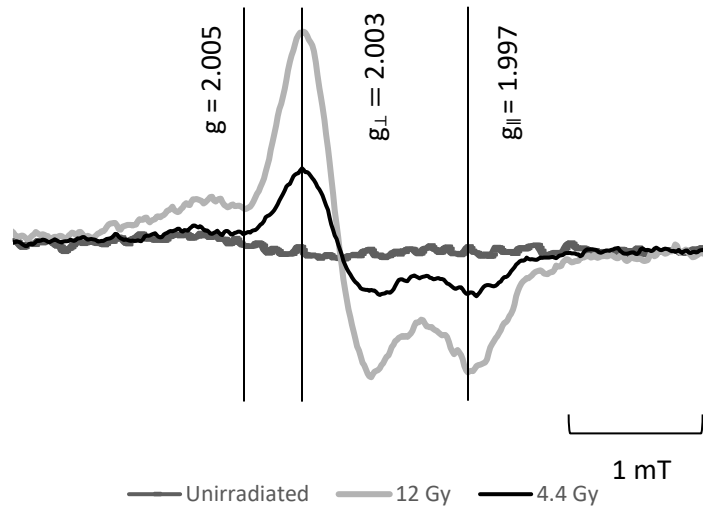
signal (RIS) originating from the CO_2^- radical is shown to increase as irradiation dose increases.

G-values were determined to be: $g = 2.005$, $g_{\perp} = 2.003$, and $g_{\parallel} = 1.997$.

4.4 Processing of the Spectra and Statistical Analysis

Data from repeated sample measurements were averaged using New ER (Ivannikov, et al. 2001), a software program used to produce Radiation Induced Signal (RIS) intensities and Background Signal (BGS) intensity values for each sample. Data were normalized using the intensity of the MgO:Mn standard marker. The normalized RIS values for aliquots from each tooth were plotted versus irradiation dose to determine linearity and variability in dose response. Values for normalized and non-normalized RIS signal intensities are shown in Appendix D along with intensity values for the MgO:Mn standard marker. Linear regression analysis was performed using Excel in addition to RStudio (Version 1.0.153) to validate assumptions of the linear regression model (normality, independence, equality of variance and linear response). A correlation test was also performed for RIS and dose. Results of this analysis are shown in Appendix J. Fig. 4.3 shows results of signal intensity plotted versus irradiation dose with linear regression analysis for Ba20170608 P_{3L} and Ba20170608 P_{3R}. Appendix L shows results for each of the four boar.

a)



b)

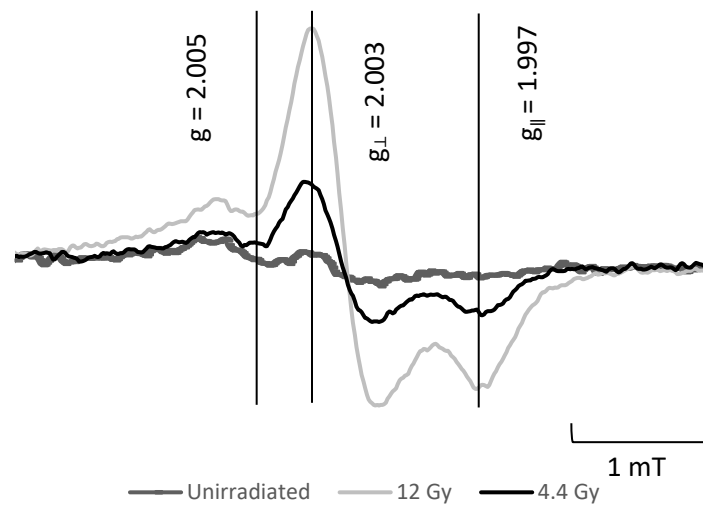


Fig. 4.2 EPR spectra of samples Ba20170608 P_{3L} a) and Ba20170609 M_{3R} b) showing the RIS for aliquots that were irradiated in the laboratory as well as an unirradiated aliquot.

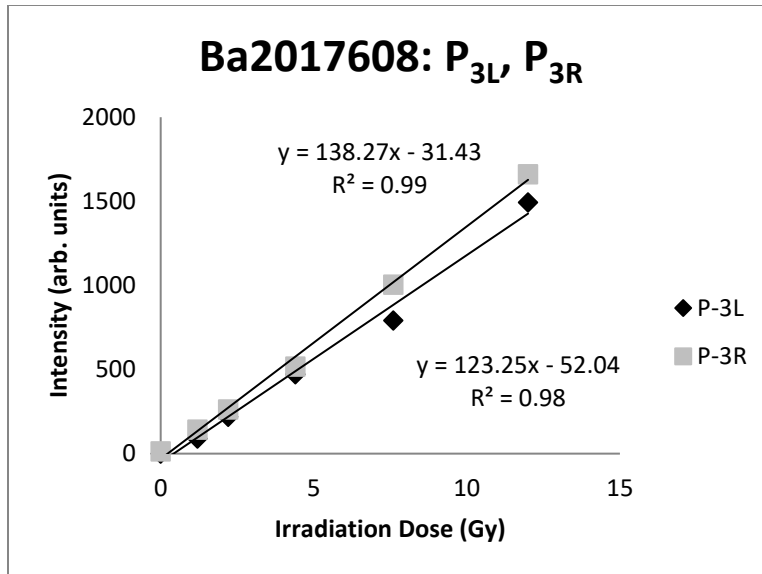


Fig. 4.3 Graph showing linearity in the lower left Pre-molar 3 and right Pre-molar 3 from boar Ba20170608

Retrospective doses and uncertainty values for tooth samples were determined using linear regression data and results are shown in Table 4.1 and Appendix M. Additionally, critical level doses (D_{CL}) and detection limit doses (D_{DL}) for each set of enamel samples were calculated and are shown in Table 4.1. Critical level dose is the dose at which a decision can be made with 95% probability regarding whether an exposure has occurred taking into account a 5% false positive rate (Wieser et al., 2008). At the critical level, the measured dose can be determined to be present and distinguishable from background at a chosen error probability (Fattibene et al., 2011). The detection limit dose indicates the minimum dose which can be measured with a chosen false negative rate and is an indication of a method's detection ability (Fattibene et al., 2011). Methodology described in Fattibene et al. (2011) together with linear regression data and irradiation dose versus RIS intensity plots were used to determine D_{CL} and D_{DL} values for the samples used in this study (Appendix E).

4.5 Results

4.5.1 Variation in Dose Response

The dose response of boar tooth enamel was found to be linear. R^2 and slope values for each tooth sample can be seen in Table 4.1. All R^2 values were between 0.98 and 0.99, and all R values were 0.99. Data were analyzed to determine variation in dose response comparing teeth from the left and right sides of the mouth of the same boar. A line was fitted to the data points, and corresponding slopes for each line were used to determine dose response. Results are shown in Table 4.1. Variation in dose response of teeth taken from the same animal based on the fitted line slopes ranged from 3.4 – 79.9%.

The boar were divided into two groups classified as “Old” (> 220 weeks) and “Young” (26 and 30 weeks). Fig. 4.4 shows a comparison of the sensitivity to dose of the boar based on age and therefore permanent versus deciduous teeth. A correlation can be seen based on age of the tooth ($p = 0.03$), with the deciduous teeth taken from young boar having a steeper slope and thus a higher dose response than the permanent teeth. R code used to obtain these results can be found in Appendix F. There was a 50% difference in dose response between the average slope of the permanent teeth versus the average slope of the deciduous teeth (79.2 and 132.0 respectively). It was noted during the study that the teeth taken from the younger boar were of higher quality and contained less visible wear, discoloration, and decay than the samples collected from older boar, and appear to have less variability.

4.5.2 Possible Causes of Dose Response Variation

EPR studies using teeth of animals have noted similar variations in dose response. Canine teeth were found to have a dose response variation ranging from 10-25% (Khan et al., 2005) and

in one study, the teeth of cows showed greater than a 10-fold variation in dose response (Toyoda et al., 2007).

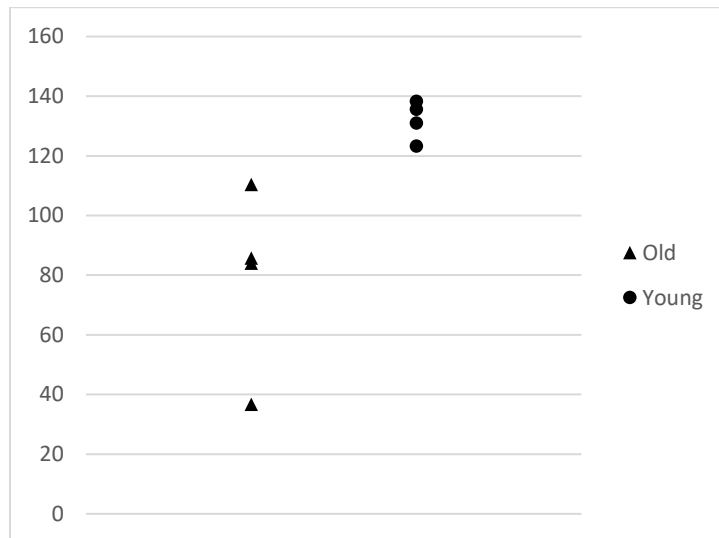


Figure 4.4 Comparison of the sensitivity to dose (slope) by age of the tooth

Based on the comparison of sensitivity to dose by age of the boar, results suggest that radiation sensitivity may be lower in permanent teeth compared to deciduous teeth. In humans, permanent teeth have been found to be more mineralized and have a lower content of water compared to deciduous teeth (Wilson and Beynon 1989; Müller and Schmitz-Feuerhake 1996), however radiation sensitivity has not been found to differ significantly between the two (Murahashi, et al. 2017; Müller and Schmitz-Feuerhake 1996). Further investigation is needed to verify this result in the teeth of wild boar.

Alternately, dentin may become more difficult to remove as the age of the boar increases, and the samples used may have contained dentin and not pure enamel. If a particular sample contains some fraction of dentin, the dose response will be less than a sample containing pure enamel due to the differences in dose response between enamel and dentin (IAEA, 2002). Finally, the age of the tooth and its condition could contribute to the discrepancy seen in the dose response of the enamel samples, as tooth disease has been shown to impact EPR measurements

due to the impact on the soundness of the enamel (Brik et al., 2000). The quality of the tooth enamel has been identified as the most likely cause of the variation in dose response seen in the measurement results.

4.6 Discussion and Synthesis of Results

Tooth specimens were collected from a total of four boar for this study. The ages of the boar are shown in Table 4.1. Samples analyzed from boar Ba20170609 and Ba20170615 that were not irradiated in the laboratory were found to have higher initial absorbed doses to the enamel as shown in Table 4.1. Initial doses are a result of exposure to radiation sources during the boar's lifetime in the Fukushima Exclusion Zone. Grinding of the teeth by boar, as made evident by visible wear and smooth enamel surfaces in older tooth samples, may have resulted in the creation of additional radicals in the enamel which could contribute to the EPR signal. Initial absorbed doses for the remaining boar tooth samples were found to be negligible prior to being irradiated in the laboratory, which is consistent with the age of the boar and the dose rates in the areas of habitation as shown in Table 4.1.

The goal of the present study is to show the potential for boar tooth enamel to be used with EPR to reconstruct doses, which are shown in Table 4.1. A comparison of doses estimated using age of the boar and collection site dose rates with ESR reconstructed doses in Table 4.1 show that the relative order is consistent. The reconstructed doses in Table 4.1 suggest that the boar in this study have been exposed to higher dose rates than those measured at their respective collection sites either by roaming to different areas or they were exposed to higher dose rates in the past or internally deposited radionuclides may have made a significant contribution to the dose. Note also that the dose rates at collection time were not corrected for radioactive decay or weathering, which could result in significantly higher air dose rates in the past. Results

calculated for critical level doses and detection limit doses suggest that at the current time this method would be useful for boar expected to have received absorbed doses greater than 1 Gy. The results discussed in the present study are preliminary, and more work is necessary in order to establish the results presented.

4.7 Conclusion

The dose response of tooth enamel from Japanese wild boar was found to be generally linear in the range of 1.2 Gy to 12.0 Gy. A significant variation in dose response exists between teeth from the same boar taken from right and left sides of the mouth and was found to be in the range of 3.4 – 79.9%. Potential causes of the large variation in dose response were identified. Furthermore, the radiation dose response of the deciduous tooth enamel of young boar was found to have less variation than enamel from permanent teeth of old boar. Based on the results of this study, the tooth enamel of the Japanese wild boar would be an appropriate dosimeter for use with EPR dosimetry in the range of 1.2-12.0 Gy. Due to the uniform sensitivity of deciduous tooth enamel, the calibration curve method of dose reconstruction could be utilized, whereas individual calibration may be needed when using tooth enamel from older boar. A low dose study, however, is necessary to verify both linearity and variability in dose response to establish usefulness of the wild boar teeth as dosimeters with EPR dosimetry for reconstructing doses below 1.2 Gy. Understanding variation in dose response of teeth taken from boar of different ages, including both deciduous and permanent teeth, and from within different positions within the mouth, will result in more reliable dose estimates to wild boar.

Chapter 5

SUITABILITY DETERMINATION PART II: DOSE RESPONSE EVALUATION (0.25- 2.0 GY)⁶

5.1 Introduction

Chapter 4 investigated linearity and variation in dose response of wild boar tooth enamel in the range of 1.2 – 12.0 Gy. Because lifetime dose estimates for boar inhabiting the Fukushima Exclusion Zone are expected to be below the range previously investigated, it is prudent to explore characteristics of boar tooth enamel in the region below 1.2 Gy. Therefore, it is the goal of Chapter 5 to further establish these characteristics in the 0.25 -2.0 Gy region and expand the range for which wild boar tooth enamel is known to be useful as an EPR dosimeter.

5.2 Materials and Methods

5.2.1 Sample Selection

Two individual tooth samples were chosen from a total of four boar for use in establishing linearity and degree of variation in EPR dose response in the region of 0.25 Gy to 2.0 Gy. Pertinent data are shown in Table 5.1 for the tooth samples selected. Also included in Table 5.1 is an estimated absorbed dose to enamel calculated using the estimated age of the boar and dose rate at the sample collection site accounting for radioactive decay. Eruption and wear patterns were used by a qualified wildlife biologist to estimate the ages of the boar in this study.

⁶ Based on: Harshman A, Johnson T. 2018. Dose Reconstruction Using Tooth Enamel from Wild Boar Living in the Fukushima Exclusion Zone with Electron Paramagnetic Resonance Dosimetry. Health Physics Journal. Submitted.

Table 5.1. Summary of information for tooth samples selected for low dose irradiation. Linearity and dose response (slope) data for irradiated tooth enamel samples, and retrospective dose estimates and left versus right tooth dose response are also included. Methodology outlined in Fattibene et. al. (2011) was used to calculate critical level doses (D_{CL}) and detection limit doses (D_{DL}).^a Estimated using collection site dose rate and estimated age of boar, neglecting possible contribution from internally deposited radionuclides.

Sample Number	Tooth Position	Linear Equation of Trendline	Slope $\pm \sigma$	% Variation relative to the average	Average Slope by boar $\pm \sigma$	R ² Value	R-Value	Estimated Lifetime Dose (Gy) ^a	Retrospective Dose \pm uncertainty (Gy)	D _{CL} (Gy)	D _{DL} (Gy)
Ba20170620	M _{2R}	$y = 1.2E-06x + 4.3E-07$	$1.2E-06 \pm 2.5E-07$	39.4	$9.8E-07 \pm 6.0E-08$	0.84	0.92	0.12	0.4 ± 0.2	1.3	3.2
	M _{2L}	$y = 7.8E-07x + 4.1E-08$	$7.8E-07 \pm 1.1E-07$						0.1 ± 0.1	0.7	1.2
Bb20170623	M _{1R}	$y = 3.2E-07x + 3.1E-07$	$3.2E-07 \pm 5.4E-08$	27.9	$2.8E-07 \pm 4.0E-08$	0.92	0.96	0.06	1.0 ± 0.2	0.4	0.8
	M _{1L}	$y = 2.4E-07x + 2.1E-07$	$2.4E-07 \pm 5.8E-08$						0.9 ± 0.3	1.0	4.5
Ba20170627	M _{2R}	$y = 7.6E-07x + 3.2E-07$	$7.6E-07 \pm 3.9E-08$	3.8	$7.4E-07 \pm 2.2E-08$	0.99	0.99	0.13	0.4 ± 0.1	0.3	0.5
	M _{2L}	$y = 7.3E-07x + 5.4E-07$	$7.3E-07 \pm 1.9E-08$						0.7 ± 0.03	0.4	0.7
Bb20170717	M _{3R}	$y = 9.2E-07x + 2.9E-07$	$9.2E-07 \pm 1.3E-07$	44.2	$7.6E-07 \pm 1.1E-07$	0.93	0.96	0.02	0.3 ± 0.1	0.7	1.2
	M _{3L}	$y = 5.9E-07x + 5.5E-07$	$5.9E-07 \pm 1.7E-07$						0.9 ± 0.4	1.4	3.2

Due to uncertainty in the developmental stages of the tooth and the estimated age of the boar, the potential exists for misclassification of the position of the tooth used. Because molars as well as pre-molars have been shown to be appropriate for use with EPR dosimetry, there is no impact to the findings of this study (IAEA, 2002).

5.2.2 Sample Preparation

Samples were rinsed in acetone before being submerged in deionized water for 24 hours. A water-cooled low-speed saw with a 10.16 cm (4-inch) diamond blade (Ameritool, Inc., Redding, CA) was then used to cut to specimens into pieces to facilitate the dentin removal process.

Chemical and mechanical methods were used to remove dentin from boar tooth enamel. Tooth pieces were submerged in a 20% KOH solution and placed in a heated ultrasonic bath at 60°C for 24 hours. Tooth pieces were rinsed with deionized water after removal from the KOH solution. Visible dentin was removed manually using either a water-cooled dental drill or dental pic. Enamel tooth pieces were again rinsed with deionized water and then ethanol prior to being dried at 40°C in an oven overnight.

Remaining enamel was ground into a powder using a mortar and pestle. Calibrated sieves ranging from 0.250-1.00 mm were used to obtain ideal grain sizes needed for EPR analysis (IAEA, 2002). A sample preparation procedure has been provided in Appendix G.

5.2.3 Sample Irradiation

Six separate aliquots were prepared from processed powder enamel for each individual tooth and used to determine radiation dose response. Samples Bb20170623 M_{1R} and Bb20170623 M_{1L} had sufficient enamel for only 5 aliquots each. In total, forty-four 90-mg ± 0.1 mg aliquots were used. Individual sample weights are listed in Appendix C. Due to insufficient

available enamel, two aliquots were used which weighed 80.6 mg and 87.2 mg from samples Bb20170623 M_{1R} and Bb20170623 M_{1L} respectively, and mass normalization was used during analysis of measurement results for these samples. Aliquots were segregated based on irradiation dose, and one aliquot from each tooth was unirradiated. Aliquots were placed between 4 mm thick acrylic plates whose dimensions were approximately 5 mm × 10 mm to ensure electronic equilibrium during irradiation. Samples were irradiated at Colorado State University using a JL Shepherd 81-14A irradiator equipped with a ¹³⁷Cs source. Aliquots were irradiated to the specified doses: 0.25 Gy, 0.50 Gy, 0.75 Gy, 1.0 Gy, and 2.0 Gy.

Table 5.2. Sample irradiation information.

Aliquot #	Rate (Gy/s)	Time (sec)	Absorbed Dose (Gy)
1	6.17E-4	405	0.25
2	6.17E-4	810	0.50
3	6.17E-4	1215	0.75
4	6.17E-4	1620	1.0
5	6.17E-4	3241	2.0
6	0	0	0

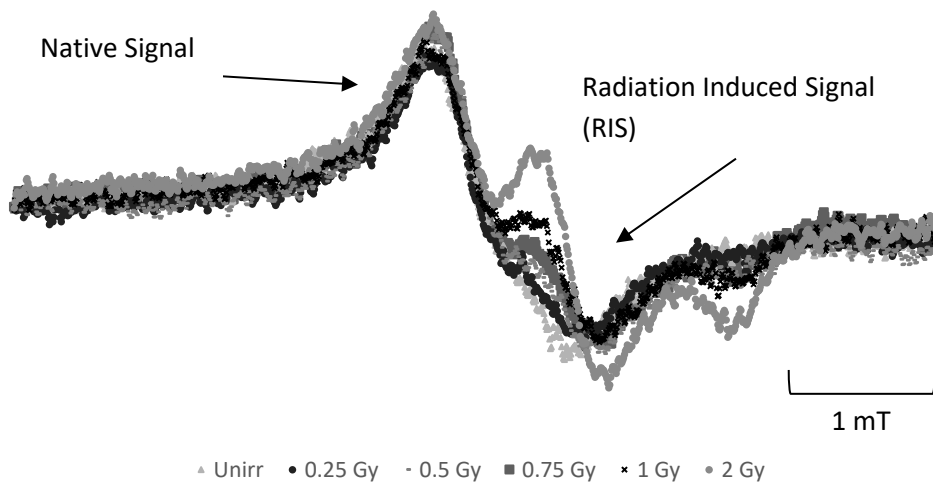
5.3 EPR Measurement

Irradiated samples were analyzed using a Bruker ELEXSYS II E 500 ESR Spectrometer at Colorado State University. Each sample was analyzed at room temperature, and individual measurements were repeated three times. The following parameters were used in the analysis: sweep width: 50 G, time of sweep: 163 s, microwave frequency: 9.72 GHz, microwave power: 2 mW, modulation frequency: 100 kHz, modulation amplitude: 2.0 G, Conversion Time: 159.18 ms, and number of scans: 6 (Ivannikov et al., 2002).

Figs. 5.1a and 5.1b show individual spectra overlaid for each set of irradiated aliquots as well as the unirradiated sample for Ba20170620 M_{2L} and M_{2R}. Results for the remaining samples

are available in Appendix K. The increase in radiation induced signal (RIS) with increasing irradiation dose can be seen. G-values for the RIS are: $g_{\perp} = 2.003$, and $g_{\parallel} = 1.997$, and $g = 2.005$ for the native signal.

a)



b)

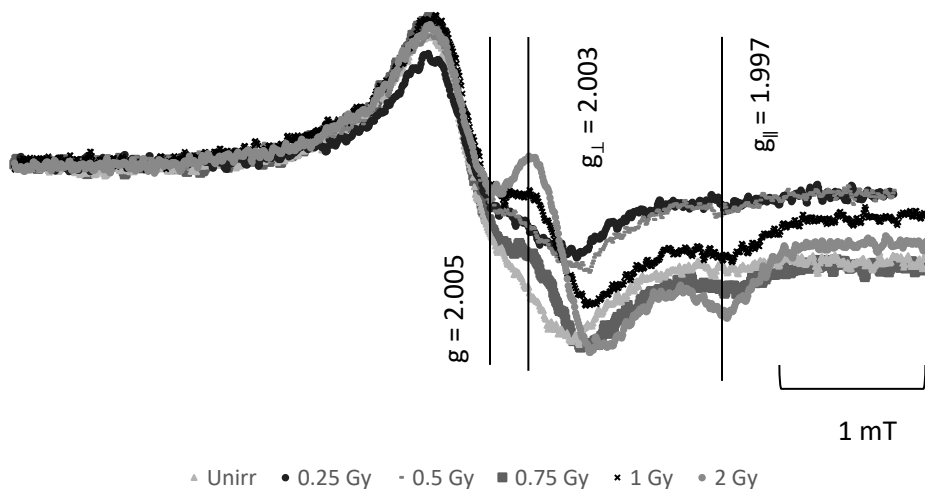


Fig. 5.1. a) EPR spectra of samples Ba20170620 M_{2L} and b) Ba20170620 M_{2R} for the unirradiated aliquot in addition to the laboratory irradiated aliquots.

5.4 Spectral Processing and Statistical Analysis

Spectra from sample measurements were analyzed using software program EPR Dosimetry version 3.3 (Koshta et al., 2000) to determine Radiation Induced Signal (RIS) intensities with empty EPR tube spectrum subtraction. EPR Dosimetry software uses spectrum deconvolution in order to determine RIS intensity. Individual components of the spectrum are isolated through spectral fitting using spectrum and Gaussian simulated lines, each of which are represented by a set of functions (IAEA, 2002). Once the RIS is isolated, the intensity can be converted into an absorbed dose using an established calibration curve (Albrecht Wieser, Computer program “EPR Dosimetry 3.3” User-guide, personal communication, September 13, 2017). RIS intensities were averaged for repeated measurements from individual samples and used to establish linearity in dose response as well as the degree of variation in dose response of the tooth enamel samples taken from the same boar. Appendix H shows individual sample RIS values for each irradiation dose.

Excel was used to perform linear regression analysis, and an example of RIS versus irradiation dose is shown in Fig. 5.2. Additional results for remaining samples are shown in Appendix L. Data obtained were used to calculate retrospective doses for the eight enamel samples, and results are listed in Table 5.1. Associated uncertainty values for retrospective doses were also calculated using data in Appendix M. Retrospective doses to the boar tooth enamel resulted from radiation exposures accumulated in the Fukushima Exclusion Zone prior to laboratory irradiation. Also listed in Table 5.1 are critical level doses (D_{CL}) and detection limit doses (D_{DL}) for the eight enamel samples. Values were determined for a one-sided 95% confidence interval (Fattibene et al., 2011). Critical level and detection limit doses were calculated using methods outlined in Wieser et al. (2008) and Fattibene et al. (2011). Values used

to determine D_{CL} and D_{DL} are listed in Appendix E. RStudio (Version 1.0.153) was used to validate assumptions of the linear model (normality, independence, equality of variance and linear response). A correlation test was performed for RIS and dose, and results are shown in Appendix J.

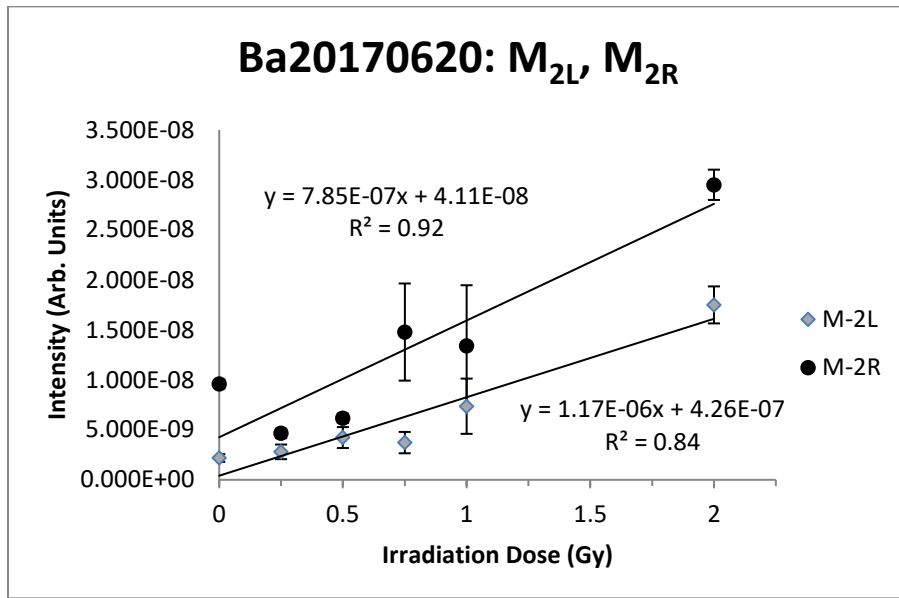


Fig. 5.2 Graph displaying linearity for left molar 2 and right molar 2 from boar Ba20170620.

5.5 Results

5.5.1 Variation in Dose Response

R^2 values for linear regression lines ranged between 0.75 – 0.99, supporting linearity in dose response of boar tooth enamel in the range of 0.25 – 2.0 Gy. R values were between 0.87-0.99. Variation in dose response was evaluated using teeth taken from opposite sides of the mouth from the same boar specimen. Variation in dose response was determined through comparison of slopes of the linear regression lines for each tooth, which ranged from 3.8 – 44.2%. Dose response (slope), R^2 and R values are shown in Table 5.1. Calculated values for variation in dose response are consistent with previous studies which investigated tooth enamel of wildlife (Khan et al., 2005; Toyoda et al., 2007; Harshman et al., 2018).

The sensitivity to dose was analyzed by age in order to determine if a correlation exists. The boar were categorized as “Old” (Bb20170623 and Bb20170717) and “Young” (Ba20170620 and Ba20170627). The dose response of the boar by age classification is shown in Fig. 5.3. No statistically significant correlation (p-value = 0.12) was found in dose response of the tooth enamel based on age of the boar. Additionally, slope values were normalized for all eight boar teeth used in the 0.25 – 2.0 Gy and 1.2 – 12.0 Gy (Chapter 4) range studies, and normalized slopes were evaluated by sex. No statistically significant correlation (p-value = 0.49) was found. R code used to obtain these results can be found in Appendix I. These results show that age of the tooth enamel does not appear to substantially impact dose response when permanent molar tooth enamel is used.

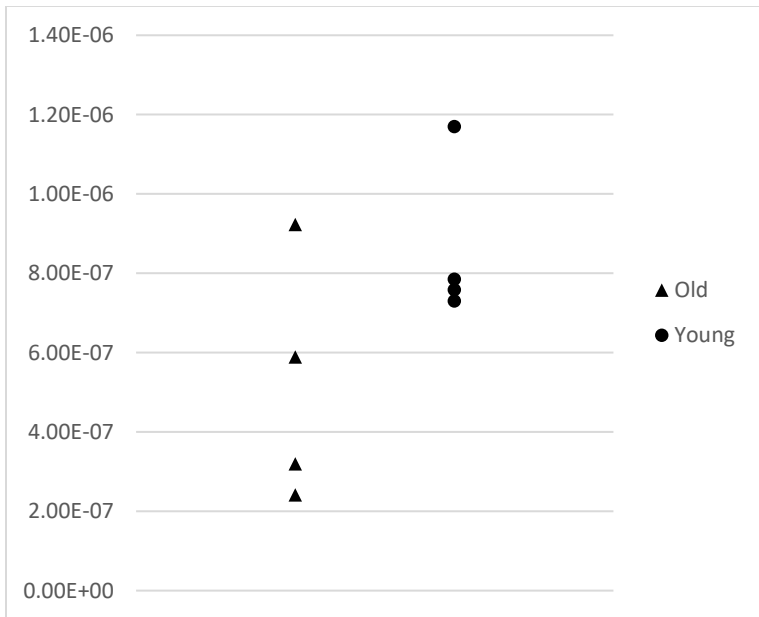


Fig. 5.3 Dose response (slope) by age of the boar

5.6 Discussion and Synthesis of Results

The goal of this section was to confirm the usefulness of wild boar tooth enamel as an EPR dosimeter in the range of 0.25 – 2.0 Gy. Results of linear regression analysis show that the dose response in this region is linear based on R^2 and R values, and that the variation in dose

response is moderate. Retrospective doses listed in Table 5.1 were compared to estimated lifetime doses and are proportional. Critical level doses and detection limit doses are similar to those calculated in Chapter 4, and further support the conclusion that although tooth enamel of Japanese wild boar are suitable dosimeters, methods used in this study would be better utilized when reconstructing doses larger than 1 Gy.

5.7 Conclusion

The radiation response of Japanese wild boar tooth enamel was linear in the 0.25 to 2.0 Gy dose range. The variation in dose response ranged from 3.8 – 44.2%, with an average of variation of approximately 30%, which is consistent with previous studies completed by Harshman et al. (2018) and outlined in Chapter 4. There is greater uncertainty in initial dose estimates for tooth enamel samples determined using the additive dose method at low doses (0.25 – 2.0 Gy) compared to the high dose region (1.2 – 12.0 Gy), and also a greater variation in the R^2 values associated with the linear regression trend line (Harshman et al., 2018). No significant variation in dose response was found to exist between samples taken from permanent molar tooth enamel from boar of different ages. Wild boar tooth enamel was found to be a suitable dosimeter for performing dose reconstructions using EPR dosimetry.

Chapter 6

CONSTRUCTION OF CALIBRATION CURVES⁷

6.1 Introduction

The calibration curve method was selected to perform dose reconstructions for the 19 boar in this study. The additive dose method of reconstruction would have also been appropriate; however, the calibration curve method was selected due to the number of samples being analyzed as well as the calculated average variation in dose response of 30% for boar tooth enamel. Section 2.1.5 outlines the basic concepts for this dose reconstruction methodology.

6.2 Materials & Methods

6.2.1 Sample Selection

Calibration curve samples were created using a homogenous mixture of powdered enamel from five molar teeth taken from different boar as shown in Table 6.1. Due to insufficient enamel available from control boar samples, molars were selected from alternate boar based on age of the boar, collection site dose rates and unirradiated sample spectrum in order to obtain samples with initial doses as low as possible. Six 90-mg aliquots were prepared from the homogenous powder enamel mixture and confirmed to be consistent to within 0.1 mg. Data regarding individual sample measurements are listed in Appendix C.

⁷ Based on: Harshman A, Johnson T. 2018. Dose Reconstruction Using Tooth Enamel from Wild Boar Living in the Fukushima Exclusion Zone with Electron Paramagnetic Resonance Dosimetry. Health Physics Journal. Submitted.

Table 6.1 Summary of data for boar whose teeth were used to construct calibration curve samples.

^a Estimated ages, ^b Measurements taken at boar capture site using a Hitachi TCS-172 NaI Scintillation Survey meter, ^c Estimated using collection site dose rate and estimated age of boar, neglecting possible contribution from internally deposited radionuclides. *Data not available.

Sample Number	Estimated Age ^a	Collection Site	GPS Coordinates	Dose Rate (μ Gy/hr) ^b	Estimated Lifetime dose (Gy) ^c	Weight of Sample (g)
Bb20170616	62 weeks	Namie	N37.49222, E141.00841	0.14	0.002	0.1103
Ba20170623	127 weeks	Namie	*	0.98	0.029	0.1101
Bc20170717	127 weeks	Namie	N37.47685, E141.00258	0.35	0.010	0.1101
Ba20170720	*	Namie	N37.29833 E141.01931	0.12	*	0.1102
Ba20170724	*	Namie	N37.48092 E140.98351	2.8	*	0.1100

6.2.2 Sample Preparation

Calibration curve samples were prepared using techniques described in section 5.2.2 and in the sample preparation procedure outlined in Appendix G.

6.2.3 Sample Irradiation

Calibration curve samples were irradiated as described in Section 5.2.3. In addition to an unirradiated aliquot, the remaining individual five aliquots were irradiated to: 0.25 Gy, 0.50 Gy, 0.75 Gy, 1.0 Gy, and 2.0 Gy. The chosen range of irradiation doses was selected based on lifetime dose estimates to the boar as shown in Table 3.1.

6.3 EPR Sample Measurement

The Bruker ELEXSYS II E 500 ESR Spectrometer at Colorado State University was used to analyze the calibration curve samples. Sample analysis procedures and spectrometer measurement parameters used were the same as those outlined in Section 5.3. Fig. 6.1 shows overlaid spectra for the set of calibration curve aliquots.

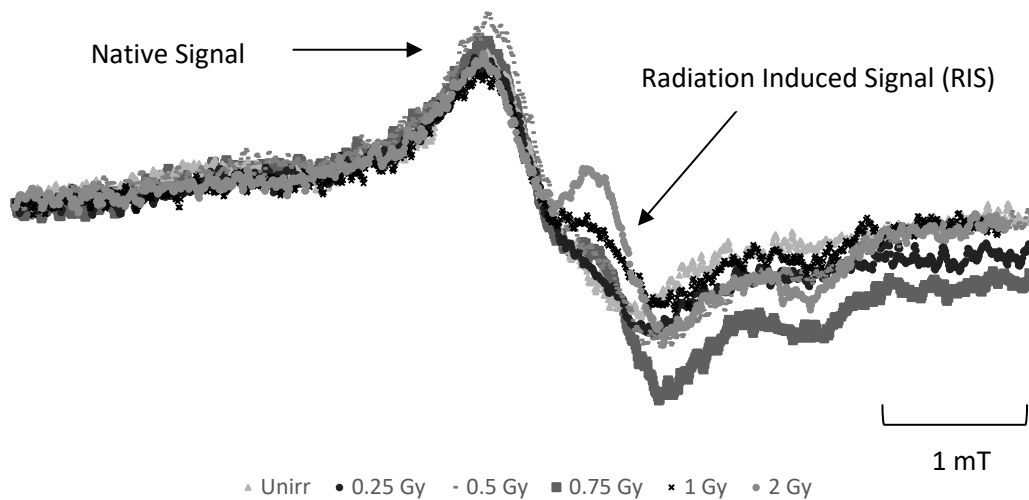


Fig. 6.1 Overlaid spectra for the calibration curve aliquots.

6.4 Spectral Processing and Statistical Analysis

EPR Dosimetry software (Koshta et al., 2000) was used to analyze spectra obtained from the calibration curve aliquots to obtain RIS intensity values for each irradiation dose. The spectrum for the empty EPR tube was measured and subtracted from each sample spectrum. Multiple measurements of the same sample were averaged and plotted with the corresponding irradiation dose, and a linear regression analysis was performed using Excel in addition to RStudio (Version 1.0.153) along with verification of linear model assumptions. Fig. 6.2 shows RIS versus irradiation dose for the calibration curve samples, and data for individual sample RIS values are available in Appendix H. The retrospective dose for the calibration curve enamel mixture consisting of 5 molar teeth was calculated using data from the linear regression analysis along with associated error as shown in Appendix M. The D_{CL} and D_{DL} were also determined for the calibration curve as explained in Section 4.4. Appendix E outlines the calculation of these values.

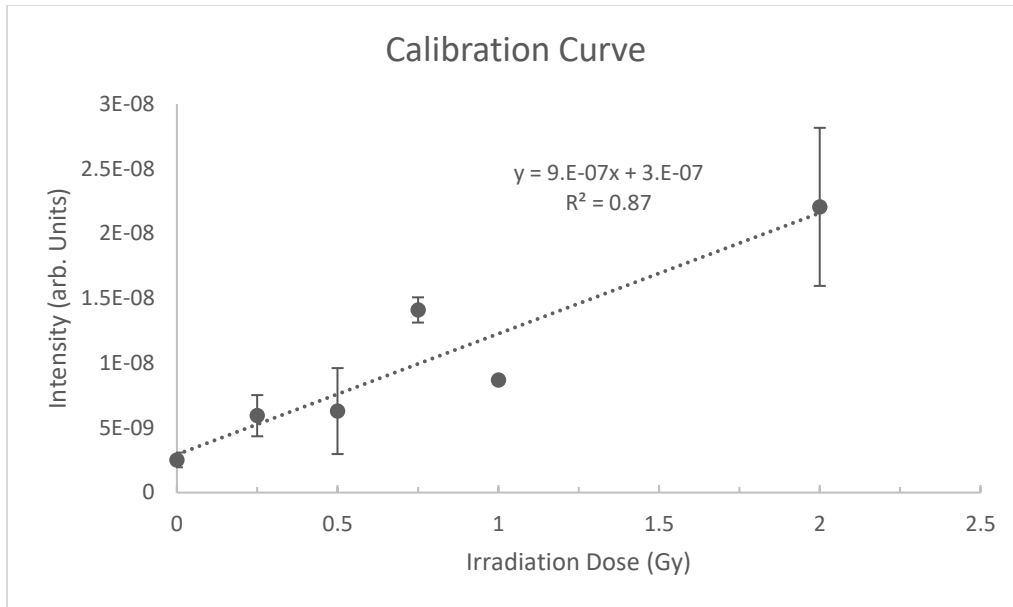


Fig. 6.2 Graph of RIS versus irradiation dose (unadjusted) for the calibration curve samples.

6.5 Results

Assumptions for linear regression analysis including: normality, independence, equality of variance and linear response, were validated, and results can be found in Appendix J along with correlation test results for dose versus RIS. The R^2 value for the calibration curve was 0.87, and the R value was 0.93. The radiation sensitivity (slope) for the calibration curve was determined to be $9E-07$ (arbitrary units). The calibration curve enamel mixture retrospective dose was calculated to be $0.3 \text{ Gy} \pm 0.2 \text{ Gy}$ (1σ). D_{CL} and D_{DL} were 1.0 Gy and 1.8 Gy, respectively.

6.6 Discussion and Synthesis of Results

The set of calibration curve samples was created for use in reconstructing doses to the 19 boar detailed in Chapter 3. Linear regression analysis was performed using the data obtained from the RIS of the calibration curve samples in both Excel and RStudio. The R^2 value of 0.87 supports linearity of the calibration curve. The R value of 0.93 is a positive indication of the linear relationship between irradiation dose and intensity of the RIS signal. Linear regression

analysis results are used to determine confidence intervals for EPR reconstructed doses. Due to D_{CL} and D_{DL} values, deviations from linearity, and standard deviations for calibration curve sample intensities, large confidence intervals and uncertainty values in reconstructed doses are expected.

Boar used in this study are of various ages, and due to the nature of the contamination in the Fukushima Exclusion Zone, dose rates that each boar is exposed to may vary widely. Because of this, a standard background dose subtraction may not be appropriate. For that reason, the calculated retrospective dose for the 5-molar enamel mixture was used instead of a zero-dose value for the unirradiated sample. This will allow for reconstructed doses using this calibration curve to be the total dose received by the boar and not the dose above background. Fig. 6.3 shows the dose adjusted calibration curve.

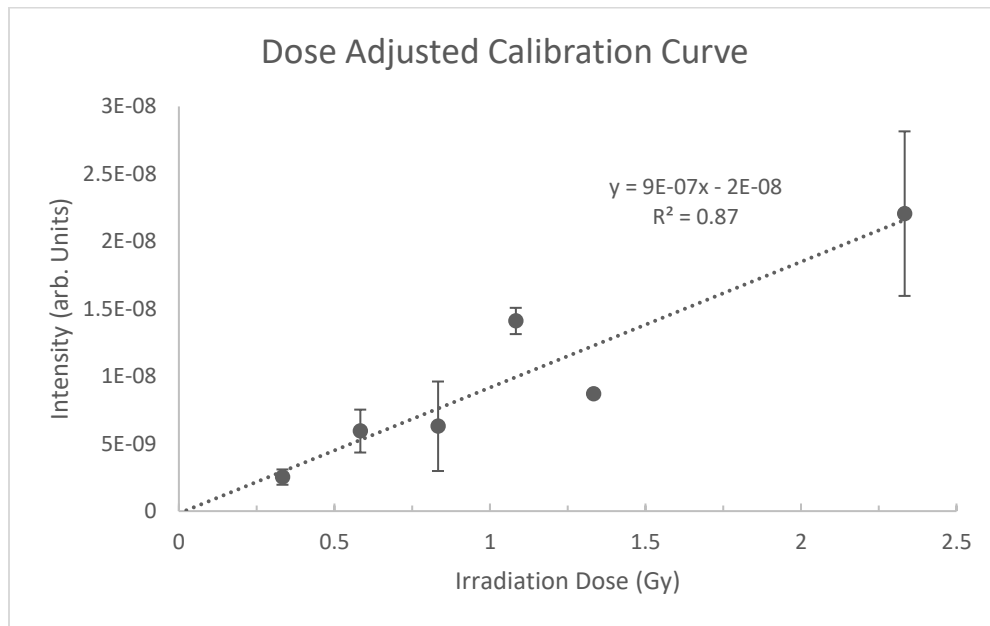


Fig. 6.3 Graph of RIS versus irradiation dose (adjusted) for the calibration curve samples.

6.7 Conclusion

The calibration curve for use in reconstructing doses to wild boar inhabiting the Fukushima Exclusion Zone was created. R^2 and R values indicate a linear response for the

calibration curve samples. D_{CL} and D_{DL} calculated values are larger than the anticipated lifetime doses to the wild boar in this study, which suggests that the calibration curve established would be more useful for reconstructing doses for boar who have received more substantial doses. In order to obtain total dose received, a dose-adjusted calibration curve was constructed. Although EPR dose reconstruction can be performed with this calibration curve, doses calculated will have large associated uncertainty values.

Chapter 7

EPR DOSE RECONSTRUCTION⁸

7.1 Introduction

The ultimate goal of this research endeavor was to use tooth enamel of wild boar as an EPR dosimeter to reconstruct lifetime absorbed doses to Japanese wild boar living in the contaminated areas of the Fukushima Exclusion Zone. In Chapters 4 and 5, suitability of wild boar tooth enamel was established through verification of a linear dose response. Through determination of the variation in radiation sensitivity of wild boar tooth enamel from teeth of the same boar, from boar of different ages, and also through investigation of permanent and deciduous teeth, a suitable EPR dose reconstruction method was chosen. This chapter outlines the completion of the goal of establishing whole body doses to boar exposed to chronic low-level radiation as a result of the nuclear accident at the FDNPP using EPR dosimetry.

7.2 Materials & Methods

7.2.1 Sample Selection

Samples used in this section include 19 boar specimens collected in various areas of Fukushima prefecture, as described in Chapter 3. Sample collection is outlined in detail in Section 3.1, and tooth extractions were performed as described in Section 3.2 and Appendix B.

7.2.2 Sample Preparation

Boar tooth enamel samples used to perform dose reconstructions were prepared using methods described in Section 5.2.2 and in Appendix G.

⁸ Based on: Harshman A, Johnson T. 2018. Dose Reconstruction Using Tooth Enamel from Wild Boar Living in the Fukushima Exclusion Zone with Electron Paramagnetic Resonance Dosimetry. Health Physics Journal. Submitted.

7.3 EPR Sample Measurement

Samples were measured at Colorado State University using a Bruker ELEXSYS II E 500. Section 5.3 lists parameters used to perform the measurements along with procedures used for sample analysis.

7.4 Spectral Processing

EPR Dosimetry Software version 3.3 was used to reconstruct doses to tooth enamel using calibration curve sample measurement data. Dose adjusted calibration curve sample intensity and doses, as well as sample masses, were entered into EPR Dosimetry software to create a calibration curve file for use in converting RIS into absorbed dose. Spectra from each boar tooth enamel sample were loaded into the EPR Dosimetry software, and the empty tube spectrum was subtracted. Masses for each sample being analyzed were also entered. Absorbed doses were determined for each of the three individual repeated sample measurements. Appendix N shows absorbed dose values for each sample along with the average of the three measurements.

7.5 Results

7.5.1 Determination of Retrospective Doses

Average values for tooth enamel dose for each boar were used to determine whole body doses. Whole body doses to the boar were calculated using a tooth enamel to effective dose ratio of 0.90 for 662 keV photons (Takahashi et al., 2001). Table 7.1 shows reconstructed doses to enamel as well as whole body doses received by the boar in this study.

Table 7.1. Summary of data for boar whose doses were reconstructed.

^a Estimated ages, ^b Control boar ^c Measurements taken at boar capture site using a Hitachi TCS-172 NaI Scintillation Survey meter, ^d Estimated using collection site dose rate and estimated age of boar, neglecting possible contribution from internally deposited radionuclides. ^e Values calculated using an enamel to effective dose ratio of 0.90 (Takahashi et al., 2001) at the 90% Confidence Interval (Nagy, 2000) *Data not available. **EPR signal contained iron and a dose could not be reconstructed.

Sample Number	Estimated Age ^a	Collection Site	GPS Coordinates	Dose Rate (μ Gy/hr) ^c	Estimated Lifetime dose (Gy) ^d	EPR Estimated Lifetime Dose to Enamel (Gy)	Estimated Whole Body Dose to Boar (Gy) ^e
170609 B-1	*	*	*	*	*	0.5	0.4 \pm 0.6
Ba20170605	26 weeks	Namie	N37.48048, E140.98898	3.05	0.014	0.3	0.3 \pm 0.6
Ba20170608	30 weeks	Namie	N37.48922, E140.99678	0.34	0.002	0.2	0.2 \pm 0.6
Ba20170609	4 years	Namie	N37.46531, E 140.92621	8.1	0.492	2.7	2.4 \pm 0.7
Bb20170609	47-52 weeks	Namie	N37.47610, E 141.00615	0.68	0.006	0.2	0.1 \pm 0.6
Ba20170615 ^b	>220 weeks	Fukushima	N37.76129, E140.49994	0.46	0.031	0.4	0.4 \pm 0.6
Ba20170616	47-52 weeks	Namie	N37.47610, E141.00615	0.68	0.006	0.6	0.5 \pm 0.5
Bb20170616	62 weeks	Namie	N37.49222, E141.00841	0.14	0.002	0.8	0.8 \pm 0.5
Ba20170617 ^b	26 weeks	Soma	N37.75646, E 140.98490	0.09	0.0004	0.2	0.2 \pm 0.6
Ba20170620	62 weeks	Namie	N37.46532, E140.92326	10.1	0.123	0.3	0.2 \pm 0.6
Ba20170623	127 weeks	Namie	*	0.98	0.029	0.4	0.4 \pm 0.6
Bb20170623	88-106 weeks	Namie	N37.59710, E140.78300	2.98	0.062	0.2	0.2 \pm 0.6
Ba20170627	62 weeks	Namie	N37.46444, E140.92354	10.5	0.128	0.6	0.6 \pm 0.5
Ba20170704	56-62 weeks	Namie	N37.28049, E140.55695	10.5	0.121	0.4	0.4 \pm 0.6
Ba20170717	57-61 weeks	Namie	N37.50570, E140.95948	1.7	0.020	**	**
Bb20170717	127 weeks	Namie	N37.48788, E140.96959	0.75	0.022	0.5	0.4 \pm 0.6
Bc20170717	127 weeks	Namie	N37.47685, E141.00258	0.35	0.010	0.5	0.4 \pm 0.6
Ba20170720	*	Namie	N37.29833 E141.01931	0.12	*	0.2	0.1 \pm 0.6
Ba20170724	*	Namie	N37.48092 E140.98351	2.8	*	0.2	0.2 \pm 0.6

7.5.2 Measurement Uncertainty

Confidence intervals for reconstructed doses using the calibration curve method were calculated using the approach described in Nagy (2000). The approach used takes into account the fit and slope of the linear regression line as well as the number of calibration points and number of repeated measurements performed on each sample (Nagy, 2000). A detailed explanation of reconstructed dose confidence interval calculations can be found in Appendix O.

7.6 Discussion and Synthesis of Results

EPR reconstructed whole body doses were compared with doses estimated based on collection site dose rates and the age of the boar, which are shown in Table 3.1. Whole body doses have large associated uncertainty values. Estimates for lifetime dose to the boar using age and collection site dose rates are generally within the calculated confidence interval for whole body doses. Note that collection site dose rates used were adjusted for radioactive decay based on effective half-life of air dose rates, which was calculated using available Fukushima Prefectural Government data (Fukushima prefecture radioactivity measurement map, 2018) as shown in Appendix P.

There are several possible factors that could contribute to the difference in estimated and reconstructed doses. As discussed in Chapter 4, collection site dose rates may not be representative of typical exposure dose rates to boar due to roaming ranges of the boar and due to inhomogeneity of dose rates in the Fukushima Exclusion Zone. Additionally, radionuclides incorporated into the body in bone, tooth enamel, or muscle, could also contribute to EPR reconstructed doses which are not accounted for when using estimates based on air dose rates. Furthermore, consumption of contaminated food or preferential chewing on one side of the mouth could have contributed to reconstructed doses to tooth enamel.

Calculated values for D_{CL} and D_{DL} , 1.0 Gy and 1.8 Gy, were generally considerably higher than whole body reconstructed doses. This result suggests that although it is possible to reconstruct doses using tooth enamel from wild boar, presently this method would be most advantageous for exposures exceeding 1.0 Gy.

Because of the considerable number of samples used in this study, the calibration curve method was selected to perform the dose reconstructions. The level of variation in radiation

sensitivity in the teeth of wild boar results in larger uncertainty values for dose estimates when using this method. Alternately, utilizing the additive dose method would serve to reduce the associated uncertainty for the EPR reconstructed doses. Comparison of doses reconstructed using the additive dose method in Table 5.1 compared to the calibration curve method shown in Table 7.1 demonstrate that they are equivalent.

7.7 Conclusion

Lifetime whole-body doses were reconstructed for 18 of the 19 boar collected for use in this study. Although it is possible to use wild boar tooth enamel as an EPR dosimeter, techniques presently used result in reconstructed doses with large corresponding uncertainty values. Doses reconstructed using the calibration curve method were nearly equal to doses estimated using the additive dose method as discussed in Chapters 4 and 5. Lifetime doses estimated using collection site dose rates, accounting for radioactive decay using effective half-life of air dose rates, were generally within two orders of magnitude of EPR reconstructed doses. This comparison shows that an internal component to tooth enamel irradiation may have contributed to reconstructed doses determined using EPR dosimetry.

Chapter 8

CESIUM-137 ANALYSIS

8.1 Introduction

The release of radioactive materials that occurred as a result of the nuclear accident at the FDNPP resulted in widespread contamination of the environment, details of which were discussed in Chapter 1. Although a number of different radionuclides were released, ^{137}Cs is of particular concern due to its long half-life, and because it can bioaccumulate in organisms. Additionally, ^{137}Cs has been shown to accumulate in mushrooms and other fungi (Yamada, 2013). Because boar consume mushrooms and root around in forest soil (Piattoni et al., 2016), it is possible that they also consume contaminated dirt, which can result in the presence of ^{137}Cs on tooth enamel. ^{137}Cs contamination of tooth enamel, if present, would add another source of exposure in addition to external exposures from environmental contamination. To help ensure that reconstructed doses to boar tooth enamel originated from external sources, teeth used in this project were analyzed for the presence of ^{137}Cs .

8.2 Materials & Methods

8.2.1 Tooth Selection

To ensure identification of ^{137}Cs in the teeth of wild boar used in this study, enamel samples from each of the 19 boar were selected and placed in small plastic bags. Samples within individual bags were combined for analysis to ensure greater probability of detection in the event that ^{137}Cs was present in the tooth enamel in quantities too low to be detected in individual samples. Analysis was performed on the aggregate samples.

8.2.2 Detector System and Software

The ^{137}Cs analysis was performed at Colorado State University using a 3 in \times 3 in Sodium Iodide (NaI) detector. The NaI detector was surrounded by lead shielding to minimize effects of background radiation. ProSpect software was used to obtain spectral information and sample count data.

8.3 Sample Measurement

ProSpect software was used to perform the measurements with a NaI detector. Necessary parameters were adjusted including count time (24 hours) and detector high voltage setting (1300 volts). A 24-hour background count was performed to establish baseline counts. Tooth enamel samples were combined and placed inside the lead shielding compartment adjacent to the NaI detector and a lead lid was placed on top of the samples. Sample measurements were then performed for 24 hours.

8.4 Results

Appendix Q shows results for channel versus counts for the 24-hour background measurement and the 24-hour combined sample measurement, and results are displayed in Figs. 8.1 and 8.2. Background counts were subtracted from sample counts to obtain net counts in order to determine whether radionuclides were present in tooth enamel samples. Results for net counts are shown in Fig. 8.3.

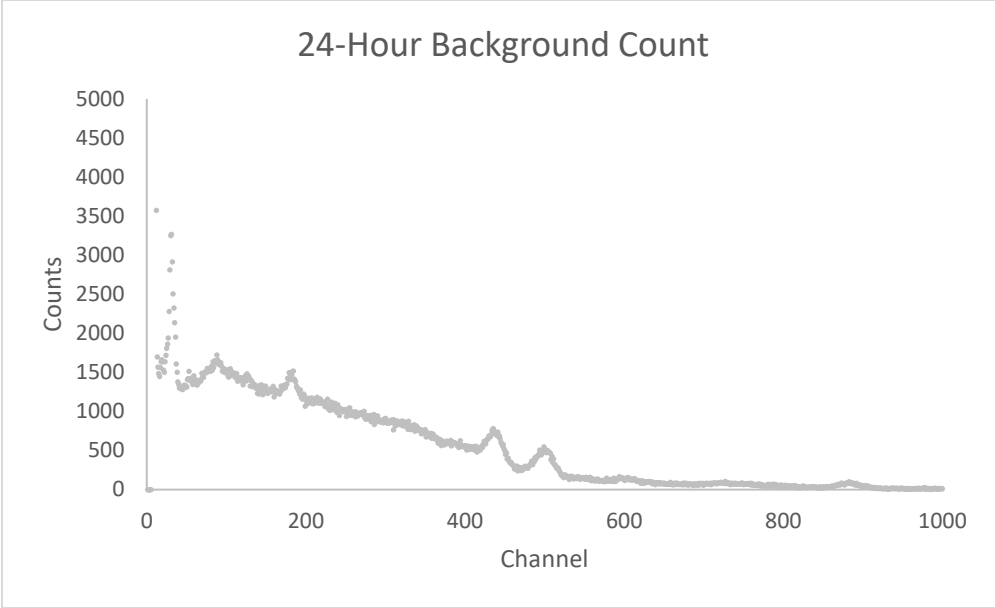


Fig. 8.1. Spectrum for the 24-hour background count of the empty NaI detector.

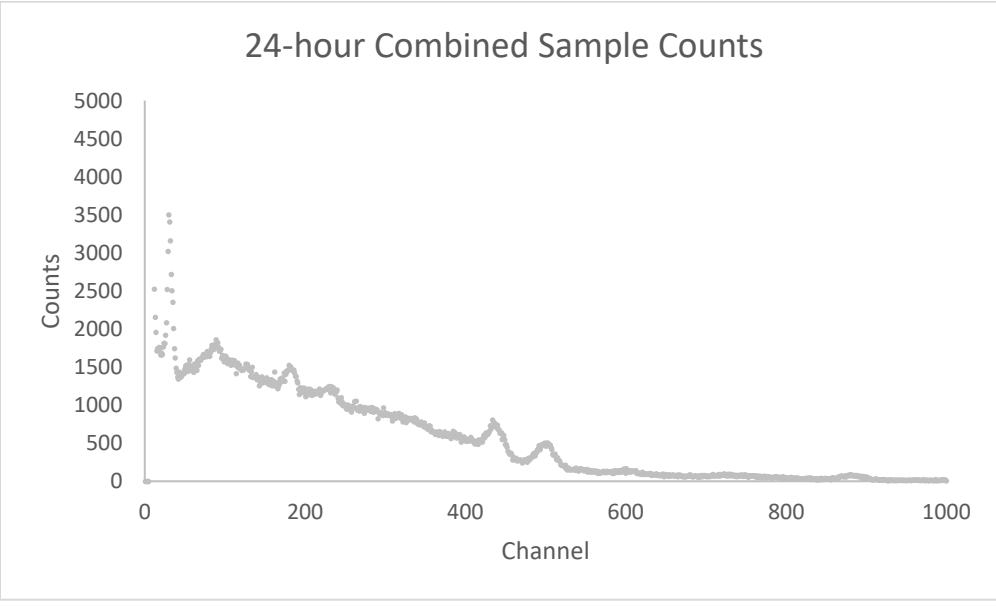


Fig. 8.2. Spectrum for the 24-hour count of the combined tooth enamel samples.

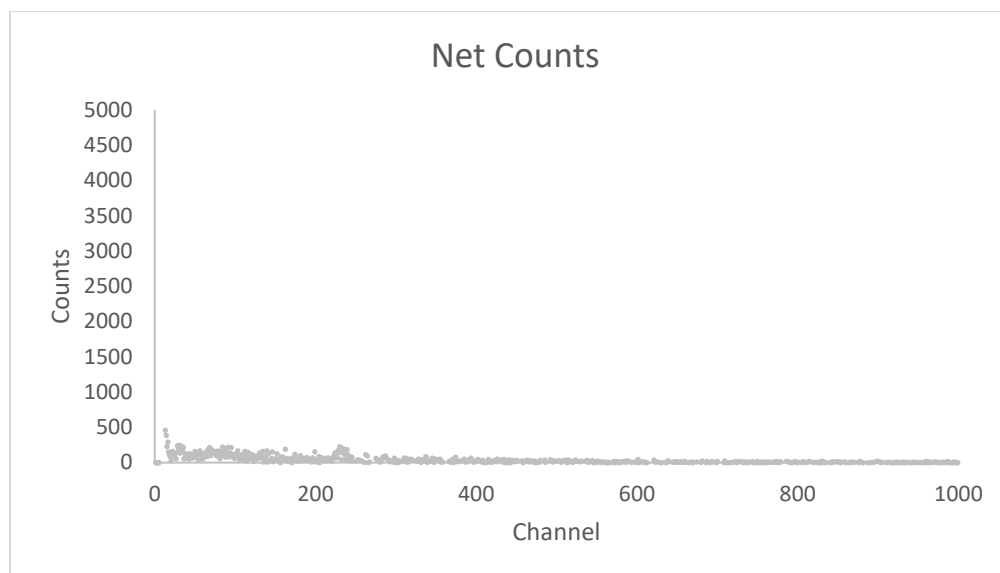


Fig. 8.3 Remaining counts after the 24-hour combined tooth enamel sample counts were subtracted from the 24-hour background count.

8.5 Discussion

No visible peaks were present in the combined sample count spectrum that were not present in the background spectrum. Background counts for all channels totaled 2,083,481 and combined sample counts totaled 1,157,475. Subtraction of background counts from combined sample measurement counts results in several channels with negative values. Background counts were likely higher than sample counts due to normal fluctuations in background and because only background levels of radioactivity were present in the samples.

8.6 Conclusion

Results of spectra and counts for the background measurement and combined sample measurements indicate the absence of ^{137}Cs in tooth enamel samples used for this research. This step is necessary in order to verify that major contributions to EPR reconstructed doses to tooth enamel are from external sources and not radionuclides within or on the tooth enamel surface. Further measurements should be conducted to determine the presence of other radionuclides of concern such as ^{90}Sr .

Chapter 9

STRONTIUM-90 ANALYSIS

9.1 Introduction

An added consideration that can have a substantial impact on the measured accumulated EPR dose is the presence of radionuclides embedded in the teeth, such as ^{90}Sr , which can result in additional radiation exposures that contribute to the overall dose that is established. When radionuclides such as ^{90}Sr are ingested, they can become embedded in the teeth of an animal. Additionally, ingested ^{90}Sr is metabolized in the body as if it were calcium and is also integrated into bones. Furthermore, if radionuclides are ingested during calcification, they can become assimilated into the tooth (Klevezal et al., 1999), generating an additional source of radiation not representative of external sources.

9.2 Materials & Methods

9.2.1 Tooth Selection

A previous study performed by Toyoda et al. (2010) which analyzed the teeth of cows exposed to ^{90}Sr found that ^{90}Sr was predominantly located in secondary dentin and to a lesser extent in the hydroxyapatite crystal of the tooth enamel (Toyoda, et al., 2010). However, another study conducted by Romanyukha et al. (2002) showed that areas of concentration varied based on the stage of tooth formation (Romanyukha, et al. 2002). Therefore, unprocessed, sterilized, whole teeth were used to determine the presence of ^{90}Sr . A portion of a whole tooth taken from each boar listed in Table 3.1 was used for analysis.

9.2.2 The Autoradiography Method

The technique of autoradiography was used to detect the presence of ^{90}Sr in the tooth samples used in this study. With this method, samples are placed on a screen containing phosphor crystals. Energy emitted by radioactive particles contained in a sample is absorbed by the phosphor crystals. The phosphor screen is then scanned using a red laser, which causes the absorbed energy to be re-emitted. The emission will appear on the phosphor screen in the same position as the radionuclide present in the sample (PerkinElmer, 2006). The re-emitted light intensity is proportional to the radionuclide activity within a sample and this allows for its quantification when compared with a standard (PerkinElmer, 2006).

9.3 Sample Measurement

Tooth enamel segments were placed on a PerkinElmer Super Resolution (SR) medium size storage phosphor screen (PerkinElmer, Downers Grove, IL) made of BaFBR:Eu²⁺ (PerkinElmer, 2006). The storage phosphor screen was positioned inside a Fisher Biotech Autoradiography cassette (Fisher Scientific, Pittsburgh, PA). A layout of the configuration is shown in Fig. 9.1. The autoradiography cassette was then closed to prevent light from entering and interfering with the measurement. Samples remained inside the cassette for a period of 3 days to allow any radioactivity present to create a latent image. At the conclusion of the monitoring period, the tooth segments were removed. The SR storage phosphor screen was subsequently placed on a carousel drum and put inside a Cyclone® Scanner (PerkinElmer, Downers Grove, IL) to be analyzed. The SR storage phosphor screen was then scanned by the reader using a red laser (PerkinElmer, 2006).

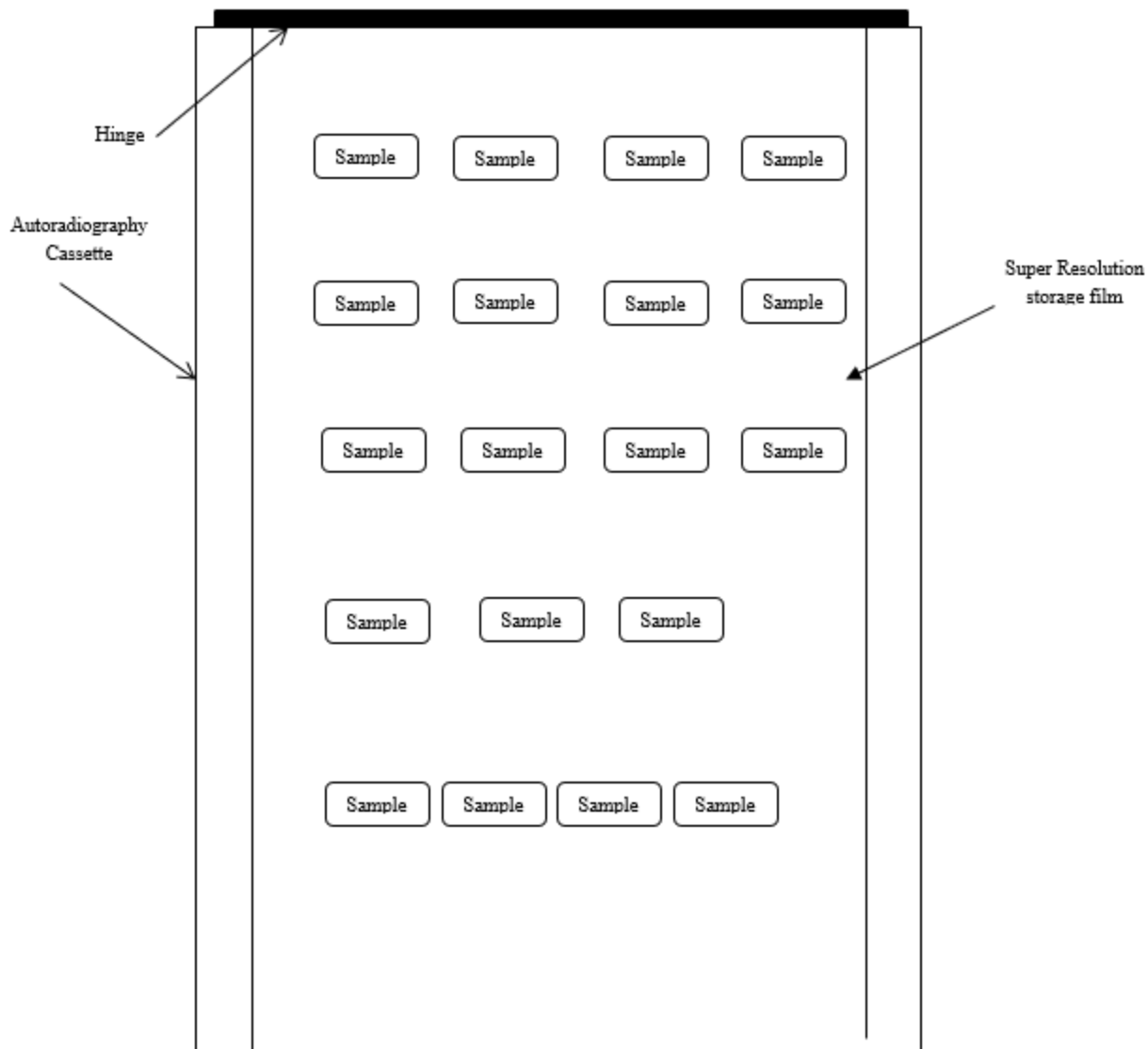


Fig. 9.1. Diagram of tooth segment placement for ^{90}Sr analysis using a PerkinElmer Super Resolution storage screen

9.4 Results

Analysis for the presence of any radionuclides was carried out using PerkinElmer OptiQuant™ Image Analysis Software (PerkinElmer, Downers Grove, IL). Appendix S shows the results for a 3-day background exposure measurement as well as from the 3-day sample exposure measurement. Results of the analyses are shown in Figs. S.1 and S.2, and the numerical data is presented in Table S.1.

9.5 Discussion

No discernable patterns or areas of increased intensity appeared in the 3-day background measurement image shown in Fig. S.1. There were, however, a small number of areas of increased intensity in the sample measurement image shown in Fig. S.2. Visual and numerical comparisons were performed between the background measurement image and the sample measurement image. The visual comparison showed that the background measurement is nearly indistinguishable from sample measurement results in almost all areas, suggesting only background levels of radioactivity were present in the samples, with the exception of a small number of teeth which showed activity levels slightly above background. This result is further corroborated by the net counts in the imaging screen regions as shown in Table S.1. In order to quantify activity levels present in the teeth, a standard sample can be measured and used to compare the activity in the standard sample in digital light units per mm² (DLU/mm²) to the areas of increased intensity for each tooth sample.

9.6 Conclusion

The results of analysis of the SR storage screen using the Cyclone® Scanner and OptiQuant™ Image Analysis Software revealed a few distinct areas of higher intensity indicating the presence of radioactivity above background levels for a small number of the 19 teeth measured. These results, combined with the results of Chapter 8: “Cesium-137 Analysis”, imply that the reconstructed EPR doses do not contain significant contributions from radionuclides embedded in tooth samples or on the surface. Although other sources of internally deposited radionuclides are expected to contribute to the EPR reconstructed doses to tooth enamel to some extent, external sources are still believed to be the biggest contributor.

Chapter 10

IMPROVEMENT OF METHODS

10.1 Introduction

EPR dosimetry using human tooth enamel as a dosimeter is a well-established technique. Characteristics of human teeth are well-known, and doses as low as 100 mGy have been reconstructed (IAEA, 2002). Multiple comparison studies have been conducted in order to harmonize techniques used to improve results of dose reconstructions using human teeth as dosimeters (Chumak et al., 1996; Wieser et al., 2000; Fattibene et al., 2011; Wieser et al., 2005). As mentioned previously, tooth enamel of wildlife has been studied much less. The methods used in the present work to analyze tooth enamel of wild boar are still in need of much refinement, as can be seen by large uncertainty values in reconstructed doses as well as large relative values in critical level doses and detection limit doses. An evaluation of techniques used in this study and possible areas for improvement are detailed in this chapter.

10.2 Improvement of Methods

10.2.1 Samples

There are several areas for improvement which have been identified related to samples used in this research which would allow for more reliable doses to be reconstructed. The first item which has been identified is the number of teeth used in this study to determine wild boar tooth enamel radiation sensitivity. In each segment of the dose response investigation, as outlined in Chapters 4 and 5, two teeth from four boar were used, for a total of 16 teeth. It would have been judicious to investigate pre-molars and molars from the same boar, as well as molars and pre-molars in different positions within the mouth to compare radiation sensitivity.

Additionally, further investigation of radiation sensitivity of deciduous versus permanent teeth could have resulted in more statistically significant results as the p-value in the comparison of the two types of teeth was 0.03. Likewise, investigation of the dose response of teeth with additional wear and discoloration versus sound teeth in wild boar could have further supported the theory that the factor most influencing the difference in radiation sensitivity of deciduous and permanent teeth is the condition of the tooth enamel in older boar. Having a larger number of teeth from additional boar for analysis would have provided additional data points with which to strengthen results obtained.

The number of control boar collected from non-contaminated areas around Fukushima Prefecture or other areas of Japan was insufficient to provide the necessary tooth enamel to prepare ideal samples for use in constructing a calibration curve. As a result, tooth enamel from boar with minimal initial doses from the contaminated areas of Fukushima Prefecture were used. Background doses accumulated by the teeth used to prepare calibration curve samples may not have been representative of background doses to boar living in non-contaminated areas. Because calibration curve samples had initial accumulated doses from a variety of different background dose rates, an adjusted calibration curve was used. Collection of a greater number of control boar for use in constructing calibration curves would have been a benefit to this research.

10.2.2 Experimental Design

There are several aspects of the experimental design which could be adjusted to produce dose estimates with smaller confidence intervals. First, increasing the number of times a measurement is repeated for a particular sample will reduce the uncertainty in the reconstructed dose (Nagy, 2000). Secondly, careful selection of irradiation doses for the calibration curve samples can produce a smaller confidence interval. Specifically, it was shown by Nagy (2000),

that use of a wide range of irradiation doses and by selecting irradiation doses close to the end points will result in smaller confidence intervals for the reconstructed doses. Using a greater number of irradiation doses for the calibration curve will produce improved results, however the improvement will not be as large as with other methods discussed (Nagy, 2000).

10.2.3 Least Squares Regression Analysis

An unweighted least squares linear regression analysis was performed on the calibration curve sample EPR intensity results. The least squares regression analysis assumes that assumptions of the model are met by the data being analyzed. This includes: normality, independence, equality of variance and a linear response, as discussed in Chapter 4. Appendix J shows results of the analysis for linear regression assumptions for the calibration curve samples. Each assumption is met, although variance among the samples is approximately equal. Using a weighted least squares regression may produce more favorable results with regards to uncertainty values in reconstructed doses as well as in critical level doses and detection limit doses for the calibration curve used (Nagy, 2000; Fattibene et al., 2011).

10.2.4. Dose Reconstruction Method Used

The calibration curve method of dose reconstruction was used to determine lifetime doses to wild boar in this project. As discussed in Chapter 2, the calibration curve method is appropriate for tooth enamel with a moderate variation in radiation sensitivity. The additive dose method would also have been appropriate for wild boar tooth enamel; however, this method is significantly more time consuming. Although it has been shown that the accuracy of EPR reconstructed doses are not significantly impacted based on the specific dose reconstruction method used (Wieser et al., 2000), the additive dose method may produce more favorable results considering the range of degree of variation between tooth samples studied in Chapters 4 and 5.

10.3 Conclusion

Dose reconstruction results and associated uncertainty values calculated using the methods outlined throughout this work have the opportunity to be improved through adoption of several factors. A greater number of teeth should be used during investigation of tooth enamel characteristics. Collection of a larger number of control boar would allow for more tooth enamel exposed to lower background doses to be available for use in developing calibration curves. Experimental design has the ability to affect the reliability of the results of dose reconstructions, and as such, calibration irradiation doses and number of measurements should be chosen carefully. Furthermore, data must be analyzed to determine if a weighted or unweighted linear regression analysis is more appropriate to produce the best results. Finally, if used, the additive dose method may produce results with greater certainty in reconstructed doses.

Chapter 11

SUMMARY AND CONCLUSIONS

11.1 Introduction

Much work has been performed in the past which has investigated the characteristics of a number of different materials for use as EPR dosimeters, including human teeth as well as the tooth enamel of several different types of wildlife. Much has been learned from past work, however, further studies are needed to determine the characteristics of tooth enamel of individual animal species. Having the ability to use tooth enamel from a variety of species receiving an unintended exposure to ionizing radiation will allow for more reliable and expedient dose reconstructions. The goal of the work outlined in previous chapters was to validate the appropriateness of use of wild boar tooth enamel for this purpose, and to reconstruct doses to wild boar exposed to radiation while living in the Fukushima Exclusion Zone. Ultimately, data collected and conclusions drawn throughout this project will reinforce past work on this topic.

11.2 Characteristics of Wild Boar Tooth Enamel

Several characteristics of wild boar tooth enamel were investigated in the 0.25 -12.0 Gy range. Tooth enamel of wild boar was confirmed to have a dose response which is linear. R^2 values ranged from 0.75 – 0.99, and R values ranged from 0.87 - 0.99. Comparison of radiation sensitivity of tooth enamel taken from a single boar showed a range in variation of 3.4 – 79.9%, with a 30% average value. Analysis of radiation sensitivity of permanent teeth compared to deciduous teeth showed a statistically significant difference, with deciduous teeth exhibiting greater sensitivity and a smaller degree of variation in enamel originating from the same boar. There was no statistically significant difference in tooth enamel radiation sensitivity of wild boar

based on sex or age. As a result of these findings, tooth enamel of wild boar was determined to be a suitable material for use as an EPR dosimeter.

11.3 Dose Reconstruction of Lifetime Doses to Wild Boar using EPR Dosimetry

Tooth enamel of wild boar demonstrated a moderate average variation in dose response, as discussed in the previous section. As a result, the calibration curve method was selected to reconstruct lifetime doses to tooth enamel, which were then converted into whole body doses. Linear regression analysis and resulting coefficients were used to establish confidence intervals for reconstructed doses, as well as the critical level dose (D_{CL}) and detection limit dose (D_{DL}) for the calibration curve used. Doses were successfully reconstructed for 18 of the 19-boar collected using calibration curve data and EPR Dosimetry software. Confidence intervals for reconstructed doses were relatively large. D_{CL} and D_{DL} values for the calibration curve are a clear indication that present methods will produce more reliable results for lifetime absorbed doses that are predicted to be on the order of 1.0 Gy or more. Several modifications for individual research design elements were identified which, if adopted, could improve results of future work.

11.4 Future Work

Recommendations for future work include investigation of a greater number of teeth, which would serve to further establish the accuracy and reliability of the results described in this study. Additionally, analysis of tooth enamel of an expanded set of wildlife species will allow the method of dose reconstruction using EPR dosimetry to be utilized in potential future situations where unintended exposures to the environment and biota occur. Adoption of suggested improvements to current methods described in Chapter 10 will allow for more reliable results to be obtained including: use of a larger number of control teeth with lower background doses, construction of newly designed calibration curves, or implementation of the additive dose

method of dose reconstruction. Furthermore, exploration of the dose response of wild boar tooth enamel compared to human tooth enamel may allow wild boar to be used as a surrogate if it becomes necessary in a nuclear or radiological accident situation. Finally, determination of individual components which contribute to EPR reconstructed doses such as: ^{137}Cs present in muscle tissue, ^{90}Sr in adjacent bone tissue of mandibles, and exposure of tooth enamel during consumption of contaminated food, may produce results more representative of actual whole-body doses to an animal. It is the hope that the findings of the present study, as well as any future work conducted, will contribute to the goal of establishing a method of reconstructing doses in wildlife, ultimately helping to bridge knowledge gaps regarding chronic low-dose exposures and resulting biological effects.

References

- Brady JM., Aarestad NO, Swartz HM. In Vivo Dosimetry by Electron Spin Resonance Spectroscopy. *Health Physics* 15(1): 43-47; 1968.
- Brenner DJ, Doll R, Goodhead DT, Hall EJ, Land CE, Little JB, Lubin JH, Preston DL, Preston RJ, Puskin JS, Ron E, Sachs RK, Samet JM, Setlow RB, Zaider M. Cancer risks attributable to low doses of ionizing radiation: Assessing what we really know. *Proceedings of the National Academy of Sciences of the United States of America* 100(24): 13761-13766; 2003.
- Brik A, Baraboy V, Atamanenko O, Shevchenko Y, Brik V. Metabolism in tooth enamel and reliability of retrospective dosimetry. *Applied Radiation and Isotopes* 52(5): 1305-1310; 2000.
- Bugai A., Baryakhtar VG, Baran N, Bartchuk V, Kolesnik S, Maksimenko V, Zakcharash MP, Berezhnoy AB, Ostapenko AN, Gaitchenko V, Radchuk V. ESR/tooth enamel dosimetry application to Chernobyl case: individual retrospective dosimetry of the liquidators and wild animals. The radiological consequences of the Chernobyl accident. Minsk. 1049-1052; 1996.
- Chino M, Nakayama H, Nagai H, Terada H, Katata G, Yamazawa H. Preliminary Estimation of Release Amounts of ¹³¹I and ¹³⁷Cs Accidentally Discharged from the Fukushima Daiichi Nuclear Power Plant into the Atmosphere. *Journal of Nuclear Science and Technology* 48(7): 1129-1134; 2011.
- Chumak V, Bailiff I, Baran N, Bugai A, Dubovsky S, Fedosov I, Finin V, Haskell E, Hayes R, Ivannikov A, Kenner G. The First International Intercomparison of EPR-dosimetry with Teeth: First Results. *Applied Radiation Isotopes* 47(11-12): 1281-1286; 1996.
- Dansoreanu IC, Fildan F. Experimental Model for Retrospective Assessment of X-Ray Exposures in Dento-Maxillary Radiology Measured by Electron Paramagnetic Resonance in Tooth Enamel. *Applied Medical Formatics* 25(3,4): 75-83; 2009.
- Eaton GR, Eaton SS, Barr DP, Weber RT. *Quantitative EPR*. Springer Science + Business Media, 2010.
- Fattibene P, Callens F. EPR dosimetry with tooth enamel: A review. *Applied Radiation and Isotopes* 68(11): 2033-2116; 2010.
- Fattibene P, Wieser A, Adolfsson E, Benevides LA, Brai M, Callens F, Chumak V, Ciesielski B, Della Monaca S, Emerich K, Gustafsson H. The 4th international comparison on EPR dosimetry with tooth enamel Part 1: Report on the results. *Radiation Measurements* 46(9): 765-771; 2011.
2018. *Fukushima prefecture radioactivity measurement map*. June 21. <http://fukushima-radioactivity.jp/pc/>.
- Gordy W, Ard WB, Shields H. Microwave Spectroscopy of Biological Substances. I. Paramagnetic Resonance In X-Irradiated Amino Acids and Proteins. *Proceedings of the National Academy of Sciences* 41(11): 983-996; 1955.
- Grant EJ, Brenner A, Sugiyama H, Sakata R, Sadakane A, Utada M, Cahoon EK, Milder CM, Soda M, Cullings HM, Preston DL. Solid Cancer Incidence among the Life Span Study of Atomic Bomb Survivors: 1958–2009. *Radiation Research* 187(5): 513-537; 2017.

- HamsterMap.com. 2018. *HamsterMap.com Custom Map*. Accessed July 2, 2018. <http://www.hamstermap.com/custommap.html>.
- Harshman A, Johnson T. A Brief Review- EPR Dosimetry and the Use of Animal Teeth as Dosimeters. *Health Physics Journal* 115(5): 600-607; 2018.
- Harshman A, Johnson T. 2018. Dose Reconstruction Using Tooth Enamel from Wild Boar Living in the Fukushima Exclusion Zone with Electron Paramagnetic Resonance Dosimetry. *Health Physics Journal*. Submitted.
- Harshman A, Toyoda S, Johnson T. Suitability of Japanese wild boar tooth enamel for use as an Electron Spin Resonance dosimeter. *Radiation Measurements* 116(2018): 46-50; 2018.
- Hasegawa A, Ohira T, Maeda M, Yasumura S, Tanigawa K. Emergency Responses and Health Consequences after the Fukushima Accident; Evacuation and Relocation. *Clinical Oncology* 28(4): 237-244; 2016.
- Hassan GM, Aboelezz E, El-Khodary A, Eissa HM. Inter-comparison study between human and cow teeth enamel for low dose measurement using ESR. *Nuclear Instruments and Methods in Physics Research Section B: Beam Interactions with Materials and Atoms* 268(14): 2329-2336; 2010.
- Hayes RB, Kenner GH, Haskell EH. EPR Dosimetry of Pacific Walrus (*ODOBENUS ROSMARUS DIVERGENS*) Teeth. *Radiation Protection Dosimetry* 77(1-2): 55-63; 1998.
- Hirose K. 2011 Fukushima Dai-ichi nuclear power plant accident: summary of regional radioactive deposition monitoring results. *Journal of Environmental Radioactivity* 111: 13-17; 2012.
- Huang PH, Peng ZC, Jin SZ, Liang RY, Wang ZR. An attempt to determine the archaeological doses of the travertine and the deer horn with ESR. *ESR Dating and Dosimetry*. Ionics, Tokyo 321-324; 1985.
- ICRP. The 2007 Recommendations of the International Commission on Radiological Protection. (ICRP Publication 103). *Annals of the ICRP* 2007; 37:1-331.
- ICRP. Environmental Protection - the Concept and Use of Reference Animals and Plants. (ICRP Publication 108). *Annals of the ICRP* 2008; 38:1-242.
- Ikeya M, Miyajima J, Okajima S. ESR dosimetry for atomic bomb survivors using shell buttons and tooth enamel. *Japanese Journal of Applied Physics* 23(9A): 697-699; 1984.
- Ikeya M, Sumimoto H, Yamanaka C, Lloyd D, Edwards A. ESR dosimetry of a deceased radiation worker. *Applied Radiation and Isotopes* 47(11-12): 1341-1344; 1996.
- International Atomic Energy Agency. Use of electron paramagnetic resonance dosimetry with tooth enamel for retrospective dose assessment. Vienna: IAEA; IAEA-TECDOC-1331. 2002.
- International Atomic Energy Agency. The Fukushima Daiichi Accident Technical Volume 1/5 Description and Context of the Accident. Vienna: IAEA. 2015.
- ISO 13304-1: Radiological protection—minimum criteria for electron paramagnetic resonance (EPR) spectroscopy for retrospective dosimetry of ionizing radiation—part 1: general principles. 2013.
- Ivannikov AI, Skvortsov VG, Stepanenko VF, Tikunov DD, Takada J, Hoshi M. EPR tooth enamel dosimetry: optimization of the automated spectra deconvolution routine. *Health Physics* 81(2): 124-137; 2001.

- Ivannikov A, Tromprier F, Gaillard-Lecanu E, Skvortsov V, Stepanenko V. Optimisation of recording conditions for the electron paramagnetic resonance signal used in dental enamel dosimetry. *Radiation Protection Dosimetry* 101(1-4): 531-538; 2002.
- Jiao L, Liu ZC, Ding YQ, Ruan SZ, Wu Q, Fan SJ, Zhang WY. Comparison study of tooth enamel ESR spectra of cows, goats and humans. *Journal of Radiation Research* 55(6): 1101-1106; 2014.
- Junwang G, Qingquan Y, Jianbo C, Lei M, Guofu D, Guoshan Y, Ke W. New Developed Cylindrical TM010 Mode EPR Cavity for X-Band In Vivo Tooth Dosimetry. *PLOS ONE* 9(9): e106587; 2014.
- Kai A, Miki T, Ikeya M. ESR dating of teeth, bones and eggshells excavated at a Paleolithic site of Douara Cave, Syria. *Quaternary Science Reviews* 7(3-4): 503-507; 1988.
- Khan RF, Rink W, Boreham D. Biophysical dose measurement using electron paramagnetic resonance in rodent teeth. *Applied Radiation and Isotopes* 59(2-3): 189-196; 2003.
- Khan RF, Pekar J, Rink W, Boreham D. Retrospective radiation dosimetry using electron paramagnetic resonance in canine dental enamel. *Applied Radiation and Isotopes* 62(2): 173-179; 2005.
- Klevezal G, Serezhenkov V, Bakhur A. Relationships between ESR-evaluated doses estimated from enamel and activity of radionuclides in bone and teeth of reindeer. *Applied Radiation and Isotopes* 50(3): 567-572; 1999.
- Klevezal G, Bakhur A, Sokolov A, Serezhenkov V, Krushinskaya N. Retrospective Estimation of Radiation Load and Its Effect on Some Biological Parameters of Reindeer (*Rangifer tarandus*) from Wrangel Island. *Russian Journal of Ecology* 32(2): 125-131; 2001.
- Koarai K, Kino Y, Takahashi A, Suzuki T, Shimizu Y, Chiba M, Osaka K, Sasaki K, Fukuda T, Isogai E, Yamashiro H, Oka T, Sekine T, Fukumoto M, Shinoda H. Sr-90 in teeth of cattle abandoned in evacuation zone: Record of pollution from the Fukushima-Daiichi Nuclear Power Plant accident. *Scientific Reports* 6: 24077; 2016.
- Koshta A, Wieser A, Ignatiev E, Bayankin S, Romanyukha A, Degteva M. New computer procedure for routine EPR-dosimetry on tooth enamel: description and verification. *Applied Radiation and Isotopes* 52(2000): 1287-1290; 2000.
- Moller AP, Mousseau TA. Biological consequences of Chernobyl: 20 years on. *Trends in Ecology & Evolution* 21(4): 200-207; 2006.
- Müller R, Schmitz-Feuerhake I. Comparison between deciduous and permanent teeth in relation to their utility for EPR dosimetry. *Proceedings of the International Workshop on the German Society for Radiation Protection Strahlentelex Mit ElektrosmogReport*. University of Portsmouth, Portsmouth, England. 380-381; 1996.
- Murahashi M, Toyoda S, Hoshi M, Ohtaki M, Endo S, Kenichi T, Yamada Y. The sensitivity variation of the radiation induced signal in deciduous teeth to be used in ESR tooth enamel dosimetry. *Radiation Measurements* 106(2017): 450-454; 2017.
- Nagy V. Accuracy considerations in EPR Dosimetry. *Applied Radiation and Isotopes* 52(2000): 1039-1050; 2000.
- Olipitz W, Wiktor-Brown D, Shuga J, Pang B, McFaline J, Lonkar P, Thomas A, Mutamba JT, Greenberger JS, Samson LD, Dedon PC. Integrated Molecular Analysis Indicates Undetectable Change in DNA damage in Mice after Continuous Irradiation at ~400-fold Natural Background Radiation. *Environmental Health Perspectives* 120(8): 1130-1136; 2012.

- PerkinElmer. Cyclone Plus Storage Phosphor System Operation Manual. Doc. Number 1694293 Rev. B. Downers Grove, IL: PerkinElmer Inc. 2006.
- Piattoni F, Ori F, Amicucci A, Salerni E, Zambonelli A. Interrelationships Between Wild Boars (*Sus scrofa*) and Truffles. In *True Truffle (Tuber spp.) in the World*. Springer, Cham, 2016. 375-389.
- Romanyukha A, Regulla D, Vasilenko E, Wieser A. Southern ural nuclear workers: comparison of individual doses from retrospective EPR dosimetry and operational personal monitoring. *Applied Radiation and Isotopes* 45(12): 1195-1199; 1994.
- Romanyukha AA, Mitch MG, Lin Z, Nagy V, Coursey BM. Mapping of Sr-90 distribution in teeth with a photostimulable phosphor imaging detector. *Radiation Research* 157(3): 341-349; 2002.
- Serezhenkov V, Moroz I, Klevezal G, Vanin A. Estimation of Accumulated Dose of Radiation by the Method of ESR-spectrometry of Dental Enamel of Mammals. *Applied Radiation and Isotopes* 47(11-12): 1321-1328; 1996.
- Steinhauser G, Brandl A, Johnson TE. Comparison of the Chernobyl and Fukushima nuclear accidents: A review of the environmental impacts. *Science of the Total Environment* 470(2014): 800-817; 2014.
- Swartz HM. Long-Lived Electron Spin Resonances in Rats Irradiated at Room Temperature. *Radiation Research* 24(4): 579-586; 1965.
- Swartz HM, Molenda RP. Electron Spin Resonance Characteristics of Some Normal Tissues: Effect of Microwave Power. *Science* 148(3666): 94-95; 1965.
- Swartz HM, Molenda RP, Lofberg RT. Long-Lived Radiation-Induced Electron Spin Resonances In An Aqueous Biological System. *Biochemical and Biophysical Research Communications* 21(1): 61-65; 1965.
- Symons M, Chandra H, Wyatt J. Electron Paramagnetic Resonance Spectra of Irradiated Fingernails: A Possible Measure of Accidental Exposure. *Radiation Protection Dosimetry* 58(1): 11-15; 1995.
- Takahashi F, Yamaguchi Y, Iwasaki M, Miyazawa C, Hamada T. Relations Between Tooth Enamel Dose and Organ Doses for Electron Spin Resonance Dosimetry Against External Photon Exposure. *Radiation Protection Dosimetry*, 95(2): 101-108; 2001.
- Thielen H. The Fukushima Daiichi Nuclear Accident—An Overview. *Health Physics* 103(2): 169-174; 2012.
- Toyoda S, Tanizawa H, Romanyukha AA, Miyazawa C, Hoshi M, Ueda Y, Nitta Y. Gamma-ray dose response of ESR signals in tooth enamel of cows and mice in comparison with human teeth. *Radiation Measurements* 37(4-5): 341-346; 2003.
- Toyoda S, Imata H, Romanyukha A, Hoshi M. Toward High Sensitivity ESR Dosimetry of Mammal Teeth: The Effect of Chemical Treatment. *Journal of Radiation Research* 47(SupplementA): A71-A74; 2006.
- Toyoda S, Romanyukha A, Hino Y, Itano S, Imata H, Tarasov O, Hoshi M. Effect of chemical treatment on ESR dosimetry of cow teeth: Application to the samples from Southern Urals. *Radiation Measurements* 42(6-7): 1178-1180; 2007.
- Toyoda S, Hino Y, Romanyukha AA, Tarasov O, Pivovarov SP, Hoshi M. Sr-90 in mammal teeth from contaminated areas in the former soviet union measured by imaging plates. *Health Physics* 98(2): 352-359; 2010.
- United Nations. *Sources and Effects of Ionizing Radiation (Report to the General Assembly)*. New York: Scientific Committee on the Effects of Atomic Radiation (UNSCEAR); 1996

- Wieser A, Romanyukha A, Degteva M, Kozheurov V, Petzoldt G. Tooth enamel as a natural beta dosemeter for bone seeking radionuclides. *Radiation Protection Dosimetry* 65(1-4): 413-416; 1996.
- Wieser A, Mehta K, Amira S, Aragno D, Bercea S, Brik A, Bugai A, Callens F, Chumak V, Ciesielski B, Debuyst R, Dubovsky S, Duliu OG, Fattibene P, Haskell EH, Hayes RB, Ignatiev EA, Ivannikov A, Toyoda S. The second international intercomparison on EPR tooth dosimetry. *Radiation Measurements* 32(5-6): 549-557; 2000.
- Wieser A, Debuyst R, Fattibene P, Meghzifene A, Onori S, Bayankin SN, Blackwell B, Brik A, Bugay A, Chumak V, Ciesielski B. The 3rd international intercomparison on EPR tooth dosimetry: Part 1, general analysis. *Applied Radiation and Isotopes* 62(2): 163-171; 2005.
- Wieser A, Fattibene P, Shishkina E, Ivanov D, De Coste V, Guttler A, Onori S. Assessment of performance parameters for EPR dosimetry with tooth enamel. *Radiation Measurements*, 43(2008): 731-736; 2008.
- Wilson PR, Beynon AD. Mineralization Differences Between Human Deciduous and Permanent Enamel Measured by Quantitative Microradiography. *Archives of Oral Biology* 34(2): 85-88; 1989.
- Yamada T. Mushrooms: radioactive contamination of widespread mushrooms in Japan. In *Agricultural Implications of the Fukushima Nuclear Accident*. Springer, Tokyo, 2013. 163-176.
- Zdravkova M, Gallez B, Debuyst R. A Comparative in vivo and in vitro L-Band EPR study of irradiated rat incisors. *Radiation Measurements* 39(2): 143-148; 2005.

Appendix A
IACUC Exemption

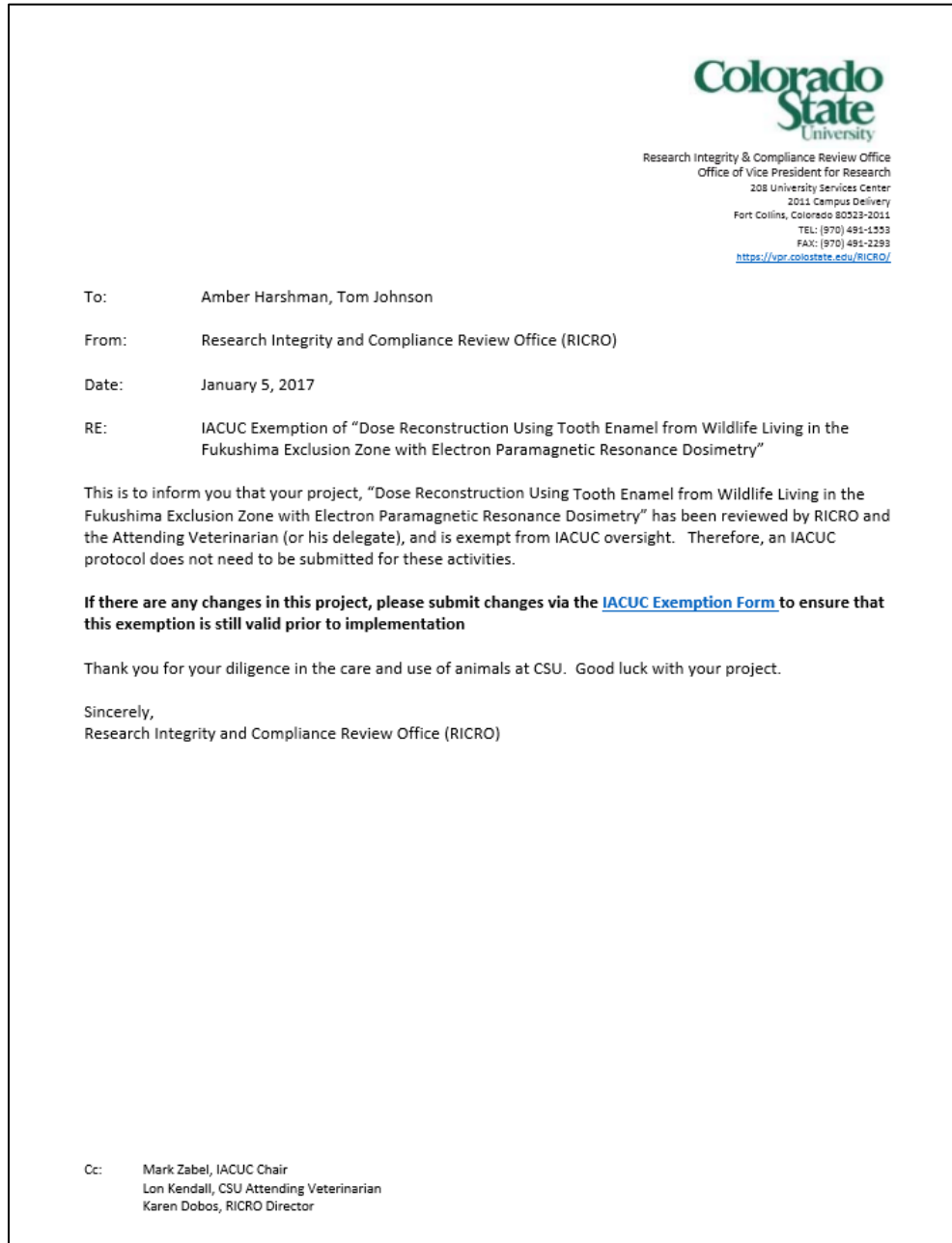


Fig. A.1. IACUC exemption document.

Appendix B

Wild Boar Tooth Extraction Procedure

This sample processing procedure was adapted from the procedures described in IAEA-TECDOC-1331, International Standard ISO 13304-1, EPR Dosimetry with Tooth Enamel: A Review (Fattibene and Callens 2010), as well as multiple studies performed using animal teeth.

B.1 Removal of the Mandible from the Wild Boar

It is important to collect samples as consistently as possible. Data about the samples should be recorded to assist in the dose reconstruction including: sex and estimated age of the specimen, geographic location for the sample collection site, and general area dose rates at the collection site. All samples should be assigned a unique identification number.

1. Once the boar has been sacrificed, remove the mandible. This should be done with an appropriate tool such as a dissection or deboning knife.
2. Once removed, place the mandible in a container or a large Ziploc bag, and label it with a unique identification number.
3. The mandible should be transported to the laboratory with environmental conditions as stable and uniform as possible. Humidity and exposure to light should be kept to a minimum.
4. If not immediately removing the teeth from the mandible, place the mandible in a freezer.

B.2 Removing the Teeth from the Mandible

For this section, a low-speed, water-cooled trim saw should be used such as the one in Fig. B1.



Fig. B.1. Saw used to perform crown amputations.

1. If the mandible is frozen, thaw it prior to proceeding to Step 2.
2. Remove the mandible from the Ziploc bag. Keep the bag for disposal of the mandible waste.
3. Photograph both sides of the mandible for the purpose of tooth identification if desired.
4. Fill the trim saw reservoir approximately half-full with cool water.

Note: Ensure a low speed is used when cutting the teeth from the mandible. It has been suggested not to exceed 10,000 rpm (IAEA, 2002).

5. Using the saw, perform a crown amputation of the desired teeth. It is best to cut the crown as close to the jaw as possible, being careful not to remove jaw bone with the tooth.

Note: Mature wild boar generally have 4 pre-molars and 3 molars on each side of the lower mandible (Fig. B2). Molars are ideal for EPR analysis; however, pre-molars can also be used.

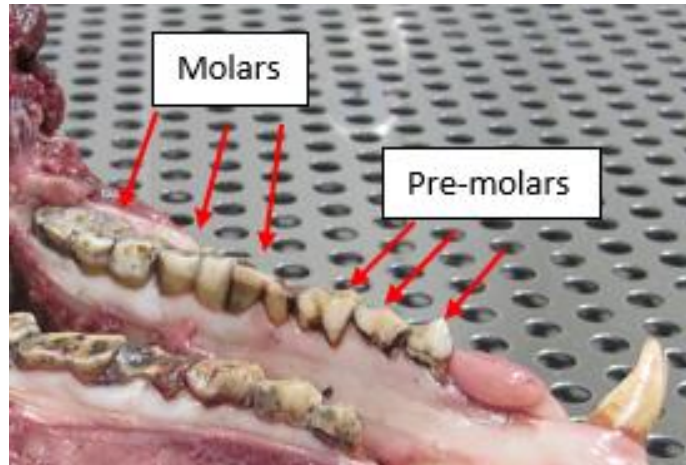


Fig. B.2. Photograph of a boar mandible showing the presence of molars and pre-molars.

6. Place each tooth onto a napkin or paper towel, or if desired, a tooth identification data sheet can be created. Photograph each tooth for the purpose of tooth identification in subsequent steps.
7. Once the crown amputation has been performed and the tooth has been photographed, the samples must be disinfected prior to being prepared for analysis

B.3 Disinfect tooth samples

This section is performed in order to avoid bacterial growth and to kill harmful viruses that may be present in the sample.

1. Place extracted teeth in a container labeled with appropriate sample identification information, in addition to being labeled 'Biohazard' until disinfected.
2. Place a solution containing 1-5% Sodium Hypochlorite diluted with deionized water into the containers until the teeth are submerged in the solution.
3. Allow teeth to remain in the solution for at least 24 hours.
4. Once sterilization is complete, remove the teeth from the containers and pour the used Sodium Hypochlorite solution into a 1L bottle for later disposal.
5. Place teeth on a paper towel to absorb any remaining Sodium Hypochlorite solution.

6. Rinse the teeth with deionized water, and then place on paper towels to absorb any remaining water (Fig. B3).

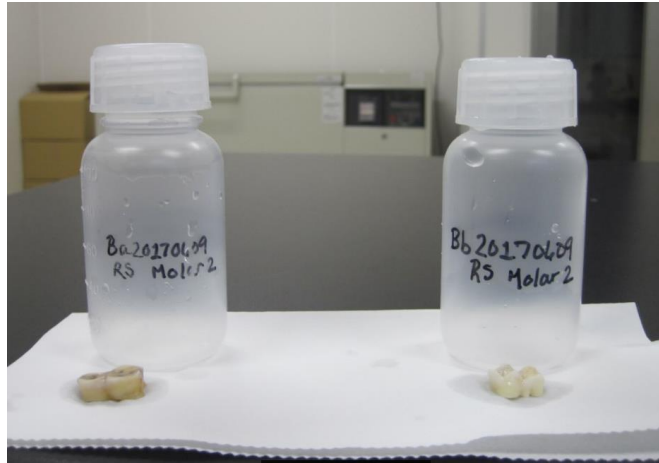


Fig. B.3. Disinfected tooth samples.

7. After the tooth has been disinfected, it should be stored in a plastic container in a dark room with low relative humidity if not immediately performing the “Tooth Sample Preparation Procedure.”

Note: After this step, the tooth is no longer considered to be biohazardous material.

Appendix C

Sample Weights

Table C.1. Individual weights for samples used to establish dose response in the 0.25 – 2.0 Gy region. * Insufficient enamel for sample

	Sample 1 (0.25 Gy)	Sample 2 (0.50 Gy)	Sample 3 (0.75 Gy)	Sample 4 (1.0 Gy)	Sample 5 (2.0 Gy)	Sample 6 (Unirradiated)
Ba20170620 M _{2L}	90.1 mg	90.0 mg	89.9 mg	90.0 mg	90.1 mg	90.1 mg
Ba20170620 M _{2R}	90.0 mg	90.1 mg	90.0 mg	90.0 mg	90.1 mg	90.0 mg
Bb200170623 M _{1L}	90.1 mg	89.9 mg	90.1 mg	87.2 mg	*	90.0 mg
Bb200170623 M _{1R}	90.1 mg	90.1 mg	90.0 mg	80.6 mg	*	89.9 mg
Ba20170627 M _{2L}	90.1 mg	90.1 mg	90.1 mg	90.0 mg	90.1 mg	90.1 mg
Ba20170627 M _{2R}	90.0 mg	90.1 mg	89.9 mg	90.0 mg	90.1 mg	89.9 mg
Bb20170717 M _{3L}	89.9 mg	89.9 mg	89.9 mg	90.0 mg	89.9 mg	90.1 mg
Bb20170717 M _{3R}	89.9 mg	90.0 mg	90.0 mg	90.0 mg	89.9 mg	89.9 mg

Table C.2. Individual weights for samples used to establish dose response in the 1.2 – 12.0 Gy region. * Insufficient enamel for sample

	Sample 1 (1.2 Gy)	Sample 2 (2.2 Gy)	Sample 3 (4.4 Gy)	Sample 4 (7.6 Gy)	Sample 5 (12.0 Gy)	Sample 6 (Unirradiated)
Ba20170608 P _{3L}	90.0 mg	90.0 mg	90.1 mg	90.1 mg	90.0 mg	90.0 mg
Ba20170608 P _{3R}	90.0 mg	90.1 mg	90.0 mg	90.1 mg	90.0 mg	89.9 mg
Ba20170609 M _{3L}	90.0 mg	90.1 mg	90.1 mg	90.1 mg	89.9 mg	90.0 mg
Ba20170609 M _{3R}	90.1 mg	89.9 mg	89.9 mg	90.0 mg	89.9 mg	90.0 mg
Ba20170615 M _{2L}	90.0 mg	90.1 mg	90.0 mg	90.0 mg	90.0 mg	89.9 mg
Ba20170615 M _{2R}	89.9 mg	90.1 mg	89.9 mg	89.9 mg	90.1 mg	89.9 mg
Ba20170617 P _{3L}	89.9 mg	89.9 mg	89.9 mg	90.1 mg	*	90.0 mg
Ba20170617 P _{3R}	90.0 mg	90.1 mg	90.0 mg	90.0 mg	90.0 mg	90.0 mg

Table C.3. Individual weights for calibration curve samples

	Sample 1 (0.25 Gy)	Sample 2 (0.50 Gy)	Sample 3 (0.75 Gy)	Sample 4 (1.0 Gy)	Sample 5 (2.0 Gy)	Sample 6 (Unirradiated)
Calibration Curve Enamel Mixture	90.0 mg	90.1 mg	89.9 mg	90.0 mg	90.1 mg	90.1 mg

Appendix D

EPR Signal Intensities (1.2 – 12.0 Gy)

D.1 Radiation Induced Signal Intensities for Individual Sample Measurements

Table D.1. Averaged Radiation Induced Signal (RIS) Intensities with associated error values (arbitrary units)

Dose (Gy)	Ba20170608 P3L		Ba20170608 P3R		Ba20170609 M3L		Ba20170609 M3R		Ba20170615 M2L		Ba20170615 M2R		Ba20170617 P3L		Ba20170617 P3R	
	RIS	Err	RIS	Err	RIS	Err	RIS	Err	RIS	Err	RIS	Err	RIS	Err	RIS	Err
1.2	102.1	3.93	166.83	3.31	247.09	4.68	243.2	4.45	109.61	3.86	37.67	3.07	262.74	6.43	132.83	2.99
2.2	316.66	4.16	371.94	3.9	454.11	5.68	401.77	5.85	257.84	3.65	66.83	2.96	502.93	4.94	307.26	4.1
4.4	752.11	6.04	591.73	5.61	543.12	6.37	889.69	8.51	382.39	3.33	140.34	3.24	1005.44	7.62	527.99	6.11
7.6	1035.62	6.75	2321.7	17.23	930.99	7.13	1071.19	8.07	793.95	5.32	287.76	3	1592.77	9.9	1080.58	8.42
12	33.08	0.22	1937.59	12.36	1306.11	9.5	2279.79	12.51	974.98	5.07	399.5	3.32	*	*	1813.35	13.66
0	0.11	0.13	14.81	3.73	127.9	4.8	132.25	4.87	16.78	11.74	29.13	3.45	23.76	4.73	5.43	4.36

Table D.2. Normalized Averaged Radiation Induced Signal (N-RIS) Intensities with associated error values (arbitrary units)

Dose (Gy)	Ba20170608 P _{3L}		Ba20170608 P _{3R}		Ba20170609 M _{3L}		Ba20170609 M _{3R}		Ba20170615 M _{2L}		Ba20170615 M _{2R}		Ba20170617 P _{3L}		Ba20170617 P _{3R}	
	N-RIS	Err	N-RIS	Err	N-RIS	Err	N-RIS	Err	N-RIS	Err	N-RIS	Err	N-RIS	Err	N-RIS	Err
1.2	90.36	3.48	142.14	2.82	205.77	3.90	192.23	3.52	104.63	3.69	46.11	3.76	169.41	4.15	137.25	3.09
2.2	218.19	2.87	261.75	2.75	322.17	4.16	317.54	4.62	204.64	2.90	85.79	3.80	320.17	3.14	278.52	3.72
4.4	471.14	3.78	518.28	4.92	461.05	5.41	608.26	5.82	365.34	3.18	183.35	4.24	600.93	4.55	485.21	5.62
7.6	790.98	5.16	1004.08	7.45	812.25	6.22	886.50	6.72	736.62	4.94	306.19	3.19	1046.79	6.51	911.29	7.11
12	1493.98	0.22	1660.32	10.60	1094.31	7.96	1422.81	7.81	1009.68	5.25	456.51	3.79	*	*	1594.76	12.01
0	0.09	0.11	13.48	3.40	103.54	3.89	103.55	3.81	16.57	11.62	38.40	4.55	15.60	3.11	4.39	3.53

D.2 MgO:Mn Standard Marker Intensity Values

Table D.3. Averaged MgO:Mn standard marker Intensity Values (arbitrary units)

	Ba20170608 P _{3L}	Ba20170608 P _{3R}	Ba20170609 M _{3L}	Ba20170609 M _{3R}	Ba20170615 M _{2L}	Ba20170615 M _{2R}	Ba20170617 P _{3L}	Ba20170617 P _{3R}
Dose (Gy)	Intensity							
1.2	1129.96	1173.68	1200.82	1265.16	1047.63	816.97	1550.95	967.77
2.2	1451.31	1420.97	1367.09	1265.26	1259.98	778.97	1570.84	1103.21
4.4	1596.35	1141.73	1178.00	1462.69	1046.66	765.41	1673.13	1088.16
7.6	1309.29	2312.26	1146.18	1208.33	1077.84	939.80	1521.57	1185.77
12	1013.93	1167.00	1193.55	1602.32	965.63	875.12	*	1137.07
0	1170.83	1098.97	1235.26	1277.12	1012.51	758.60	1523.48	1236.38

Table D.4. Normalized Averaged MgO:Mn standard marker Intensity Values (arbitrary units)

	Ba20170608 P _{3L}	Ba20170608 P _{3R}	Ba20170609 M _{3L}	Ba20170609 M _{3R}	Ba20170615 M _{2L}	Ba20170615 M _{2R}	Ba20170617 P _{3L}	Ba20170617 P _{3R}
Dose (Gy)	N-Intensity							
1.2	1.13	1.17	1.20	1.27	1.05	0.82	1.55	0.97
2.2	1.45	1.42	1.37	1.27	1.26	0.78	1.57	1.10
4.4	1.60	1.14	1.18	1.46	1.05	0.77	1.67	1.09
7.6	1.31	2.31	1.15	1.21	1.08	0.94	1.52	1.19
12	1.01	1.17	1.19	1.60	0.97	0.88	*	1.14
0	1.17	1.10	1.24	1.28	1.01	0.76	1.52	1.24

Appendix E⁹

Critical Level Dose (D_{CL}) and Decision Level Dose (D_{DL}) Equations and Values

The following equations were used to calculate D_{CL} (E.1) and D_{DL} (E.3):

$$D_{CL} = \frac{I_{CL} - b_0}{b_1} \quad (E.1)$$

$$\text{Where } I_{CL} = b_0 + t_{(0.95, n-2)} s \sqrt{1 + \frac{1}{n} + \frac{D_M^2}{SSD}} \quad (E.2)$$

and

$$D_{DL} = D_{CL} + \frac{t_{(0.95, n-2)} s}{b_1} \sqrt{1 + \frac{1}{n} + \frac{(D_{DL} - D_M)^2}{SSD}} \quad (E.3)$$

$$\text{Where } SSD = \sum (D_i - D_M)^2 \quad (E.4)$$

$$s = \sqrt{\frac{\sum (I_i - I)^2}{n-2}} \quad (E.5)$$

and

$$I = b_0 + b_1 D \quad (E.6)$$

Definition of Variables:

I – Intensity of the EPR signal

D – Irradiation dose

b_0 – Intercept of the linear regression line

b_1 – Slope of the linear regression line

I_{CL} – EPR signal intensity critical level

t – Student's t-distribution critical value for the single-sided 95% confidence interval

n – Number of irradiation and intensity data points

D_i – Applied irradiation dose

D_M – Mean value of irradiation doses (D_i)

SSD – Equation (4), square sum of the variation in dose

s – Equation (5), standard deviation residual value

I_i – Intensity of the EPR signal at irradiation dose D_i

I – Equation (6), Intensity of the EPR signal determined using the linear regression line and irradiation dose D_i

⁹ (Fattibene et al., 2011)

Table E.1. Values used to calculate Critical Level Dose (D_{CL}) and Decision Level Dose (D_{DL}) for all tooth samples and results

Ba20170608			Ba20170609		
	P_{3L} -RIS	P_{3R} - RIS	M_{3L} -RIS	M_{3R} - RIS	
D	I_i	I_i	D	I_i	I_i
1.2	90.357	142.143	1.2	205.769	192.229
2.2	218.190	261.751	2.2	322.172	317.541
4.4	471.144	518.275	4.4	461.053	608.256
7.6	790.977	1004.081	7.6	812.251	886.504
12.0	1493.975	1660.324	12.0	1094.305	1422.808
0.0	0.094	13.476	0.0	103.541	103.553
b_0	-52.043	-31.432	b_0	116.150	84.262
b_1	123.248	138.272	b_1	84.022	110.410
n	6	6	n	6	6
t	2.132	2.132	t	2.132	2.132
s	63.996	41.631	s	37.297	31.899
D_M	4.570	4.570	D_M	4.570	4.570
D_M^2	20.885	20.885	D_M^2	20.885	20.885
SSD	102.300	102.300	SSD	102.300	102.300
$1 + 1/n$	1.666	1.666	$1 + 1/n$	1.666	1.666
D	I	I	D	I	I
1.2	95.855	134.494	1.2	216.976	216.754
2.2	219.103	272.765	2.2	300.998	327.164
4.4	490.248	576.963	4.4	485.847	570.066
7.6	884.641	1019.433	7.6	754.717	923.378
12.0	1426.932	1627.828	12.0	1124.414	1409.182
0.0	-52.043	-31.432	0.0	116.150	84.262
D	$(I_i - I)^2$	$(I_i - I)^2$	D	$(I_i - I)^2$	$(I_i - I)^2$
1.2	30.223	58.516	1.2	125.617	601.485
2.2	0.834	121.319	2.2	448.313	92.608
4.4	364.977	3444.270	4.4	614.752	1458.472
7.6	8772.990	235.672	7.6	3310.161	1359.692
12.0	4494.737	1055.984	12.0	906.552	185.668
0.0	2718.220	2016.779	0.0	158.992	372.158
Sum	16381.980	6932.539	Sum	5564.387	4070.084
s	63.996	41.631	s	37.297	31.899
I_{CL}	134.543	89.946	I_{CL}	224.894	177.265
D_{CL}	1.514	0.878	D_{CL}	1.294	0.842
D_{DL}	3.028	1.756	D_{DL}	2.588	1.685

	D_{DL} - Iterations			D_{DL} - Iterations	
I-1	2.721	1.594	I-1	2.333	1.530
I-2	2.727	1.596	I-2	2.338	1.533
I-3	2.727	1.596	I-3	2.338	1.533
I-4	2.727	1.596	I-4	2.338	1.533
I-5	2.727	1.596	I-5	2.338	1.533

	Ba20170615	
	M _{2L} - RIS	M _{2R} - RIS
D	I _i	I _i
1.2	104.626	46.110
2.2	204.638	85.793
4.4	365.344	183.353
7.6	736.615	306.194
12.0	1009.680	456.508
0.0	16.573	38.400
b ₀	14.805	18.260
b ₁	85.717	36.744
n	6	6
t	2.132	2.132
s	41.748	15.335
D _M	4.570	4.570
D _M ²	20.885	20.885
SSD	102.300	102.300
1 + 1/n	1.666	1.666
D	I	I
1.2	117.665	62.353
2.2	203.382	99.097
4.4	391.960	179.934
7.6	666.254	297.514
12.0	1043.409	459.188
0.0	14.805	18.260
D	(I _i - I) ²	(I _i - I) ²
1.2	170.021	263.843
2.2	1.576	176.989
4.4	708.427	11.691
7.6	4950.642	75.332
12.0	1137.645	7.185
0.0	3.125	405.610
Sum	6971.436	940.650
s	41.748	15.335
I _{CL}	136.524	62.971
D _{CL}	1.420	1.217
D _{DL}	2.840	2.434

	D _{DL} - Iterations	
I-1	2.556	2.196
I-2	2.560	2.200
I-3	2.560	2.200
I-4	2.560	2.200
I-5	2.560	2.200

	Ba20170617	
	P _{3L} - RIS	P _{3R} - RIS
D	I _i	I _i
1.2	169.405	137.254
2.2	320.167	278.516
4.4	600.934	485.213
7.6	1046.794	911.289
12.0	*	1594.760
0.0	15.596	4.392
b ₀	12.998	-29.603
b ₁	135.580	130.990
n	5	6
t	2.353	2.132
s	11.155	52.851
D _M	3.080	4.570
D _M ²	9.486	20.885
SSD	35.968	102.300
1 + 1/n	1.200	1.666
D	I	I
1.2	175.694	127.585
2.2	311.274	258.575
4.4	609.550	546.753
7.6	1043.406	965.921
12.0	*	1542.277
0.0	12.998	-29.603
D	(I _i - I) ²	(I _i - I) ²
1.2	39.546	93.490
2.2	79.087	397.626
4.4	74.229	3787.165
7.6	11.479	2984.666
12.0	*	2754.465
0.0	168.948	1155.649
Sum	373.289	11173.062
s	11.155	52.851
I _{CL}	44.753	124.490
D _{CL}	0.234	1.176
D _{DL}	0.468	2.353

	D _{DL} - Iterations	
I-1	0.462	2.124
I-2	0.463	2.128
I-3	0.463	2.128
I-4	0.463	2.128
I-5	0.463	2.128

Ba20170620		
	M _{2L} -RIS	M _{2R} -RIS
D	I _i	I _i
0.25	2.80E-07	4.64E-07
0.5	4.23E-07	6.16E-07
0.75	3.72E-07	1.48E-06
1	7.36E-07	1.34E-06
2	1.75E-06	2.95E-06
0	2.18E-07	9.59E-07
b ₀	4.00E-08	4.00E-07
b ₁	8.00E-07	1.00E-06
n	6	6
t	2.132	2.132
s	1.79E-07	4.59E-07
D _M	0.750	0.750
D _M ²	0.563	0.563
SSD	2.5	2.5
1 + 1/n	1.666	1.666
D	I	I
0.25	2.40E-07	6.50E-07
0.5	4.40E-07	9.00E-07
0.75	6.40E-07	1.15E-06
1	8.40E-07	1.40E-06
2	1.64E-06	2.40E-06
0	4.00E-08	4.00E-07
D	(I _i - I) ²	(I _i - I) ²
0.25	1.57E-15	3.44E-14
0.5	3.00E-16	8.08E-14
0.75	7.17E-14	1.08E-13
1	1.08E-14	3.64E-15
2	1.20E-14	3.04E-13
0	3.17E-14	3.12E-13
Sum	1.28E-13	8.42E-13
s	1.79E-07	4.59E-07
I _{CL}	5.65E-07	1.75E-06
D _{CL}	0.656	1.345
D _{DL}	1.312	2.690

	D _{DL} - Iterations	
I-1	1.198	2.944
I-2	1.188	3.066
I-3	1.188	3.125
I-4	1.188	3.155
I-5	1.188	3.170

Bb20170623		
	M _{1L} -RIS	M _{1R} -RIS
D	I _i	I _i
0.25	2.60E-07	4.06E-07
0.5	3.46E-07	5.06E-07
0.75	4.52E-07	5.69E-07
1	4.05E-07	5.86E-07
2		
0	1.99E-07	2.69E-07
b ₀	2.00E-07	3.00E-07
b ₁	2.00E-07	3.00E-07
n	5	5
t	2.353	2.353
s	6.47E-08	4.21E-08
D _M	0.500	0.500
D _M ²	0.250	0.250
SSD	0.625	0.625
1 + 1/n	1.2	1.2
D	I	I
0.25	2.50E-07	3.75E-07
0.5	3.00E-07	4.50E-07
0.75	3.50E-07	5.25E-07
1	4.00E-07	6.00E-07
2		
0	2.00E-07	3.00E-07
D	(I _i - I) ²	(I _i - I) ²
0.25	1.07E-16	9.32E-16
0.5	2.13E-15	3.11E-15
0.75	1.03E-14	1.93E-15
1	2.02E-17	1.90E-16
2		
0	2.05E-18	9.34E-16
Sum	1.26E-14	7.10E-15
s	6.47E-08	4.21E-08
I _{CL}	3.93E-07	4.25E-07
D _{CL}	0.963	0.418
D _{DL}	1.926	0.836

	D _{DL} - Iterations	
I-1	2.569	0.806
I-2	3.123	0.802
I-3	3.623	0.801
I-4	4.083	0.801
I-5	4.513	0.801

Ba20170627		
	M _{2L} -RIS	M _{2R} - RIS
D	I _i	I _i
0.25	6.98E-07	4.63E-07
0.5	9.05E-07	6.94E-07
0.75	1.12E-06	8.31E-07
1	1.23E-06	1.08E-06
2	2.01E-06	1.87E-06
0	5.66E-07	4.13E-07
b ₀	5.00E-07	3.00E-07
b ₁	7.00E-07	8.00E-07
n	6	6
t	2.132	2.132
s	8.75E-08	7.12E-08
D _M	0.750	0.750
D _M ²	0.563	0.563
SSD	2.5	2.5
1 + 1/n	1.666	1.666
D	I	I
0.25	6.75E-07	5.00E-07
0.5	8.50E-07	7.00E-07
0.75	1.03E-06	9.00E-07
1	1.20E-06	1.10E-06
2	1.90E-06	1.90E-06
0	5.00E-07	3.00E-07
D	(I _i - I) ²	(I _i - I) ²
0.25	5.27E-16	1.36E-15
0.5	3.01E-15	3.21E-17
0.75	8.71E-15	4.77E-15
1	1.20E-15	5.44E-16
2	1.28E-14	7.11E-16
0	4.32E-15	1.29E-14
Sum	3.06E-14	2.03E-14
s	8.75E-08	7.12E-08
I _{CL}	7.56E-07	5.09E-07
D _{CL}	0.366	0.261
D _{DL}	0.733	0.522

	D _{DL} - Iterations	
I-1	0.654	0.468
I-2	0.655	0.469
I-3	0.655	0.469
I-4	0.655	0.469
I-5	0.655	0.469

Bb20170717		
	M _{3L} -RIS	M _{3R} -RIS
D	I _i	I _i
0.25	9.57E-07	5.64E-07
0.5	1.08E-06	6.67E-07
0.75	7.37E-07	1.06E-06
1	8.76E-07	8.80E-07
2	1.87E-06	2.28E-06
0	4.38E-07	4.18E-07
b ₀	6.00E-07	3.00E-07
b ₁	6.00E-07	9.00E-07
n	6	6
t	2.132	2.132
s	2.78E-07	2.03E-07
D _M	0.750	0.750
D _M ²	0.563	0.563
SSD	2.5	2.5
1 + 1/n	1.666	1.666
D	I	I
0.25	7.50E-07	5.25E-07
0.5	9.00E-07	7.50E-07
0.75	1.05E-06	9.75E-07
1	1.20E-06	1.20E-06
2	1.80E-06	2.10E-06
0	6.00E-07	3.00E-07
D	(I _i - I) ²	(I _i - I) ²
0.25	4.30E-14	1.49E-15
0.5	3.29E-14	6.90E-15
0.75	9.80E-14	7.56E-15
1	1.05E-13	1.02E-13
2	4.27E-15	3.20E-14
0	2.64E-14	1.40E-14
Sum	3.10E-13	1.64E-13
s	2.78E-07	2.03E-07
I _{CL}	1.42E-06	8.94E-07
D _{CL}	1.360	0.660
D _{DL}	2.719	1.320

	D _{DL} - Iterations	
I-1	2.989	1.207
I-2	3.121	1.197
I-3	3.187	1.196
I-4	3.220	1.196
I-5	3.237	1.196

Table E.2. Values used to calculate Critical Level Dose (D_{CL}) and Decision Level Dose (D_{DL}) for the calibration curve

Calibration Curve	
D	I_i
0.583	5.93E-07
0.833	6.29E-07
1.083	1.41E-06
1.333	8.69E-07
2.333	2.21E-06
0.333	2.52E-07
b_0	-2.00E-08
b_1	9.00E-07
n	6
t	2.132
s	2.91E-07
D_M	1.083
D_M^2	1.173
SSD	2.5
$1 + 1/n$	1.666
D	I
0.583	5.05E-07
0.833	7.30E-07
1.083	9.55E-07
1.333	1.18E-06
2.333	2.08E-06
0.333	2.80E-07
D	$(I_i - I)^2$
0.25	7.87E-15
0.5	1.01E-14
0.75	2.07E-13
1	9.67E-14
2	1.58E-14
0	7.56E-16
Sum	3.38E-13
s	2.91E-07
I_{CL}	8.86E-07
D_{CL}	1.006
D_{DL}	2.010

D_{DL} - Iterations	
I-1	1.854
I-2	1.823
I-3	1.817
I-4	1.816
I-5	1.816

Appendix F

Deciduous versus Permanent Tooth Slope Comparison

F.1 R Data Used for Deciduous versus Permanent Tooth Slope Comparison

F.1.1 Data Used in CSV File:

Table F.1. Data used in CSV File 'slope'

Tooth	Slope	Type
608P3L	123.2479	D
608P3R	138.2717	D
609M3L	84.022	P
609M3R	110.41	P
615M2L	85.717	P
615M2R	36.744	P
617P3L	135.58	D
617P3R	130.99	D

F. 1.2. R Code used and Generated Results

```
slope <- read.csv(file.choose())  
t.test(Slope ~ Type, data=slope, paired = T)
```

Paired t-test

```
data: Slope by Type  
t = -3.6344, df = 3, p-value = 0.03588  
alternative hypothesis: true difference in means is not equal to 0  
95 percent confidence interval:  
-99.032073 -6.566227  
sample estimates:  
mean of the differences  
-52.79915
```

```
t.test(Slope ~ Type, data=slope)
```

welch Two Sample t-test

```
data: Slope by Type  
t = -3.355, df = 3.2734, p-value = 0.03853  
alternative hypothesis: true difference in means is not equal to 0  
95 percent confidence interval:  
-100.598182 -5.000118  
sample estimates:  
mean in group M mean in group P  
79.22325 132.02240
```

Appendix G

Tooth Sample Preparation Procedure

This sample processing procedure was adapted from the procedures described in IAEA-TECDOC-1331, International Standard ISO 13304-1, EPR Dosimetry with Tooth Enamel: A Review (Fattibene and Callens 2010), as well as multiple studies performed using animal teeth.

G.1 Sample Preparation:

1. Rinse specimens in acetone and store in deionized water for a minimum of 24 hours.
 - a. Using tweezers, hold tooth samples over a glass beaker and rinse with acetone using a squeeze bottle.
 - b. Place all teeth into individual beakers and cover teeth with approximately 100 mL deionized water for a minimum of 24 hours (Fig. G1).

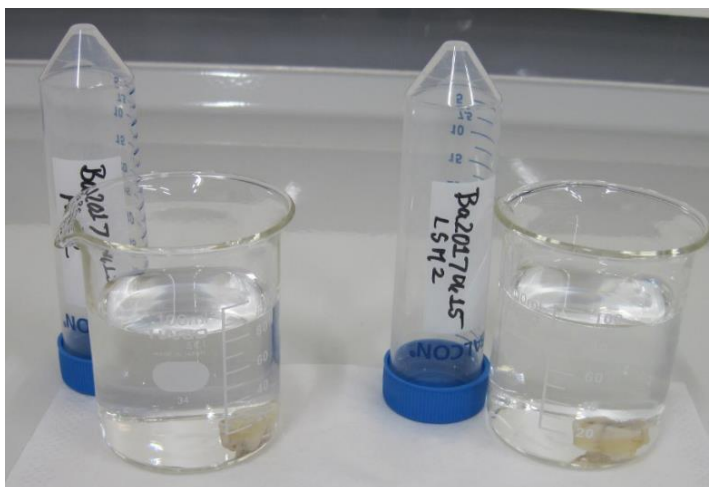


Fig. G.1. Boar teeth in individual beakers containing deionized water.

- c. Pour the used acetone solution into a 1L bottle for later disposal.

2. Cut the separated crown into smaller pieces to facilitate removal of dentin from the enamel. Excess bone or tissue attached to the tooth can also be removed at this time. A water-cooled saw should be used for this step.
 - a. Place the tooth into the saw vice so that the saw blade is in line with the center of the tooth (Fig. G2).



Fig. G.2. Boar tooth in position to be cut into smaller pieces.

- b. Tighten the screw on the vice to ensure steady placement of the tooth so that it does not move during cutting.
 - c. Engage the saw and cut the tooth in half.
 - d. Place each tooth into individual containers labeled with sample identification information.
3. Dentin must be removed from the enamel. The most effective method to remove dentin involves a combination of mechanical removal using a water-cooled drill and also chemical separation through alkaline denaturation with Potassium Hydroxide solution.
 - a. Place tooth segments in individual beakers containing approximately 150 ml of 20% Potassium Hydroxide solution.

- b. Place beakers in an ultrasonic bath for period of 24 hours at a temperature of 60°C (Fig. G3).



Fig. G.3. Ultrasonic bath containing tooth samples inside beakers of KOH.

- c. Remove the tooth segments from each beaker and rinse with deionized water.

Note: This process will result in a visible color difference between the enamel and dentin (Fig. G4), where the enamel will be white and the dentin will appear as a yellowish color.



Fig. G.4. Tooth sample fragments inside beakers of KOH. Visible differences in color between dentin and enamel is shown.

- d. Remove visible dentin from enamel using a dental pic or dental drill with burs made of a hard metal alloy.

Note: Tooth segments should be held with tweezers or pliers to avoid contact with the dental bur.
Perform this step under a sink faucet or while using a water irrigation system (Fig. G5).



Fig. G.5. Removal of dentin from enamel with a dental drill

- e. Rinse the tooth segments with deionized water.
- f. Repeat steps 2-5 as necessary until all visible dentin is removed.
- g. Place tooth segments on a paper towel to absorb any excess water remaining.
- h. Rinse tooth segments with ethanol by submerging the tooth in a beaker containing a 70% ethanol solution or by rinsing with ethanol from a squeeze bottle.
- i. Allow the tooth segments to air dry for approximately 30 minutes.
- j. Place remaining enamel into individual containers and heat in a drying oven overnight at 40°C (Fig. G6).



Fig. G.6. Tooth enamel pieces dried overnight in an oven.

- k. Remove samples from the oven.
4. Grind the enamel into a powder.
 - a. Using a mortar and pestle, grind the enamel into a powder.
 - b. A grain size of 0.250-1.00 mm is desired. Assemble a stack consisting of a 1.00 mm sieve, a 0.500 mm sieve and a 0.250 mm sieve to be used to for obtaining the desired powder enamel particle size. Other sized sieves within this range may also be used. A small container should be placed under the sieves to catch powder that passes through the bottom sieve as shown below in Fig. G7.



Fig. G.7. Mortar and pestle used to grind enamel into a powder for measurement in an EPR spectrometer alongside sieves used to ensure desired particle sizes are obtained.

- c. Pour the powder into 1.00 mm sieve.

Note: The powder enamel smaller than 1.00 mm will go through the sieve and into the 0.500 mm sieve. Pieces smaller than 0.500 mm will pass through the second sieve and into the 0.250 mm sieve. Particles smaller than 0.250 mm can be disposed of.

Note: A sample of between 70-100 mg is necessary to sufficiently perform the analysis.

5. Place the powder into small plastic containers.
6. Finally, store samples prior to analysis at room temperature in a low humidity (<60%) environment for approximately 7 days prior to EPR measurement.

Appendix H

Individual RIS values and Irradiation Doses: 0.25 Gy – 2.0 Gy Range

Table H.1. Individual RIS values for each sample measurement and irradiation doses for sample Ba20170620 M_{2L} and M_{2R}.

Ba20170620						
M _{2L}						
Meas	0.25 Gy	0.5 Gy	0.75 Gy	1.0 Gy	2.0 Gy	Unirradiated
1	2.12E-07	4.16E-07	2.93E-07	1.05E-06	1.89E-06	2.58E-07
2	2.70E-07	5.31E-07	3.30E-07	6.46E-07	1.54E-06	2.15E-07
3	3.57E-07	3.22E-07	4.94E-07	5.16E-07	1.81E-06	1.81E-07
Avg	2.80E-07	4.23E-07	3.72E-07	7.36E-07	1.75E-06	2.18E-07
SD	7.32E-08	1.05E-07	1.07E-07	2.76E-07	1.85E-07	3.89E-08
M _{2R}						
Meas	0.25 Gy	0.5 Gy	0.75 Gy	1.0 Gy	2.0 Gy	Unirradiated
1	4.50E-07	6.68E-07	1.76E-06	6.67E-07	2.78E-06	1.01E-06
2	4.26E-07	5.78E-07	1.76E-06	1.85E-06	3.04E-06	9.38E-07
3	5.17E-07	6.02E-07	9.17E-07	1.51E-06	3.04E-06	9.27E-07
Avg	4.64E-07	6.16E-07	1.48E-06	1.34E-06	2.95E-06	9.59E-07
SD	4.75E-08	4.68E-08	4.86E-07	6.07E-07	1.52E-07	4.57E-08

Table H.2 Individual RIS values for each sample measurement and irradiation doses for sample Bb20170623 M_{1L} and M_{1R}.

Bb20170623					
M _{1L}					
Meas	0.25 Gy	0.5 Gy	0.75 Gy	1.0 Gy	Unirradiated
1	2.83E-07	3.08E-07	4.86E-07	3.97E-07	1.98E-07
2	2.26E-07	3.96E-07	4.14E-07	4.00E-07	2.33E-07
3	2.72E-07	3.34E-07	4.55E-07	4.17E-07	1.65E-07
Avg	2.60E-07	3.46E-07	4.52E-07	4.05E-07	1.99E-07
SD	3.05E-08	4.50E-08	3.61E-08	1.06E-08	3.38E-08
M _{1R}					
Meas	0.25 Gy	0.5 Gy	0.75 Gy	1.0 Gy	Unirradiated
1	3.57E-07	4.94E-07	5.23E-07	5.98E-07	2.40E-07
2	3.13E-07	5.25E-07	6.54E-07	6.04E-07	2.32E-07
3	5.46E-07	4.98E-07	5.30E-07	5.57E-07	3.36E-07
Avg	4.06E-07	5.06E-07	5.69E-07	5.86E-07	2.69E-07
SD	1.24E-07	1.67E-08	7.40E-08	2.56E-08	5.80E-08

Table H.3 Individual RIS values for each sample measurement and irradiation doses for sample Ba20170627 M_{2L} and M_{2R}.

Ba20170627						
M _{2L}						
Meas	0.25 Gy	0.5 Gy	0.75 Gy	1.0 Gy	2.0 Gy	Unirradiated
1	7.19E-07	8.34E-07	1.16E-06	1.22E-06	1.97E-06	4.24E-07
2	6.49E-07	9.85E-07	1.04E-06	1.33E-06	2.09E-06	6.32E-07
3	7.26E-07	8.96E-07	1.16E-06	1.16E-06	1.98E-06	6.41E-07
Avg	6.98E-07	9.05E-07	1.12E-06	1.23E-06	2.01E-06	5.66E-07
SD	4.26E-08	7.58E-08	6.87E-08	8.53E-08	6.65E-08	1.23E-07
M _{2R}						
Meas	0.25 Gy	0.5 Gy	0.75 Gy	1.0 Gy	2.0 Gy	Unirradiated
1	4.69E-07	7.34E-07	8.38E-07	1.07E-06	1.84E-06	4.87E-07
2	4.40E-07	7.01E-07	8.16E-07	1.12E-06	1.91E-06	2.57E-07
3	4.81E-07	6.48E-07	8.39E-07	1.04E-06	1.87E-06	4.96E-07
Avg	4.63E-07	6.94E-07	8.31E-07	1.08E-06	1.87E-06	4.13E-07
SD	2.07E-08	4.34E-08	1.26E-08	4.14E-08	3.51E-08	1.36E-07

Table H.4 Individual RIS values for each sample measurement and irradiation doses for sample Bb20170717 M_{3L} and M_{3R}.

Bb20170717						
M _{3L}						
Meas	0.25 Gy	0.5 Gy	0.75 Gy	1.0 Gy	2.0 Gy	Unirradiated
1	9.31E-07	1.10E-06	8.06E-07	8.90E-07	1.52E-06	3.96E-07
2	9.04E-07	1.06E-06	7.50E-07	8.95E-07	1.50E-06	4.29E-07
3	1.04E-06	1.08E-06	6.55E-07	8.42E-07	2.58E-06	4.88E-07
Avg	9.57E-07	1.08E-06	7.37E-07	8.76E-07	1.87E-06	4.38E-07
SD	7.02E-08	2.35E-08	7.61E-08	2.93E-08	6.16E-07	4.68E-08
M _{3R}						
Meas	0.25 Gy	0.5 Gy	0.75 Gy	1.0 Gy	2.0 Gy	Unirradiated
1	5.39E-07	7.44E-07	1.19E-06	8.78E-07	2.68E-06	4.58E-07
2	5.70E-07	6.06E-07	9.47E-07	8.71E-07	2.62E-06	2.77E-07
3	5.83E-07	6.50E-07	1.05E-06	8.92E-07	1.53E-06	5.20E-07
Avg	5.64E-07	6.67E-07	1.06E-06	8.80E-07	2.28E-06	4.18E-07
SD	2.27E-08	7.05E-08	1.20E-07	1.08E-08	6.49E-07	1.26E-07

Table H.5 Individual RIS values for each sample measurement and irradiation doses for calibration curve samples.

Calibration Curve Samples						
Meas	0.583* Gy	0.833* Gy	1.083* Gy	1.333* Gy	2.333* Gy	0.333* Gy
1	7.72E-07	9.86E-07	1.52E-06	8.58E-07	1.58E-06	3.16E-07
2	5.42E-07	3.30E-07	1.35E-06	8.65E-07	2.80E-06	2.09E-07
3	4.66E-07	5.71E-07	1.36E-06	8.83E-07	2.23E-06	2.31E-07
Avg	5.93E-07	6.29E-07	1.41E-06	8.69E-07	2.21E-06	2.52E-07
SD	1.59E-07	3.32E-07	9.74E-08	1.30E-08	6.10E-07	5.67E-08

*Adjusted values

Appendix I

R Code for Tooth Slope Comparison

I.1 R Data Used for “Old” versus “Young” Tooth Slope Comparison

I.1.1 Data Used in CSV File

Table I.1. Data used in CSV File ‘slope’

Tooth	Slope	Age
620L	7.85E-07	Y
620R	1.17E-06	Y
b623L	2.41E-07	O
b623R	3.19E-07	O
627L	7.30E-07	Y
627R	7.58E-07	Y
b717L	5.89E-07	O
b717R	9.23E-07	O

I.1.2. R Code used and Generated Results

```
> slope <- read.csv(file.choose())  
> t.test(Slope ~ Age, data=slope, paired = T)
```

Paired t-test

```
data: Slope by Age  
t = -1.5362, df = 3, p-value = 0.2221  
alternative hypothesis: true difference in means is not equal to 0  
95 percent confidence interval:  
-1.052783e-06 3.672831e-07  
sample estimates:  
mean of the differences  
-3.4275e-07
```

```
> t.test(Slope ~ Age, data=slope)
```

welch Two Sample t-test

```
data: Slope by Age  
t = -1.8444, df = 5.2522, p-value = 0.1216  
alternative hypothesis: true difference in means is not equal to 0  
95 percent confidence interval:  
-8.136394e-07 1.281394e-07  
sample estimates:  
mean in group O mean in group Y  
5.1800e-07 8.6075e-07
```

I.2 R Data Used for Tooth Slope and Sex Comparison

I.2.1. Data Used in CSV File

Table I.2. Normalized slope data used in CSV File 'slopedata2':

Tooth	Slope	Sex
608P3L	8.52E-01	Female
608P3R	1.00E+00	Female
609M3L	4.66E-01	Female
609M3R	7.26E-01	Female
615M2L	4.83E-01	Female
615M2R	0.00E+00	Female
617P3L	9.74E-01	Male
617P3R	9.29E-01	Male
620M2L	6.30E-01	Female
620M2R	1.04E+00	Female
b623M1L	4.41E-02	Male
b623M1R	1.28E-01	Male
627M2L	5.71E-01	Male
627M2R	6.01E-01	Male
b717M3L	4.19E-01	Male
b717M3R	7.78E-01	Male

I.2.1 R Code Used and Generated Results

```
> Slopedata2<- read.csv(file.choose())  
> t.test(Slope ~ Sex, data=Slopedata2)
```

Welch Two Sample t-test

```
data: Slope by Sex  
t = 0.55075, df = 13.997, p-value = 0.5905  
alternative hypothesis: true difference in means is not equal to 0  
95 percent confidence interval:  
-0.2723963 0.4606213  
sample estimates:  
mean in group Female    mean in group Male  
0.6496250                0.5555125
```

```
> t.test(Slope ~ Sex, data=Slopedata2, paired=T)
```

Paired t-test

```
data: Slope by Sex  
t = 0.71627, df = 7, p-value = 0.497  
alternative hypothesis: true difference in means is not equal to 0  
95 percent confidence interval:  
-0.2165811 0.4048061  
sample estimates:
```

mean of the differences
0.0941125

Appendix J

Results for the Linear Regression and Correlation Analysis: Chapters 4 – 6

J.1 Summary of Results

Table J.1. Summary of results for linear regression analysis assumptions for tooth enamel studied in Chapters 4 and 5, and also for the calibration curve tooth enamel samples. ✓ = Assumption met, ✗ = Assumption not met, ~ = Assumption Questionable

	Independence	Linearity	Equal Variance	Normality
Ba20170608 P _{3L}	✓	✓	✗	✓
Ba20170608 P _{3R}	✓	✓	✗	✓
Ba20170609 M _{3L}	✓	✓	✗	✓
Ba20170609 M _{3R}	✓	✓	✓	✓
Ba20170615 M _{2L}	✓	✓	✗	✓
Ba20170615 M _{2R}	✓	✓	✓	✓
Ba20170617 P _{3L}	✓	✓	✓	✓
Ba20170617 P _{3R}	✓	✓	✓	✓
Ba20170620 M _{2L}	✓	✓	~	✓
Ba20170620 M _{2R}	✓	✓	✓	✓
Ba20170623 M _{1L}	✓	✓	✗	✓
Ba20170623 M _{1R}	✓	✓	✓	~
Ba20170627 M _{2L}	✓	✓	✓	✓
Ba20170627 M _{2R}	✓	✓	~	✓
Bb20170717 M _{3L}	✓	✓	✓	~
Bb20170717 M _{3R}	✓	✓	✗	✓
Calibration Curve	✓	✓	✓	✓

J.2 Linear Regression Analysis R Code and Results for Chapter 4

J.2.1 Sample Ba20170608 P_{3L}

Table J.2. Data used in CSV File for sample Ba20170608 P_{3L}

Dose	Intensity
1.2	90.36
2.2	218.19
4.4	471.14
7.6	790.98
12	1493.98
0	0.09

J.2.1.1 R Code for Linear Regression Assumptions for sample Ba20170608 P_{3L}

```
> PL <- read.csv(file.choose())
> str(PL)
'data.frame': 7 obs. of 2 variables:
 $ Dose      : num  1.2 2.2 4.4 7.6 12 0 NA
 $ Intensity: num  90.4 218.2 471.1 791 1494 ...
> plot(Intensity ~ Dose, data = PL, pch = 15)
> abline(lm(Intensity ~ Dose, data = PL))
> Fit <- lm(Intensity ~ Dose, data = PL)
> Fit
```

```
Call:
lm(formula = Intensity ~ Dose, data = PL)
```

```
Coefficients:
(Intercept)      Dose
   -52.04      123.25
```

```
> summary(Fit)
```

```
Call:
lm(formula = Intensity ~ Dose, data = PL)
```

```
Residuals:
    1     2     3     4     5     6
-5.494 -0.912 -19.109 -93.664  67.043  52.135
```

```
Coefficients:
              Estimate Std. Error t value Pr(>|t|)
(Intercept)  -52.045     38.957  -1.336   0.253
Dose          123.248     6.328   19.477  4.1e-05 ***
---
Signif. codes:  0 '***' 0.001 '**' 0.01 '*' 0.05 '.' 0.1 ' ' 1
```

```
Residual standard error: 64 on 4 degrees of freedom
(1 observation deleted due to missingness)
Multiple R-squared:  0.9896, Adjusted R-squared:  0.987
F-statistic: 379.3 on 1 and 4 DF, p-value: 4.097e-05
```

```

> par(mfrow = c(2, 2))
> plot(residuals(Fit) ~ fitted(Fit), xlab = "Fitted Values", ylab =
"Residuals", main = "Residuals vs Fitted"); abline(h = 0)
> qqnorm(residuals(Fit)); qqline(residuals(Fit))

```

J.2.1.2 Plot Output for Linear Regression Analysis for Sample Ba20170608 P_{3L}

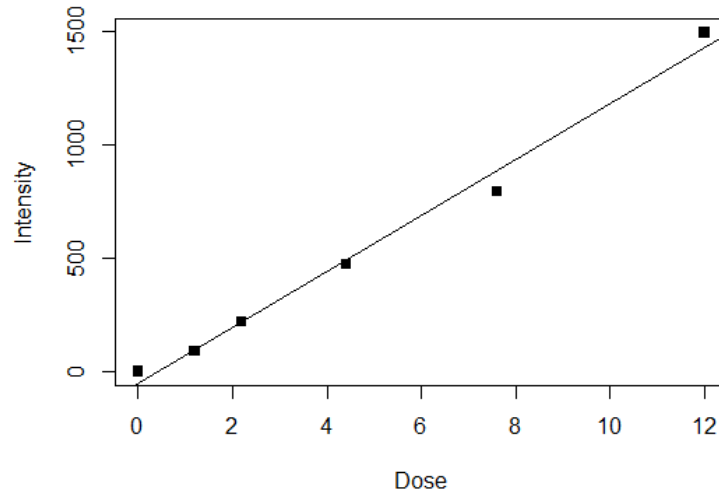


Fig. J.1. Intensity versus irradiation dose for sample Ba20170608 P_{3L}

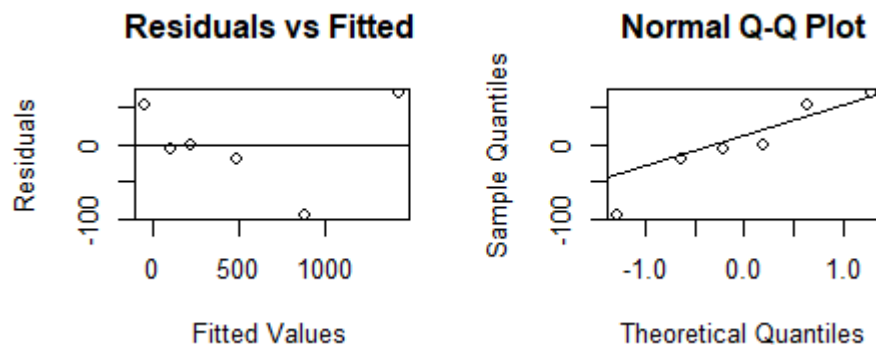


Fig. J.2. R generated plots which were used to verify linear regression assumptions for sample Ba20170608 P_{3L}

J.2.1.3 R Code for Correlation for sample Ba20170608 P_{3L}

```

> InData <- read.csv(file.choose())
> head(InData)
  Dose Intensity
1  1.2    90.36
2  2.2   218.19
3  4.4   471.14
4  7.6   790.98
5 12.0  1493.98
6  0.0    0.09
> pairs(InData)
> cor(InData)
      Dose Intensity
Dose  1.000 0.999
Intensity 0.999 1.000

```

```

Dose      1      NA
Intensity NA      1
> cor(InData, method = "spearman")
      Dose Intensity
Dose      1      NA
Intensity NA      1
> cor.test(InData$Dose, InData$Intensity)

Pearson's product-moment correlation

data: InData$Dose and InData$Intensity
t = 19.477, df = 4, p-value = 4.097e-05
alternative hypothesis: true correlation is not equal to 0
95 percent confidence interval:
 0.9508191 0.9994546
sample estimates:
      cor
0.9947689

> cor.test(InData$Dose, InData$Intensity, method = "spearman")

Spearman's rank correlation rho

data: InData$Dose and InData$Intensity
S = 0, p-value = 0.002778
alternative hypothesis: true rho is not equal to 0
sample estimates:
rho
 1

```

J.2.1.4 Plot Output for Correlation Analysis for sample Ba20170608 P_{3L}

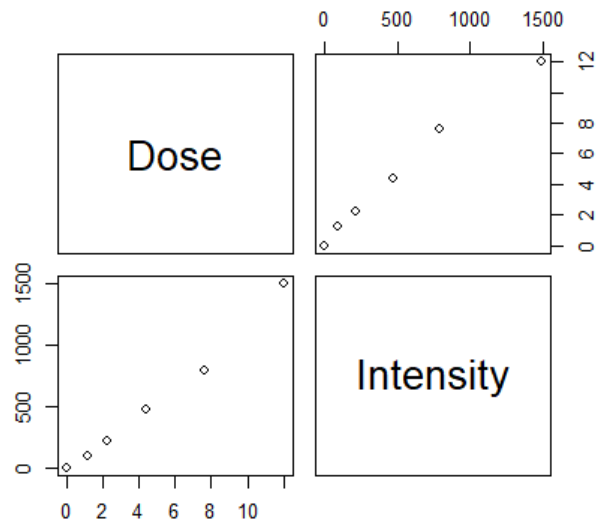


Fig. J.3. R generated plot showing the correlation between irradiation dose and intensity for sample Ba20170608 P_{3L}

J.2.2 Sample Ba20170608 P_{3R}

Table J.3. Data used in CSV File for sample Ba20170608 P_{3R}

Dose	Intensity
1.2	142.14
2.2	261.75
4.4	518.28
7.6	1004.08
12	1660.32
0	13.48

J.2.2.1 R Code for Linear Regression Assumptions for sample Ba20170608 P_{3R}

```
> PR <- read.csv(file.choose())
> str(PR)
'data.frame': 6 obs. of 2 variables:
 $ Dose      : num  1.2 2.2 4.4 7.6 12 0
 $ Intensity: num  142 262 518 1004 1660 ...
> plot(Intensity ~ Dose, data = PR, pch = 15)
> abline(lm(Intensity ~ Dose, data = PR))
> Fit <- lm(Intensity ~ Dose, data = PR)
> Fit
```

```
Call:
lm(formula = Intensity ~ Dose, data = PR)
```

```
Coefficients:
(Intercept)      Dose
    -31.43      138.27
```

```
>
> summary(Fit)
```

```
Call:
lm(formula = Intensity ~ Dose, data = PR)
```

```
Residuals:
    1     2     3     4     5     6
 7.645 -11.016 -58.683 -15.351  32.495  44.911
```

```
Coefficients:
              Estimate Std. Error t value Pr(>|t|)
(Intercept)  -31.431    25.342   -1.24   0.283
Dose          138.271     4.116   33.59 4.69e-06 ***
---
Signif. codes:  0 '***' 0.001 '**' 0.01 '*' 0.05 '.' 0.1 ' ' 1
```

```
Residual standard error: 41.63 on 4 degrees of freedom
Multiple R-squared:  0.9965, Adjusted R-squared:  0.9956
F-statistic: 1128 on 1 and 4 DF, p-value: 4.685e-06
```

```
> par(mfrow = c(2, 2))
```

```

> plot(residuals(Fit) ~ fitted(Fit), xlab = "Fitted values", ylab =
"Residuals", main = "Residuals vs Fitted"); abline(h = 0)
> qqnorm(residuals(Fit)); qqline(residuals(Fit))

```

J.2.2.2 Plot Output for Linear Regression Analysis for Sample Ba20170608 P_{3R}

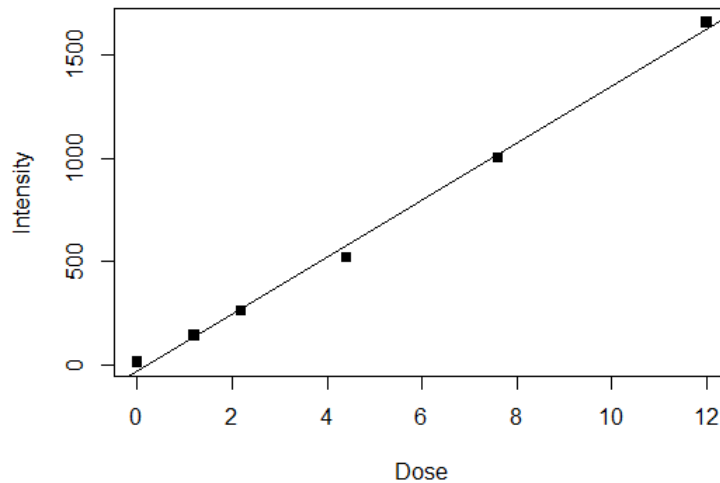


Fig. J.4. Intensity versus irradiation dose for sample Ba20170608 P_{3R}

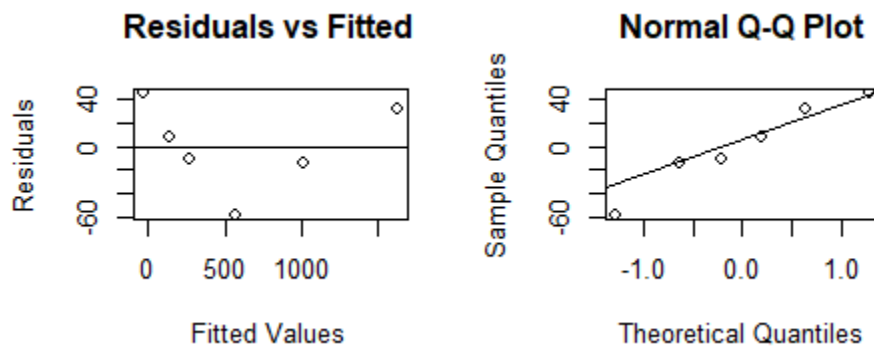


Fig. J.5. R generated plots which were used to verify linear regression assumptions for sample Ba20170608 P_{3R}

J.2.2.3 R Code for Correlation for sample Ba20170608 P_{3R}

```

> InData <- read.csv(file.choose())
> head(InData)
  Dose Intensity
1  1.2   142.14
2  2.2   261.75
3  4.4   518.28
4  7.6  1004.08
5 12.0  1660.32
6  0.0    13.48
> pairs(InData)
> cor(InData)

```

```

          Dose Intensity
Dose      1.000000 0.9982321
Intensity 0.9982321 1.0000000
>
> cor(InData, method = "spearman")
          Dose Intensity
Dose      1      1
Intensity 1      1
> cor.test(InData$Dose, InData$Intensity)

Pearson's product-moment correlation

data: InData$Dose and InData$Intensity
t = 33.59, df = 4, p-value = 4.685e-06
alternative hypothesis: true correlation is not equal to 0
95 percent confidence interval:
 0.9831329 0.9998160
sample estimates:
      cor
0.9982321

> cor.test(InData$Dose, InData$Intensity, method = "spearman")

Spearman's rank correlation rho

data: InData$Dose and InData$Intensity
S = 0, p-value = 0.002778
alternative hypothesis: true rho is not equal to 0
sample estimates:
rho
1

```

J.2.2.4 Plot Output for Correlation Analysis for sample Ba20170608 P_{3R}

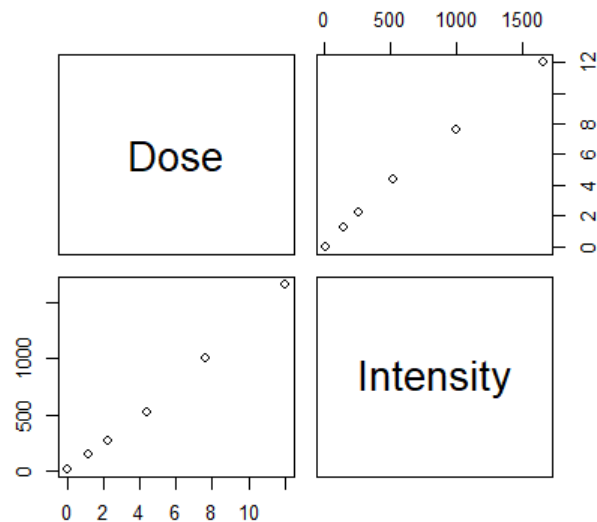


Fig. J.6. R generated plot showing the correlation between irradiation dose and intensity for sample Ba20170608 P_{3R}

J.2.3 Sample Ba20170609 M_{3L}

Table J.4. Data used in CSV File for Sample Ba20170609 M_{3L}

Dose	Intensity
1.2	205.77
2.2	322.17
4.4	461.05
7.6	812.25
12	1094.31
0	103.54

J.2.3.1 R Code for Linear Regression Assumptions for sample Ba20170609 M_{3L}

```
> ML <- read.csv(file.choose())
> str(ML)
'data.frame': 6 obs. of 2 variables:
 $ Dose      : num  1.2 2.2 4.4 7.6 12 0
 $ Intensity: num  206 322 461 812 1094 ...
> plot(Intensity ~ Dose, data = ML, pch = 15)
> abline(lm(Intensity ~ Dose, data = ML))
>
> Fit <- lm(Intensity ~ Dose, data = ML)
> Fit
```

```
Call:
lm(formula = Intensity ~ Dose, data = ML)
```

```
Coefficients:
(Intercept)      Dose
    116.14         84.02
```

```
>
> summary(Fit)
```

```
Call:
lm(formula = Intensity ~ Dose, data = ML)
```

```
Residuals:
    1     2     3     4     5     6
-11.20  21.18 -24.79  57.53 -30.11 -12.60
```

```
Coefficients:
              Estimate Std. Error t value Pr(>|t|)
(Intercept)  116.144    22.704   5.116 0.00691 **
Dose          84.023     3.688  22.783 2.2e-05 ***
---
Signif. codes:  0 '***' 0.001 '**' 0.01 '*' 0.05 '.' 0.1 ' ' 1
```

```
Residual standard error: 37.3 on 4 degrees of freedom
Multiple R-squared:  0.9924, Adjusted R-squared:  0.9904
F-statistic: 519.1 on 1 and 4 DF, p-value: 2.199e-05
```

```

> par(mfrow = c(2, 2))
> plot(residuals(Fit) ~ fitted(Fit), xlab = "Fitted Values", ylab =
"Residuals", main = "Residuals vs Fitted"); abline(h = 0)
> qqnorm(residuals(Fit)); qqline(residuals(Fit))

```

J.2.3.2 Plot Output for Linear Regression Analysis for Sample Ba20170609 M_{3L}

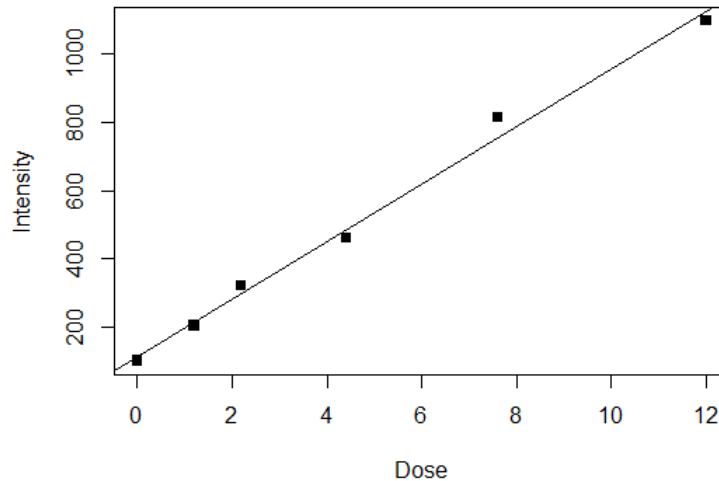


Fig. J.7. Intensity versus irradiation dose for sample Ba20170609 M_{3L}

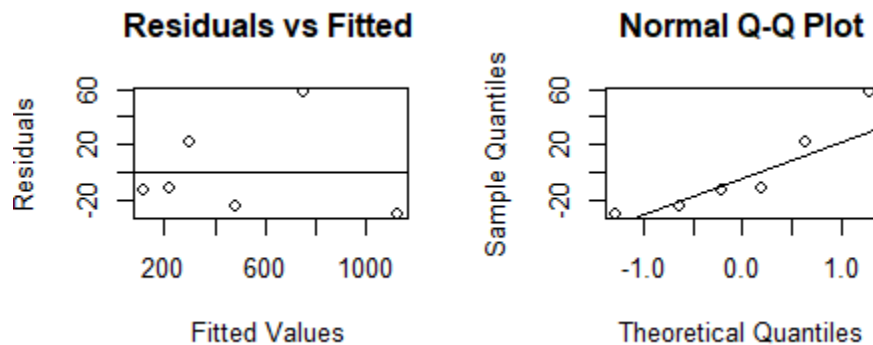


Fig. J.8. R generated plots which were used to verify linear regression assumptions for sample Ba20170609 M_{3L}

J.2.3.3 R Code for Correlation for sample Ba20170609 M_{3L}

```

> InData <- read.csv(file.choose())
> head(InData)
  Dose Intensity
1  1.2    205.77
2  2.2    322.17
3  4.4    461.05
4  7.6    812.25
5 12.0   1094.31
6  0.0    103.54
> pairs(InData)
> cor(InData)

```

```

          Dose Intensity
Dose      1.0000000 0.9961691
Intensity 0.9961691 1.0000000
> cor(InData, method = "spearman")
          Dose Intensity
Dose      1      1
Intensity 1      1
> cor.test(InData$Dose, InData$Intensity)

Pearson's product-moment correlation

data: InData$Dose and InData$Intensity
t = 22.783, df = 4, p-value = 2.199e-05
alternative hypothesis: true correlation is not equal to 0
95 percent confidence interval:
 0.9637695 0.9996008
sample estimates:
      cor
0.9961691

> cor.test(InData$Dose, InData$Intensity, method = "spearman")

Spearman's rank correlation rho

data: InData$Dose and InData$Intensity
S = 0, p-value = 0.002778
alternative hypothesis: true rho is not equal to 0
sample estimates:
rho
1

```

J.2.3.4 Plot Output for Correlation Analysis for sample Ba20170609 M_{3L}

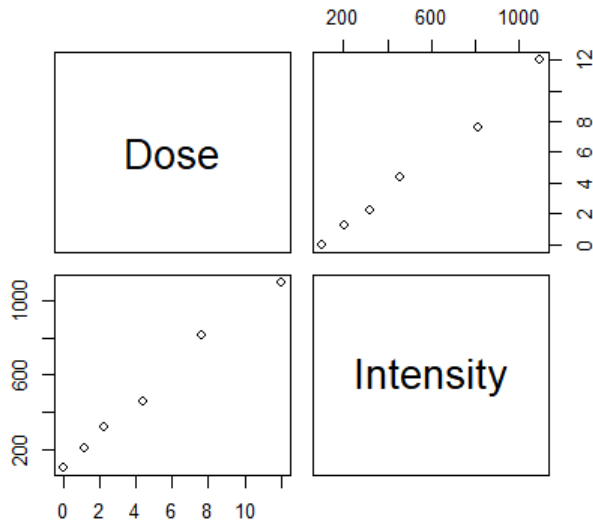


Fig. J.9. R generated plot showing the correlation between irradiation dose and intensity for sample Ba20170609 M_{3L}

J.2.4 Sample Ba20170609 M_{3R}

Table J.5. Data used in CSV File for sample Ba20170609 M_{3R}

Dose	Intensity
1.2	192.23
2.2	317.54
4.4	608.26
7.6	886.5
12	1422.81
0	103.55

J.2.4.1 R Code for Linear Regression Assumptions for sample Ba20170609 M_{3R}

```
> MR <- read.csv(file.choose())
> str(MR)
'data.frame': 6 obs. of 2 variables:
 $ Dose      : num  1.2 2.2 4.4 7.6 12 0
 $ Intensity: num  192 318 608 886 1423 ...
> plot(Intensity ~ Dose, data = MR, pch = 15)
> abline(lm(Intensity ~ Dose, data = MR))
>
> Fit <- lm(Intensity ~ Dose, data = MR)
> Fit

Call:
lm(formula = Intensity ~ Dose, data = MR)

Coefficients:
(Intercept)      Dose
      84.26      110.41

> summary(Fit)

Call:
lm(formula = Intensity ~ Dose, data = MR)

Residuals:
    1     2     3     4     5     6
-24.53  -9.63  38.18 -36.90  13.59  19.29

Coefficients:
            Estimate Std. Error t value Pr(>|t|)
(Intercept)  84.261    19.419   4.339  0.0123 *
Dose        110.413     3.154  35.003 3.98e-06 ***
---
Signif. codes:  0 '***' 0.001 '**' 0.01 '*' 0.05 '.' 0.1 ' ' 1

Residual standard error: 31.9 on 4 degrees of freedom
Multiple R-squared:  0.9967, Adjusted R-squared:  0.9959
F-statistic: 1225 on 1 and 4 DF, p-value: 3.975e-06

> par(mfrow = c(2, 2))
```

```

> plot(residuals(Fit) ~ fitted(Fit), xlab = "Fitted values", ylab =
"Residuals", main = "Residuals vs Fitted"); abline(h = 0)
> qqnorm(residuals(Fit)); qqline(residuals(Fit))

```

J.2.4.2 Plot Output for Linear Regression Analysis for Sample Ba20170609 M_{3R}

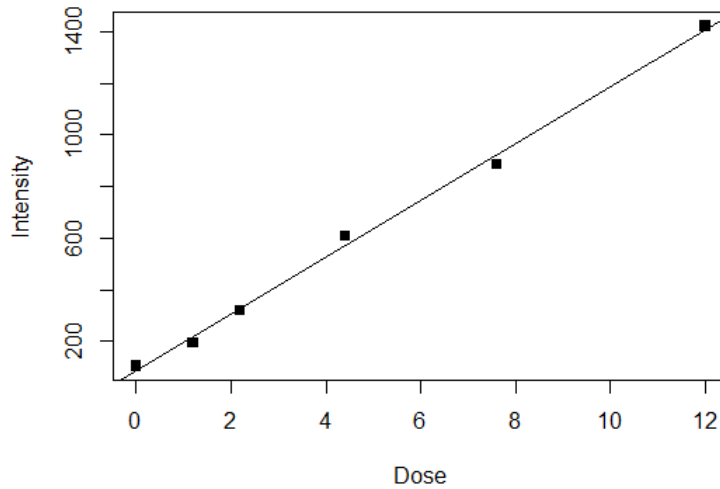


Fig. J.10. Intensity versus irradiation dose for sample Ba20170609 M_{3R}

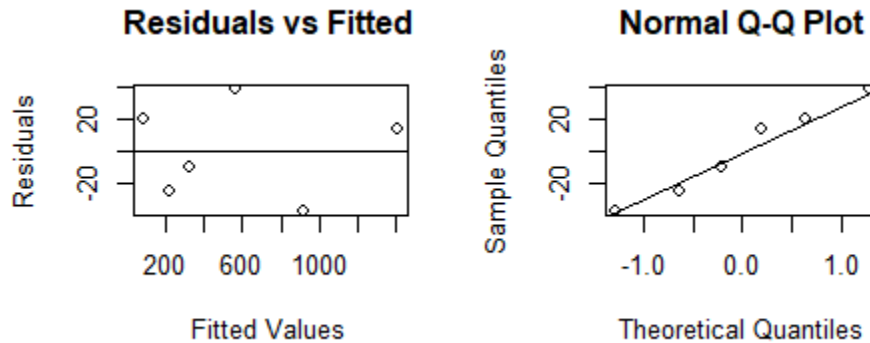


Fig. J.11. R generated plots which were used to verify linear regression assumptions for sample Ba20170609 M_{3R}

J.2.4.3 R Code for Correlation for sample Ba20170609 M_{3R}

```

> InData <- read.csv(file.choose())
> head(InData)
  Dose Intensity
1  1.2   192.23
2  2.2   317.54
3  4.4   608.26
4  7.6   886.50
5 12.0  1422.81
6  0.0   103.55
> pairs(InData)
> cor(InData)
           Dose Intensity
Dose      1.000000 0.9983716

```

```

Intensity 0.9983716 1.0000000
> cor(InData, method = "spearman")
      Dose Intensity
Dose      1         1
Intensity 1         1
> cor.test(InData$Dose, InData$Intensity)

Pearson's product-moment correlation

data: InData$Dose and InData$Intensity
t = 35.003, df = 4, p-value = 3.975e-06
alternative hypothesis: true correlation is not equal to 0
95 percent confidence interval:
 0.9844545 0.9998305
sample estimates:
      cor
0.9983716

> cor.test(InData$Dose, InData$Intensity, method = "spearman")

Spearman's rank correlation rho

data: InData$Dose and InData$Intensity
S = 0, p-value = 0.002778
alternative hypothesis: true rho is not equal to 0
sample estimates:
rho
 1

```

J.2.4.4 Plot Output for Correlation Analysis for sample Ba20170609 M_{3R}

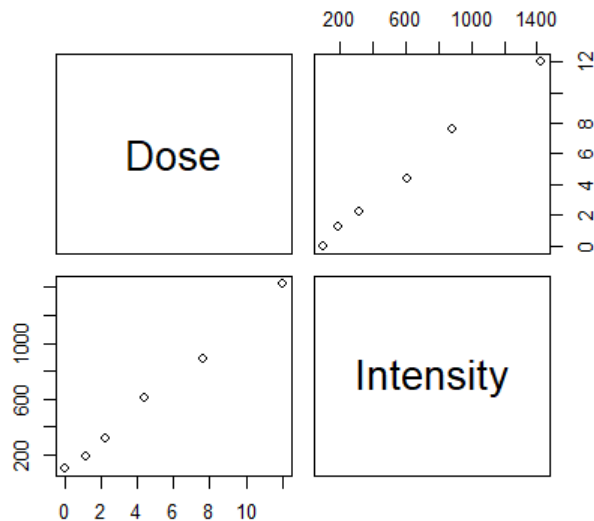


Fig. J.12. R generated plot showing the correlation between irradiation dose and intensity for sample Ba20170609 M_{3R}

J.2.5 Sample Ba20170615 M_{2L}

Table J.6. Data used in CSV File for sample Ba20170615 M_{2L}

Dose	Intensity
1.2	104.63
2.2	204.64
4.4	365.34
7.6	736.62
12	1009.68
0	16.57

J.2.5.1 R Code for Linear Regression Assumptions for sample Ba20170615 M_{2L}

```
> ML <- read.csv(file.choose())
> str(ML)
'data.frame': 6 obs. of 2 variables:
 $ Dose      : num  1.2 2.2 4.4 7.6 12 0
 $ Intensity: num  105 205 365 737 1010 ...
> plot(Intensity ~ Dose, data = ML, pch = 15)
> abline(lm(Intensity ~ Dose, data = ML))
>
> Fit <- lm(Intensity ~ Dose, data = ML)
> Fit
```

```
Call:
lm(formula = Intensity ~ Dose, data = ML)
```

```
Coefficients:
(Intercept)      Dose
      14.81         85.72
```

```
> summary(Fit)
```

```
Call:
lm(formula = Intensity ~ Dose, data = ML)
```

```
Residuals:
    1     2     3     4     5     6
-13.036  1.257 -26.620  70.365 -33.730  1.765
```

```
Coefficients:
              Estimate Std. Error t value Pr(>|t|)
(Intercept)   14.805      25.415   0.583   0.591
Dose           85.717       4.128  20.763 3.18e-05 ***
---
```

```
Signif. codes:  0 '***' 0.001 '**' 0.01 '*' 0.05 '.' 0.1 ' ' 1
```

```
Residual standard error: 41.75 on 4 degrees of freedom
Multiple R-squared:  0.9908, Adjusted R-squared:  0.9885
F-statistic: 431.1 on 1 and 4 DF, p-value: 3.179e-05
```

```
> par(mfrow = c(2, 2))
```

```

> plot(residuals(Fit) ~ fitted(Fit), xlab = "Fitted values", ylab =
"Residuals", main = "Residuals vs Fitted"); abline(h = 0)
> qqnorm(residuals(Fit)); qqline(residuals(Fit))

```

J.2.5.2 Plot Output for Linear Regression Analysis for Sample Ba20170615 M_{2L}

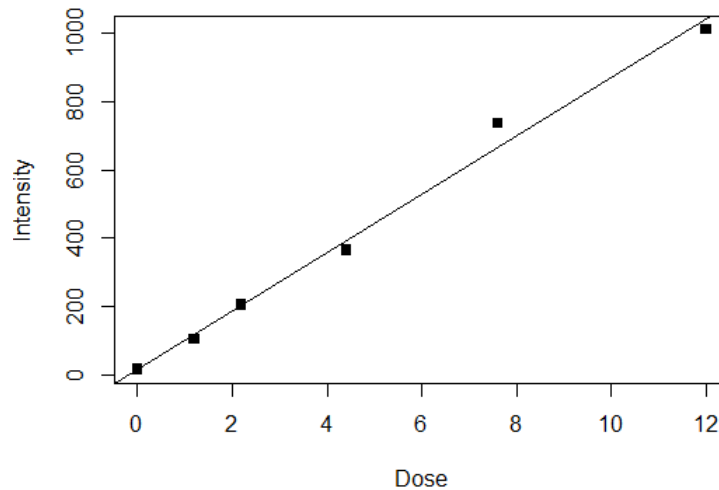


Fig. J.13. Intensity versus irradiation dose for sample Ba20170615 M_{2L}

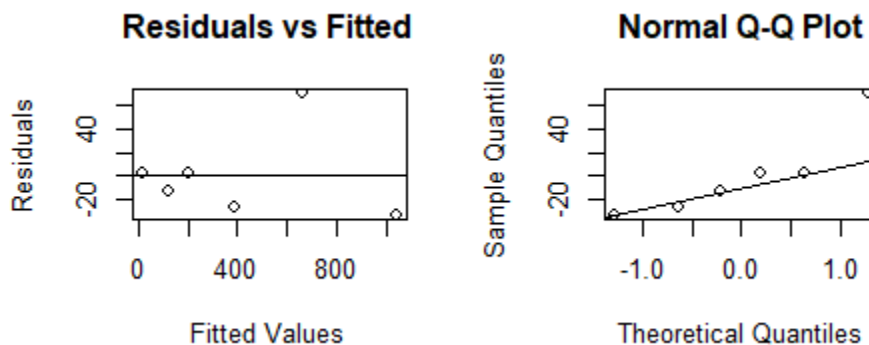


Fig. J.14. R generated plots which were used to verify linear regression assumptions for sample Ba20170615 M_{2L}

J.2.5.3 R Code for Correlation for sample Ba20170615 M_{2L}

```

> InData <- read.csv(file.choose())
> head(InData)
  Dose Intensity
1  1.2   104.63
2  2.2   204.64
3  4.4   365.34
4  7.6   736.62
5 12.0  1009.68
6  0.0    16.57
> pairs(InData)
> cor(InData)

```

```

          Dose Intensity
Dose      1.0000000 0.9953928
Intensity 0.9953928 1.0000000
> cor(InData, method = "spearman")
          Dose Intensity
Dose      1      1
Intensity 1      1
> cor.test(InData$Dose, InData$Intensity)

Pearson's product-moment correlation

data: InData$Dose and InData$Intensity
t = 20.763, df = 4, p-value = 3.179e-05
alternative hypothesis: true correlation is not equal to 0
95 percent confidence interval:
 0.9565705 0.9995198
sample estimates:
      cor
0.9953928

> cor.test(InData$Dose, InData$Intensity, method = "spearman")

Spearman's rank correlation rho

data: InData$Dose and InData$Intensity
S = 0, p-value = 0.002778
alternative hypothesis: true rho is not equal to 0
sample estimates:
rho
1

```

J.2.5.4 Plot Output for Correlation Analysis for sample Ba20170615 M_{2L}

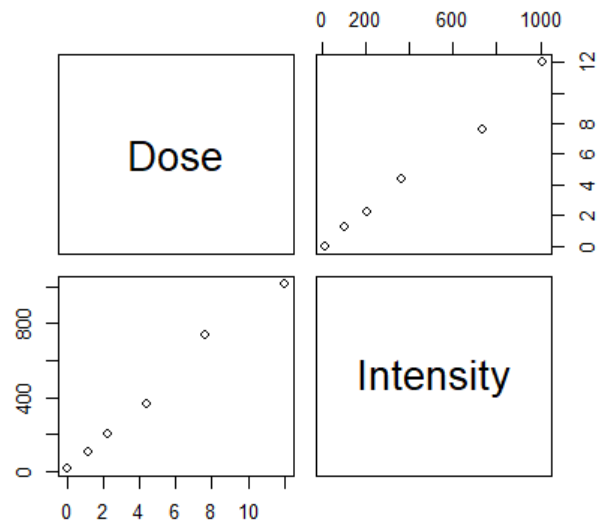


Fig. J.15. R generated plot showing the correlation between irradiation dose and intensity for sample Ba20170615 M_{2L}.

J.2.6 Sample Ba20170615 M_{2R}

Table J.7. Data used in CSV File for sample Ba20170615 M_{2R}

Dose	Intensity
1.2	46.11
2.2	85.79
4.4	183.35
7.6	306.19
12	456.51
0	38.4

J.2.6.1 R Code for Linear Regression Assumptions for sample Ba20170615 M_{2R}

```
> MR <- read.csv(file.choose())
> str(MR)
'data.frame': 6 obs. of 2 variables:
 $ Dose      : num  1.2 2.2 4.4 7.6 12 0
 $ Intensity: num  46.1 85.8 183.3 306.2 456.5 ...
> plot(Intensity ~ Dose, data = MR, pch = 15)
> abline(lm(Intensity ~ Dose, data = MR))
> Fit <- lm(Intensity ~ Dose, data = MR)
> Fit
```

```
Call:
lm(formula = Intensity ~ Dose, data = MR)
```

```
Coefficients:
(Intercept)      Dose
      18.26         36.74
```

```
>
> summary(Fit)
```

```
Call:
lm(formula = Intensity ~ Dose, data = MR)
```

```
Residuals:
    1     2     3     4     5     6
-16.242 -13.307  3.416  8.674 -2.682 20.141
```

```
Coefficients:
              Estimate Std. Error t value Pr(>|t|)
(Intercept)  18.259     9.335    1.956  0.122
Dose         36.744     1.516   24.232 1.72e-05 ***
---

```

```
Signif. codes:  0 '***' 0.001 '**' 0.01 '*' 0.05 '.' 0.1 ' ' 1
```

```
Residual standard error: 15.33 on 4 degrees of freedom
Multiple R-squared:  0.9932, Adjusted R-squared:  0.9915
F-statistic: 587.2 on 1 and 4 DF, p-value: 1.721e-05
```

```
> par(mfrow = c(2, 2))
```

```

> plot(residuals(Fit) ~ fitted(Fit), xlab = "Fitted values", ylab =
"Residuals", main = "Residuals vs Fitted"); abline(h = 0)
> qqnorm(residuals(Fit)); qqline(residuals(Fit))

```

J.2.6.2 Plot Output for Linear Regression Analysis for Sample Ba20170615 M_{2R}

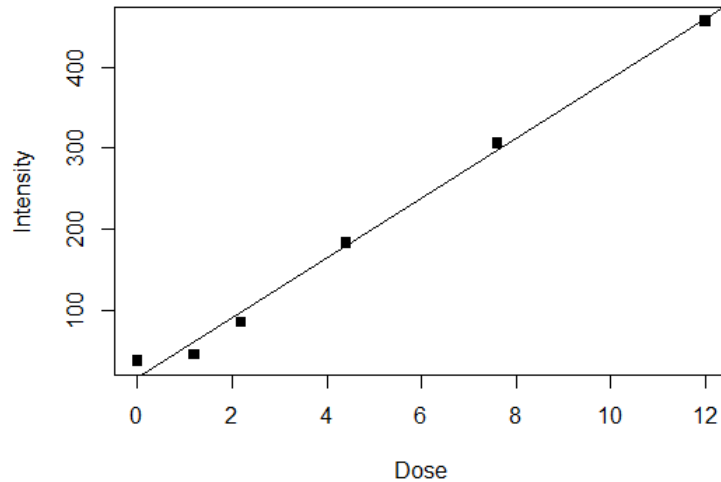


Fig. J.16. Intensity versus irradiation dose for sample Ba20170615 M_{2R}

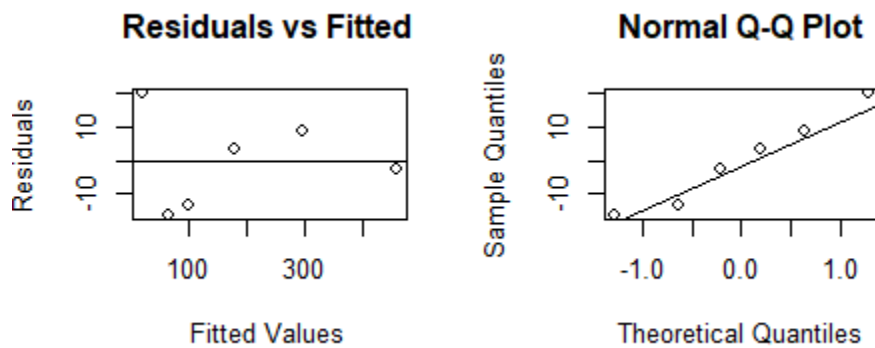


Fig. J.17. R generated plots which were used to verify linear regression assumptions for sample Ba20170615 M_{2R}

J.2.6.3 R Code for Correlation for sample Ba20170615 M_{2R}

```

> InData <- read.csv(file.choose())
> head(InData)
  Dose Intensity
1  1.2    46.11
2  2.2    85.79
3  4.4   183.35
4  7.6   306.19
5 12.0   456.51
6  0.0    38.40
> pairs(InData)
> cor(InData)
           Dose Intensity
Dose      1.000000 0.9966113

```

```

Intensity 0.9966113 1.0000000
> cor(InData, method = "spearman")
      Dose Intensity
Dose      1      1
Intensity 1      1
> cor.test(InData$Dose, InData$Intensity)

Pearson's product-moment correlation

data: InData$Dose and InData$Intensity
t = 24.232, df = 4, p-value = 1.721e-05
alternative hypothesis: true correlation is not equal to 0
95 percent confidence interval:
 0.9678914 0.9996470
sample estimates:
      cor
0.9966113

> cor.test(InData$Dose, InData$Intensity, method = "spearman")

Spearman's rank correlation rho

data: InData$Dose and InData$Intensity
S = 0, p-value = 0.002778
alternative hypothesis: true rho is not equal to 0
sample estimates:
rho
 1

```

J.2.6.4 Plot Output for Correlation Analysis for sample Ba20170615 M_{2R}

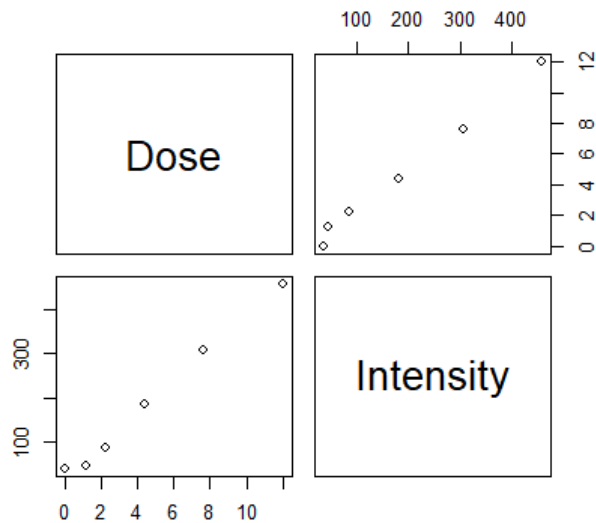


Fig. J.18. R generated plot showing the correlation between irradiation dose and intensity for sample Ba20170615 M_{2R}

J.2.7 Sample Ba20170617 P_{3L}

Table J.8. Data used in CSV File for sample Ba20170617 P_{3L}

Dose	Intensity
1.2	169.41
2.2	320.17
4.4	600.93
7.6	1046.79
0	15.6

J.2.7.1 R Code for Linear Regression Assumptions for sample Ba20170617 P_{3L}

```
> PL <- read.csv(file.choose())
> str(PL)
'data.frame': 5 obs. of 2 variables:
 $ Dose      : num  1.2 2.2 4.4 7.6 0
 $ Intensity: num  169.4 320.2 600.9 1046.8 15.6
> plot(Intensity ~ Dose, data = PL, pch = 15)
> abline(lm(Intensity ~ Dose, data = PL))
> Fit <- lm(Intensity ~ Dose, data = PL)
> Fit
Call:
lm(formula = Intensity ~ Dose, data = PL)

Coefficients:
(Intercept)      Dose
      13.0         135.6

>
> summary(Fit)

Call:
lm(formula = Intensity ~ Dose, data = PL)

Residuals:
    1     2     3     4     5
-6.285  8.898 -8.612  3.402  2.597

Coefficients:
            Estimate Std. Error t value Pr(>|t|)
(Intercept)  13.003     5.713   2.276   0.107
Dose        135.577     1.399  96.918 2.42e-06 ***
---
Signif. codes:  0 '***' 0.001 '**' 0.01 '*' 0.05 '.' 0.1 ' ' 1

Residual standard error: 8.39 on 3 degrees of freedom
Multiple R-squared:  0.9997, Adjusted R-squared:  0.9996
F-statistic: 9393 on 1 and 3 DF, p-value: 2.422e-06

> par(mfrow = c(2, 2))
> plot(residuals(Fit) ~ fitted(Fit), xlab = "Fitted values", ylab =
"Residuals", main = "Residuals vs Fitted"); abline(h = 0)
```

```
> qqnorm(residuals(Fit)); qqline(residuals(Fit))
```

J.2.7.2 Plot Output for Linear Regression Analysis for Sample Ba20170617 P_{3L}

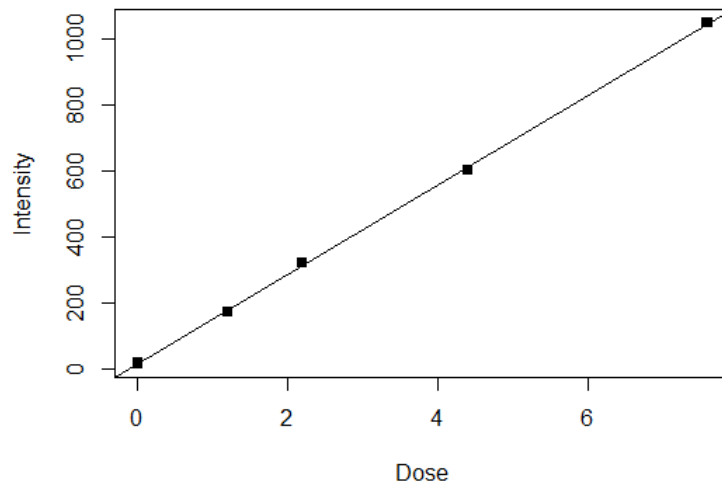


Fig. J.19. Intensity versus irradiation dose for sample Ba20170617 P_{3L}

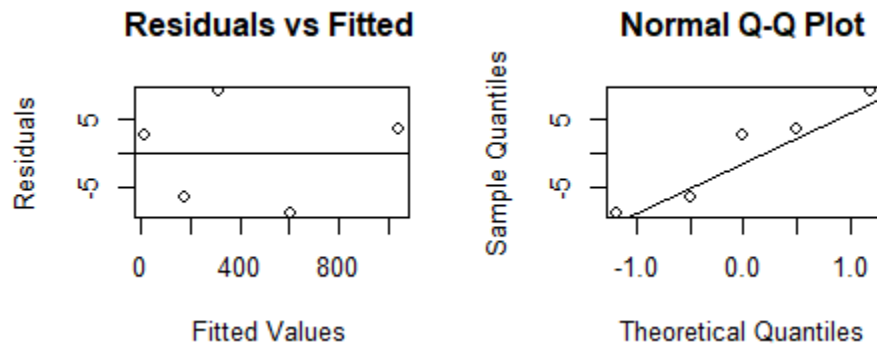


Fig. J.20. R generated plots which were used to verify linear regression assumptions for sample Ba20170617 P_{3L}

J.2.7.3 R Code for Correlation for sample Ba20170617 P_{3L}

```
> InData <- read.csv(file.choose())
> head(InData)
  Dose Intensity
1  1.2   169.41
2  2.2   320.17
3  4.4   600.93
4  7.6  1046.79
5  0.0    15.60
> pairs(InData)
> cor(InData)
           Dose Intensity
Dose      1.000000 0.9998403
Intensity 0.9998403 1.0000000
> cor(InData, method = "spearman")
```

```

      Dose Intensity
Dose      1      1
Intensity 1      1
> cor.test(InData$Dose, InData$Intensity)

Pearson's product-moment correlation

data: InData$Dose and InData$Intensity
t = 96.918, df = 3, p-value = 2.422e-06
alternative hypothesis: true correlation is not equal to 0
95 percent confidence interval:
 0.9974506 0.9999900
sample estimates:
      cor
0.9998403

> cor.test(InData$Dose, InData$Intensity, method = "spearman")

Spearman's rank correlation rho

data: InData$Dose and InData$Intensity
S = 4.4409e-15, p-value = 0.01667
alternative hypothesis: true rho is not equal to 0
sample estimates:
rho
 1

```

J.2.7.4 Plot Output for Correlation Analysis for sample Ba20170617 P_{3L}

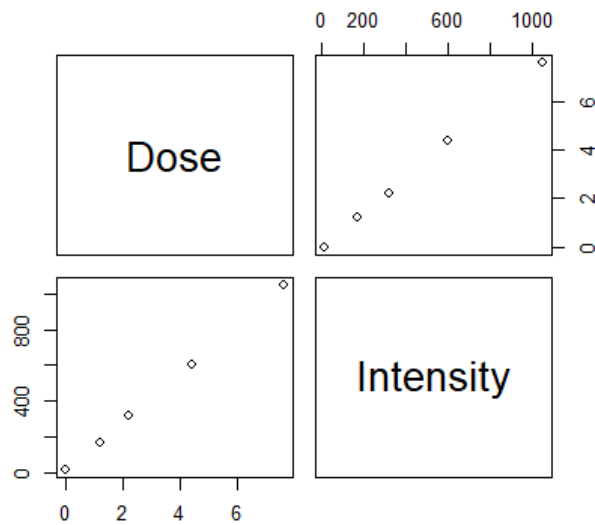


Fig. J.21. R generated plot showing the correlation between irradiation dose and intensity for sample Ba20170617 P_{3L}.

J.2.8 Sample Ba20170617 P_{3R}

Table J.9. Data used in CSV File for sample Ba20170617 P_{3R}

Dose	Intensity
1.2	137.25
2.2	278.52
4.4	485.21
7.6	911.29
12	1594.76
0	4.39

J.2.8.1 R Code for Linear Regression Assumptions for sample Ba20170617 P_{3R}

```
> PR <- read.csv(file.choose())
> str(PR)
'data.frame': 6 obs. of 2 variables:
 $ Dose      : num  1.2 2.2 4.4 7.6 12 0
 $ Intensity: num  137 279 485 911 1595 ...
> plot(Intensity ~ Dose, data = PR, pch = 15)
> abline(lm(Intensity ~ Dose, data = PR))
>
> Fit <- lm(Intensity ~ Dose, data = PR)
> Fit
```

```
Call:
lm(formula = Intensity ~ Dose, data = PR)
```

```
Coefficients:
(Intercept)      Dose
      -29.6         131.0
```

```
>
> summary(Fit)
```

```
Call:
lm(formula = Intensity ~ Dose, data = PR)
```

```
Residuals:
    1     2     3     4     5     6
 9.669 19.952 -61.529 -54.607  52.520  33.994
```

```
Coefficients:
              Estimate Std. Error t value Pr(>|t|)
(Intercept)  -29.604     32.174   -0.92   0.41
Dose         130.987     5.226   25.06 1.5e-05 ***
```

```
---
Signif. codes:  0 '***' 0.001 '**' 0.01 '*' 0.05 '.' 0.1 ' ' 1
```

```
Residual standard error: 52.85 on 4 degrees of freedom
Multiple R-squared:  0.9937, Adjusted R-squared:  0.9921
F-statistic: 628.2 on 1 and 4 DF, p-value: 1.504e-05
```

```

> par(mfrow = c(2, 2))
> plot(residuals(Fit) ~ fitted(Fit), xlab = "Fitted Values", ylab =
"Residuals", main = "Residuals vs Fitted"); abline(h = 0)
> qqnorm(residuals(Fit)); qqline(residuals(Fit))

```

J.2.8.2 Plot Output for Linear Regression Analysis for Sample Ba20170617 P_{3R}

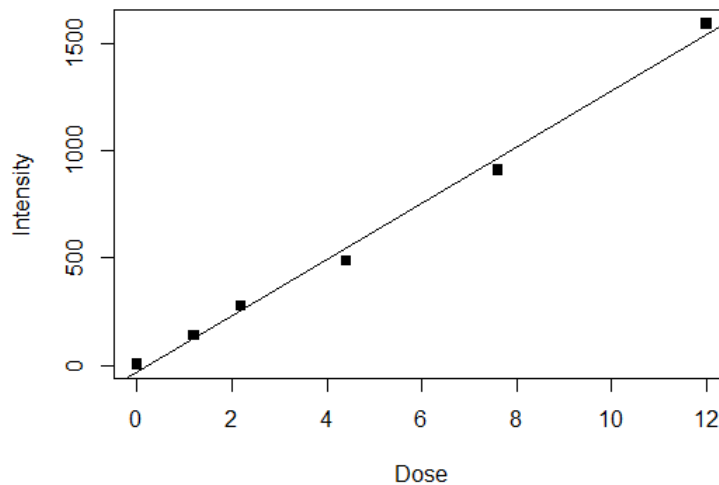


Fig. J.22. Intensity versus irradiation dose for sample Ba20170617 P_{3R}

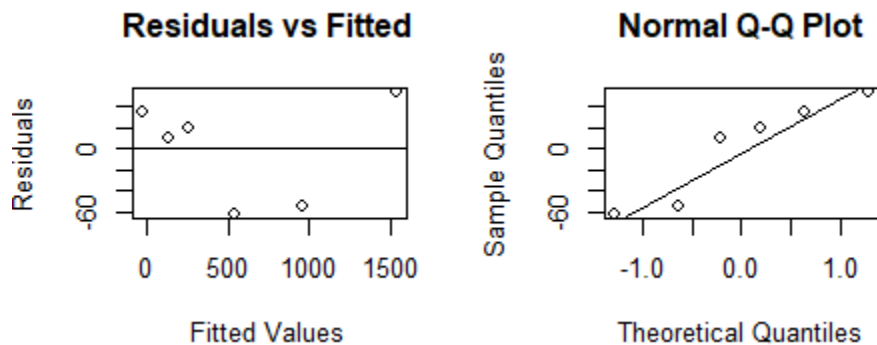


Fig. J.23. R generated plots which were used to verify linear regression assumptions for sample Ba20170617 P_{3R}

J.2.8.3 R Code for Correlation for sample Ba20170617 P_{3R}

```

> InData <- read.csv(file.choose())
> head(InData)
  Dose Intensity
1  1.2   137.25
2  2.2   278.52
3  4.4   485.21
4  7.6   911.29
5 12.0  1594.76
6  0.0    4.39
> pairs(InData)
> cor(InData)

```

```

          Dose Intensity
Dose      1.0000000 0.9968314
Intensity 0.9968314 1.0000000
> cor(InData, method = "spearman")
          Dose Intensity
Dose      1      1
Intensity 1      1
> cor.test(InData$Dose, InData$Intensity)

Pearson's product-moment correlation

data: InData$Dose and InData$Intensity
t = 25.064, df = 4, p-value = 1.504e-05
alternative hypothesis: true correlation is not equal to 0
95 percent confidence interval:
 0.9699489 0.9996699
sample estimates:
      cor
0.9968314

> cor.test(InData$Dose, InData$Intensity, method = "spearman")

Spearman's rank correlation rho

data: InData$Dose and InData$Intensity
S = 0, p-value = 0.002778
alternative hypothesis: true rho is not equal to 0
sample estimates:
rho
1

```

J.2.8.4 Plot Output for Correlation Analysis for sample Ba20170617 P_{3R}

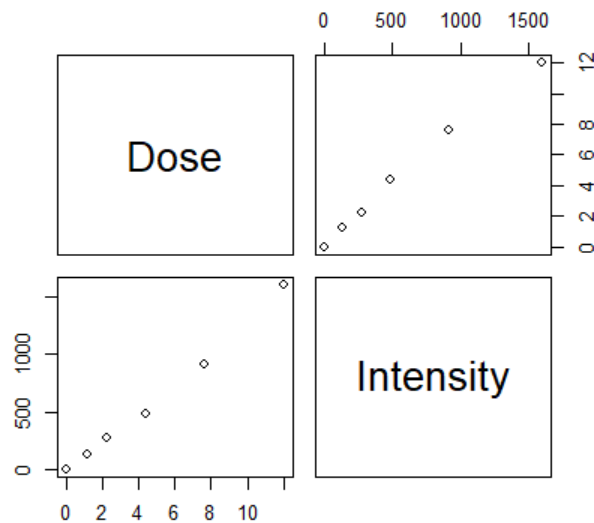


Fig. J.24. R generated plot showing the correlation between irradiation dose and intensity for sample Ba20170617 P_{3R}

J.3_Linear Regression Analysis R Code and Results for Chapter 5

J.3.1 Sample Ba20170620 M_{2L}

Table J.10. Data used in CSV File for sample Ba20170620 M_{2L}

Dose	Intensity
0.25	2.80E-07
0.5	4.23E-07
0.75	3.72E-07
1	7.36E-07
2	1.75E-06
0	2.18E-07

J.3.1.1 R Code for Linear Regression Assumptions for sample Ba20170620 M_{2L}

```
> ML <- read.csv(file.choose())
> str(ML)
'data.frame': 6 obs. of 2 variables:
 $ Dose      : num  0.25 0.5 0.75 1 2 0
 $ Intensity: num  2.80e-07 4.23e-07 3.72e-07 7.36e-07 1.75e-06 2.18e-07
> plot(Intensity ~ Dose, data = ML, pch = 15)
> abline(lm(Intensity ~ Dose, data = ML))
>
> Fit <- lm(Intensity ~ Dose, data = ML)
> Fit
```

```
Call:
lm(formula = Intensity ~ Dose, data = ML)
```

```
Coefficients:
(Intercept)      Dose
 4.116e-08    7.849e-07
```

```
>
> summary(Fit)
```

```
Call:
lm(formula = Intensity ~ Dose, data = ML)
```

```
Residuals:
    1         2         3         4         5
4.262e-08 -1.061e-08 -2.578e-07 -9.006e-08  1.390e-07
    6
1.768e-07
```

```
Coefficients:
              Estimate Std. Error t value Pr(>|t|)
(Intercept) 4.116e-08  1.116e-07  0.369  0.73089
Dose        7.849e-07  1.128e-07  6.961  0.00224 **
---
Signif. codes:  0 '***' 0.001 '**' 0.01 '*' 0.05 '.' 0.1 ' ' 1
```

Residual standard error: 1.783e-07 on 4 degrees of freedom
 Multiple R-squared: 0.9238, Adjusted R-squared: 0.9047
 F-statistic: 48.46 on 1 and 4 DF, p-value: 0.002238

```
> par(mfrow = c(2, 2))
> plot(residuals(Fit) ~ fitted(Fit), xlab = "Fitted values", ylab =
"Residuals", main = "Residuals vs Fitted"); abline(h = 0)
> qqnorm(residuals(Fit)); qqline(residuals(Fit))
```

J.3.1.2 Plot Output for Linear Regression Analysis for Sample Ba20170620 M_{2L}

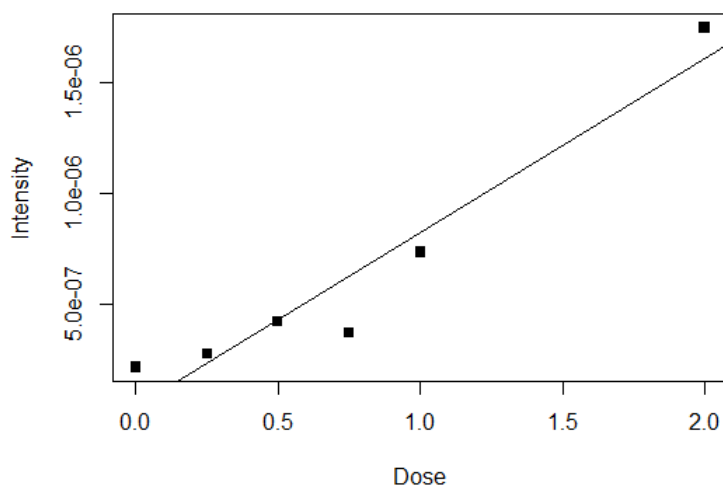


Fig. J.25. Intensity versus irradiation dose for sample Ba20170620 M_{2L}

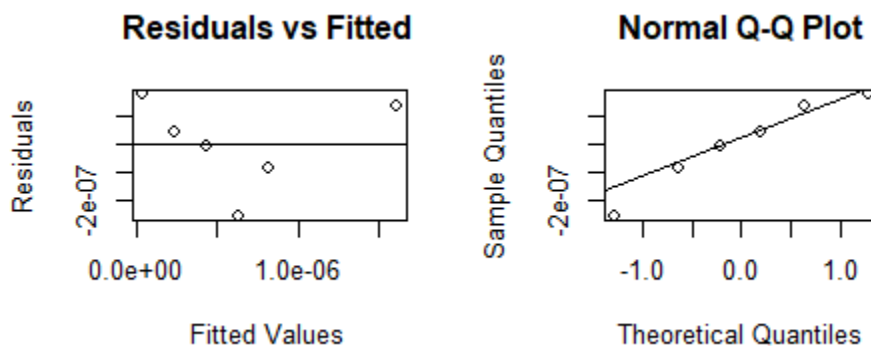


Fig. J.26 R generated plots which were used to verify linear regression assumptions for sample Ba20170620 M_{2L}

J.3.1.3 R Code for Correlation for sample Ba20170620 M_{2L}

```
> InData <- read.csv(file.choose())
> head(InData)
  Dose Intensity
1 0.25  2.80e-07
2 0.50  4.23e-07
3 0.75  3.72e-07
4 1.00  7.36e-07
5 2.00  1.75e-06
```

```

6 0.00 2.18e-07
> pairs(InData)
> cor(InData)
      Dose Intensity
Dose   1.0000000 0.9611217
Intensity 0.9611217 1.0000000
> cor(InData, method = "spearman")
      Dose Intensity
Dose   1.0000000 0.9428571
Intensity 0.9428571 1.0000000
> cor.test(InData$Dose, InData$Intensity)

```

Pearson's product-moment correlation

```

data: InData$Dose and InData$Intensity
t = 6.9615, df = 4, p-value = 0.002238
alternative hypothesis: true correlation is not equal to 0
95 percent confidence interval:
 0.6798485 0.9958842
sample estimates:
      cor
0.9611217

```

```
> cor.test(InData$Dose, InData$Intensity, method = "spearman")
```

Spearman's rank correlation rho

```

data: InData$Dose and InData$Intensity
S = 2, p-value = 0.01667
alternative hypothesis: true rho is not equal to 0
sample estimates:
      rho
0.9428571

```

J.3.1.4 Plot Output for Correlation Analysis for sample Ba20170620 M_{2L}

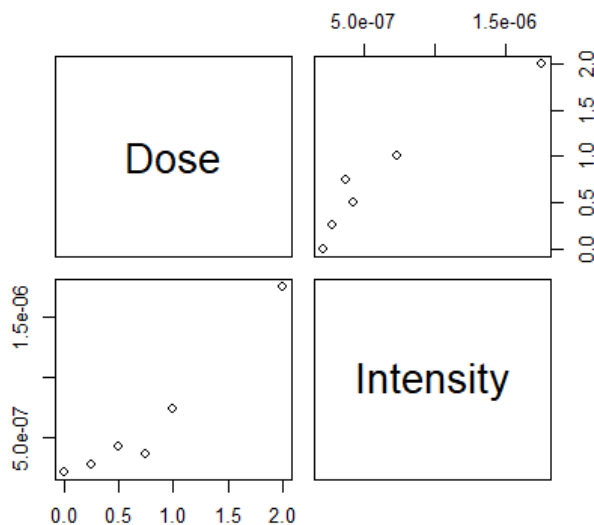


Fig. J.27. R generated plot showing the correlation between irradiation dose and intensity for sample Ba20170620 M_{2L}.

J.3.2 Sample Ba20170620 M_{2R}

Table J.11. Data used in CSV File for sample Ba20170620 M_{2R}

Dose	Intensity
0.25	4.64E-07
0.5	6.16E-07
0.75	1.48E-06
1	1.34E-06
2	2.95E-06
0	9.59E-07

J.3.2.1 R Code for Linear Regression Assumptions for sample Ba20170620 M_{2R}

```
> MR <- read.csv(file.choose())
> str(MR)
'data.frame': 6 obs. of 2 variables:
 $ Dose      : num  0.25 0.5 0.75 1 2 0
 $ Intensity: num  4.64e-07 6.16e-07 1.48e-06 1.34e-06 2.95e-06 ...
> plot(Intensity ~ Dose, data = MR, pch = 15)
> abline(lm(Intensity ~ Dose, data = MR))
> Fit <- lm(Intensity ~ Dose, data = MR)
> Fit
```

```
Call:
lm(formula = Intensity ~ Dose, data = MR)
```

```
Coefficients:
(Intercept)      Dose
 4.261e-07      1.167e-06
```

```
>
> summary(Fit)
```

```
Call:
lm(formula = Intensity ~ Dose, data = MR)
```

```
Residuals:
    1      2      3      4      5
-2.540e-07 -3.938e-07  1.783e-07 -2.535e-07  1.901e-07
    6
 5.329e-07
```

```
Coefficients:
            Estimate Std. Error t value Pr(>|t|)
(Intercept) 4.261e-07  2.495e-07   1.708  0.16285
Dose        1.167e-06  2.521e-07   4.630  0.00981 **
---
Signif. codes:  0 '***' 0.001 '**' 0.01 '*' 0.05 '.' 0.1 ' ' 1
```

```
Residual standard error: 3.987e-07 on 4 degrees of freedom
Multiple R-squared:  0.8427, Adjusted R-squared:  0.8034
F-statistic: 21.44 on 1 and 4 DF, p-value: 0.009808
```

```

> par(mfrow = c(2, 2))
> plot(residuals(Fit) ~ fitted(Fit), xlab = "Fitted Values", ylab =
"Residuals", main = "Residuals vs Fitted"); abline(h = 0)
> qqnorm(residuals(Fit)); qqline(residuals(Fit))

```

J.3.2.2 Plot Output for Linear Regression Analysis for Sample Ba20170620 M_{2R}

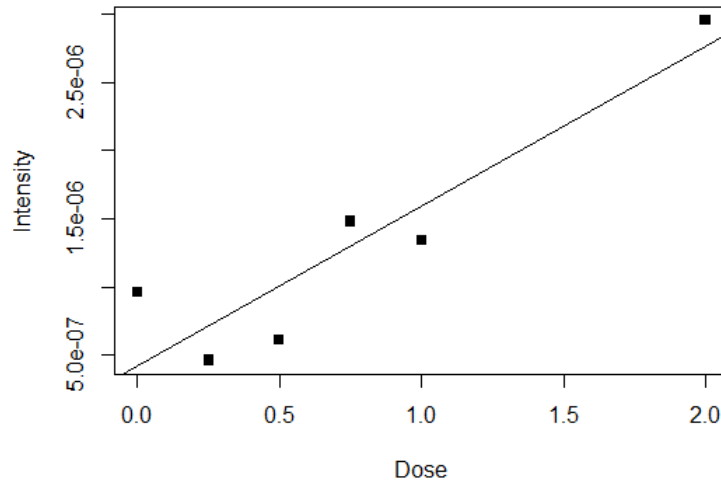


Fig. J.28 Intensity versus irradiation dose for sample Ba20170620 M_{2R}

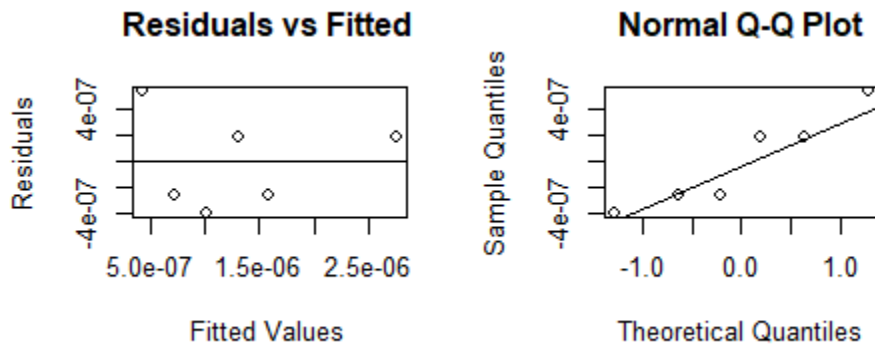


Fig. J.29 R generated plots which were used to verify linear regression assumptions for sample Ba20170620 M_{2R}

J.3.2.3 R Code for Correlation for sample Ba20170620 M_{2R}

```

> InData <- read.csv(file.choose())
> head(InData)
  Dose Intensity
1 0.25 4.640e-07
2 0.50 6.160e-07
3 0.75 1.480e-06
4 1.00 1.340e-06
5 2.00 2.951e-06
6 0.00 9.590e-07
> pairs(InData)
> cor(InData)

```

```

      Dose Intensity
Dose      1.000000 0.9180105
Intensity 0.9180105 1.0000000
> cor(InData, method = "spearman")
      Dose Intensity
Dose      1.0000000 0.7714286
Intensity 0.7714286 1.0000000
> cor.test(InData$Dose, InData$Intensity)

Pearson's product-moment correlation

data: InData$Dose and InData$Intensity
t = 4.6299, df = 4, p-value = 0.009808
alternative hypothesis: true correlation is not equal to 0
95 percent confidence interval:
 0.4174834 0.9911462
sample estimates:
      cor
0.9180105
> cor.test(InData$Dose, InData$Intensity, method = "spearman")

Spearman's rank correlation rho

data: InData$Dose and InData$Intensity
S = 8, p-value = 0.1028
alternative hypothesis: true rho is not equal to 0
sample estimates:
      rho
0.7714286

```

J.3.2.4 Plot Output for Correlation Analysis for sample Ba20170620 M_{2R}

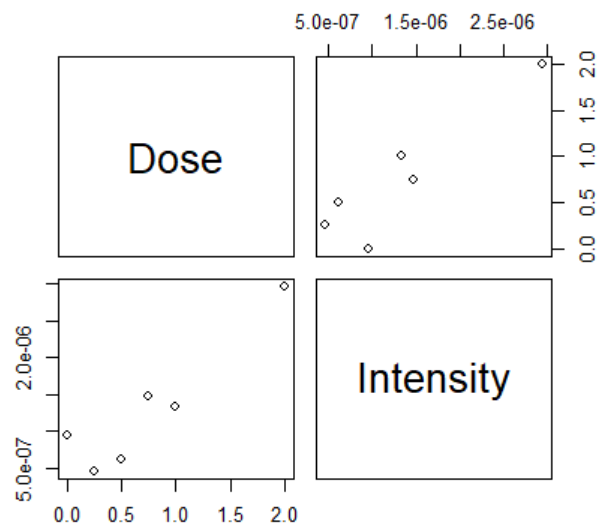


Fig. J.30. R generated plot showing the correlation between irradiation dose and intensity for sample Ba20170620 M_{2R}

J.3.3 Sample Bb20170623 M_{IL}

Table J.12. Data used in CSV File for Sample Bb20170623 M_{IL}

Dose	Intensity
0.25	2.60E-07
0.5	3.46E-07
0.75	4.52E-07
1	4.05E-07
0	1.99E-07

J.3.3.1 R Code for Linear Regression Assumptions for sample Bb20170623 M_{IL}

```
> ML <- read.csv(file.choose())
> str(ML)
'data.frame': 5 obs. of 2 variables:
 $ Dose      : num  0.25 0.5 0.75 1 0
 $ Intensity: num  2.60e-07 3.46e-07 4.51e-07 4.04e-07 1.99e-07
> plot(Intensity ~ Dose, data = ML, pch = 15)
> abline(lm(Intensity ~ Dose, data = ML))
>
> Fit <- lm(Intensity ~ Dose, data = ML)
> Fit
```

```
Call:
lm(formula = Intensity ~ Dose, data = ML)
```

```
Coefficients:
(Intercept)      Dose
 2.116e-07      2.412e-07
```

```
> summary(Fit)
```

```
Call:
lm(formula = Intensity ~ Dose, data = ML)
```

```
Residuals:
    1         2         3         4         5
-1.155e-08  1.392e-08  5.899e-08 -4.831e-08 -1.305e-08
```

```
Coefficients:
              Estimate Std. Error t value Pr(>|t|)
(Intercept) 2.116e-07  3.553e-08   5.956  0.00946 **
Dose        2.412e-07  5.802e-08   4.157  0.02530 *
```

```
---
Signif. codes:  0 '***' 0.001 '**' 0.01 '*' 0.05 '.' 0.1 ' ' 1
```

```
Residual standard error: 4.587e-08 on 3 degrees of freedom
Multiple R-squared:  0.8521, Adjusted R-squared:  0.8028
F-statistic: 17.28 on 1 and 3 DF, p-value: 0.0253
```

```
> par(mfrow = c(2, 2))
```

```
> plot(residuals(Fit) ~ fitted(Fit), xlab = "Fitted values", ylab =
"Residuals", main = "Residuals vs Fitted"); abline(h = 0)
> qqnorm(residuals(Fit)); qqline(residuals(Fit))
```

J.3.3.2 Plot Output for Linear Regression Analysis for Sample Bb20170623 M_{IL}

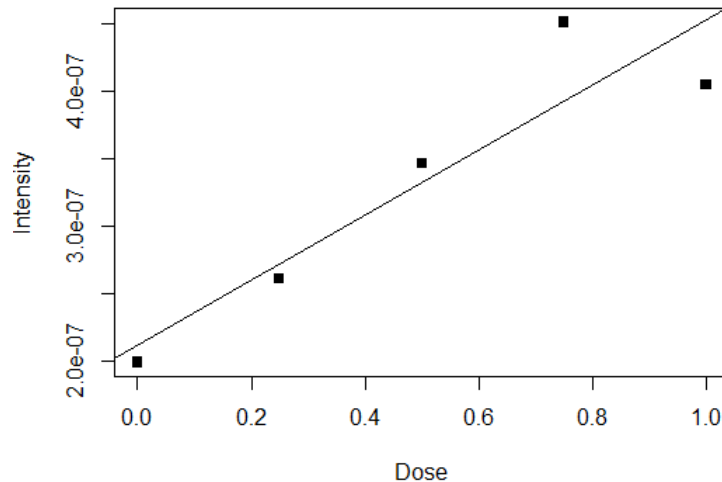


Fig. J.31. Intensity versus irradiation dose for sample Bb20170623 M_{IL}

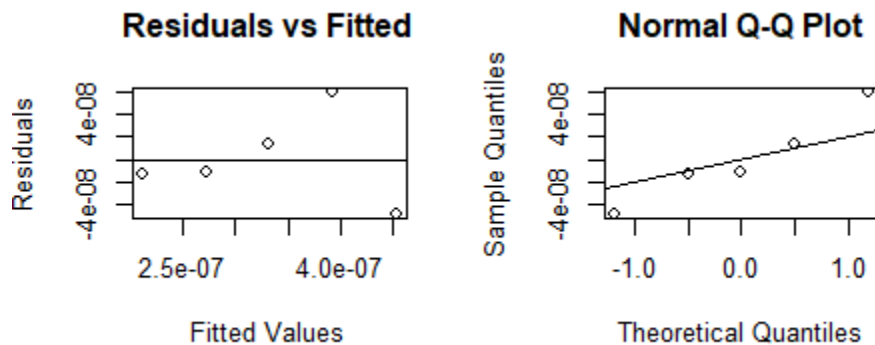


Fig. J.32. R generated plots which were used to verify linear regression assumptions for sample Bb20170623 M_{IL}

J.3.3.3 R Code for Correlation for sample Bb20170623 M_{IL}

```
> InData <- read.csv(file.choose())
> head(InData)
  Dose Intensity
1 0.25 2.60367e-07
2 0.50 3.46133e-07
3 0.75 4.51500e-07
4 1.00 4.04500e-07
5 0.00 1.98567e-07
> pairs(InData)
> cor(InData)
           Dose Intensity
Dose      1.0000000 0.9230958
Intensity 0.9230958 1.0000000
> cor(InData, method = "spearman")
```

```

      Dose Intensity
Dose      1.0      0.9
Intensity 0.9      1.0
> cor.test(InData$Dose, InData$Intensity)

Pearson's product-moment correlation

data: InData$Dose and InData$Intensity
t = 4.1575, df = 3, p-value = 0.0253
alternative hypothesis: true correlation is not equal to 0
95 percent confidence interval:
 0.2200056 0.9950099
sample estimates:
      cor
0.9230958

> cor.test(InData$Dose, InData$Intensity, method = "spearman")

Spearman's rank correlation rho

data: InData$Dose and InData$Intensity
S = 2, p-value = 0.08333
alternative hypothesis: true rho is not equal to 0
sample estimates:
rho
0.9

```

J.3.3.4 Plot Output for Correlation Analysis for sample Bb20170623 M_{IL}

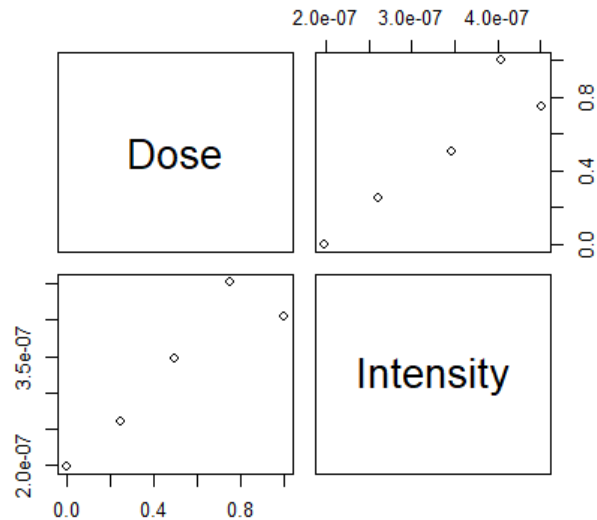


Fig. J.33. R generated plot showing the correlation between irradiation dose and intensity for sample Bb20170623 M_{IL}

J.3.4 Sample Bb20170623 M_{1R}

Table J.13. Data used in CSV File for Sample Bb20170623 M_{1R}

Dose	Intensity
0.25	4.06E-07
0.5	5.06E-07
0.75	5.69E-07
1	5.86E-07
0	2.69E-07

J.3.4.1 R Code for Linear Regression Assumptions for sample Bb20170623 M_{1R}

```
> MR <- read.csv(file.choose())
> str(MR)
'data.frame':  5 obs. of  2 variables:
 $ Dose      : num  0.25 0.5 0.75 1 0
 $ Intensity: num  4.06e-07 5.06e-07 5.69e-07 5.86e-07 2.69e-07
> plot(Intensity ~ Dose, data = MR, pch = 15)
> abline(lm(Intensity ~ Dose, data = MR))
> Fit <- lm(Intensity ~ Dose, data = MR)
> Fit

Call:
lm(formula = Intensity ~ Dose, data = MR)

Coefficients:
(Intercept)      Dose 
 3.078e-07      3.188e-07

> summary(Fit)

Call:
lm(formula = Intensity ~ Dose, data = MR)

Residuals:
    1         2         3         4         5 
1.805e-08  3.859e-08  2.207e-08 -4.036e-08 -3.835e-08

Coefficients:
            Estimate Std. Error t value Pr(>|t|)
(Intercept) 3.078e-07  3.287e-08   9.364  0.00258 **
Dose        3.188e-07  5.368e-08   5.939  0.00954 **
---
Signif. codes:  0 '***' 0.001 '**' 0.01 '*' 0.05 '.' 0.1 ' ' 1

Residual standard error: 4.244e-08 on 3 degrees of freedom
Multiple R-squared:  0.9216, Adjusted R-squared:  0.8955
F-statistic: 35.27 on 1 and 3 DF, p-value: 0.009544

> par(mfrow = c(2, 2))
> plot(residuals(Fit) ~ fitted(Fit), xlab = "Fitted values", ylab =
"Residuals", main = "Residuals vs Fitted"); abline(h = 0)
> qqnorm(residuals(Fit)); qqline(residuals(Fit))
```

J.3.4.2 Plot Output for Linear Regression Analysis for Sample Bb20170623 M_{IR}

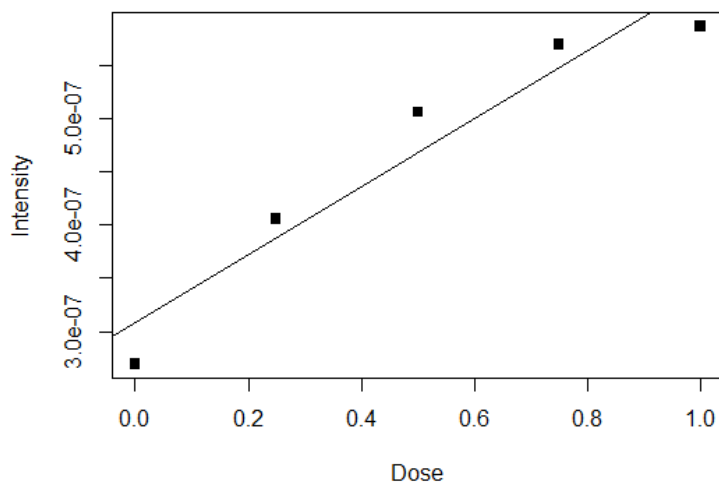


Fig. J.34. Intensity versus irradiation dose for sample Bb20170623 M_{IR}

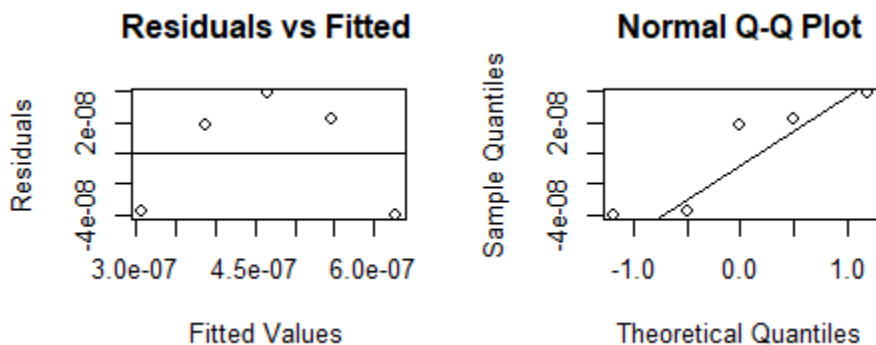


Fig. J.35. R generated plots which were used to verify linear regression assumptions for sample Bb20170623 M_{IR}

J.3.4.3 R Code for Correlation for sample Bb20170623 M_{IR}

```
> InData <- read.csv(file.choose())
> head(InData)
  Dose Intensity
1 0.25 4.05533e-07
2 0.50 5.05767e-07
3 0.75 5.68933e-07
4 1.00 5.86200e-07
5 0.00 2.69433e-07
> pairs(InData)
> cor(InData)
           Dose Intensity
Dose      1.0000000 0.9600039
Intensity 0.9600039 1.0000000
> cor(InData, method = "spearman")
           Dose Intensity
Dose          1          1
Intensity      1          1
> cor.test(InData$Dose, InData$Intensity)
```

Pearson's product-moment correlation

```
data: InData$Dose and InData$Intensity
t = 5.9388, df = 3, p-value = 0.009544
alternative hypothesis: true correlation is not equal to 0
95 percent confidence interval:
 0.5080187 0.9974505
sample estimates:
      cor
0.9600039
```

```
> cor.test(InData$Dose, InData$Intensity, method = "spearman")
```

Spearman's rank correlation rho

```
data: InData$Dose and InData$Intensity
S = 4.4409e-15, p-value = 0.01667
alternative hypothesis: true rho is not equal to 0
sample estimates:
rho
 1
```

J.3.4.4 Plot Output for Correlation Analysis for sample Bb20170623 M_{1R}

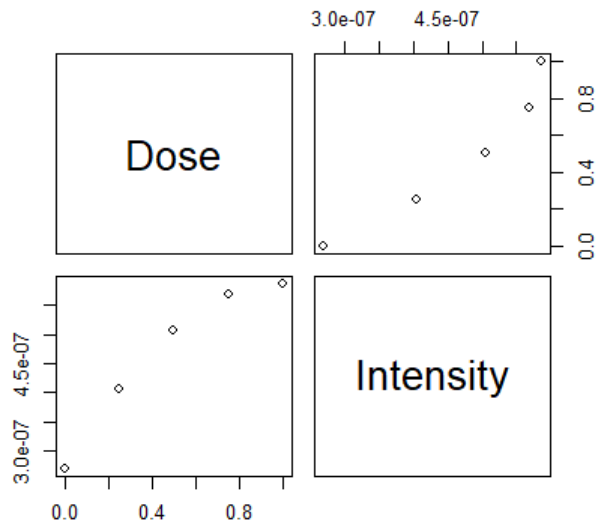


Fig. J.36. R generated plot showing the correlation between irradiation dose and intensity for sample Bb20170623 M_{1R}

J.3.5 Sample Ba20170627 M_{2L}

Table J.14. Data used in CSV File for Sample Ba20170627 M_{2L}

Dose	Intensity
0.25	6.98E-07
0.5	9.05E-07
0.75	1.12E-06
1	1.23E-06
2	2.01E-06
0	5.66E-07

J.3.5.1 R Code for Linear Regression Assumptions for sample Ba20170627 M_{2L}

```
> ML <- read.csv(file.choose())
> str(ML)
'data.frame': 6 obs. of 2 variables:
 $ Dose      : num  0.25 0.5 0.75 1 2 0
 $ Intensity: num  6.98e-07 9.05e-07 1.12e-06 1.23e-06 2.01e-06 ...
> plot(Intensity ~ Dose, data = ML, pch = 15)
> abline(lm(Intensity ~ Dose, data = ML))
>
> Fit <- lm(Intensity ~ Dose, data = ML)
> Fit
```

```
Call:
lm(formula = Intensity ~ Dose, data = ML)
```

```
Coefficients:
(Intercept)      Dose
 5.414e-07      7.303e-07
```

```
>
> summary(Fit)
```

```
Call:
lm(formula = Intensity ~ Dose, data = ML)
```

```
Residuals:
    1      2      3      4      5
-2.600e-08 -1.719e-09  2.919e-08 -3.705e-08  1.126e-08
    6
 2.432e-08
```

```
Coefficients:
            Estimate Std. Error t value Pr(>|t|)
(Intercept) 5.414e-07  1.883e-08  28.75 8.72e-06 ***
Dose        7.304e-07  1.903e-08  38.37 2.75e-06 ***
---
Signif. codes:  0 '***' 0.001 '**' 0.01 '*' 0.05 '.' 0.1 ' ' 1
```

```
Residual standard error: 3.009e-08 on 4 degrees of freedom
Multiple R-squared:  0.9973, Adjusted R-squared:  0.9966
```

F-statistic: 1473 on 1 and 4 DF, p-value: 2.755e-06

```
> par(mfrow = c(2, 2))  
> plot(residuals(Fit) ~ fitted(Fit), xlab = "Fitted values", ylab =  
"Residuals", main = "Residuals vs Fitted"); abline(h = 0)  
> qqnorm(residuals(Fit)); qqline(residuals(Fit))
```

J.3.5.2 Plot Output for Linear Regression Analysis for Sample Ba20170627 M_{2L}

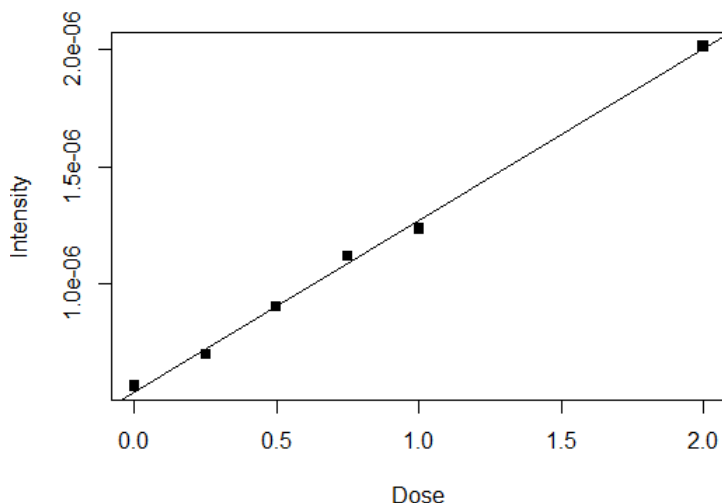


Fig. J.37. Intensity versus irradiation dose for sample Ba20170627 M_{2L}

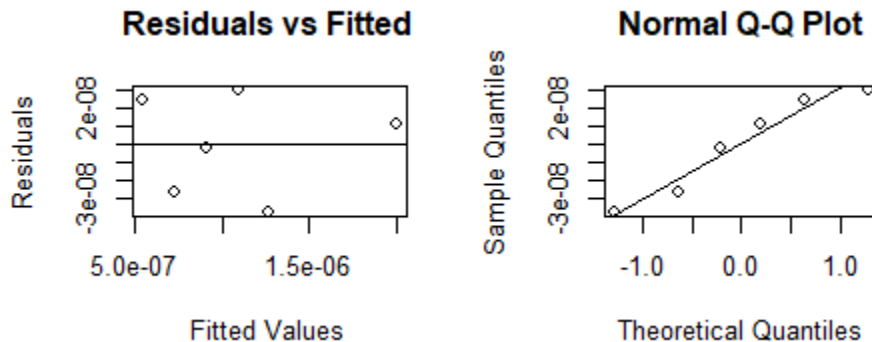


Fig. J.38. R generated plots which were used to verify linear regression assumptions for sample Ba20170627 M_{2L}

J.3.5.3 R Code for Correlation for sample Ba20170627 M_{2L}

```
> InData <- read.csv(file.choose())  
> head(InData)  
  Dose Intensity  
1 0.25 6.97967e-07  
2 0.50 9.04833e-07  
3 0.75 1.11833e-06  
4 1.00 1.23467e-06  
5 2.00 2.01333e-06  
6 0.00 5.65700e-07  
> pairs(InData)  
> cor(InData)
```

```

      Dose Intensity
Dose    1.0000000 0.9986446
Intensity 0.9986446 1.0000000
> cor(InData, method = "spearman")
      Dose Intensity
Dose      1      1
Intensity 1      1
> cor.test(InData$Dose, InData$Intensity)

Pearson's product-moment correlation

data: InData$Dose and InData$Intensity
t = 38.374, df = 4, p-value = 2.755e-06
alternative hypothesis: true correlation is not equal to 0
95 percent confidence interval:
 0.9870450 0.9998589
sample estimates:
      cor
0.9986446

> cor.test(InData$Dose, InData$Intensity, method = "spearman")

Spearman's rank correlation rho

data: InData$Dose and InData$Intensity
S = 0, p-value = 0.002778
alternative hypothesis: true rho is not equal to 0
sample estimates:
rho
 1

```

J.3.5.4 Plot Output for Correlation Analysis for sample Ba20170627 M_{2L}

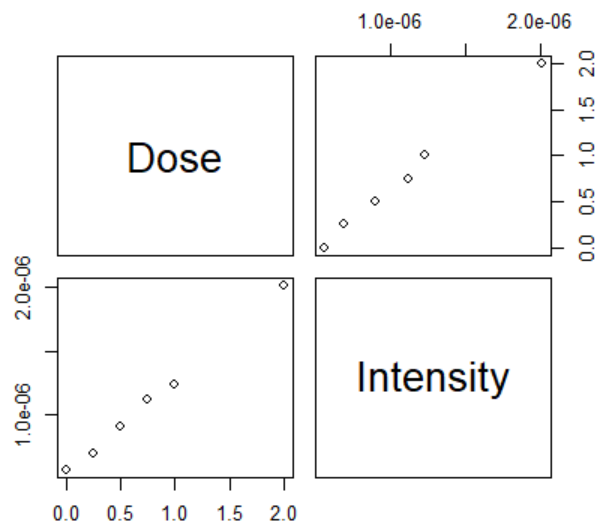


Fig. J.39. R generated plot showing the correlation between irradiation dose and intensity for sample Ba20170627 M_{2L}.

J.3.6 Sample Ba20170627 M_{2R}

Table J.15. Data used in CSV File for Sample Ba20170627 M_{2R}

Dose	Intensity
0.25	4.63E-07
0.5	6.94E-07
0.75	8.31E-07
1	1.08E-06
2	1.87E-06
0	4.13E-07

J.3.6.1 R Code for Linear Regression Assumptions for sample Ba20170627 M_{2R}

```
> MR <- read.csv(file.choose())
> str(MR)
'data.frame': 6 obs. of 2 variables:
 $ Dose      : num  0.25 0.5 0.75 1 2 0
 $ Intensity: num  4.63e-07 6.94e-07 8.31e-07 1.08e-06 1.87e-06 ...
> plot(Intensity ~ Dose, data = MR, pch = 15)
> abline(lm(Intensity ~ Dose, data = MR))
>
> Fit <- lm(Intensity ~ Dose, data = MR)
> Fit
```

```
Call:
lm(formula = Intensity ~ Dose, data = MR)
```

```
Coefficients:
(Intercept)      Dose
 3.233e-07      7.582e-07
```

```
>
> summary(Fit)
```

```
Call:
lm(formula = Intensity ~ Dose, data = MR)
```

```
Residuals:
    1         2         3         4         5
-4.968e-08 -8.072e-09 -6.107e-08 -4.858e-09  3.356e-08
    6
 9.012e-08
```

```
Coefficients:
              Estimate Std. Error t value Pr(>|t|)
(Intercept) 3.233e-07  3.900e-08   8.289  0.00116 **
Dose        7.583e-07  3.941e-08  19.239  4.3e-05 ***
---
Signif. codes:  0 '***' 0.001 '**' 0.01 '*' 0.05 '.' 0.1 ' ' 1
```

```
Residual standard error: 6.232e-08 on 4 degrees of freedom
Multiple R-squared:  0.9893, Adjusted R-squared:  0.9866
```

F-statistic: 370.1 on 1 and 4 DF, p-value: 4.302e-05

```
> par(mfrow = c(2, 2))  
> plot(residuals(Fit) ~ fitted(Fit), xlab = "Fitted values", ylab =  
"Residuals", main = "Residuals vs Fitted"); abline(h = 0)  
> qqnorm(residuals(Fit)); qqline(residuals(Fit))
```

J.3.6.2 Plot Output for Linear Regression Analysis for Sample Ba20170627 M_{2R}

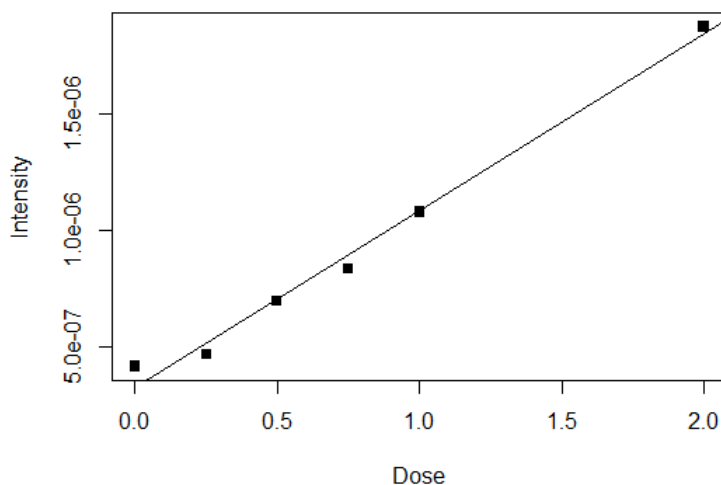


Fig. J.40. Intensity versus irradiation dose for sample Ba20170627 M_{2R}

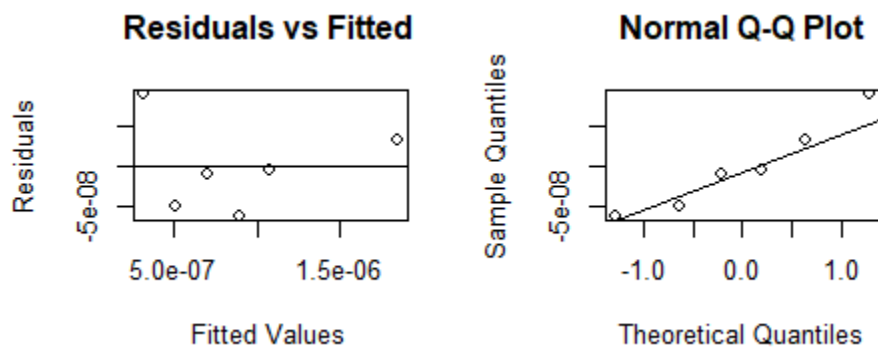


Fig. J.41. R generated plots which were used to verify linear regression assumptions for sample Ba20170627 M_{2R}

J.3.6.3 R Code for Correlation for sample Ba20170627 M_{2R}

```
> InData <- read.csv(file.choose())  
> head(InData)  
  Dose Intensity  
1 0.25 4.63167e-07  
2 0.50 6.94333e-07  
3 0.75 8.30900e-07  
4 1.00 1.07667e-06  
5 2.00 1.87333e-06  
6 0.00 4.13400e-07  
> pairs(InData)  
> cor(InData)
```

```

          Dose Intensity
Dose      1.0000000 0.9946401
Intensity 0.9946401 1.0000000
> cor(InData, method = "spearman")
          Dose Intensity
Dose           1           1
Intensity      1           1
> cor.test(InData$Dose, InData$Intensity)

Pearson's product-moment correlation

data: InData$Dose and InData$Intensity
t = 19.239, df = 4, p-value = 4.302e-05
alternative hypothesis: true correlation is not equal to 0
95 percent confidence interval:
 0.9496347 0.9994411
sample estimates:
      cor
0.9946401

> cor.test(InData$Dose, InData$Intensity, method = "spearman")

Spearman's rank correlation rho

data: InData$Dose and InData$Intensity
S = 0, p-value = 0.002778
alternative hypothesis: true rho is not equal to 0
sample estimates:
rho
 1

```

J.3.6.4 Plot Output for Correlation Analysis for sample Ba20170627 M_{2R}

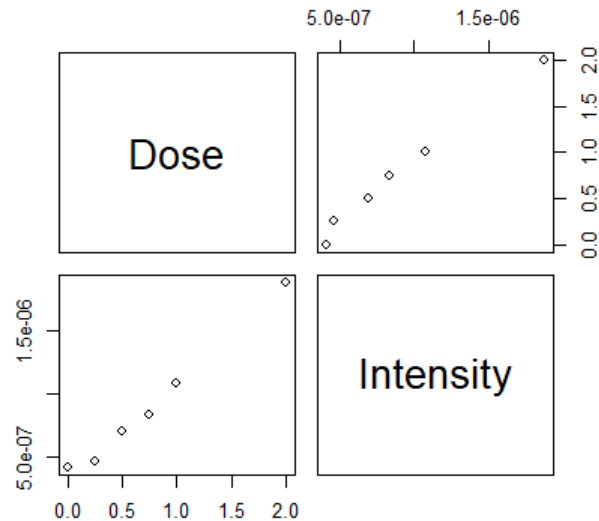


Fig. J.42. R generated plot showing the correlation between irradiation dose and intensity for sample Ba20170627 M_{2R}

J.3.7 Sample Bb20170717 M_{3L}

Table J.16. Data used in CSV File for Sample Bb20170717 M_{3L}

Dose	Intensity
0.25	9.57E-07
0.5	1.08E-06
0.75	7.37E-07
1	8.76E-07
2	1.87E-06
0	4.38E-07

J.3.7.1 R Code for Linear Regression Assumptions for sample Bb20170717 M_{3L}

```
> ML <- read.csv(file.choose())
> str(ML)
'data.frame': 6 obs. of 2 variables:
 $ Dose      : num  0.25 0.5 0.75 1 2 0
 $ Intensity: num  9.57e-07 1.08e-06 7.37e-07 8.76e-07 1.87e-06 ...
> plot(Intensity ~ Dose, data = ML, pch = 15)
> abline(lm(Intensity ~ Dose, data = ML))
> Fit <- lm(Intensity ~ Dose, data = ML)
> Fit
```

```
Call:
lm(formula = Intensity ~ Dose, data = ML)
```

```
Coefficients:
(Intercept)      Dose
 5.504e-07      5.893e-07
```

```
>
> summary(Fit)
```

```
Call:
lm(formula = Intensity ~ Dose, data = ML)
```

```
Residuals:
    1      2      3      4      5
2.597e-07 2.362e-07 -2.554e-07 -2.640e-07 1.363e-07
    6
-1.128e-07
```

```
Coefficients:
              Estimate Std. Error t value Pr(>|t|)
(Intercept) 5.504e-07  1.684e-07   3.269  0.0308 *
Dose        5.893e-07  1.701e-07   3.464  0.0257 *
```

```
---
Signif. codes:  0 '***' 0.001 '**' 0.01 '*' 0.05 '.' 0.1 ' ' 1
```

```
Residual standard error: 2.69e-07 on 4 degrees of freedom
Multiple R-squared: 0.75, Adjusted R-squared: 0.6874
```

F-statistic: 12 on 1 and 4 DF, p-value: 0.02573

```
> par(mfrow = c(2, 2))
> plot(residuals(Fit) ~ fitted(Fit), xlab = "Fitted values", ylab =
"Residuals", main = "Residuals vs Fitted"); abline(h = 0)
> qqnorm(residuals(Fit)); qqline(residuals(Fit))
```

J.3.7.2 Plot Output for Linear Regression Analysis for Sample Bb20170717 M_{3L}

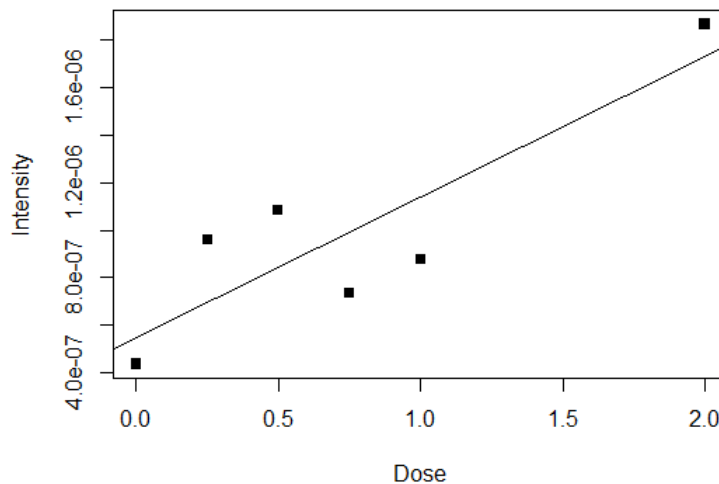


Fig. J.43. Intensity versus irradiation dose for sample Bb20170717 M_{3L}

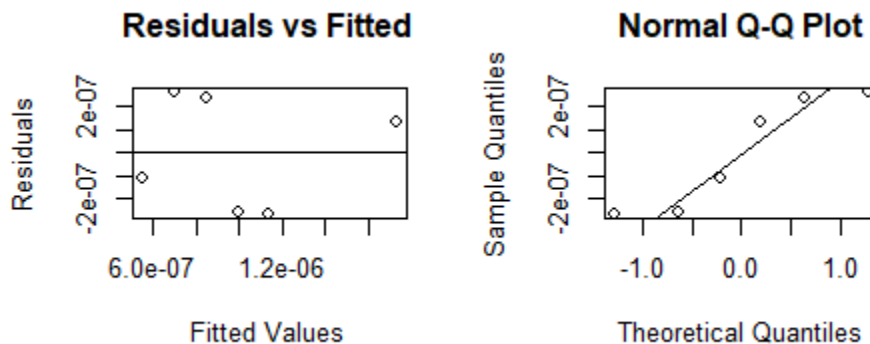


Fig. J.44 R generated plots which were used to verify linear regression assumptions for sample Bb20170717 M_{3L}

J.3.7.3 R Code for Correlation for sample Bb20170717 M_{3L}

```
> InData <- read.csv(file.choose())
> head(InData)
  Dose Intensity
1 0.25 9.57433e-07
2 0.50 1.08133e-06
3 0.75 7.36997e-07
4 1.00 8.75700e-07
5 2.00 1.86533e-06
6 0.00 4.37667e-07
> pairs(InData)
> cor(InData)
```

```

      Dose Intensity
Dose      1.000000 0.8659975
Intensity 0.8659975 1.000000
> cor(InData, method = "spearman")
      Dose Intensity
Dose      1.000000 0.5428571
Intensity 0.5428571 1.000000
> cor.test(InData$Dose, InData$Intensity)

```

Pearson's product-moment correlation

```

data: InData$Dose and InData$Intensity
t = 3.4637, df = 4, p-value = 0.02573
alternative hypothesis: true correlation is not equal to 0
95 percent confidence interval:
 0.1831698 0.9851708
sample estimates:
      cor
0.8659975

```

```
> cor.test(InData$Dose, InData$Intensity, method = "spearman")
```

Spearman's rank correlation rho

```

data: InData$Dose and InData$Intensity
S = 16, p-value = 0.2972
alternative hypothesis: true rho is not equal to 0
sample estimates:
      rho
0.5428571

```

J.3.7.4 Plot Output for Correlation Analysis for sample Bb20170717 M_{3L}

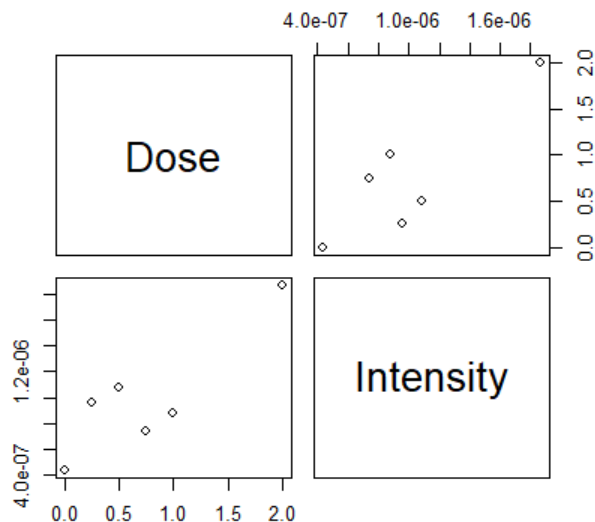


Fig. J.45. R generated plot showing the correlation between irradiation dose and intensity for sample Bb20170717 M_{3L}.

J.3.8 Sample Bb20170717 M_{3R}

Table J.17. Data used in CSV File for Sample Bb20170717 M_{3R}

Dose	Intensity
0.25	5.64E-07
0.5	6.67E-07
0.75	1.06E-06
1	8.80E-07
2	2.28E-06
0	4.18E-07

J.3.8.1 R Code for Linear Regression Assumptions for sample Bb20170717 M_{3R}

```
> MR <- read.csv(file.choose())
> str(MR)
'data.frame': 6 obs. of 2 variables:
 $ Dose      : num  0.25 0.5 0.75 1 2 0
 $ Intensity: num  5.64e-07 6.67e-07 1.06e-06 8.80e-07 2.28e-06 ...
> plot(Intensity ~ Dose, data = MR, pch = 15)
> abline(lm(Intensity ~ Dose, data = MR))
>
> Fit <- lm(Intensity ~ Dose, data = MR)
> Fit
```

```
Call:
lm(formula = Intensity ~ Dose, data = MR)
```

```
Coefficients:
(Intercept)      Dose
 2.865e-07      9.226e-07
```

```
>
> summary(Fit)
```

```
Call:
lm(formula = Intensity ~ Dose, data = MR)
```

```
Residuals:
    1         2         3         4         5
4.654e-08 -8.078e-08  8.356e-08 -3.287e-07  1.474e-07
    6
1.320e-07
```

```
Coefficients:
              Estimate Std. Error t value Pr(>|t|)
(Intercept) 2.865e-07  1.263e-07   2.268  0.08591 .
Dose        9.226e-07  1.276e-07   7.228  0.00194 **
---

```

```
Signif. codes:  0 '***' 0.001 '**' 0.01 '*' 0.05 '.' 0.1 ' ' 1
```

```
Residual standard error: 2.018e-07 on 4 degrees of freedom
```

Multiple R-squared: 0.9289, Adjusted R-squared: 0.9111
F-statistic: 52.25 on 1 and 4 DF, p-value: 0.001943

```
> par(mfrow = c(2, 2))  
> plot(residuals(Fit) ~ fitted(Fit), xlab = "Fitted values", ylab =  
"Residuals", main = "Residuals vs Fitted"); abline(h = 0)  
> qqnorm(residuals(Fit)); qqline(residuals(Fit))
```

J.3.8.2 Plot Output for Linear Regression Analysis for Sample Bb20170717 M_{3R}

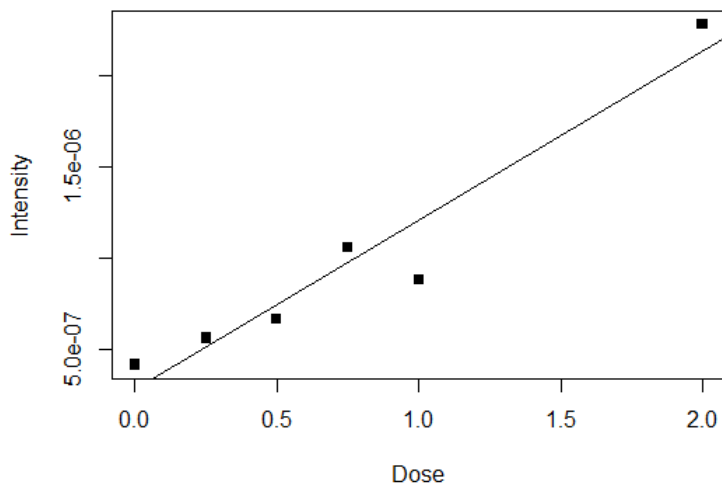


Fig. J.46. Intensity versus irradiation dose for sample Bb20170717 M_{3R}

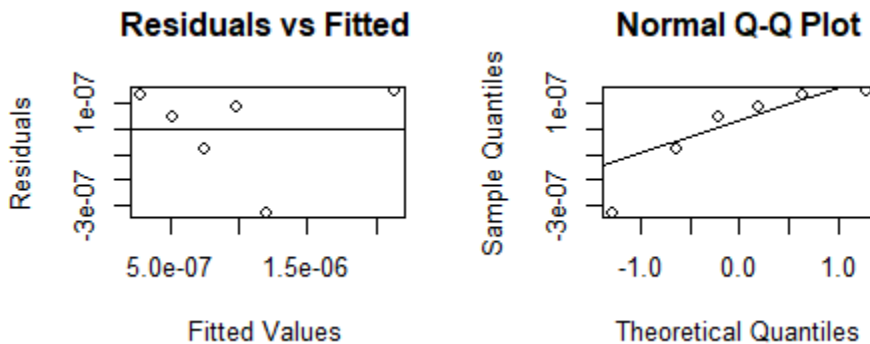


Fig. J.47. R generated plots which were used to verify linear regression assumptions for sample Bb20170717 M_{3R}

J.3.8.3 R Code for Correlation for sample Bb20170717 M_{3R}

```
> InData <- read.csv(file.choose())  
> head(InData)  
  Dose Intensity  
1 0.25 5.63633e-07  
2 0.50 6.66950e-07  
3 0.75 1.06193e-06  
4 1.00 8.80267e-07  
5 2.00 2.27900e-06  
6 0.00 4.18467e-07  
> pairs(InData)
```

```

> cor(InData)
      Dose Intensity
Dose    1.0000000 0.9637857
Intensity 0.9637857 1.0000000
> cor(InData, method = "spearman")
      Dose Intensity
Dose    1.0000000 0.9428571
Intensity 0.9428571 1.0000000
> cor.test(InData$Dose, InData$Intensity)

Pearson's product-moment correlation

data: InData$Dose and InData$Intensity
t = 7.2281, df = 4, p-value = 0.001943
alternative hypothesis: true correlation is not equal to 0
95 percent confidence interval:
 0.6988255 0.9961709
sample estimates:
      cor
0.9637857

> cor.test(InData$Dose, InData$Intensity, method = "spearman")

Spearman's rank correlation rho

data: InData$Dose and InData$Intensity
S = 2, p-value = 0.01667
alternative hypothesis: true rho is not equal to 0
sample estimates:
      rho
0.9428571

```

J.3.8.4 Plot Output for Correlation Analysis for sample Bb20170717 M_{3R}

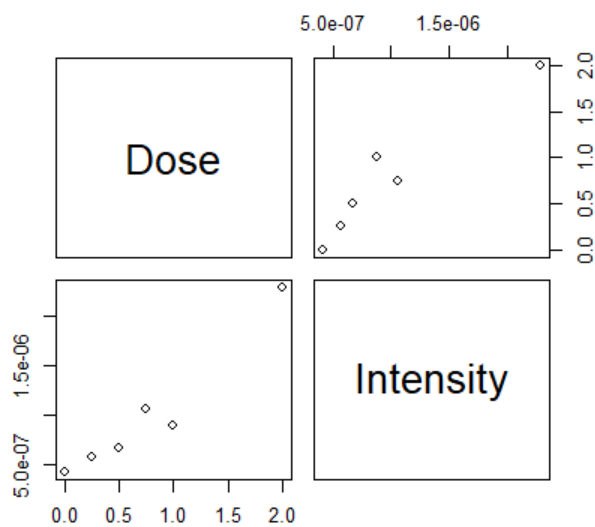


Fig. J.48. R generated plot showing the correlation between irradiation dose and intensity for sample Bb20170717 M_{3R}

J.4 Linear Regression Analysis R Code and Results for Chapter 6

J.4.1 Adjusted Calibration Curve:

Table J.18. Data used in CSV File for the adjusted calibration curve samples

Dose	Intensity
0.583	5.93E-07
0.833	6.29E-07
1.083	1.41E-06
1.333	8.69E-07
2.333	2.21E-06
0.333	2.52E-07

J.4.1.1 R Code for Linear Regression Assumptions for the Adjusted Calibration Curve Samples

```
> CCLRA <- read.csv(file.choose())
> str(CCLRA)
'data.frame': 6 obs. of 2 variables:
 $ Dose      : num  0.583 0.833 1.083 1.333 2.333 ...
 $ Intensity: num  5.93e-07 6.29e-07 1.41e-06 8.69e-07 2.21e-06 ...
> plot(Intensity ~ Dose, data = CCLRA, pch = 15)
> abline(lm(Intensity ~ Dose, data = CCLRA))
> Fit <- lm(Intensity ~ Dose, data = CCLRA)
> Fit
```

```
Call:
lm(formula = Intensity ~ Dose, data = CCLRA)
```

```
Coefficients:
(Intercept)      Dose
-1.659e-08    9.323e-07
```

```
> summary(Fit)
```

```
Call:
lm(formula = Intensity ~ Dose, data = CCLRA)
```

```
Residuals:
    1         2         3         4         5
6.650e-08 -1.309e-07  4.166e-07 -3.574e-07  4.688e-08
    6
-4.166e-08
```

```
Coefficients:
              Estimate Std. Error t value Pr(>|t|)
(Intercept) -1.659e-08  2.279e-07  -0.073  0.94547
Dose         9.323e-07  1.808e-07   5.158  0.00671 **
---
```

```
Signif. codes:  0 '***' 0.001 '**' 0.01 '*' 0.05 '.' 0.1 ' ' 1
```

```
Residual standard error: 2.858e-07 on 4 degrees of freedom
```

Multiple R-squared: 0.8693, Adjusted R-squared: 0.8366
 F-statistic: 26.6 on 1 and 4 DF, p-value: 0.006709

```
> par(mfrow = c(2, 2))
> plot(residuals(Fit) ~ fitted(Fit), xlab = "Fitted values", ylab =
"Residuals", main = "Residuals vs Fitted"); abline(h = 0)
> qqnorm(residuals(Fit)); qqline(residuals(Fit))
```

J.4.1.2 Plot Output for Linear Regression Analysis for the Adjusted Calibration Curve Samples

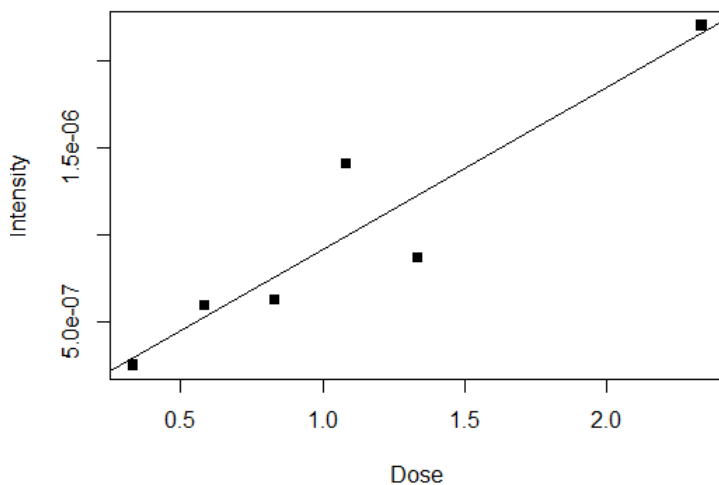


Fig. J.49. Intensity versus irradiation dose for the adjusted calibration curve samples

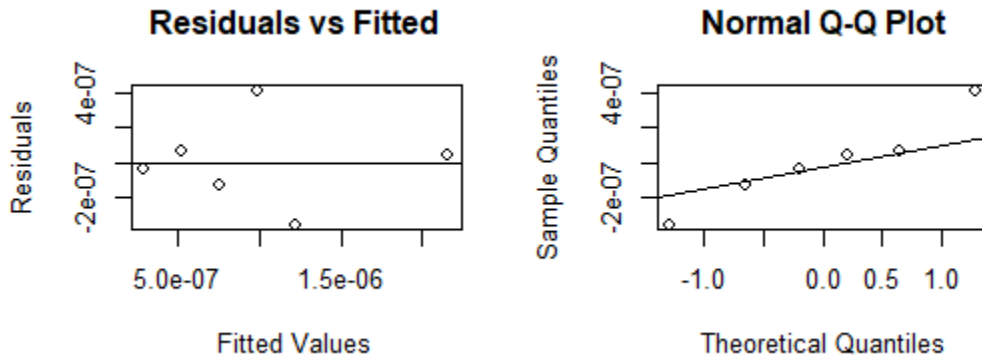


Fig. J.50. R generated plots which were used to verify linear regression assumptions for the adjusted calibration curve samples

J.4.1.3 R Code for Correlation for the Adjusted Calibration Curve Samples

```
> InData <- read.csv(file.choose())
> head(InData)
  Dose Intensity
1 0.583 5.93433e-07
2 0.833 6.29067e-07
3 1.083 1.40967e-06
4 1.333 8.68800e-07
5 2.333 2.20533e-06
6 0.333 2.52200e-07
> pairs(InData)
> cor(InData)
```

```

      Dose Intensity
Dose      1.0000000 0.9323534
Intensity 0.9323534 1.0000000
> cor(InData, method = "spearman")
      Dose Intensity
Dose      1.0000000 0.9428571
Intensity 0.9428571 1.0000000
> cor.test(InData$Dose, InData$Intensity)

Pearson's product-moment correlation

data: InData$Dose and InData$Intensity
t = 5.1576, df = 4, p-value = 0.006709
alternative hypothesis: true correlation is not equal to 0
95 percent confidence interval:
 0.4963962 0.9927435
sample estimates:
      cor
0.9323534

> cor.test(InData$Dose, InData$Intensity, method = "spearman")

Spearman's rank correlation rho

data: InData$Dose and InData$Intensity
S = 2, p-value = 0.01667
alternative hypothesis: true rho is not equal to 0
sample estimates:
      rho
0.9428571

```

J.4.1.4 Plot Output for Correlation Analysis for the Adjusted Calibration Curve Samples

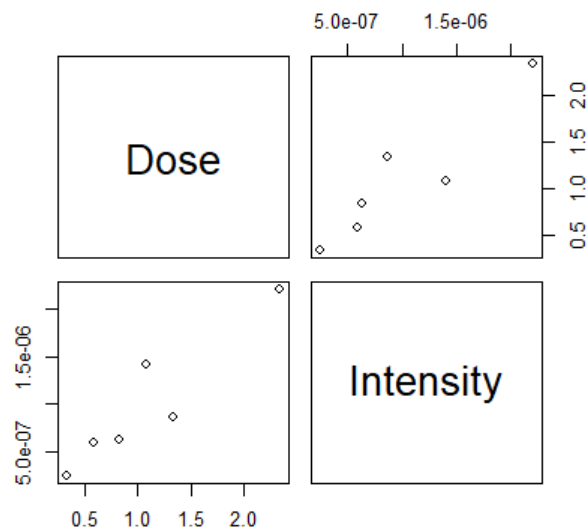
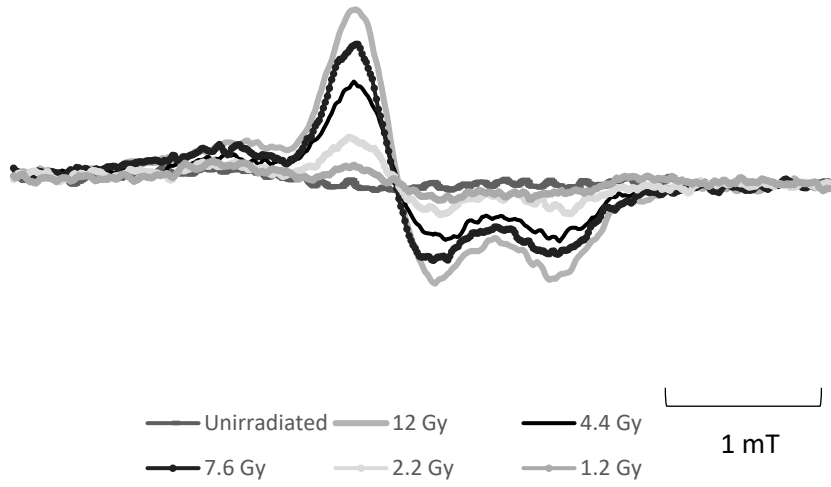


Fig. J.51. R generated plot showing the correlation between irradiation dose and intensity for the adjusted calibration curve samples

Appendix K

EPR Spectra of samples: Chapters 4 – 6

a)



b)

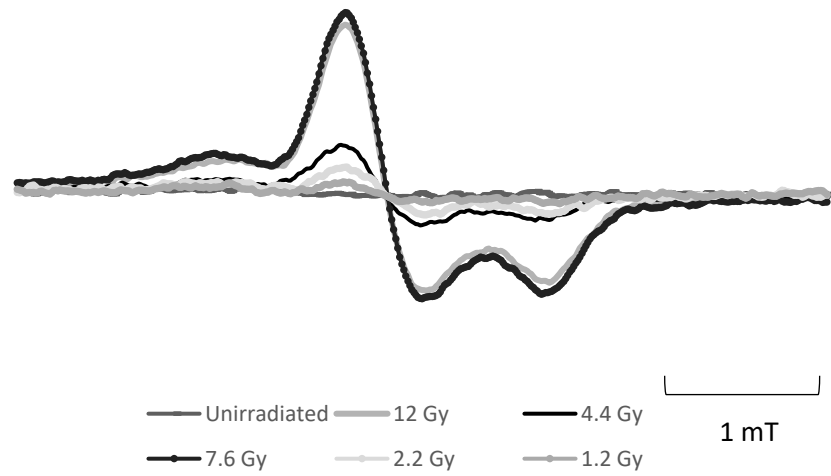
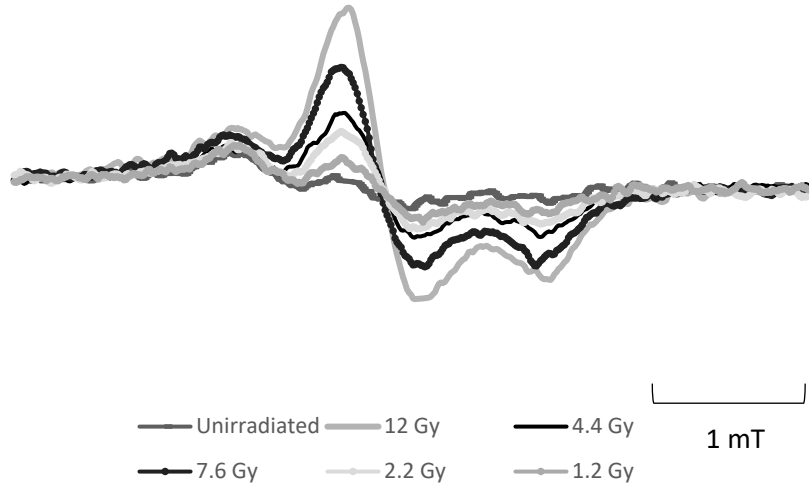


Fig. K.1. EPR spectra of samples Ba20170608 P_{3L} a) and Ba20170608 P_{3R} b) showing the RIS for aliquots that were irradiated in the laboratory as well as the unirradiated aliquot.

a)



b)

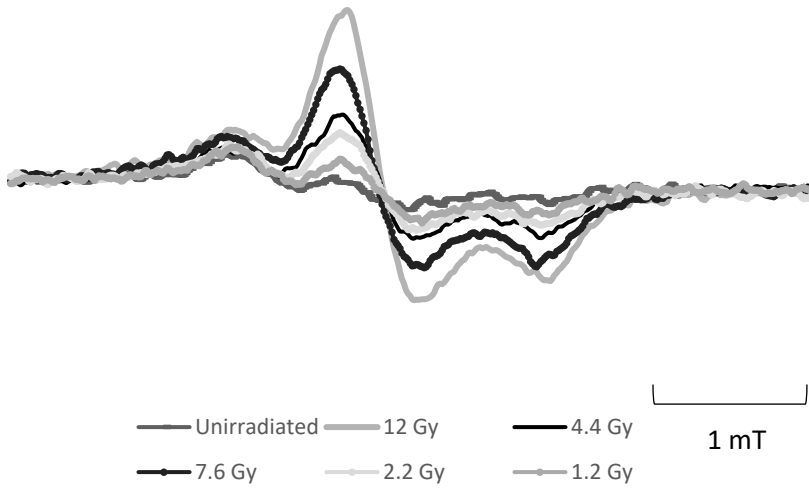
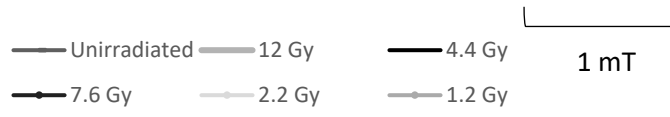
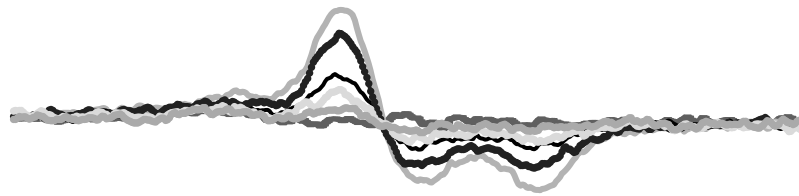


Fig. K.2. EPR spectra of samples Ba20170609 M_{3L} a) and Ba20170609 M_{3R} b) showing the RIS for aliquots that were irradiated in the laboratory as well as the unirradiated aliquot.

a)



b)

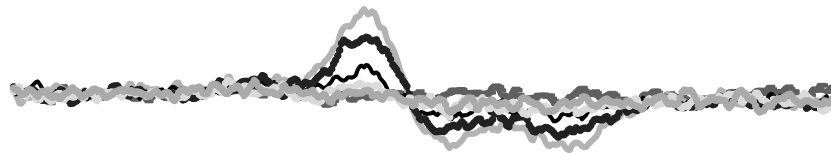
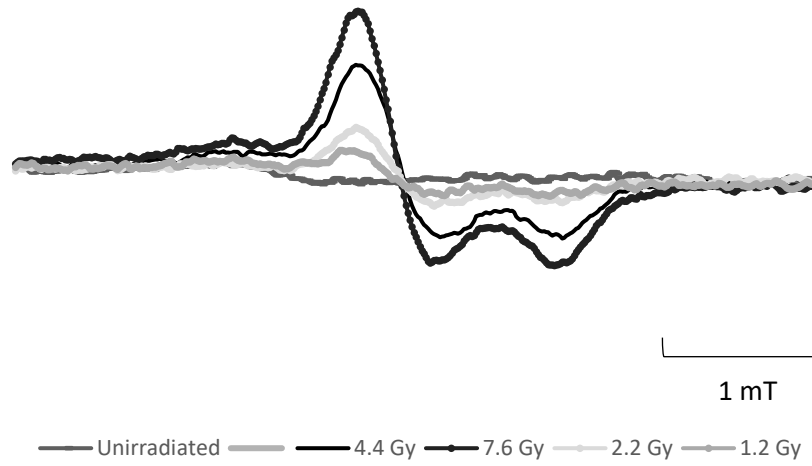


Fig. K.3. EPR spectra of samples Ba20170615 M_{2L} a) and Ba20170615 M_{2R} b) showing the RIS for aliquots that were irradiated in the laboratory as well as the unirradiated aliquot.

a)



b)

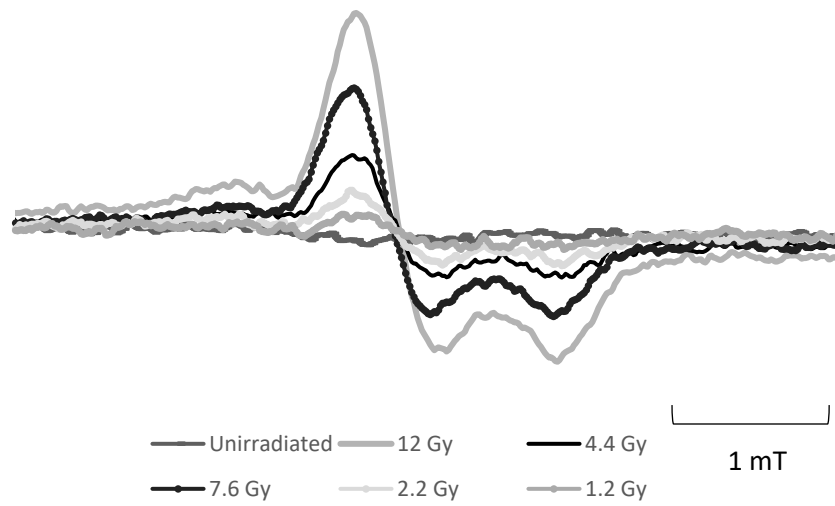
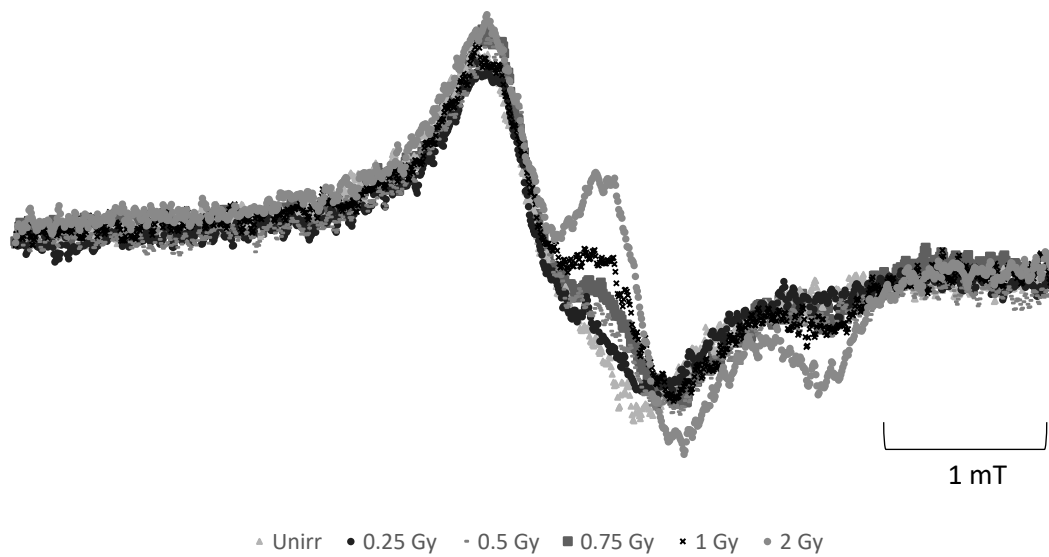


Fig. K.4. EPR spectra of samples Ba20170617 P_{3L} a) and Ba20170617 P_{3R} b) showing the RIS for aliquots that were irradiated in the laboratory as well as the unirradiated aliquot.

a)



b)

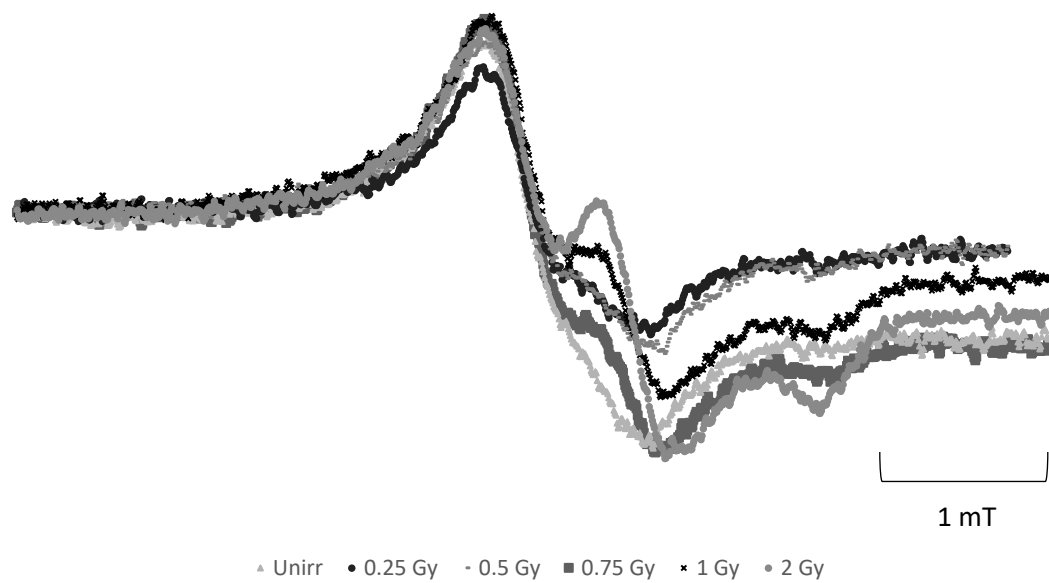
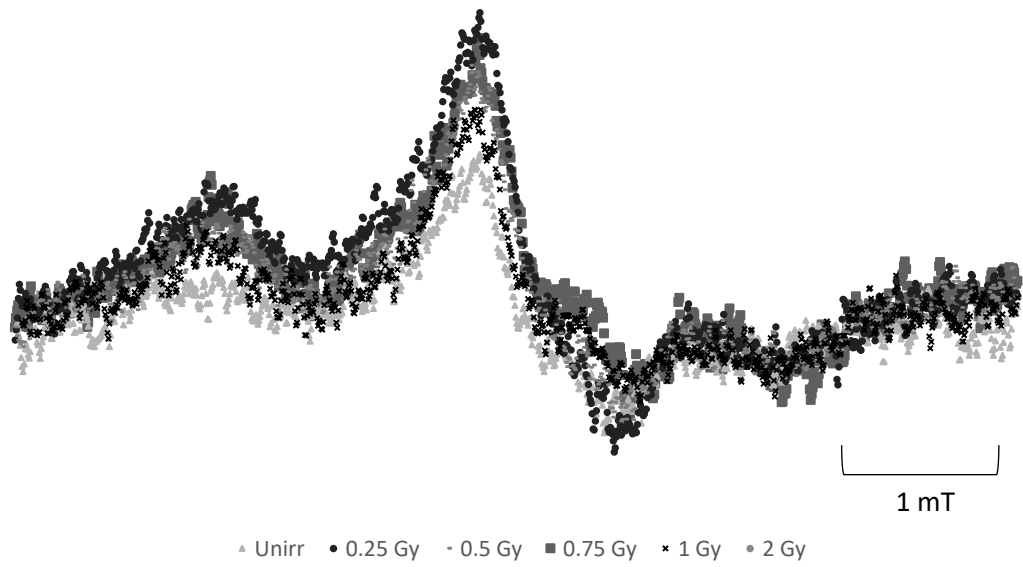


Fig. K.5. EPR spectra of samples Ba20170620 M_{2L} a) and Ba20170620 M_{2R} b) for the unirradiated aliquot in addition to the laboratory irradiated aliquots.

a)



b)

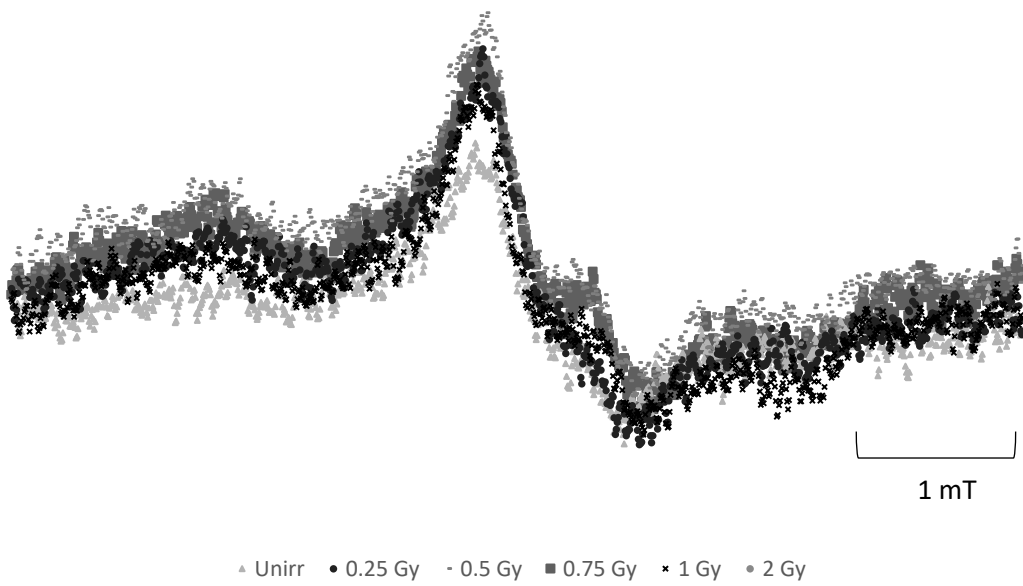
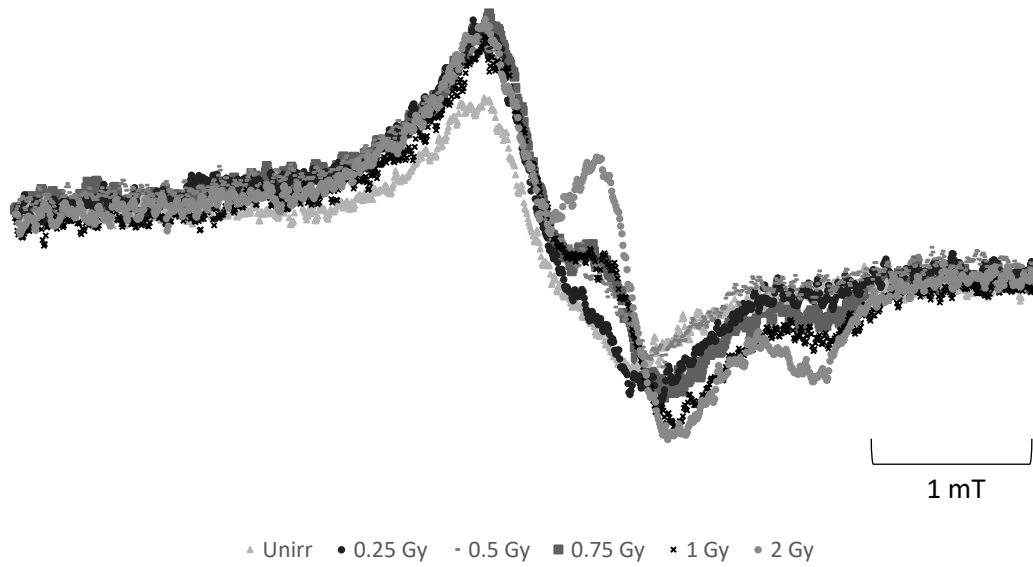


Fig. K.6. EPR spectra of samples Bb20170623 M_{IL} a) and Bb20170623 M_{IR} b) for the unirradiated aliquot in addition to the laboratory irradiated aliquots.

a)



b)

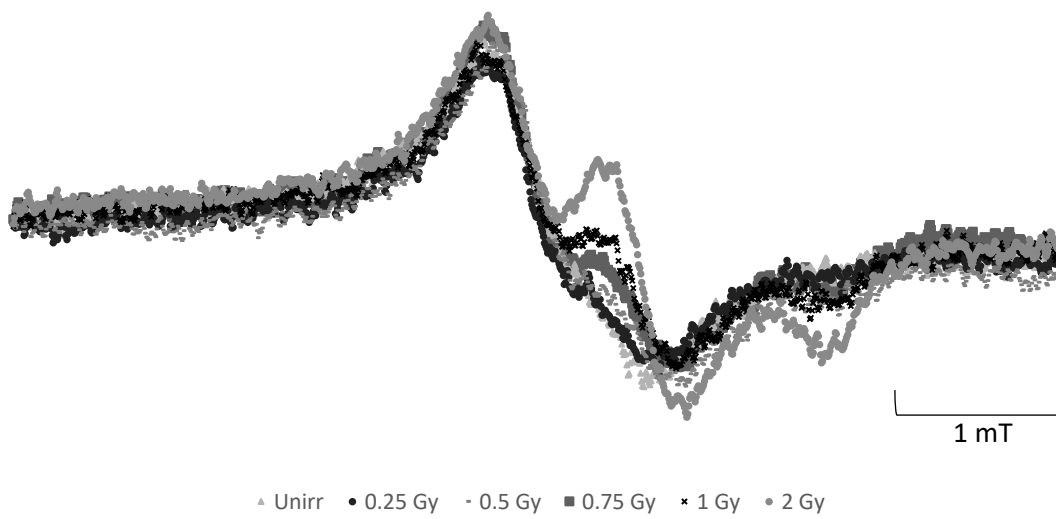
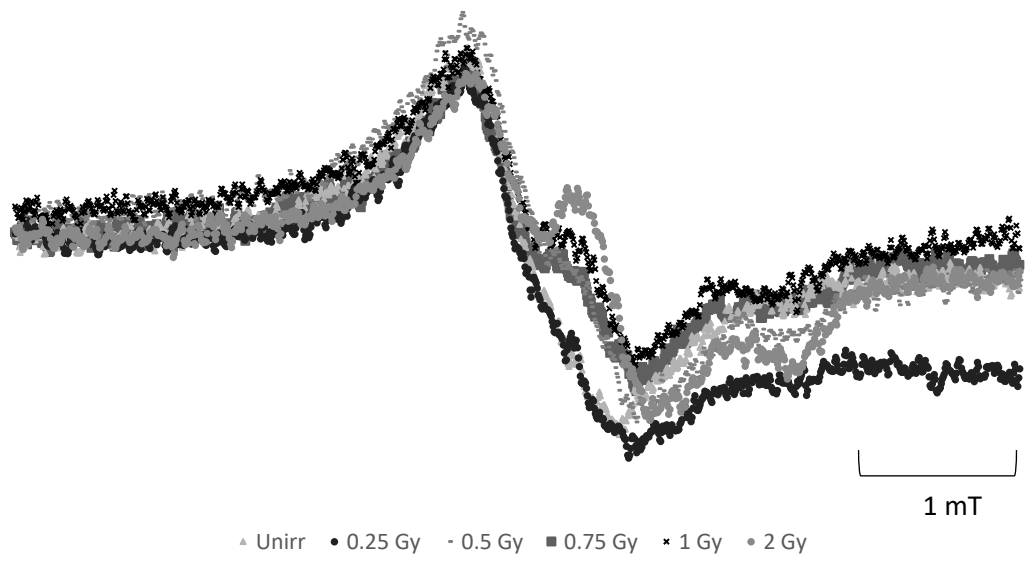


Fig. K.7. EPR spectra of samples Ba20170627 M_{2L} a) and Ba20170627 M_{2R} b) for the unirradiated aliquot in addition to the laboratory irradiated aliquots.

a)



b)

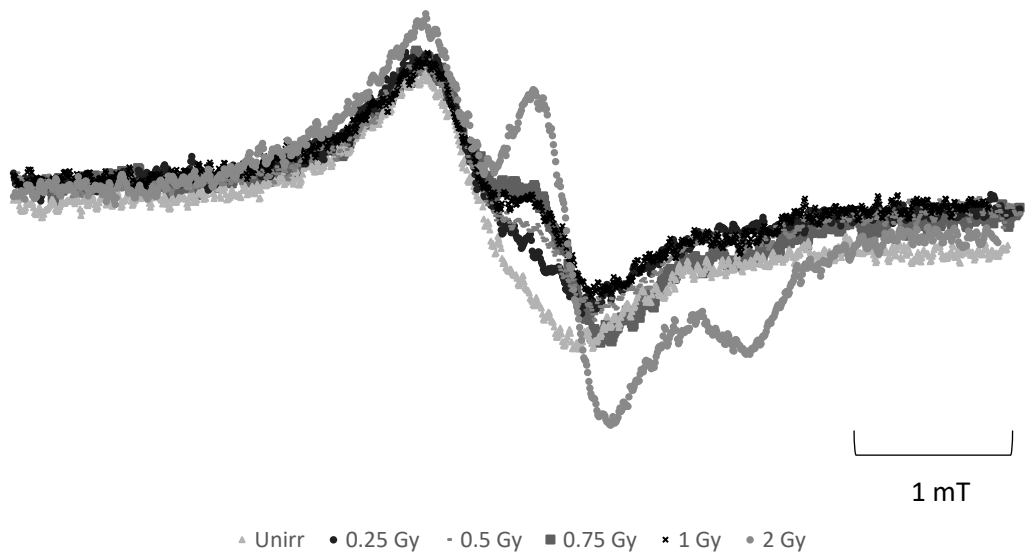


Fig. K.8. EPR spectra of samples Bb20170717 M_{3L} a) and Bb20170717 M_{3R} b) for the unirradiated aliquot in addition to the laboratory irradiated aliquots.

Appendix L

Signal Intensity Versus Irradiation Dose with Linear Regression Analysis

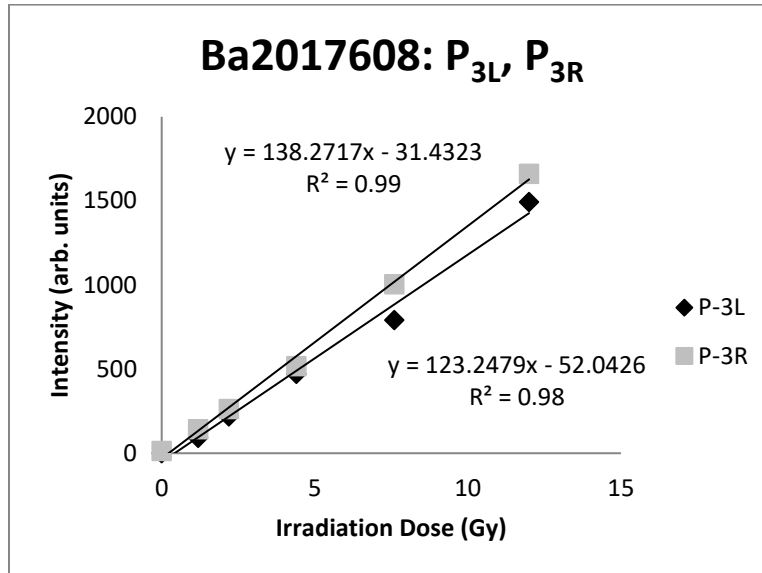


Fig. L.1. Graph showing linearity in the lower left Pre-molar 3 and right Pre-molar 3 from boar Ba20170608

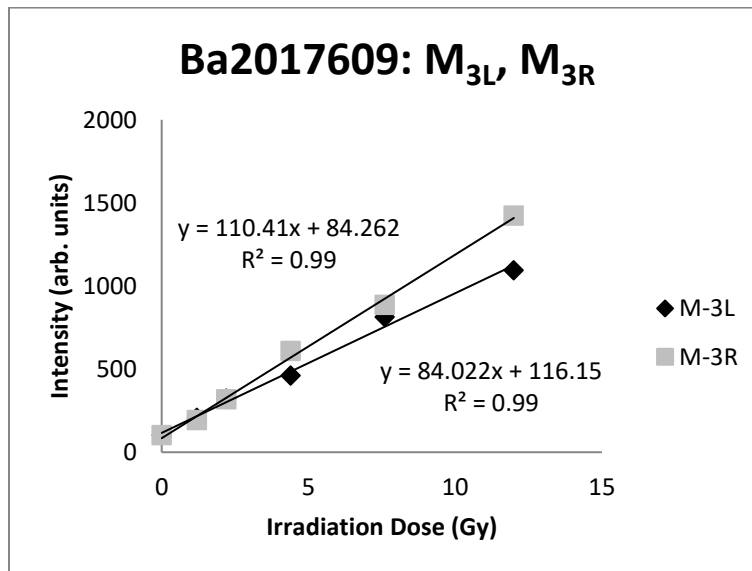


Fig. L.2. Graph showing linearity in the lower left molar 3 and right molar 3 from boar Ba20170609

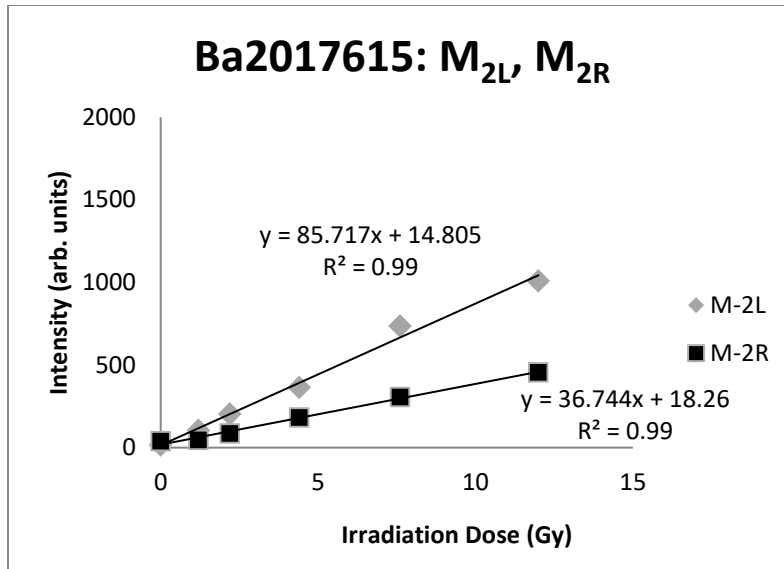


Fig. L.3. Graph showing linearity in the lower left molar 2 and right molar 2 from boar Ba20170615

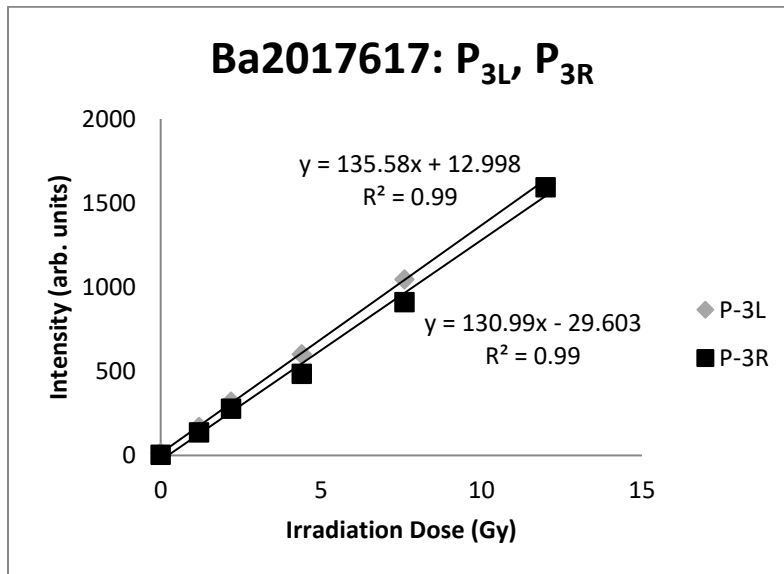


Fig. L.4. Graph showing linearity in the lower left Pre-molar 3 and right Pre-molar 3 from boar Ba20170617

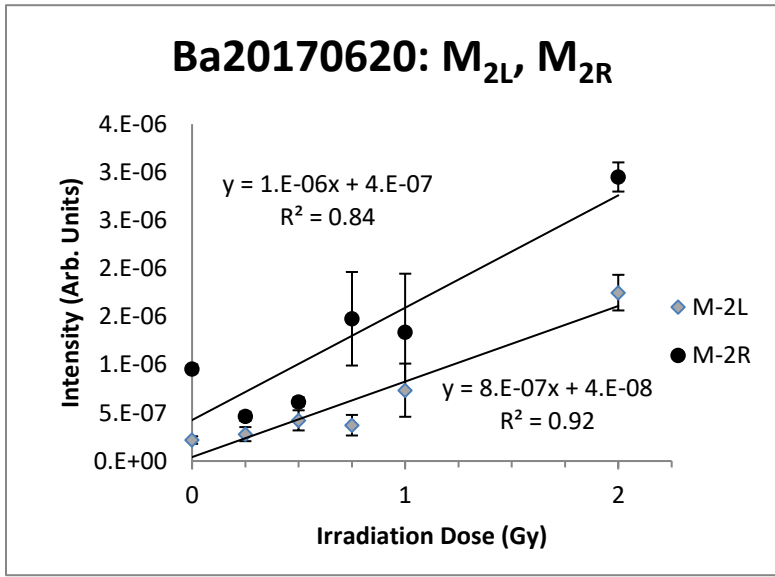


Fig. L.5. Graph displaying linearity for left molar 2 and right molar 2 from boar Ba20170620

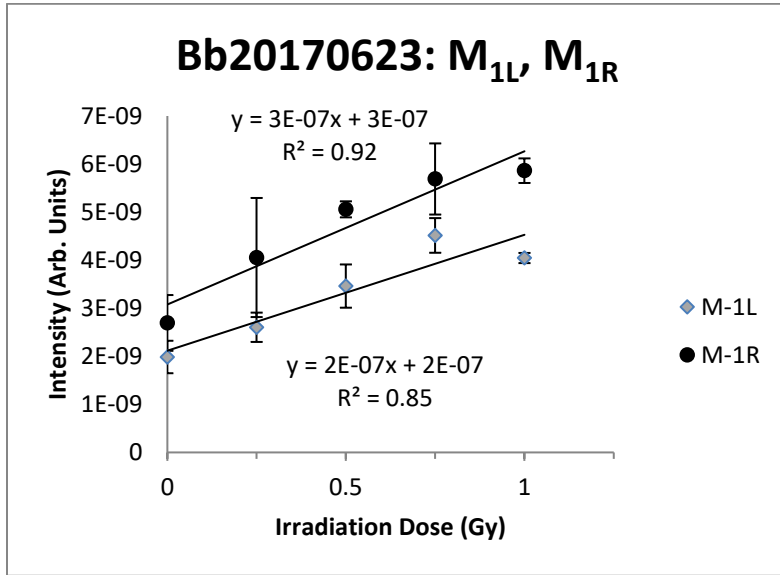


Fig. L.6. Graph displaying linearity for left molar 1 and right molar 1 from boar Bb20170623

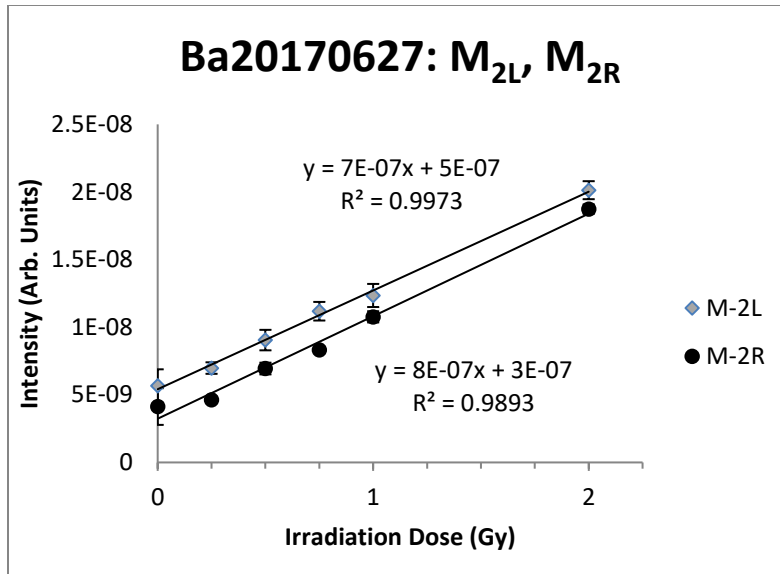


Fig. L.7. Graph displaying linearity for left molar 2 and right molar 2 from boar Ba20170627

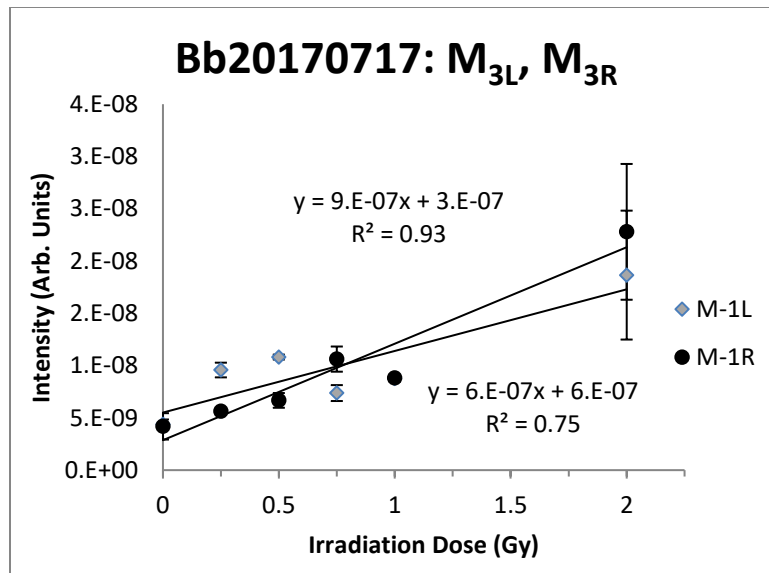


Fig. L.8. Graph displaying linearity for left molar 3 and right molar 3 from boar Bb20170717

Appendix M

Excel LINEST Results: Uncertainty in Retrospective Dose Calculations

Retrospective doses using the additive dose method were determined by dividing the intercept and slope of the line of best fit for each set of enamel samples. Uncertainty in retrospective dose values were determined using the LINEST function in Excel along with the following equation, which follows from the rules of error propagation:

$$\text{Uncertainty in Retrospective Dose} = \sqrt{\left(\frac{SD \text{ Slope}}{Slope}\right)^2 + \left(\frac{SD \text{ intercept}}{intercept}\right)^2} \quad (\text{M.1})$$

Table M.1. Data from Excel LINEST function used to calculate retrospective doses. Retrospective dose estimates and associated uncertainty values are also shown.

	Slope	SD Slope	R ²	Intercept	SD Intercept	SD Y	Retrospective Dose (Gy)	Uncertainty (Gy)
Ba20170608 P3L	1.23E+02	6.33E+00	9.90E-01	-5.20E+01	3.90E+01	6.40E+01	*	*
Ba20170608 P3R	1.38E+02	4.12E+00	9.96E-01	-3.14E+01	2.53E+01	4.16E+01	*	*
Ba20170609 M3L	8.40E+01	3.69E+00	9.92E-01	1.16E+02	2.27E+01	3.73E+01	1.4	0.3
Ba20170609 M3R	1.10E+02	3.15E+00	9.97E-01	8.43E+01	1.94E+01	3.19E+01	0.8	0.2
Ba20170615 M2L	8.57E+01	4.13E+00	9.91E-01	1.48E+01	2.54E+01	4.17E+01	0.2	0.03
Ba20170615 M2R	3.67E+01	1.52E+00	9.93E-01	1.83E+01	9.34E+00	1.53E+01	0.5	0.3
Ba20170617 P3L	1.36E+02	1.40E+00	1.00E+00	1.30E+01	5.71E+00	8.39E+00	*	*
Ba20170617 P3R	1.31E+02	5.23E+00	9.94E-01	-2.96E+01	3.22E+01	5.29E+01	*	*
Ba20170620 M2L	7.85E-07	1.13E-07	9.24E-01	4.11E-08	1.11E-07	1.78E-07	0.1	0.1
Ba20170620 M2R	1.17E-06	2.52E-07	8.43E-01	4.26E-07	2.49E-07	3.98E-07	0.4	0.2
Bb20170623 M1L	2.41E-07	5.80E-08	8.52E-01	2.12E-07	3.55E-08	4.59E-08	0.9	0.3
Bb20170623 M1R	3.19E-07	5.37E-08	9.22E-01	3.08E-07	3.29E-08	4.24E-08	1.0	0.2
Ba20170627 M2L	7.30E-07	1.90E-08	9.97E-01	5.41E-07	1.88E-08	3.01E-08	0.7	0.03

	Slope	SD Slope	R ²	Intercept	SD Intercept	SD Y	Retrospective Dose (Gy)	Uncertainty (Gy)
Ba20170627 M2R	7.58E-07	3.94E-08	9.89E-01	3.23E-07	3.90E-08	6.23E-08	0.4	0.1
Bb20170717 M3L	5.89E-07	1.70E-07	7.50E-01	5.50E-07	1.68E-07	2.69E-07	0.9	0.4
Bb20170717 M3R	9.23E-07	1.28E-07	9.29E-01	2.86E-07	1.26E-07	2.02E-07	0.3	0.1
Calibration Curve	9.32E-07	1.81E-07	8.69E-01	2.94E-07	1.79E-07	2.86E-07	0.3	0.2

Appendix N

Dose Reconstruction Measurement Results

Table N.1. Individual dose measurement results measured to determine EPR reconstructed doses

	Dose 1 (mGy)	Dose 2 (mGy)	Dose 3 (mGy)	Avg (mGy)
170609B1	413.3	679.4	348.0	480.2
Ba20170605	294.4	307.8	275.9	292.7
Ba20170608	265.7	141.7	244.1	217.2
Ba20170609	2529.6	2560.2	2920.0	2669.9
Bb20170609	144.7	184.9	155.9	161.8
Ba20170615	359.7	390.5	507.8	419.3
Ba20170616	505.2	741.3	562.9	603.1
Bb20170616	1084.4	949.4	513.5	849.1
Ba20170617	140.1	136.1	292.3	189.5
Ba20170620	295.4	249.4	212.3	252.3
Ba20170623	310.4	278.4	618.6	402.5
Bb20170623	231.3	270.9	195.8	232.7
Ba20170627	472.3	695.2	705.0	624.2
Ba20170704	385.2	488.7	306.4	393.5
Ba20170717	*Signal contained iron and dose reconstruction could not be performed			
Bb20170717	442.3	478.1	541.2	487.2
Bc20170717	510.0	486.6	484.8	493.8
Ba20170720	176.4	168.4	146.4	163.7
Ba20170724	315.3	273.8	139.5	242.9

Appendix O

Reconstructed Dose Confidence Interval Calculations

Nagy (2000) describes how to construct confidence intervals for EPR reconstructed doses using the calibration curve method with the following equation:

$$X = X_0 \pm t_{n-2,P} \times \frac{s_{fit}}{b} \times \sqrt{\frac{1}{m} + \frac{1}{n} + \frac{(X_0 - X_{mean})^2}{\sum_{i=1}^n (X_i - X_{mean})^2}} \quad (O.1)$$

Definition of Variables:

X_0 – Reconstructed dose

X_{mean} – Mean value of irradiation doses

X_i – Applied irradiation dose

b – Slope of the linear regression line

t – Student’s t-distribution critical value for a desired probability

n – Number of calibration curve samples or data points

m – Number of repeated measurements for each sample

s_{fit} – line fit standard error

Table O.1. Confidence interval parameter values used to calculate confidence intervals for EPR reconstructed doses

Confidence Interval Parameters			
$t_{4,0.9}$	2.132	X_1	0.583
s_{fit}	0.000000286	X_2	0.833
b	9.00E-07	X_3	1.083
m	3	X_4	1.333
n	6	X_5	2.333
X_{mean}	1.083	X_6	0.333
X_0	See Table		

Table O.2. EPR reconstructed doses to enamel with corresponding whole-body doses with confidence intervals

	Reconstructed Dose to Enamel (Gy)	Whole Body Dose (Gy) (X_0)	\pm
170609B1	0.5	0.4	0.6
Ba20170605	0.3	0.3	0.6
Ba20170608	0.2	0.2	0.6
Ba20170609	2.7	2.4	0.7
Bb20170609	0.2	0.1	0.6
Ba20170615	0.4	0.4	0.6
Ba20170616	0.6	0.5	0.5
Bb20170616	0.8	0.8	0.5
Ba20170617	0.2	0.2	0.6
Ba20170620	0.3	0.2	0.6
Ba20170623	0.4	0.4	0.6
Bb20170623	0.2	0.2	0.6
Ba20170627	0.6	0.6	0.5
Ba20170704	0.4	0.4	0.6
Bb20170717	0.5	0.4	0.6
Bc20170717	0.5	0.4	0.6
Ba20170720	0.2	0.1	0.6
Ba20170724	0.2	0.2	0.6

Appendix P

Calculation of Effective Half-Life of Air Dose Rates and Estimated Lifetime Doses

P.1 Calculation of Air Dose Rate Effective Half-Life

The effective half-life for air dose rates in the Fukushima Exclusion Zone was calculated using the following equation:

$$\dot{D}(t) = \dot{D}_0 e^{-\lambda t} \quad (\text{P.1})$$

Where $\dot{D}(t)$ is the air dose rate at time t , \dot{D}_0 is the initial dose rate, and λ is the decay constant,

which in this case equals: $\frac{\ln(2)}{t_{eff}}$.

Table P.1. Data used to calculate average effective half-life of air dose rates in areas surrounding the Fukushima Exclusion Zone

Monitoring Point #	Air Dose Rate ($\mu\text{Sv/hr}$)				t_{eff}
	6/25/2012 8:00	6/25/2013 8:00	6/25/2014 8:00	6/25/2015 8:00	
705	5.34	4.43	2.84	2.1	2.23 y
691	4.06	3.11	2.3	2	2.94 y
1465	1.4	0.99	0.82	0.68	2.88 y
706	3.56	2.33	1.82	1.49	2.39 y
702	2.64	2.19	1.51	1.18	2.58 y
1468	2.15	1.46	1.16	0.93	2.48 y
702	2.64	2.19	1.51	1.18	2.58 y
704	4.96	4.16	2.85	2.32	2.74 y
717	9.52	8.61	6.55	5.09	3.32 y
117	5.19	4.17	3.27*	2.61	3.03 y
				Average t_{eff}	2.72 y

* Recorded on 6/25/2014 at 05:00

The calculated t_{eff} is 2.72 years or 141.44 weeks.

P.2 Calculation of Estimated Lifetime Doses to Boar

The following equations were used to Calculate estimated lifetime doses to boar in this study, using a t_{eff} of 141.44 weeks:

$$\text{Initial Dose Rate: } \frac{\text{Dose Rate at the Collection Site}}{e^{-\left(\frac{\ln(2)}{t_{eff}}\right)(\text{Age in weeks})}} \quad (\text{P.2})$$

$$\text{Lifetime Dose: } \frac{\text{Dose } \left(\frac{\mu\text{Gy}}{\text{week}}\right)}{\lambda} \cdot 1 - e^{-\lambda(\text{Age in weeks})} \quad (\text{P.3})$$

Table P.2. Data used to estimate lifetime doses to wild boar

Boar Sample Number	Est. Age (weeks)	Dose Rate at Collection Site (μGy/hr)	Initial Dose Rate (μGy/hr)	μGy/week	Lifetime Dose (μGy)	Estimated Lifetime Dose (Gy)
170604 B-1	*	*	*	*	*	*
Ba20170605	26	3.05	3.46	582.01	14208.18	0.014
Ba20170608	30	0.34	0.39	66.16	1845.94	0.002
Ba20170609	208	8.1	22.44	3770.44	491802.01	0.492
Bb20170609	50	0.68	0.87	145.95	6472.48	0.006
Ba20170615	220	0.46	1.35	227.09	30576.02	0.031
Ba20170616	50	0.68	0.87	145.95	6472.48	0.006
Bb20170616	62	0.14	0.19	31.87	1703.97	0.002
Ba20170617	26	0.09	0.10	17.17	419.26	0.0004
Ba20170620	62	10.1	13.69	2299.10	122929.16	0.123
Ba20170623	127	0.98	1.83	306.74	29003.00	0.029
Bb20170623	97	2.98	4.79	805.25	62169.69	0.062
Ba20170627	62	10.5	14.23	2390.16	127797.64	0.128
Ba20170704	59	10.5	14.02	2355.28	120679.61	0.121
Ba20170717	59	1.7	2.27	381.33	19538.60	0.020
Bb20170717	127	0.75	1.40	234.75	22196.17	0.022
Bc20170717	127	0.35	0.65	109.55	10358.21	0.010
Ba20170720	*	0.12	*	*	*	*
Ba20170724	*	2.8	*	*	*	*

Appendix Q

¹³⁷Cs Measurements for Combined Tooth Enamel Samples and Background Measurements

Table Q.1. Data for background and combined sample measurement recording times

Background Measurement	
Start Time	Thu Mar 8 12:51:45 GMT-0700 2018
Energy calibration	Offset: -6.293735980987549
Live Time (s)	86397.71
Real Time (s)	86400
Combined Sample Measurement	
Start Time	Wed Mar 7 12:42:41 GMT-0700 2018
Energy calibration	Offset: -6.293735980987549
Live Time (s)	86398.38
Real Time (s)	86400

Table Q.2. Counts per channel data for background and combined sample counts for ¹³⁷Cs measurements in tooth enamel

Channel	Energy (keV)	Background Counts	Sample Counts	Net
1	-4.615996957	0	0	0
2	-2.938257933	0	0	0
3	-1.260518909	0	0	0
4	0.417220116	0	0	0
5	2.09495914	0	0	0
6	3.772698164	309014	173780	-135234
7	5.450437188	377542	153979	-223563
8	7.128176212	348341	119639	-228702
9	8.805915236	295961	92065	-203896
10	10.48365426	173858	47253	-126605
11	12.16139328	36900	9952	-26948
12	13.83913231	3574	2526	-1048
13	15.51687133	1698	2155	457
14	17.19461036	1570	1958	388
15	18.87234938	1486	1712	226
16	20.55008841	1451	1744	293
17	22.22782743	1564	1713	149
18	23.90556645	1639	1758	119
19	25.58330548	1664	1753	89
20	27.2610445	1637	1659	22

Channel	Energy (keV)	Background Counts	Sample Counts	Net
21	28.93878353	1532	1683	151
22	30.61652255	1502	1662	160
23	32.29426157	1636	1763	127
24	33.9720006	1720	1814	94
25	35.64973962	1811	1810	-1
26	37.32747865	1863	1920	57
27	39.00521767	1943	2083	140
28	40.6829567	2281	2522	241
29	42.36069572	2815	3021	206
30	44.03843474	3253	3500	247
31	45.71617377	3269	3405	136
32	47.39391279	2915	3158	243
33	49.07165182	2506	2719	213
34	50.74939084	2326	2503	177
35	52.42712986	2136	2354	218
36	54.10486889	1952	2009	57
37	55.78260791	1610	1743	133
38	57.46034694	1501	1620	119
39	59.13808596	1380	1488	108
40	60.81582499	1349	1430	81
41	62.49356401	1301	1370	69
42	64.17130303	1292	1343	51
43	65.84904206	1309	1435	126
44	67.52678108	1308	1373	65
45	69.20452011	1283	1370	87
46	70.88225913	1297	1380	83
47	72.55999815	1341	1410	69
48	74.23773718	1313	1424	111
49	75.9154762	1332	1413	81
50	77.59321523	1313	1473	160
51	79.27095425	1410	1516	106
52	80.94869328	1419	1525	106
53	82.6264323	1515	1489	-26
54	84.30417132	1400	1444	44
55	85.98191035	1412	1540	128
56	87.65964937	1430	1597	167
57	89.3373884	1363	1492	129
58	91.01512742	1347	1456	109
59	92.69286644	1459	1512	53
60	94.37060547	1408	1481	73
61	96.04834449	1355	1433	78
62	97.72608352	1404	1541	137

Channel	Energy (keV)	Background Counts	Sample Counts	Net
63	99.40382254	1340	1473	133
64	101.0815616	1389	1492	103
65	102.7593006	1366	1456	90
66	104.4370396	1401	1582	181
67	106.1147786	1396	1523	127
68	107.7925177	1391	1605	214
69	109.4702567	1490	1591	101
70	111.1479957	1443	1592	149
71	112.8257347	1439	1620	181
72	114.5034738	1486	1633	147
73	116.1812128	1509	1667	158
74	117.8589518	1507	1630	123
75	119.5366908	1498	1651	153
76	121.2144299	1554	1667	113
77	122.8921689	1542	1638	96
78	124.5699079	1540	1706	166
79	126.2476469	1543	1670	127
80	127.925386	1516	1653	137
81	129.603125	1579	1641	62
82	131.280864	1526	1689	163
83	132.958603	1636	1742	106
84	134.636342	1565	1787	222
85	136.3140811	1650	1755	105
86	137.9918201	1625	1732	107
87	139.6695591	1626	1771	145
88	141.3472981	1724	1803	79
89	143.0250372	1661	1862	201
90	144.7027762	1615	1749	134
91	146.3805152	1602	1822	220
92	148.0582542	1625	1762	137
93	149.7359933	1627	1710	83
94	151.4137323	1579	1710	131
95	153.0914713	1519	1734	215
96	154.7692103	1517	1618	101
97	156.4469494	1547	1653	106
98	158.1246884	1500	1620	120
99	159.8024274	1513	1572	59
100	161.4801664	1536	1632	96
101	163.1579055	1519	1644	125
102	164.8356445	1459	1566	107
103	166.5133835	1443	1610	167
104	168.1911225	1457	1543	86

Channel	Energy (keV)	Background Counts	Sample Counts	Net
105	169.8688616	1547	1595	48
106	171.5466006	1517	1593	76
107	173.2243396	1469	1576	107
108	174.9020786	1485	1525	40
109	176.5798177	1498	1591	93
110	178.2575567	1450	1573	123
111	179.9352957	1469	1556	87
112	181.6130347	1430	1588	158
113	183.2907737	1485	1530	45
114	184.9685128	1390	1413	23
115	186.6462518	1422	1510	88
116	188.3239908	1408	1552	144
117	190.0017298	1435	1489	54
118	191.6794689	1435	1523	88
119	193.3572079	1394	1487	93
120	195.0349469	1403	1479	76
121	196.7126859	1342	1457	115
122	198.390425	1416	1470	54
123	200.068164	1441	1459	18
124	201.745903	1457	1483	26
125	203.423642	1394	1486	92
126	205.1013811	1482	1541	59
127	206.7791201	1441	1500	59
128	208.4568591	1454	1538	84
129	210.1345981	1426	1495	69
130	211.8123372	1326	1462	136
131	213.4900762	1395	1462	67
132	215.1678152	1394	1377	-17
133	216.8455542	1320	1440	120
134	218.5232933	1340	1498	158
135	220.2010323	1353	1365	12
136	221.8787713	1332	1372	40
137	223.5565103	1306	1370	64
138	225.2342494	1292	1386	94
139	226.9119884	1233	1402	169
140	228.5897274	1324	1335	11
141	230.2674664	1226	1353	127
142	231.9452055	1336	1366	30
143	233.6229445	1272	1254	-18
144	235.3006835	1342	1309	-33
145	236.9784225	1234	1293	59
146	238.6561615	1218	1371	153

Channel	Energy (keV)	Background Counts	Sample Counts	Net
147	240.3339006	1278	1294	16
148	242.0116396	1293	1330	37
149	243.6893786	1327	1320	-7
150	245.3671176	1278	1334	56
151	247.0448567	1257	1295	38
152	248.7225957	1231	1360	129
153	250.4003347	1260	1313	53
154	252.0780737	1254	1299	45
155	253.7558128	1288	1271	-17
156	255.4335518	1270	1271	1
157	257.1112908	1258	1335	77
158	258.7890298	1253	1335	82
159	260.4667689	1324	1254	-70
160	262.1445079	1188	1263	75
161	263.8222469	1278	1316	38
162	265.4999859	1242	1434	192
163	267.177725	1274	1249	-25
164	268.855464	1245	1270	25
165	270.533203	1234	1293	59
166	272.210942	1262	1218	-44
167	273.8886811	1223	1251	28
168	275.5664201	1256	1280	24
169	277.2441591	1326	1342	16
170	278.9218981	1301	1304	3
171	280.5996372	1291	1356	65
172	282.2773762	1299	1355	56
173	283.9551152	1338	1319	-19
174	285.6328542	1305	1424	119
175	287.3105932	1349	1316	-33
176	288.9883323	1351	1406	55
177	290.6660713	1424	1448	24
178	292.3438103	1412	1447	35
179	294.0215493	1499	1458	-41
180	295.6992884	1447	1526	79
181	297.3770274	1407	1506	99
182	299.0547664	1477	1504	27
183	300.7325054	1513	1464	-49
184	302.4102445	1518	1460	-58
185	304.0879835	1415	1460	45
186	305.7657225	1401	1460	59
187	307.4434615	1379	1424	45
188	309.1212006	1322	1383	61

Channel	Energy (keV)	Background Counts	Sample Counts	Net
189	310.7989396	1300	1375	75
190	312.4766786	1289	1320	31
191	314.1544176	1261	1292	31
192	315.8321567	1225	1209	-16
193	317.5098957	1278	1141	-137
194	319.1876347	1178	1230	52
195	320.8653737	1193	1203	10
196	322.5431128	1160	1227	67
197	324.2208518	1223	1168	-55
198	325.8985908	1208	1171	-37
199	327.5763298	1069	1225	156
200	329.2540689	1149	1171	22
201	330.9318079	1099	1111	12
202	332.6095469	1100	1154	54
203	334.2872859	1171	1167	-4
204	335.9650249	1123	1212	89
205	337.642764	1133	1136	3
206	339.320503	1136	1160	24
207	340.998242	1177	1210	33
208	342.675981	1100	1167	67
209	344.3537201	1131	1127	-4
210	346.0314591	1101	1157	56
211	347.7091981	1114	1176	62
212	349.3869371	1162	1185	23
213	351.0646762	1160	1147	-13
214	352.7424152	1185	1161	-24
215	354.4201542	1115	1184	69
216	356.0978932	1110	1171	61
217	357.7756323	1133	1170	37
218	359.4533713	1164	1212	48
219	361.1311103	1105	1127	22
220	362.8088493	1135	1154	19
221	364.4865884	1114	1175	61
222	366.1643274	1109	1194	85
223	367.8420664	1124	1190	66
224	369.5198054	1065	1200	135
225	371.1975445	1092	1203	111
226	372.8752835	1069	1209	140
227	374.5530225	1158	1227	69
228	376.2307615	1036	1210	174
229	377.9085006	1082	1238	156
230	379.5862396	1014	1242	228

Channel	Energy (keV)	Background Counts	Sample Counts	Net
231	381.2639786	1103	1248	145
232	382.9417176	1121	1164	43
233	384.6194566	1045	1241	196
234	386.2971957	1024	1223	199
235	387.9749347	1042	1231	189
236	389.6526737	1060	1174	114
237	391.3304127	1104	1144	40
238	393.0081518	1036	1166	130
239	394.6858908	991	1179	188
240	396.3636298	1084	1200	116
241	398.0413688	1012	1097	85
242	399.7191079	952	1045	93
243	401.3968469	1041	1067	26
244	403.0745859	1037	1027	-10
245	404.7523249	1018	1098	80
246	406.430064	1024	1048	24
247	408.107803	998	993	-5
248	409.785542	1025	1016	-9
249	411.463281	1022	1012	-10
250	413.1410201	1001	998	-3
251	414.8187591	936	966	30
252	416.4964981	1032	950	-82
253	418.1742371	959	1003	44
254	419.8519762	1020	997	-23
255	421.5297152	1048	944	-104
256	423.2074542	954	949	-5
257	424.8851932	953	981	28
258	426.5629323	959	911	-48
259	428.2406713	995	988	-7
260	429.9184103	985	989	4
261	431.5961493	994	971	-23
262	433.2738883	934	1048	114
263	434.9516274	994	960	-34
264	436.6293664	954	1052	98
265	438.3071054	940	941	1
266	439.9848444	969	937	-32
267	441.6625835	962	974	12
268	443.3403225	974	923	-51
269	445.0180615	985	980	-5
270	446.6958005	961	948	-13
271	448.3735396	962	949	-13
272	450.0512786	983	968	-15

Channel	Energy (keV)	Background Counts	Sample Counts	Net
273	451.7290176	1002	915	-87
274	453.4067566	923	894	-29
275	455.0844957	906	968	62
276	456.7622347	906	955	49
277	458.4399737	949	934	-15
278	460.1177127	919	960	41
279	461.7954518	903	946	43
280	463.4731908	938	948	10
281	465.1509298	948	964	16
282	466.8286688	872	920	48
283	468.5064079	905	960	55
284	470.1841469	886	968	82
285	471.8618859	963	910	-53
286	473.5396249	836	909	73
287	475.217364	855	953	98
288	476.895103	937	933	-4
289	478.572842	878	935	57
290	480.250581	945	940	-5
291	481.9283201	905	821	-84
292	483.6060591	875	902	27
293	485.2837981	878	891	13
294	486.9615371	864	883	19
295	488.6392761	881	903	22
296	490.3170152	889	882	-7
297	491.9947542	856	863	7
298	493.6724932	901	967	66
299	495.3502322	898	884	-14
300	497.0279713	912	901	-11
301	498.7057103	868	870	2
302	500.3834493	853	880	27
303	502.0611883	885	889	4
304	503.7389274	851	874	23
305	505.4166664	880	869	-11
306	507.0944054	874	873	-1
307	508.7721444	859	878	19
308	510.4498835	889	847	-42
309	512.1276225	895	794	-101
310	513.8053615	767	833	66
311	515.4831005	894	854	-40
312	517.1608396	823	888	65
313	518.8385786	819	827	8
314	520.5163176	857	872	15

Channel	Energy (keV)	Background Counts	Sample Counts	Net
315	522.1940566	880	847	-33
316	523.8717957	849	862	13
317	525.5495347	840	892	52
318	527.2272737	836	870	34
319	528.9050127	860	830	-30
320	530.5827518	829	875	46
321	532.2604908	879	816	-63
322	533.9382298	836	779	-57
323	535.6159688	814	797	-17
324	537.2937078	867	830	-37
325	538.9714469	826	848	22
326	540.6491859	814	771	-43
327	542.3269249	847	826	-21
328	544.0046639	774	826	52
329	545.682403	877	826	-51
330	547.360142	792	810	18
331	549.037881	820	825	5
332	550.71562	768	810	42
333	552.3933591	815	810	-5
334	554.0710981	820	815	-5
335	555.7488371	798	826	28
336	557.4265761	830	780	-50
337	559.1043152	749	834	85
338	560.7820542	767	817	50
339	562.4597932	813	819	6
340	564.1375322	795	760	-35
341	565.8152713	786	751	-35
342	567.4930103	756	778	22
343	569.1707493	770	744	-26
344	570.8484883	771	758	-13
345	572.5262274	717	782	65
346	574.2039664	762	749	-13
347	575.8817054	728	735	7
348	577.5594444	738	716	-22
349	579.2371835	718	767	49
350	580.9149225	771	720	-51
351	582.5926615	676	719	43
352	584.2704005	716	692	-24
353	585.9481395	730	691	-39
354	587.6258786	710	683	-27
355	589.3036176	679	728	49
356	590.9813566	713	724	11

Channel	Energy (keV)	Background Counts	Sample Counts	Net
357	592.6590956	719	652	-67
358	594.3368347	658	669	11
359	596.0145737	702	651	-51
360	597.6923127	711	641	-70
361	599.3700517	654	646	-8
362	601.0477908	655	633	-22
363	602.7255298	651	618	-33
364	604.4032688	670	648	-22
365	606.0810078	641	629	-12
366	607.7587469	598	619	21
367	609.4364859	603	602	-1
368	611.1142249	647	653	6
369	612.7919639	601	617	16
370	614.469703	565	612	47
371	616.147442	627	618	-9
372	617.825181	585	590	5
373	619.50292	597	614	17
374	621.1806591	573	650	77
375	622.8583981	605	632	27
376	624.5361371	603	618	15
377	626.2138761	624	589	-35
378	627.8916152	591	614	23
379	629.5693542	609	628	19
380	631.2470932	618	601	-17
381	632.9248322	605	595	-10
382	634.6025712	629	563	-66
383	636.2803103	561	594	33
384	637.9580493	612	587	-25
385	639.6357883	606	658	52
386	641.3135273	601	611	10
387	642.9912664	601	640	39
388	644.6690054	591	606	15
389	646.3467444	589	571	-18
390	648.0244834	567	606	39
391	649.7022225	577	574	-3
392	651.3799615	539	573	34
393	653.0577005	552	617	65
394	654.7354395	628	572	-56
395	656.4131786	553	517	-36
396	658.0909176	567	579	12
397	659.7686566	551	562	11
398	661.4463956	562	581	19

Channel	Energy (keV)	Background Counts	Sample Counts	Net
399	663.1241347	547	577	30
400	664.8018737	545	537	-8
401	666.4796127	564	530	-34
402	668.1573517	509	555	46
403	669.8350908	541	526	-15
404	671.5128298	558	549	-9
405	673.1905688	514	533	19
406	674.8683078	525	538	13
407	676.5460469	552	580	28
408	678.2237859	521	552	31
409	679.9015249	523	530	7
410	681.5792639	533	536	3
411	683.2570029	553	506	-47
412	684.934742	510	490	-20
413	686.612481	504	510	6
414	688.29022	557	523	-34
415	689.967959	484	532	48
416	691.6456981	533	486	-47
417	693.3234371	522	545	23
418	695.0011761	523	528	5
419	696.6789151	507	524	17
420	698.3566542	539	550	11
421	700.0343932	560	514	-46
422	701.7121322	540	566	26
423	703.3898712	581	608	27
424	705.0676103	620	571	-49
425	706.7453493	586	600	14
426	708.4230883	589	639	50
427	710.1008273	633	611	-22
428	711.7785664	648	619	-29
429	713.4563054	652	638	-14
430	715.1340444	687	660	-27
431	716.8117834	687	730	43
432	718.4895225	680	689	9
433	720.1672615	709	739	30
434	721.8450005	758	806	48
435	723.5227395	781	723	-58
436	725.2004786	772	772	0
437	726.8782176	728	736	8
438	728.5559566	726	746	20
439	730.2336956	704	704	0
440	731.9114347	695	738	43

Channel	Energy (keV)	Background Counts	Sample Counts	Net
441	733.5891737	739	679	-60
442	735.2669127	680	680	0
443	736.9446517	686	633	-53
444	738.6223907	652	632	-20
445	740.3001298	604	637	33
446	741.9778688	588	547	-41
447	743.6556078	562	577	15
448	745.3333468	576	602	26
449	747.0110859	525	544	19
450	748.6888249	499	480	-19
451	750.3665639	450	481	31
452	752.0443029	471	446	-25
453	753.722042	395	392	-3
454	755.399781	406	391	-15
455	757.07752	374	358	-16
456	758.755259	362	357	-5
457	760.4329981	341	368	27
458	762.1107371	348	348	0
459	763.7884761	327	279	-48
460	765.4662151	315	313	-2
461	767.1439542	306	303	-3
462	768.8216932	268	289	21
463	770.4994322	271	307	36
464	772.1771712	290	272	-18
465	773.8549103	302	272	-30
466	775.5326493	242	270	28
467	777.2103883	271	280	9
468	778.8881273	288	277	-11
469	780.5658664	257	281	24
470	782.2436054	282	275	-7
471	783.9213444	246	243	-3
472	785.5990834	263	267	4
473	787.2768224	258	281	23
474	788.9545615	282	283	1
475	790.6323005	298	279	-19
476	792.3100395	300	272	-28
477	793.9877785	285	252	-33
478	795.6655176	293	297	4
479	797.3432566	276	307	31
480	799.0209956	302	278	-24
481	800.6987346	310	303	-7
482	802.3764737	329	314	-15

Channel	Energy (keV)	Background Counts	Sample Counts	Net
483	804.0542127	335	313	-22
484	805.7319517	368	341	-27
485	807.4096907	321	360	39
486	809.0874298	361	368	7
487	810.7651688	362	334	-28
488	812.4429078	410	381	-29
489	814.1206468	392	380	-12
490	815.7983859	423	413	-10
491	817.4761249	434	425	-9
492	819.1538639	430	471	41
493	820.8316029	460	413	-47
494	822.509342	509	444	-65
495	824.187081	473	482	9
496	825.86482	445	476	31
497	827.542559	499	479	-20
498	829.2202981	475	493	18
499	830.8980371	548	503	-45
500	832.5757761	496	466	-30
501	834.2535151	515	465	-50
502	835.9312541	475	503	28
503	837.6089932	480	504	24
504	839.2867322	499	473	-26
505	840.9644712	473	461	-12
506	842.6422102	474	479	5
507	844.3199493	471	444	-27
508	845.9976883	384	419	35
509	847.6754273	431	354	-77
510	849.3531663	352	345	-7
511	851.0309054	395	347	-48
512	852.7086444	324	360	36
513	854.3863834	320	321	1
514	856.0641224	297	286	-11
515	857.7418615	273	309	36
516	859.4196005	280	277	-3
517	861.0973395	274	272	-2
518	862.7750785	247	262	15
519	864.4528176	228	216	-12
520	866.1305566	210	217	7
521	867.8082956	189	210	21
522	869.4860346	187	204	17
523	871.1637737	169	206	37
524	872.8415127	156	183	27

Channel	Energy (keV)	Background Counts	Sample Counts	Net
525	874.5192517	189	212	23
526	876.1969907	187	162	-25
527	877.8747298	178	148	-30
528	879.5524688	164	160	-4
529	881.2302078	160	173	13
530	882.9079468	169	151	-18
531	884.5856858	131	155	24
532	886.2634249	172	154	-18
533	887.9411639	160	153	-7
534	889.6189029	160	154	-6
535	891.2966419	173	157	-16
536	892.974381	139	164	25
537	894.65212	149	145	-4
538	896.329859	142	175	33
539	898.007598	146	150	4
540	899.6853371	158	143	-15
541	901.3630761	145	137	-8
542	903.0408151	167	143	-24
543	904.7185541	153	166	13
544	906.3962932	140	167	27
545	908.0740322	134	159	25
546	909.7517712	153	153	0
547	911.4295102	154	154	0
548	913.1072493	153	135	-18
549	914.7849883	142	149	7
550	916.4627273	140	145	5
551	918.1404663	134	156	22
552	919.8182054	160	131	-29
553	921.4959444	148	121	-27
554	923.1736834	135	147	12
555	924.8514224	140	146	6
556	926.5291615	125	133	8
557	928.2069005	161	121	-40
558	929.8846395	146	135	-11
559	931.5623785	113	124	11
560	933.2401175	138	135	-3
561	934.9178566	136	137	1
562	936.5955956	118	121	3
563	938.2733346	121	133	12
564	939.9510736	111	111	0
565	941.6288127	133	134	1
566	943.3065517	129	105	-24

Channel	Energy (keV)	Background Counts	Sample Counts	Net
567	944.9842907	134	121	-13
568	946.6620297	112	106	-6
569	948.3397688	114	118	4
570	950.0175078	116	122	6
571	951.6952468	115	124	9
572	953.3729858	117	131	14
573	955.0507249	112	114	2
574	956.7284639	117	129	12
575	958.4062029	104	115	11
576	960.0839419	121	133	12
577	961.761681	112	114	2
578	963.43942	146	124	-22
579	965.117159	109	121	12
580	966.794898	122	126	4
581	968.4726371	130	119	-11
582	970.1503761	110	125	15
583	971.8281151	112	109	-3
584	973.5058541	114	134	20
585	975.1835932	135	104	-31
586	976.8613322	106	111	5
587	978.5390712	148	142	-6
588	980.2168102	105	132	27
589	981.8945493	108	128	20
590	983.5722883	121	137	16
591	985.2500273	127	117	-10
592	986.9277663	144	138	-6
593	988.6055053	134	141	7
594	990.2832444	166	141	-25
595	991.9609834	156	121	-35
596	993.6387224	155	144	-11
597	995.3164614	145	154	9
598	996.9942005	151	162	11
599	998.6719395	133	141	8
600	1000.349679	145	108	-37
601	1002.027418	119	165	46
602	1003.705157	135	138	3
603	1005.382896	138	134	-4
604	1007.060635	155	122	-33
605	1008.738374	130	140	10
606	1010.416113	151	130	-21
607	1012.093852	127	123	-4
608	1013.771591	127	135	8

Channel	Energy (keV)	Background Counts	Sample Counts	Net
609	1015.44933	125	136	11
610	1017.127069	136	132	-4
611	1018.804808	128	128	0
612	1020.482547	125	125	0
613	1022.160286	145	142	-3
614	1023.838025	120	105	-15
615	1025.515764	124	116	-8
616	1027.193503	105	102	-3
617	1028.871242	119	99	-20
618	1030.548981	112	107	-5
619	1032.22672	109	100	-9
620	1033.904459	116	89	-27
621	1035.582198	82	121	39
622	1037.259937	98	108	10
623	1038.937676	115	91	-24
624	1040.615415	104	100	-4
625	1042.293154	82	91	9
626	1043.970893	103	94	-9
627	1045.648632	94	93	-1
628	1047.326371	104	97	-7
629	1049.00411	96	96	0
630	1050.681849	102	102	0
631	1052.359588	107	105	-2
632	1054.037327	99	80	-19
633	1055.715066	104	91	-13
634	1057.392805	96	91	-5
635	1059.070544	77	84	7
636	1060.748283	100	86	-14
637	1062.426022	82	85	3
638	1064.103761	84	98	14
639	1065.7815	66	92	26
640	1067.459239	80	77	-3
641	1069.136979	88	86	-2
642	1070.814718	88	76	-12
643	1072.492457	89	79	-10
644	1074.170196	75	80	5
645	1075.847935	90	74	-16
646	1077.525674	86	93	7
647	1079.203413	79	92	13
648	1080.881152	77	63	-14
649	1082.558891	76	91	15
650	1084.23663	86	78	-8

Channel	Energy (keV)	Background Counts	Sample Counts	Net
651	1085.914369	74	78	4
652	1087.592108	71	83	12
653	1089.269847	72	65	-7
654	1090.947586	71	87	16
655	1092.625325	71	82	11
656	1094.303064	71	68	-3
657	1095.980803	73	78	5
658	1097.658542	94	77	-17
659	1099.336281	70	87	17
660	1101.01402	74	72	-2
661	1102.691759	63	70	7
662	1104.369498	82	73	-9
663	1106.047237	72	69	-3
664	1107.724976	80	83	3
665	1109.402715	65	62	-3
666	1111.080454	87	76	-11
667	1112.758193	75	86	11
668	1114.435932	68	74	6
669	1116.113671	69	69	0
670	1117.79141	65	72	7
671	1119.469149	75	63	-12
672	1121.146888	69	66	-3
673	1122.824627	76	57	-19
674	1124.502366	60	71	11
675	1126.180105	84	60	-24
676	1127.857844	75	67	-8
677	1129.535583	79	64	-15
678	1131.213322	81	71	-10
679	1132.891061	63	70	7
680	1134.5688	71	86	15
681	1136.246539	62	84	22
682	1137.924278	76	64	-12
683	1139.602018	64	62	-2
684	1141.279757	71	62	-9
685	1142.957496	70	62	-8
686	1144.635235	67	68	1
687	1146.312974	54	73	19
688	1147.990713	74	68	-6
689	1149.668452	73	63	-10
690	1151.346191	61	57	-4
691	1153.02393	65	68	3
692	1154.701669	77	51	-26

Channel	Energy (keV)	Background Counts	Sample Counts	Net
693	1156.379408	59	75	16
694	1158.057147	83	60	-23
695	1159.734886	68	79	11
696	1161.412625	67	63	-4
697	1163.090364	76	73	-3
698	1164.768103	82	80	-2
699	1166.445842	68	70	2
700	1168.123581	58	75	17
701	1169.80132	71	63	-8
702	1171.479059	73	64	-9
703	1173.156798	80	69	-11
704	1174.834537	80	62	-18
705	1176.512276	76	70	-6
706	1178.190015	72	66	-6
707	1179.867754	77	74	-3
708	1181.545493	80	81	1
709	1183.223232	67	92	25
710	1184.900971	80	68	-12
711	1186.57871	83	75	-8
712	1188.256449	79	80	1
713	1189.934188	86	74	-12
714	1191.611927	85	72	-13
715	1193.289666	77	76	-1
716	1194.967405	87	89	2
717	1196.645144	76	70	-6
718	1198.322883	81	73	-8
719	1200.000622	84	91	7
720	1201.678361	89	81	-8
721	1203.3561	96	79	-17
722	1205.033839	96	83	-13
723	1206.711578	82	99	17
724	1208.389318	86	89	3
725	1210.067057	88	87	-1
726	1211.744796	88	69	-19
727	1213.422535	108	82	-26
728	1215.100274	76	95	19
729	1216.778013	87	73	-14
730	1218.455752	83	75	-8
731	1220.133491	85	90	5
732	1221.81123	84	90	6
733	1223.488969	67	72	5
734	1225.166708	71	79	8

Channel	Energy (keV)	Background Counts	Sample Counts	Net
735	1226.844447	82	83	1
736	1228.522186	82	66	-16
737	1230.199925	70	79	9
738	1231.877664	78	79	1
739	1233.555403	81	60	-21
740	1235.233142	83	77	-6
741	1236.910881	70	80	10
742	1238.58862	78	72	-6
743	1240.266359	73	71	-2
744	1241.944098	75	88	13
745	1243.621837	73	75	2
746	1245.299576	74	74	0
747	1246.977315	82	67	-15
748	1248.655054	85	87	2
749	1250.332793	79	71	-8
750	1252.010532	65	83	18
751	1253.688271	76	69	-7
752	1255.36601	71	73	2
753	1257.043749	77	52	-25
754	1258.721488	73	69	-4
755	1260.399227	68	76	8
756	1262.076966	73	75	2
757	1263.754705	80	74	-6
758	1265.432444	65	68	3
759	1267.110183	65	74	9
760	1268.787922	82	70	-12
761	1270.465661	60	66	6
762	1272.1434	59	61	2
763	1273.821139	68	72	4
764	1275.498878	58	48	-10
765	1277.176618	59	58	-1
766	1278.854357	61	70	9
767	1280.532096	57	52	-5
768	1282.209835	72	67	-5
769	1283.887574	52	56	4
770	1285.565313	69	45	-24
771	1287.243052	68	50	-18
772	1288.920791	50	65	15
773	1290.59853	49	64	15
774	1292.276269	60	65	5
775	1293.954008	59	63	4
776	1295.631747	45	49	4

Channel	Energy (keV)	Background Counts	Sample Counts	Net
777	1297.309486	45	53	8
778	1298.987225	51	61	10
779	1300.664964	43	55	12
780	1302.342703	60	51	-9
781	1304.020442	69	57	-12
782	1305.698181	51	46	-5
783	1307.37592	49	47	-2
784	1309.053659	59	45	-14
785	1310.731398	64	51	-13
786	1312.409137	42	61	19
787	1314.086876	68	58	-10
788	1315.764615	42	57	15
789	1317.442354	71	47	-24
790	1319.120093	50	56	6
791	1320.797832	52	53	1
792	1322.475571	61	41	-20
793	1324.15331	39	42	3
794	1325.831049	55	51	-4
795	1327.508788	53	42	-11
796	1329.186527	43	60	17
797	1330.864266	63	40	-23
798	1332.542005	50	52	2
799	1334.219744	44	36	-8
800	1335.897483	41	48	7
801	1337.575222	54	46	-8
802	1339.252961	55	39	-16
803	1340.9307	56	41	-15
804	1342.608439	46	35	-11
805	1344.286178	45	46	1
806	1345.963917	36	52	16
807	1347.641657	48	38	-10
808	1349.319396	44	37	-7
809	1350.997135	38	45	7
810	1352.674874	45	44	-1
811	1354.352613	47	38	-9
812	1356.030352	33	39	6
813	1357.708091	47	34	-13
814	1359.38583	28	48	20
815	1361.063569	52	33	-19
816	1362.741308	45	29	-16
817	1364.419047	36	35	-1
818	1366.096786	24	30	6

Channel	Energy (keV)	Background Counts	Sample Counts	Net
819	1367.774525	38	36	-2
820	1369.452264	36	29	-7
821	1371.130003	26	33	7
822	1372.807742	33	29	-4
823	1374.485481	33	27	-6
824	1376.16322	30	34	4
825	1377.840959	47	39	-8
826	1379.518698	40	42	2
827	1381.196437	36	37	1
828	1382.874176	35	37	2
829	1384.551915	29	46	17
830	1386.229654	28	34	6
831	1387.907393	24	45	21
832	1389.585132	34	25	-9
833	1391.262871	32	29	-3
834	1392.94061	31	34	3
835	1394.618349	29	33	4
836	1396.296088	42	32	-10
837	1397.973827	36	33	-3
838	1399.651566	38	21	-17
839	1401.329305	27	25	-2
840	1403.007044	36	36	0
841	1404.684783	31	19	-12
842	1406.362522	24	25	1
843	1408.040261	21	35	14
844	1409.718	30	39	9
845	1411.395739	34	24	-10
846	1413.073478	35	27	-8
847	1414.751217	28	25	-3
848	1416.428957	19	30	11
849	1418.106696	23	39	16
850	1419.784435	36	34	-2
851	1421.462174	36	32	-4
852	1423.139913	28	36	8
853	1424.817652	29	34	5
854	1426.495391	30	33	3
855	1428.17313	39	31	-8
856	1429.850869	28	21	-7
857	1431.528608	37	28	-9
858	1433.206347	35	48	13
859	1434.884086	38	35	-3
860	1436.561825	43	44	1

Channel	Energy (keV)	Background Counts	Sample Counts	Net
861	1438.239564	40	37	-3
862	1439.917303	44	38	-6
863	1441.595042	51	36	-15
864	1443.272781	38	43	5
865	1444.95052	56	57	1
866	1446.628259	52	43	-9
867	1448.305998	59	65	6
868	1449.983737	56	64	8
869	1451.661476	65	64	-1
870	1453.339215	70	68	-2
871	1455.016954	63	67	4
872	1456.694693	64	57	-7
873	1458.372432	84	71	-13
874	1460.050171	70	65	-5
875	1461.72791	79	58	-21
876	1463.405649	72	75	3
877	1465.083388	61	79	18
878	1466.761127	81	77	-4
879	1468.438866	76	73	-3
880	1470.116605	80	87	7
881	1471.794344	88	88	0
882	1473.472083	84	75	-9
883	1475.149822	103	78	-25
884	1476.827561	86	78	-8
885	1478.5053	79	71	-8
886	1480.183039	92	72	-20
887	1481.860778	77	78	1
888	1483.538517	72	69	-3
889	1485.216256	81	69	-12
890	1486.893996	62	60	-2
891	1488.571735	66	69	3
892	1490.249474	80	64	-16
893	1491.927213	59	64	5
894	1493.604952	59	48	-11
895	1495.282691	64	45	-19
896	1496.96043	55	64	9
897	1498.638169	49	44	-5
898	1500.315908	56	40	-16
899	1501.993647	38	61	23
900	1503.671386	48	43	-5
901	1505.349125	45	39	-6
902	1507.026864	45	54	9

Channel	Energy (keV)	Background Counts	Sample Counts	Net
903	1508.704603	34	39	5
904	1510.382342	52	32	-20
905	1512.060081	31	36	5
906	1513.73782	48	31	-17
907	1515.415559	38	25	-13
908	1517.093298	32	21	-11
909	1518.771037	31	19	-12
910	1520.448776	24	24	0
911	1522.126515	32	28	-4
912	1523.804254	25	31	6
913	1525.481993	21	27	6
914	1527.159732	25	19	-6
915	1528.837471	24	18	-6
916	1530.51521	28	15	-13
917	1532.192949	18	19	1
918	1533.870688	19	20	1
919	1535.548427	18	19	1
920	1537.226166	16	20	4
921	1538.903905	24	16	-8
922	1540.581644	18	25	7
923	1542.259383	16	19	3
924	1543.937122	15	16	1
925	1545.614861	15	19	4
926	1547.2926	12	10	-2
927	1548.970339	12	13	1
928	1550.648078	18	8	-10
929	1552.325817	25	20	-5
930	1554.003556	12	18	6
931	1555.681296	11	13	2
932	1557.359035	9	20	11
933	1559.036774	14	16	2
934	1560.714513	17	12	-5
935	1562.392252	14	9	-5
936	1564.069991	21	10	-11
937	1565.74773	17	21	4
938	1567.425469	21	12	-9
939	1569.103208	15	9	-6
940	1570.780947	14	17	3
941	1572.458686	17	17	0
942	1574.136425	20	14	-6
943	1575.814164	11	16	5
944	1577.491903	17	11	-6

Channel	Energy (keV)	Background Counts	Sample Counts	Net
945	1579.169642	12	14	2
946	1580.847381	9	14	5
947	1582.52512	19	11	-8
948	1584.202859	13	17	4
949	1585.880598	18	10	-8
950	1587.558337	20	9	-11
951	1589.236076	14	13	-1
952	1590.913815	13	16	3
953	1592.591554	10	15	5
954	1594.269293	17	14	-3
955	1595.947032	13	10	-3
956	1597.624771	8	10	2
957	1599.30251	16	15	-1
958	1600.980249	3	14	11
959	1602.657988	11	15	4
960	1604.335727	7	21	14
961	1606.013466	9	16	7
962	1607.691205	14	15	1
963	1609.368944	12	16	4
964	1611.046683	11	19	8
965	1612.724422	11	15	4
966	1614.402161	14	16	2
967	1616.0799	12	10	-2
968	1617.757639	18	11	-7
969	1619.435378	8	16	8
970	1621.113117	19	9	-10
971	1622.790856	12	18	6
972	1624.468596	11	19	8
973	1626.146335	10	17	7
974	1627.824074	17	6	-11
975	1629.501813	20	15	-5
976	1631.179552	16	17	1
977	1632.857291	11	17	6
978	1634.53503	27	8	-19
979	1636.212769	10	13	3
980	1637.890508	8	15	7
981	1639.568247	13	17	4
982	1641.245986	17	10	-7
983	1642.923725	10	13	3
984	1644.601464	13	12	-1
985	1646.279203	6	17	11
986	1647.956942	11	5	-6

Channel	Energy (keV)	Background Counts	Sample Counts	Net
987	1649.634681	11	24	13
988	1651.31242	10	11	1
989	1652.990159	15	11	-4
990	1654.667898	13	13	0
991	1656.345637	21	10	-11
992	1658.023376	13	16	3
993	1659.701115	11	13	2
994	1661.378854	8	20	12
995	1663.056593	10	21	11
996	1664.734332	17	19	2
997	1666.412071	14	14	0
998	1668.08981	11	13	2
999	1669.767549	16	19	3
1000	1671.445288	11	5	-6
1001	1673.123027	18	13	-5
1002	1674.800766	11	10	-1
1003	1676.478505	11	11	0
1004	1678.156244	11	12	1
1005	1679.833983	11	18	7
1006	1681.511722	15	20	5
1007	1683.189461	14	10	-4
1008	1684.8672	15	11	-4
1009	1686.544939	17	12	-5
1010	1688.222678	13	21	8
1011	1689.900417	9	13	4
1012	1691.578156	12	13	1
1013	1693.255895	10	7	-3
1014	1694.933635	17	10	-7
1015	1696.611374	16	8	-8
1016	1698.289113	16	11	-5
1017	1699.966852	11	12	1
1018	1701.644591	3	15	12
1019	1703.32233	10	6	-4
1020	1705.000069	9	9	0
1021	1706.677808	13	9	-4
1022	1708.355547	19	13	-6
1023	1710.033286	10	15	5
1024	1711.711025	16	11	-5

Appendix R

USDA Permit for Shipment of Tooth Samples



**United States
Department of
Agriculture**

Animal and Plant
Health Inspection
Service

Veterinary Services

National Center for
Import and Export

Animal Products

4700 River Road
Unit 40
Riverdale, MD 20737

Telephone:
(301) 851-3300

FAX:
(301) 734-8226

Prof. Thomas E. Johnson / Colorado State University
Environmental and Radiological Health Science Building
1618 Campus Delivery
Fort Collins, CO 80523

Tuesday, July 25, 2017

Dear Prof. Thomas E. Johnson:

Your USDA Veterinary Permit to import and/or transport controlled materials, organisms, or vectors accompanies this cover letter.

Review this permit carefully, as the statements and language may have changed to reflect the requirements of newly published regulations.

Please note the following:

- USDA Veterinary Permits no longer require a signature. Use of the permit for importation of the described commodity(ies) is acknowledgement that the permittee is legally responsible for complying with the permit conditions.
- Review the import permit for errors. Should you identify any errors, please contact our office immediately.
- A copy of the permit must accompany every shipment.

Do Not send the permit back to this office.

Contact our office with any questions or concerns at 301-851-3300, option 1.

Sincerely,

A handwritten signature in blue ink that reads "D. Langford".

Dr. Deborah Langford
Staff Veterinarian
Import Animal Products
National Import Export Services (NIES)

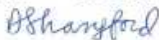
PLEASE VISIT OUR WEBSITE WWW.APHIS.USDA.GOV AND ENJOY OUR QUARTERLY NEWSLETTER WHICH HIGHLIGHTS THE IMPORT AND EXPORT STAFF CONTINUED EFFORTS TOWARD SAFEGUARDING U.S. AGRICULTURE AND LIVESTOCK. THIS NEWSLETTER ALSO FEATURES CURRENT TRENDS SHAPING APHIS/NIES AND THE IMPORT PERMIT PROCESS.



Safeguarding Animal Health
APHIS is an agency of USDA's Marketing and Regulatory Programs
An Equal Opportunity Provider and Employer

Federal Helpline Service
(Voice/TTY/ASL/Spasid)
1-800-675-8339

Fig. R.1 .Cover Letter: USDA Veterinary permit to import/transport controlled materials, organisms, or vectors

U.S. DEPARTMENT OF AGRICULTURE ANIMAL AND PLANT HEALTH INSPECTION SERVICE VETERINARY SERVICES RIVERDALE, MARYLAND 20737 file:///D:/inetpub/wwwroot/epemba/mageu/		PERMIT NUMBER 192546 (Amended 07/25/2017) Research	
UNITED STATES VETERINARY PERMIT FOR IMPORTATION AND TRANSPORTATION OF CONTROLLED MATERIALS AND ORGANISMS AND VECTORS		DATE ISSUED 12/12/2016	DATE EXPIRES 12/12/2017
NAME AND ADDRESS OF SHIPPER(S) Various shippers within... Japan		CC: Service Center, CO (Lakewood, CR)	
NAME AND ADDRESS OF PERMITTEE INCLUDING ZIP CODE AND TELEPHONE NUMBER Prof. Thomas E. Johnson Colorado State University Environmental and Radiological Health Science Building 1618 Campus Delivery Fort Collins, Colorado 80523 970-491-0562		U.S. PORT(S) OF ARRIVAL DENVER, CO	
		MODE OF TRANSPORTATION	AIR
AS REQUESTED IN YOUR APPLICATION, YOU ARE AUTHORIZED TO IMPORT OR TRANSPORT THE FOLLOWING MATERIALS			
Teeth, hair, blood, and/or tissue samples (fixed and/or on slides) from wild boar (porcine origin)			
RESTRICTIONS AND PRECAUTIONS FOR TRANSPORTING AND HANDLING MATERIALS AND ALL DERIVATIVES			
THIS PERMIT IS ISSUED UNDER AUTHORITY CONTAINED IN 9 CFR CHAPTER 1, PARTS 94.95 AND 122. THE AUTHORIZED MATERIALS OR THEIR DERIVATIVES SHALL BE USED ONLY IN ACCORDANCE WITH THE RESTRICTIONS AND PRECAUTIONS SPECIFIED BELOW (ALTERATIONS OF RESTRICTIONS CAN BE MADE ONLY WHEN AUTHORIZED BY USDA, APHIS, VS).			
o Adequate safety precautions shall be maintained during shipment and handling to prevent dissemination of disease.			
o With the use of this permit I, Thomas E. Johnson, Permittee, acknowledge that the regulated material(s) will be imported/transported within the United States in accordance with the terms and conditions as are specified in the permit. The Permittee is the legal importer/recipient [as applicable] of regulated article(s) and is responsible for complying with the permit conditions. The Permittee must be at least 18 years of age and have and maintain an address in the United States that is specified on the permit; or if another legal entity, maintain an address or business office in the United States with a designated individual for service of process; and serve as the contact for the purpose of communications associated with the import, transit, or transport of the regulated article(s). **Note: Import/Permit requirements are subject to change at any time during the duration of this permit.			
o ***Each shipment shall be accompanied by an ORIGINAL signed document from the producer/manufacture confirming that: 1) the exported material was derived from wild boar (porcine) that originated in Japan; 2) prior to export to the United States, the exported materials were treated as follows: (a) the teeth were treated using a solution of bleach in an ultrasonic cleansing system, (b) the hair samples were washed with isopropanol and air dried, (c) the slides contain blood fixed with methanol and acetic acid then sealed with a fixative and coverslip, ... [continued on page 2]...			
continued on subsequent page(s)....			
TO EXPEDITE CLEARANCES AT THE PORT OF ENTRY, BILL OF LADING, AIRBILL OR OTHER DOCUMENTS ACCOMPANYING THE SHIPMENT SHALL BEAR THE PERMIT NUMBER			
SIGNATURE Deborah Langford 	TITLE Staff Veterinarian National Import Export Services	NO. LABELS	

VS FORM 16-6A (MAR 95)

Replaces VS Form 16-3A and 16-28 which are obsolete

Page 1 of 2

Fig. R.2. Page 1: USDA Veterinary permit to import/transport controlled materials, organisms, or vectors

RESTRICTIONS AND PRECAUTIONS: (continued from Permit Form VS 16-6)

- o ...[continued from page 1]... (d) the blood samples were fixed with methanol and acetic acid plus glutaraldehyde to achieve a final concentration of 0.2% glutaraldehyde, and (e) the tissue samples were fully fixed in 10% formalin before being transferred to 70% ethyl alcohol; and 4) the exported material was not exposed to or commingled with any other animal origin material.
(This certification must CLEARLY correspond to the shipment by means of an invoice number or shipping marks or lot number or other identification method. An English translation must be provided.)

- o ***Materials shall be consigned directly to the permittee at the permittee address specified above. Materials imported under this permit may be hand carried in personal baggage from the country of origin to the port of arrival, but must be declared and made available to port officials for inspection, and must be transported directly to the permittee by someone with identification and current, signed written authority from the permittee. The permittee's authorizing document must be original, on letterhead, and specific to the particular shipment(s), and shall be valid for no more than 2 months from the date of issuance.

- o COMMERCIAL DISTRIBUTION OF THE IMPORTED MATERIAL AND/OR THEIR DERIVATIVES IS PROHIBITED.

- o This permit DOES NOT authorize direct or indirect exposure of or inoculation into laboratory and domestic livestock (including but not limited to: birds/poultry/eggs, cattle, sheep, goats, swine, and/or horses). Work shall be limited to *in vitro* uses only. No extraction of nucleic acids is to be performed on imported material.

- o Packaging, containers, and all equipment in contact with these materials shall be sterilized or considered a biohazard and be disposed of accordingly.

- o THIS PERMIT IS VALID ONLY FOR WORK CONDUCTED OR DIRECTED BY YOU OR YOUR DESIGNEE IN YOUR PRESENT U.S. FACILITY OR APPROPRIATELY INSPECTED LABORATORY. THE AUTHORIZED IMPORTED MATERIAL(S) MUST BE SHIPPED/CONSIGNEE DIRECTLY TO THE ADDRESS OF THE PERMITTEE OR TO THE ADDRESS OF THE ADDITIONAL PERMITTEE(S) AS IDENTIFIED ON THIS PERMIT. (MATERIALS SHALL NOT BE MOVED TO ANOTHER U.S. LOCATION, OR DISTRIBUTED WITHIN THE U.S., WITHOUT USDA, APHIS, VS, NIES AUTHORIZATION.)

- o On completion of your work, all permitted materials and all derivatives therefrom shall be destroyed.

- o This permit does not exempt the permittee from responsibility for compliance with any other applicable federal, state, or local laws and regulations.

Fig. R.3. Page 2: USDA Veterinary permit to import/transport controlled materials, organisms, or vectors

RESTRICTIONS AND PRECAUTIONS: (continued from Permit Form VS 16-6)

- o Imported material may be subject to regulations enforced by the United States Department of Interior, Fish and Wildlife Service (FWS). Importer must contact FWS, information is available at web pages <http://www.FWS.gov/permits/> and/or <http://www.FWS.gov/le/travelers.html>
 - o The restrictions on this permit remain in force as long as the material is in the United States.
 - o Any person who VIOLATES the terms and conditions of permits, and/or who forge, counterfeit, or deface permits may be subject to criminal and civil penalties in accordance with applicable law. In addition, all current permits may be cancelled and future permit applications denied.
 - o A copy of this permit must be included with the shipping documents. For imported materials, these documents must be presented to CBF Agricultural Specialists upon arrival at the U.S. port of arrival. This permit replaces previous editions and has been amended to authorize hand carry.
-

Fig. R.4. Page 3: USDA Veterinary permit to import/transport controlled materials, organisms, or vectors

Appendix S

^{90}Sr Analysis Results

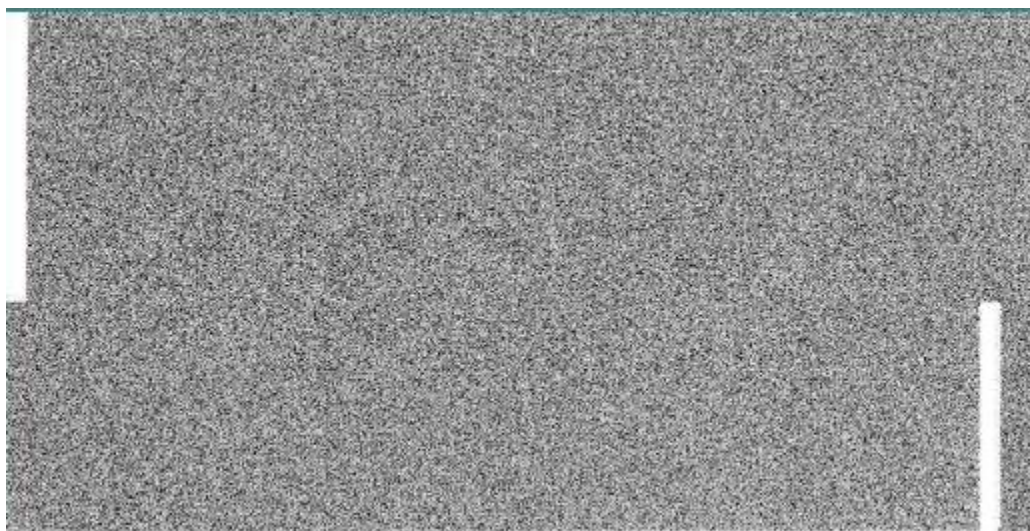


Fig. S.1. Screenshot of OptiQuant™ Image Analysis Software for a 3-day background.

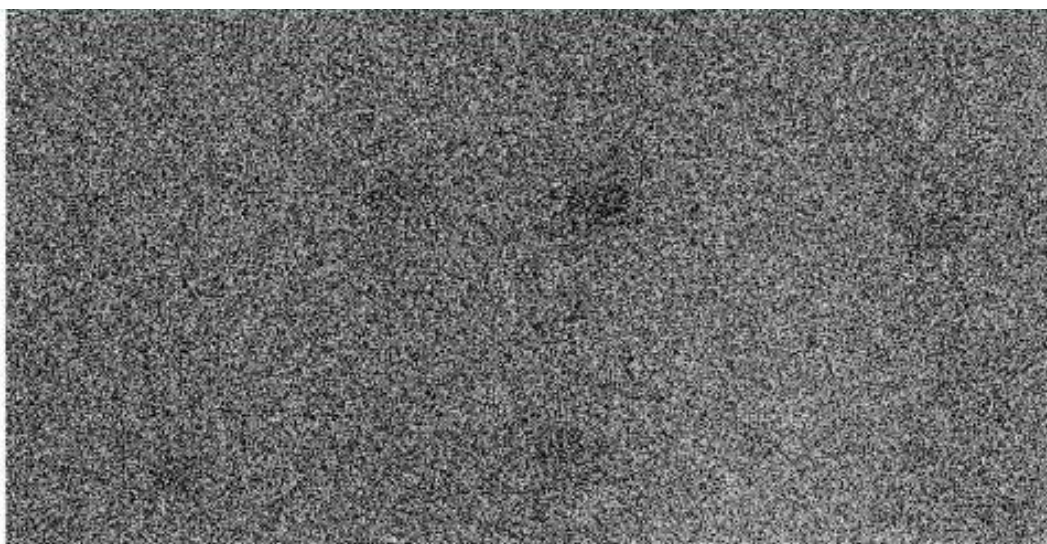


Fig. S.2. Screenshot of OptiQuant™ Image Analysis Software for the 3-day tooth sample count

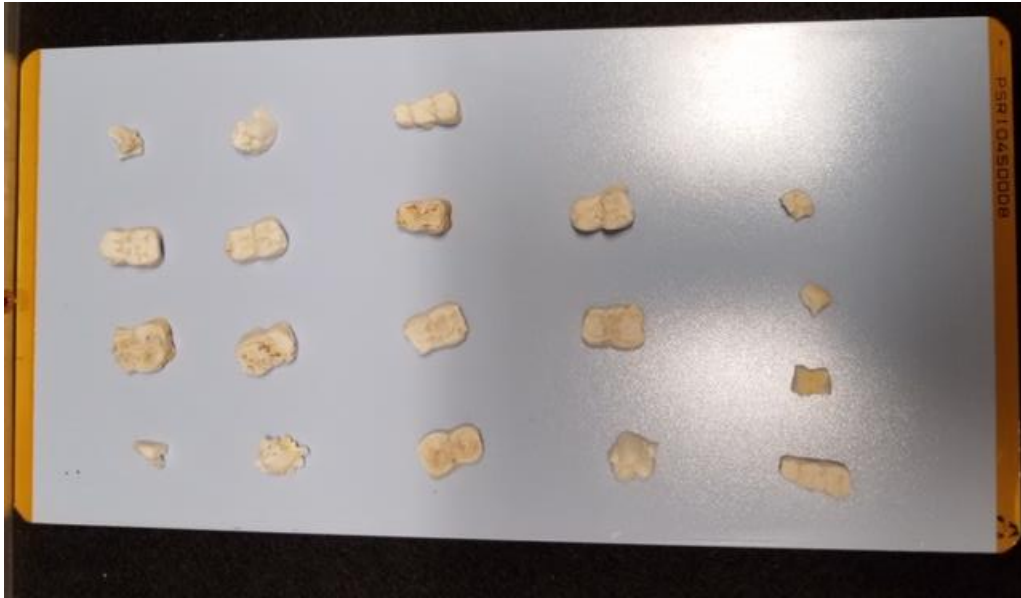


Fig. S.3. Tooth sample placement on the imaging plate

Table S.1. Data collected from imaging plate containing tooth samples. Digital light units per mm² (DLU/mm²) are shown for each region for the background and sample counts. Net counts for each region after background subtraction are shown for comparison.

Background 3-Day DLU/mm ²					
	1	2	3	4	5
A	7467.4	7218.2	7244.6	7148.9	7059.0
B	7456.0	7217.4	7136.5	7089.7	7080.7
C	7277.0	7186.3	7075.7	6799.7	6855.2
D	7275.2	7062.5	6967.0	6643.8	6064.0
Boar Tooth Sample 3-Day DLU/mm ²					
	1	2	3	4	5
A	7310.8	7186.4	7362.2	7037.7	6835.1
B	7374.2	7504.3	7899.8	6755.3	6990.8
C	7396.9	7337.9	7174.2	6451.7	6868.3
D	7632.4	7359.3	7335.8	6089.1	6816.3
Net Counts DLU/mm ²					
	1	2	3	4	5
A	-156.6	-31.8	117.6	-111.2	-223.9
B	-81.8	286.9	763.3	-334.4	-89.9
C	119.9	151.6	98.5	-348.0	13.1
D	357.2	296.8	368.8	-554.7	752.3